



UvA-DARE (Digital Academic Repository)

Going beyond your form

T-cell dependent B-cell fate determination

Verstegen, N.J.M.C.

Publication date

2023

Document Version

Final published version

[Link to publication](#)

Citation for published version (APA):

Verstegen, N. J. M. C. (2023). *Going beyond your form: T-cell dependent B-cell fate determination*. [Thesis, fully internal, Universiteit van Amsterdam].

General rights

It is not permitted to download or to forward/distribute the text or part of it without the consent of the author(s) and/or copyright holder(s), other than for strictly personal, individual use, unless the work is under an open content license (like Creative Commons).

Disclaimer/Complaints regulations

If you believe that digital publication of certain material infringes any of your rights or (privacy) interests, please let the Library know, stating your reasons. In case of a legitimate complaint, the Library will make the material inaccessible and/or remove it from the website. Please Ask the Library: <https://uba.uva.nl/en/contact>, or a letter to: Library of the University of Amsterdam, Secretariat, Singel 425, 1012 WP Amsterdam, The Netherlands. You will be contacted as soon as possible.

Going beyond your form

T-cell dependent B-cell fate determination



Niels J.M.C. Verstegen

Going beyond your form

T-cell dependent B-cell fate determination

Niels Josephus Martinus Cornelis Verstegen



Sanquin

The research described in this thesis was performed at the Department of Immunopathology of Sanquin Research, Amsterdam, The Netherlands and Synthetic Systems Biology and Nuclear Organization, Swammerdam Institute for Life Sciences, University of Amsterdam, The Netherlands.

The printing of this thesis was financially supported by Sanquin Research

Copyright © Niels J.M.C. Verstegen, 2023

ISBN: 978-94-6483-020-0

Cover created with Midjourney

Lay-out and design by Niels J.M.C. Verstegen

printed by Ridderprint | www.ridderprint.nl

Going beyond your form

T-cell dependent B-cell fate determination

ACADEMISCH PROEFSCHRIFT

ter verkrijging van de graad van doctor
aan de Universiteit van Amsterdam
op gezag van de Rector Magnificus
prof. dr. ir. P.P.C.C. Verbeek

ten overstaan van een door het College voor Promoties ingestelde commissie,
in het openbaar te verdedigen in de Agnietenkapel
op vrijdag, 14 april 2023, te 13.00 uur

door Niels Josephus Martinus Cornelis Verstegen
geboren te Goirle

Promotiecommissie

<i>Promotor:</i>	prof. dr. S.M. van Ham	Universiteit van Amsterdam
<i>Copromotores:</i>	dr. J.A. ten Brinke dr. M. Barberis	Sanquin Research University of Surrey
<i>Overige leden:</i>	prof. dr. ing. A.H.C. van Kampen prof. dr. C.E. van der Schoot prof. dr. M.A. Haniffa prof. dr. R.W. Hendriks dr. J. de Wit prof. dr. S. Brul	Universiteit van Amsterdam Universiteit van Amsterdam Newcastle University Erasmus Universiteit Rotterdam RIVM Universiteit van Amsterdam

Faculteit der Natuurwetenschappen, Wiskunde en Informatica

Table of contents

Chapter 1	General introduction and outline of the thesis	7
Chapter 2	System-level scenarios for the elucidation of T cell-mediated germinal center B cell differentiation	21
Chapter 3	Human B cells engage the NCK/PI3K/RAC1 axis to internalize large particles via the IgM-BCR	57
Chapter 4	TCR signal strength regulates the plastic co-expression of IL-4 and IFN- γ by Tfh-like cells	87
Chapter 5	Minimalistic <i>in vitro</i> culture to drive human naive B cell differentiation into antibody-secreting cells	107
Chapter 6	Single-cell analysis reveals dynamics of human B cell differentiation and identifies novel B and antibody-secreting cell intermediates	141
Chapter 7	Summarizing discussion	173
Appendix	Nederlandse samenvatting	190
	List of publications	195
	Contributing authors	199
	PhD portfolio	204
	Curriculum vitae	206
	Dankwoord	207

Chapter 1

General introduction and outline of the thesis

The recent SARS-CoV-2 pandemic has made it increasingly apparent to the public how reliant we are on our immune system to function effectively. Our immune system protects us from the billions of different microorganisms that surround us, such as viruses, bacteria, fungi, and parasites, which may invade us in our lifetime. The immune system is a complex biological system that consists of two yet highly integrated parts: the innate (natural) immune system and the adaptive (specific) immune system¹. An appropriate interplay between these two parts leads to highly effective recognition and clearance of pathogens. After a pathogen has entered the body, the innate immune system serves as the first line of defense¹. The innate immune system contains complement proteins and cells such as macrophages, neutrophils, and dendritic cells (DCs)^{2,3}. A primary role of named cells is to quickly bind to molecules on the pathogens via specific receptors (Pattern Recognition Receptors (PRRs) and Scavenger Receptors) to subsequently become activated and engulf (or secrete toxic molecules) and destroy invading pathogens⁴. In addition, the innate immune system provides multiple cues to support the activation of the adaptive immune system⁵. The adaptive immune system comprises two types of cells, B and T cells. B and T cells recognize parts of pathogens termed antigens with their antigen receptor, called B cell receptors (BCR) or membrane-bound antibodies and T cell receptors (TCR), respectively. By targeting the immune defense against specific antigens on the pathogen and activating receptors that enhance the effector functions of the immune system to eliminate the pathogen, these cells contribute to pathogen elimination by ensuring a higher level of specificity and efficiency in the attack against the pathogen⁶. Although it takes a longer time to get the adaptive immune system activated, long-term memory of the previously encountered pathogen is maintained in the form of memory T and B cells that are activated rapidly upon reencounter with the same pathogen, and long-lived plasma cells that can take residence in the bone marrow and secrete large amounts of antibodies with the same specificity that were initially bound as BCR on the surface of their B cell precursor (**Figure 1a**)⁷. BCRs and TCRs are not encoded by a single gene but are composed of multiprotein chains containing variable antigen-binding regions at the tip of each chain⁸.

As this thesis focuses on B cell responses, the recombination process that results in the expression of a functional BCR will be explained. A BCR comprises two identical heavy and light chains (kappa or lambda) (**Figure 1a**)⁸. The heavy and light chains contain a constant and a variable region. The heavy chain constant region defines the isotype of the BCR (in humans IgA, IgD, IgE, IgG, and IgM) and confers the antibody's effector function once it is secreted. The function of these secreted antibodies includes neutralization of the pathogen or toxin, facilitation of phagocytosis and antibody-dependent cellular cytotoxicity (ADCC), and activation of complement-mediated lysis (**Figure 1b**)^{9,10}. The variable region of the heavy and light chain confers the antigen-binding site and is encoded by a somatic combination of hundreds of V, D, and J or V and J segments that assemble for heavy or light chains, respectively (**Figure 1c**). One of every segment is randomly recombined and joined, which by nature is an imprecise process and adds even more variation (**Figure 1c**)^{8,11-14}. Although TCRs consist of different protein chains than BCRs, the combinatorial processes that provide the diversity are highly homologous.

Together, the combination of multiprotein chains, the V(D)J rearrangement, and the joining imperfections give rise to an enormous ($\sim 10^{14}$ and 10^{16}) diversity of antigen receptors that allows the recognition of a nearly infinite number of molecules.

B cells are generated in the bone marrow, acquiring the unique BCR. After maturation in the bone marrow and elimination of B cells containing self-reactive BCRs, they circulate between the lymph and blood and seed secondary lymphoid organs such as lymph nodes, the spleen, and mucosal-associated lymphoid tissues. Secondary lymphoid tissues serve as a means of efficiently trapping foreign antigens that enter the body through the bloodstream, peripheral tissues, and mucosal sites, respectively¹⁵. Adaptive immune responses against antigens are centered in these secondary lymphoid tissues. Antigens are functionally divided into T cell-independent (TI) and

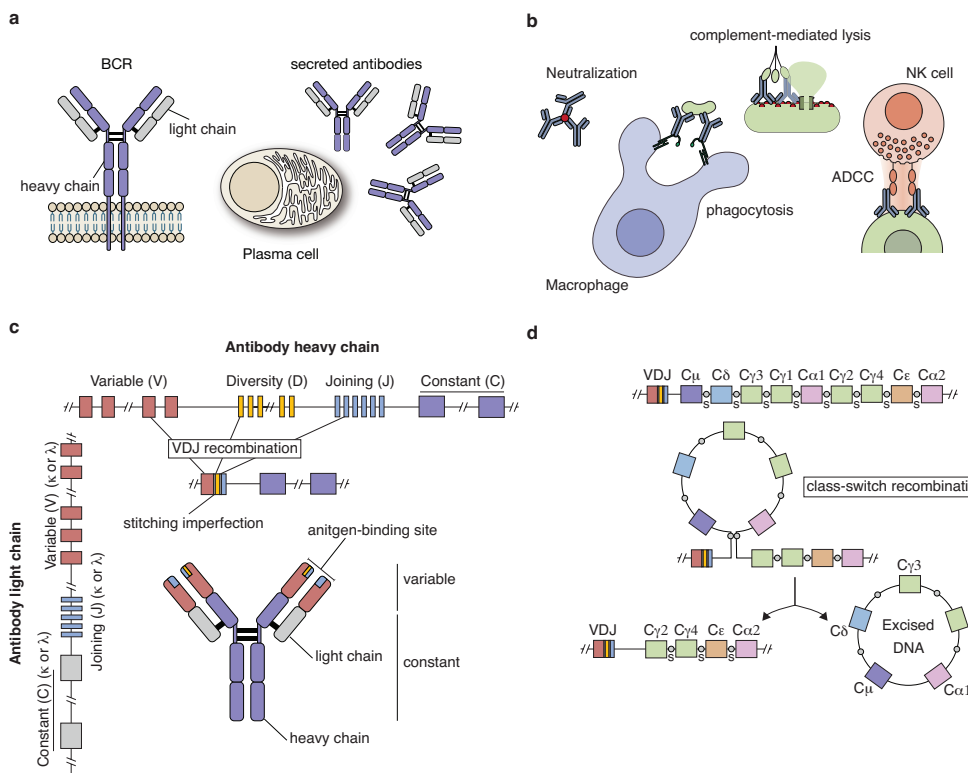


Figure 1 | B cell receptor (BCR) and antibody structure and function. (A) The BCR is a transmembrane protein on the surface of a B cell. It contains two identical heavy chains and two identical light chains. The antibodies secreted by antibody-secreting plasmablasts and plasma cells are the secreted form of the BCR bound by the B cell precursor. (B) Secreted antibodies have different effector functions, including pathogen neutralization, facilitation of FC receptor-mediated phagocytosis, pathogen opsonization to drive complement deposition, and antibody-dependent cellular cytotoxicity (ADCC). (C) The antibody variable domain contains the antigen-binding site. The exons encoding the antigen binding site are assembled from so-called V (variable), D (diversity), and J (joining) gene segments by DNA rearrangements. (D) The heavy chain constant region defines the antibody isotype. Each segment encodes for a different isotype and has its switch region (s). Switching occurs by recombining between these switch regions, excluding the excised DNA.

T cell-dependent (TD) antigens, depending on whether help from a CD4⁺ helper T (Th) cell is needed to induce an antibody response¹⁶. TI antigens are often enriched for polysaccharide and/or lipopolysaccharide repeating structures that extensively cross-link the BCRs and activate PRRs¹⁶. The overall binding avidity of the cross-linked BCRs is generally sufficient to initiate the immune response. TI responses do not stimulate efficient immunological memory, and the antibody-secreting cells generated during these responses secrete antibodies of the IgM and IgA isotype^{17–20}. Without T cell help, class-switch recombination (CSR) is not efficiently induced. CSR replaces the BCR constant region from IgM-IgD, expressed by mature B cells after their development in the bone marrow, to the IgA, IgG, or IgE class most effective in protecting against a particular pathogen (**Figure 1d**)^{21,22}. The IgM antibodies made first in any infection are instrumental in early host defense²³. IgM antibodies form hexameric (or pentameric) complexes, which are effective at fixing complement²⁴. Although the affinity of the antigen-binding site of IgM molecules is relatively low, complex formation provides the molecules with relatively high avidity for multivalent antigens. IgA is secreted into body fluids to protect mucosal surfaces²⁵. IgE binds to specific receptors on mast cells and triggers the production of histamine and other mediators of allergy, but these cells are also vital in defense against helminths²⁶. IgG is potent for opsonization by interacting with FC gamma receptors on different cell types, including macrophages²⁷. IgG also facilitates ADCC, which can fix complement to different degrees depending on the different IgG subclasses (IgG1, IgG2, IgG3, and IgG4)²⁸.

Responses to TD antigens require assistance from Th cells. B and Th cells in secondary lymphoid organs are separated into distinct areas (**Figure 2**)²⁹. To engage in a TD antigen response, naive CD4⁺ T cells must first recognize cognate antigens in the T cell zone. Th cells use the TCR to bind antigens presented as antigen-derived peptides in complex with major histocompatibility complex (MHC) class II proteins (**Figure 2**)³⁰. Cells that can internalize antigens, process them into smaller antigen-derived peptides and display p:MHCII are termed antigen-presenting cells (APCs) and include macrophages, DCs, and B cells³¹. During a foreign antigen challenge, DCs bearing antigens from peripheral tissues migrate to secondary lymphoid organs to present antigens to naive CD4⁺ T cells (**Figure 2**)³². The antigen-specific TCR and p:MHCII initially mediates the interaction between naive CD4⁺ T cells and antigen-presenting DCs to provide the first activation signal. Naive CD4⁺ T cells are further modulated by cytokines and CD28 costimulation necessary for full and productive T cell activation (**Figure 2**). Costimulation is a fail-safe mechanism of the immune system to prevent unnecessary activation^{33,34}. This contact allows Th cell activation, clonal expansion, and effector fate determination.

The Th cell fate is plastic, capable of acquiring distinct functions to combat specific pathogens and redirecting these functions in response to changing circumstances or different pathogens^{35,36}. Upon their activation by DCs, human naive CD4⁺ T cells mainly develop a Th1 phenotype following infections by intracellular bacteria and viruses³⁷. In contrast, Th2 cells are programmed in response to extracellular bacterial and certain gut infections³⁸, whereas Th17 responses are directed against fungal infection³⁹. Th1, Th2, and Th17 cells leave the secondary

lymphoid organs and migrate to the peripheral side of infection or inflammation to help locally terminate the foreign antigen threat. Other helper T cells acquire an early T follicular helper (Tfh) cell phenotype programmed to help the B cell response and stay in secondary lymphoid organs (**Figure 2**)^{40–43}. The notion that the Tfh cell is crucial for the B cell response was cemented when the key transcriptional regulator of this population, BCL6, was discovered^{44–46}. BCL6 is vital for many aspects of Tfh cell function, but it is essential for orchestrating CXCR5-mediated migration towards and into the B cell follicles (**Figure 2**). Each Th subset produces a specific cytokine signature in high amounts while retaining the ability to produce other cytokines to a lesser extent. Conditions that polarize a particular subset of Th cells inhibit the differentiation of other subsets, thus enhancing the desired response. Th1 development is accompanied by IFN- γ secretion, whereas IL-4 secretion correlates with Th2 and Tfh. Likewise, IL-21 is the main cytokine secreted by (early) Tfh cells to regulate B cell differentiation to ASC. Since antibody responses are desired against all pathogens, whether viral, bacterial, or fungal, Tfh cell responses are helpful against 99% of them. Hence, Tfh cell differentiation and function require a high degree of plasticity.

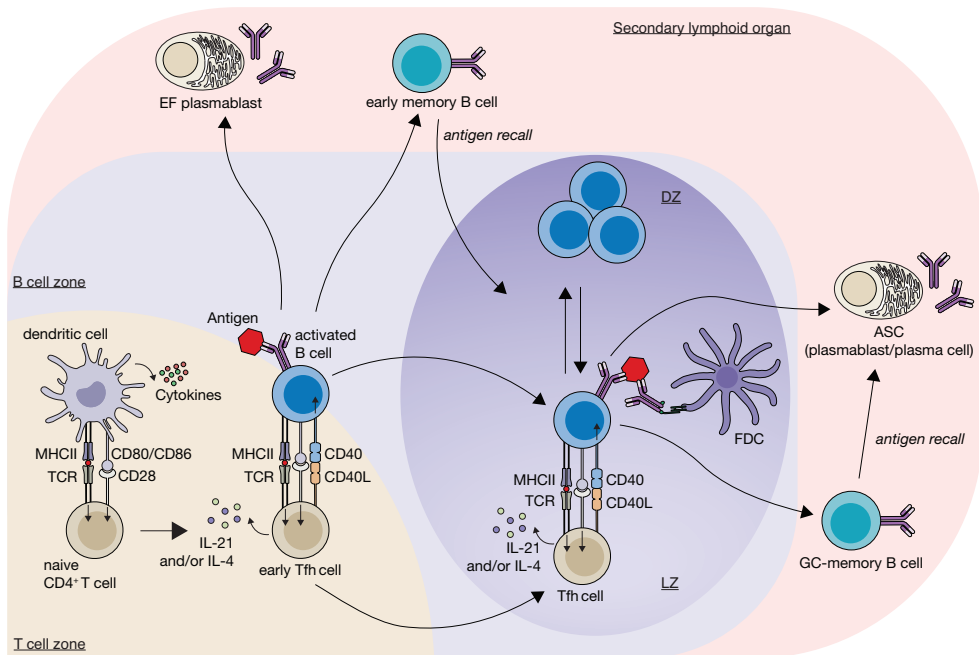


Figure 2 | Multiple signals and steps for generating Tfh cells, T-dependent memory B cells, and antibody-secreting cells. Naive CD4⁺ T cells are activated by dendritic cells (DCs) that take up antigens in the periphery to acquire an early T follicular helper (Tfh) cell phenotype. Early Tfh cells interact with antigen-activated B cells to drive extrafollicular (EF) plasmablast or early memory B cell differentiation or to induce a germinal center (GC) B cell response. Simultaneously, interaction with the antigen-activated B cells complements the differentiation of the early Tfh to the Tfh cell phenotype, facilitating the migration into the GC where they reside with GC B cells. Tfh and GC B cells interact in the GC regularly to drive affinity-based selection and fate determination into antibody-secreting plasmablast/plasma cells and GC-memory B cells.

When a naive B cell gets activated by a TD antigen, the first activation signal is classically delivered when the antigen binds to the BCR (**Figure 2**). After recognition, the antigen is internalized, which is fundamental for the correct function of the humoral immune response to TD antigens. Various cellular mechanisms are involved in acquiring antigens, which include endocytosis, micropinocytosis, and phagocytosis. B cells acquire antigens primarily by endocytosis (for antigens $<0.2 \mu\text{m}$)⁴⁷. In phagocytosis, large particles ($>0.5 \mu\text{m}$) are acquired through an intense remodeling of the actin cytoskeleton. In the early paradigm, phagocytosis was only carried out by professional phagocytes, such as macrophages and dendritic cells. Due to the membrane and cytosolic rearrangements needed, B cells were thought to lack such phagocytic properties. In the last decade, multiple studies demonstrated BCR-mediated phagocytosis of large particles, including beads and bacteria, by B cells⁴⁸⁻⁵². Subsequent recognition and internalization, the antigen is processed to be presented as p:MHCII. The B cell now acts as a professional APC, showing p:MHCII to the TCR of antigen-experienced early Tfh cells (**Figure 2**). TCR interaction with p:MHCII controls the specificity of the immune response and is essential for B and T cells to engage in cognate interactions.

Although B cells bind and are activated by native unprocessed antigens, they require additional signals from early Tfh cells to get fully primed and participate in the TD immune response. These additional signals come in many forms, but the most important is provided by the surface receptor CD40 ligand (CD40L) on early Tfh cells that binds CD40 on the primed B cell and the soluble cytokines IL-21 and IL-4 that are secreted by the Tfh cell and interact with the cytokine receptors on B cells (**Figure 2**)⁵³⁻⁵⁵. Simultaneously, early Tfh to Tfh differentiation becomes extremely B cell dependent⁴³. Since DC cells will be around for a few days (at least during acute antigen exposure) before they die by apoptosis, B cells become the primary antigen source for Tfh cells. Tfh cells have a highly symbiotic relationship with B cells⁵⁶, and B cells are required for Tfh development under almost all *in vivo* conditions^{40,42,43}. After this contact at the border of the T:B zones, activated B cells acquire multiple phenotypes (**Figure 2**). Some differentiate into extrafollicular plasmablasts (PB) that secrete the early wave of sometimes class-switched but unmutated antibodies^{57,58}, whereas others acquire an early-memory B cell phenotype (**Figure 2**)⁵⁹. These early-memory B cells are of low affinity and are retained locally to contribute to GC responses upon antigen recall (**Figure 2**)⁶⁰⁻⁶². Other activated B cells enter the primary follicle and start proliferating rapidly, forming germinal centers (GC) (for detailed information, see chapter 2 of this thesis) (**Figure 2**)⁶³⁻⁶⁶. The initial fate determination depends on the BCR affinity for the target antigen, where high-affinity B cells are more prevalent in the extrafollicular plasma cell versus the GC B cell response^{58,67}. Although it has been thought for quite a while that CSR occurs predominantly during the GC reaction, recently, it was shown that these processes are uncoupled and that most class switch events are triggered before differentiation into GC B cells or PB⁶⁸.

B cells acquiring the GC fate divide rapidly and acquire somatic mutations in the genes that encode the BCR, which can change BCR binding properties for the target antigen. This process

relies highly on the activation-induced cytidine deaminase protein (AID) expression in GC B cells^{69,70}. Mature GCs polarize into two distinct zones, the dark zone (DZ) and the light zone (LZ) (**Figure 2**). During the GC reactions, B cells alternate between periods of proliferation in the DZ and periods of antigen reencounter and re-engagement with cognate Tfh cells in the LZ (**Figure 2**)^{71,72}. Since the mutations are random, many are deleterious to the GC B cell⁷³. However, occasionally a mutation will improve the affinity of the BCR. The growing population of B cells expresses these hypermutated genes, giving BCRs a range of affinities for the target antigen. Inside the GC, the antigen is retained as immune complexes by follicular dendritic cells (FDCs) in the LZ (**Figure 2**)⁷⁴⁻⁷⁷. Competition for this limited quantity of antigen will provide the basis for selection among the random GC B cell mutants. High-affinity interaction induces the B cell to spread on the surface of the FDC, capturing more antigens⁷⁸. The captured antigen is internalized and presented to Tfh cells that, upon their differentiation, migrate into the GC and return CD40L and the cytokines IL-21 and IL-4 required for B cell survival and selection (**Figure 2**). Tfh cells progressively differentiate from producing mainly IL-21 in the early GC response to IL-4 production in the late GC response⁷⁹. Interestingly, Tfh cells engage in positive feedback loops whereby signals delivered by Tfh cells stimulate B cells to increase surface and soluble mediators that attract further help from Tfh cells⁸⁰⁻⁸². As such, those B cells with low affinity are likely outcompeted to receive Tfh-driven selection signals and die by apoptosis. This selection, termed affinity maturation, allows preferentially the highest affinity B cells to remain from the variable population. It has been demonstrated recently that positive selection is not only based on BCR affinity but also on BCR isotype, with IgG-expressing cells showing an advantage over IgM-expressing cells⁸³. Selected B cells will continue to mutate and divide again^{84,85}. Over several generations, like in Darwinian-based selection, only the fittest high-affinity population of GC B cells remains within the germinal center. The GC reaction ultimately gives rise to higher-affinity memory B cells relatively early in the GC and antibody-secreting PB and plasma cells (PCs), later (**Figure 2**)^{64,86-88}. High-affinity memory B cells that reencounter antigens infrequently reengage in GC for further diversification and account for most secondary antibody responses (**Figure 2**)⁸⁹. What cues determine the export of GC B cells into the memory or antibody-secreting cell compartment is studied extensively. Likely it is a combination of the strength of Tfh cell help and BCR signaling^{64,90}.

Scope of this thesis

This thesis aims to investigate the role of antigen and B-Tfh cell communication in T cell-dependent B cell responses and fate determination. **Chapter 2** reviews internal and external factors driving various GC dynamics, such as GC initiation, maturation, and GC B cell fate determination. We describe the most potent signals delivered by Tfh cells – CD40L and the cytokines IL-21 and IL-4 – and provide insight into how these extracellular signals integrate to activate different transcriptional effector profiles. We elaborate on current strategies of system modeling efforts to elucidate B cell behavior during the GC tract. **Chapter 3** describes

how downstream signaling molecules contribute to the BCR-mediated phagocytosis of large particulate antigens. In **Chapter 4**, we investigate how TCR stimulation, CD28 co-stimulation, and cytokines direct the differentiation of naive CD4⁺ Th cells to secrete the Tfh-associated cytokines IL-4 and IL-21. We describe the plasticity that allows Tfh cells to possess characteristics of other effector Th cell populations. In **Chapter 5**, the level and dynamics of CD40 co-stimulation in human naive B cells were studied in the presence of IL-21 and/or IL-4 to understand their contribution to antibody-secreting cell differentiation. In **Chapter 6**, we investigate the trajectories of human naive B cell differentiation into antibody-secreting cells by combining single-cell RNA sequencing of B cell differentiation *in vitro* with *ex vivo* datasets of isolated B cells and ASCs and state-of-the-art analysis pipelines. We identify a novel ASC-precursor population and *in vitro* B cell differentiation pathways that recapitulate GC B cell reactions and (early) memory B cell formation. **Chapter 7** summarizes the findings of this thesis and explores the implications for T-cell-dependent B-cell fate determination research.

REFERENCES

1. Marshall, J. S., Warrington, R., Watson, W. & Kim, H. L. An introduction to immunology and immunopathology. *Allergy, Asthma and Clinical Immunology* **14**, 1–10 (2018).
2. Dunkelberger, J. R. & Song, W. C. Complement and its role in innate and adaptive immune responses. *Cell Research* **20**, 34–50 (2009).
3. Paludan, S. R., Pradeu, T., Masters, S. L. & Mogensen, T. H. Constitutive immune mechanisms: mediators of host defence and immune regulation. *Nature Reviews Immunology* **20**, 137–150 (2020).
4. Akira, S., Uematsu, S. & Takeuchi, O. Pathogen Recognition and Innate Immunity. *Cell* **124**, 783–801 (2006).
5. Jain, A. & Pasare, C. Innate control of adaptive immunity: Beyond the three-signal paradigm. *J Immunol* **198**, 3791 (2017).
6. Flajnik, M. F. & Kasahara, M. Origin and evolution of the adaptive immune system: genetic events and selective pressures. *Nature Reviews Genetics* **10**, 47–59 (2009).
7. Netea, M. G., Schlitzer, A., Placek, K., Joosten, L. A. B. & Schultze, J. L. Innate and Adaptive Immune Memory: an Evolutionary Continuum in the Host's Response to Pathogens. *Cell Host Microbe* **25**, 13–26 (2019).
8. Jung, D. & Alt, F. W. Unraveling V(D)J Recombination: Insights into Gene Regulation. *Cell* **116**, 299–311 (2004).
9. Lu, L. L., Suscovich, T. J., Fortune, S. M. & Alter, G. Beyond binding: antibody effector functions in infectious diseases. *Nature Reviews Immunology* **17**, 46–61 (2017).
10. van Erp, E. A., Luytjes, W., Ferwerda, G. & van Kasteren, P. B. Fc-mediated antibody effector functions during respiratory syncytial virus infection and disease. *Front Immunol* **10**, 548 (2019).
11. Alt, F. W. & Baltimore, D. Joining of immunoglobulin heavy chain gene segments. *Proc. Natl. Acad. Sci. USA* **79**, 4118–4122 (1982).
12. Agrawal, A., Eastman, Q. M. & Schatz, D. G. Transposition mediated by RAG1 and RAG2 and its implications for the evolution of the immune system. *Nature* **394**, 744–751 (1998).
13. Bassing, C. H., Swat, W. & Alt, F. W. The mechanism and regulation of chromosomal V(D)J recombination. *Cell* **109**, S45–S55 (2002).
14. Bassing, C. H. *et al.* Recombination signal sequences restrict chromosomal V(D)J recombination beyond the 12/23 rule. *Nature* **405**, 583–586 (2000).
15. Batista, F. D. & Harwood, N. E. The who, how and where of antigen presentation to B cells. *Nat Rev Immunol* **9**, 15–27 (2009).
16. Mond, J. J., Lees, A. & Snapper, C. M. T Cell-Independent Antigens Type 2. <https://doi.org/10.1146/annurev-ij.13.040195.003255> **13**, 655–692 (2003).
17. Allman, D., Wilmore, J. R. & Gaudette, B. T. The Continuing Story of T-cell Independent Antibodies. *Immunol Rev* **288**, 128 (2019).
18. Macpherson, A. J. *et al.* A primitive T cell-independent mechanism of intestinal mucosal IgA responses to commensal bacteria. *Science* **288**, 2222–2226 (2000).
19. Bunker, J. J. & Bendelac, A. IgA responses to microbiota. *Immunity* **49**, 211 (2018).
20. Bunker, J. J. *et al.* Innate and Adaptive Humoral Responses Coat Distinct Commensal Bacteria with Immunoglobulin A. *Immunity* **43**, 541–553 (2015).
21. Chaudhuri, J. & Alt, F. W. Class-switch recombination: interplay of transcription, DNA deamination and DNA repair. *Nat Rev Immunol* **4**, 541–52 (2004).
22. Xu, Z., Zan, H., Pone, E. J., Mai, T. & Casali, P. Immunoglobulin class-switch DNA recombination: induction, targeting and beyond. *Nat Rev Immunol* **12**, 517–31 (2012).
23. Boes, M. Role of natural and immune IgM antibodies in immune responses. *Mol Immunol* **37**, 1141–1149 (2000).
24. Sharp, T. H. *et al.* Insights into IgM-mediated complement activation based on in situ structures of IgM-C1-C4b. *Proc Natl Acad Sci U S A* **116**, 11900–11905 (2019).
25. Corthésy, B. Multi-Faceted Functions of Secretory IgA at Mucosal Surfaces. *Front Immunol* **4**, (2013).
26. Sutton, B. J., Davies, A. M., Bax, H. J. & Karagiannis, S. N. IgE Antibodies: From Structure to Function and Clinical Translation. *Antibodies* **8**, (2019).
27. de Taeye, S. W., Rispens, T. & Vidarsson, G. The Ligands for Human IgG and Their Effector Functions. *Antibodies (Basel)* **8**, (2019).

28. Vidarsson, G., Dekkers, G. & Rispen, T. IgG subclasses and allotypes: From structure to effector functions. *Front Immunol* **5**, 520 (2014).
29. Ruddle, N. H. & Akirav, E. M. Secondary Lymphoid Organs: Responding to Genetic and Environmental Cues in Ontogeny and the Immune Response. *J Immunol* **183**, 2205 (2009).
30. Sundberg, E. J., Deng, L. & Mariuzza, R. A. TCR recognition of peptide/MHC class II complexes and superantigens. *Semin Immunol* **19**, 262 (2007).
31. Gaudino, S. J. & Kumar, P. Cross-talk between antigen presenting cells and T cells impacts intestinal homeostasis, bacterial infections, and tumorigenesis. *Front Immunol* **10**, 360 (2019).
32. Alvarez, D., Vollmann, E. H. & von Andrian, U. H. Mechanisms and consequences of dendritic cell migration. *Immunity* **29**, 325–342 (2008).
33. Sharpe, A. H. Mechanisms of Costimulation. *Immunol Rev* **229**, 5 (2009).
34. June, C. H., Ledbetter, J. A., Linsley, P. S. & Thompson, C. B. Role of the CD28 receptor in T-cell activation. *Immunol Today* **11**, 211–216 (1990).
35. Geginat, J. *et al.* Plasticity of human CD4 T cell subsets. *Front Immunol* **5**, 630 (2014).
36. Kaiko, G. E., Horvat, J. C., Beagley, K. W. & Hansbro, P. M. Immunological decision-making: how does the immune system decide to mount a helper T-cell response? *Immunology* **123**, 326 (2008).
37. Kidd, P. Th1/Th2 balance: the hypothesis, its limitations, and implications for health and disease. *Altern Med Rev* **8**, 223–46 (2003).
38. Spellberg, B. & Edwards, J. E. Type 1/Type 2 Immunity in Infectious Diseases. *Clinical Infectious Diseases* **32**, 76–102 (2001).
39. Li, J., Casanova, J. L. & Puel, A. Mucocutaneous IL-17 immunity in mice and humans: host defense vs. excessive inflammation. *Mucosal Immunology* **2018 11:3** **11**, 581–589 (2017).
40. Crotty, S. T Follicular Helper Cell Biology: A Decade of Discovery and Diseases. *Immunity* **50**, 1132–1148 (2019).
41. Crotty, S. A brief history of T cell help to B cells. *Nat Rev Immunol* **15**, 185–9 (2015).
42. Crotty, S. T follicular helper cell differentiation, function, and roles in disease. *Immunity* **41**, 529–42 (2014).
43. Crotty, S. Follicular helper CD4 T cells (TFH). *Annu Rev Immunol* **29**, 621–63 (2011).
44. Choi, J. & Crotty, S. Bcl6-Mediated Transcriptional Regulation of Follicular Helper T cells (TFH). *Trends Immunol* **42**, 336–349 (2021).
45. Choi, Y. S. *et al.* ICOS receptor instructs T follicular helper cell versus effector cell differentiation via induction of the transcriptional repressor Bcl6. *Immunity* **34**, 932–46 (2011).
46. Nurieva, R. I. *et al.* Bcl6 mediates the development of T follicular helper cells. *Science (1979)* **325**, 1001–1005 (2009).
47. McShane, A. N. & Malinova, D. The Ins and Outs of Antigen Uptake in B cells. *Front Immunol* **13**, 1–10 (2022).
48. Souwer, Y. *et al.* B cell receptor-mediated internalization of salmonella: a novel pathway for autonomous B cell activation and antibody production. *J Immunol* **182**, 7473–81 (2009).
49. Souwer, Y. *et al.* Selective Infection of Antigen-Specific B Lymphocytes by Salmonella Mediates Bacterial Survival and Systemic Spreading of Infection. *PLoS One* **7**, e50667 (2012).
50. Parra, D. *et al.* Pivotal advance: peritoneal cavity B-1 B cells have phagocytic and microbicidal capacities and present phagocytosed antigen to CD4+ T cells. *J Leukoc Biol* **91**, 525–36 (2012).
51. Gao, J. *et al.* Novel functions of murine B1 cells: active phagocytic and microbicidal abilities. *Eur J Immunol* **42**, 982–92 (2012).
52. Martínez-Riaño, A. *et al.* Antigen phagocytosis by B cells is required for a potent humoral response. *EMBO Rep* **19**, 1–15 (2018).
53. Bélanger, S. & Crotty, S. Dances with cytokines, featuring TFH cells, IL-21, IL-4 and B cells. *Nat Immunol* **17**, 1135–6 (2016).
54. Saito, T. *et al.* Effective collaboration between IL-4 and IL-21 on B cell activation. *Immunobiology* **213**, 545–55 (2008).
55. McGuire, H. M. *et al.* IL-21 and IL-4 Collaborate To Shape T-Dependent Antibody Responses. *The Journal of Immunology* **195**, 5123–35 (2015).
56. Merkenschlager, J. *et al.* Dynamic regulation of TFH selection during the germinal centre reaction. *Nature* 1–6 (2021) doi:10.1038/s41586-021-03187-x.
57. O'Connor, B. P. *et al.* Imprinting the fate of antigen-reactive B cells through the affinity of the B cell receptor. *J Immunol* **177**, 7723–32 (2006).

58. Paus, D. *et al.* Antigen recognition strength regulates the choice between extrafollicular plasma cell and germinal center B cell differentiation. *J Exp Med* **203**, 1081–91 (2006).
59. Glaros, V. *et al.* Limited access to antigen drives generation of early B cell memory while restraining the plasmablast response. *Immunity* **54**, 2005-2023.e10 (2021).
60. Taylor, J. J., Pape, K. A. & Jenkins, M. K. A germinal center-independent pathway generates unswitched memory B cells early in the primary response. *Journal of Experimental Medicine* **209**, 597–606 (2012).
61. Kuraoka, M. *et al.* Recall of B cell memory depends on relative locations of prime and boost immunization. *Sci Immunol* **7**, (2022).
62. van Beek, M., Nussenzweig, M. C. & Chakraborty, A. K. Two complementary features of humoral immune memory confer protection against the same or variant antigens. *Proc Natl Acad Sci U S A* **119**, 1–10 (2022).
63. Allen, C. D. C., Okada, T. & Cyster, J. G. Germinal-center organization and cellular dynamics. *Immunity* **27**, 190–202 (2007).
64. Victora, G. D. & Nussenzweig, M. C. Germinal Centers. *Annu Rev Immunol* **40**, 413–442 (2022).
65. Victora, G. D. & Nussenzweig, M. C. Germinal Centers. *Annu Rev Immunol* **30**, 429–457 (2012).
66. MacLennan, I. C. M. Germinal Centers. *Annu Rev Immunol* **12**, 117–139 (1994).
67. Wishnie, A. J., Chwat-Edelstein, T., Attaway, M. & Vuong, B. Q. BCR Affinity Influences T-B Interactions and B Cell Development in Secondary Lymphoid Organs. *Front Immunol* **12**, 703918 (2021).
68. Roco, J. A. *et al.* Class-Switch Recombination Occurs Infrequently in Germinal Centers. *Immunity* **51**, 337–350.e7 (2019).
69. Longrich, S., Basu, U., Alt, F. & Storb, U. AID in somatic hypermutation and class switch recombination. *Curr Opin Immunol* **18**, 164–174 (2006).
70. Maul, R. W. & Gearhart, P. J. AID AND SOMATIC HYPERMUTATION. *Adv Immunol* **105**, 159 (2010).
71. Beltman, J. B., Allen, C. D. C., Cyster, J. G. & de Boer, R. J. B cells within germinal centers migrate preferentially from dark to light zone. *Proc Natl Acad Sci U S A* **108**, 8755–60 (2011).
72. Bannard, O. *et al.* Germinal center centroblasts transition to a centrocyte phenotype according to a timed program and depend on the dark zone for effective selection. *Immunity* **39**, 912–24 (2013).
73. Stewart, I., Radtke, D., Phillips, B., McGowan, S. J. & Bannard, O. Germinal Center B Cells Replace Their Antigen Receptors in Dark Zones and Fail Light Zone Entry when Immunoglobulin Gene Mutations are Damaging. *Immunity* **49**, 477–489.e7 (2018).
74. Heesters, B. A. *et al.* Characterization of human FDCs reveals regulation of T cells and antigen presentation to B cells. *Journal of Experimental Medicine* **218**, (2021).
75. Reimer, D. *et al.* B Cell Speed and B-FDC Contacts in Germinal Centers Determine Plasma Cell Output via Swiprosin-1/EFhd2. *Cell Rep* **32**, 108030 (2020).
76. Arulraj, T., Binder, S. C. & Meyer-Hermann, M. Rate of Immune Complex Cycling in Follicular Dendritic Cells Determines the Extent of Protecting Antigen Integrity and Availability to Germinal Center B Cells. *The Journal of Immunology* **206**, 1436–1442 (2021).
77. Heesters, B. A. *et al.* Endocytosis and recycling of immune complexes by follicular dendritic cells enhances B cell antigen binding and activation. *Immunity* **38**, 1164–75 (2013).
78. Aydar, Y., Sukumar, S., Szakal, A. K. & Tew, J. G. The influence of immune complex-bearing follicular dendritic cells on the IgM response, Ig class switching, and production of high affinity IgG. *J Immunol* **174**, 5358–5366 (2005).
79. Weinstein, J. S. *et al.* TFH cells progressively differentiate to regulate the germinal center response. *Nat Immunol* **17**, 1197–205 (2016).
80. Papa, I. *et al.* TFH-derived dopamine accelerates productive synapses in germinal centres. *Nature* **547**, 318–323 (2017).
81. Liu, B. *et al.* Affinity-coupled CCL22 promotes positive selection in germinal centres. *Nature* **592**, 133–137 (2021).
82. Liu, D. *et al.* T-B-cell entanglement and ICOSL-driven feed-forward regulation of germinal centre reaction. *Nature* **517**, 214–8 (2015).
83. Sundling, C. *et al.* Positive selection of IgG+ over IgM+ B cells in the germinal center reaction. *Immunity* **54**, 988-1001.e5 (2021).
84. Dominguez-Sola, D. *et al.* The proto-oncogene MYC is required for selection in the germinal center and cyclic reentry. *Nat Immunol* **13**, 1083–1091 (2012).
85. Meyer-Hermann, M. *et al.* A Theory of Germinal Center B Cell Selection, Division, and Exit. *Cell Rep* **2**, 162–174 (2012).

86. Mesin, L., Ersching, J. & Victora, G. D. Germinal Center B Cell Dynamics. *Immunity* **45**, 471–482 (2016).
87. Weisel, F. J., Zuccarino-Catania, G. v., Chikina, M. & Shlomchik, M. J. A Temporal Switch in the Germinal Center Determines Differential Output of Memory B and Plasma Cells. *Immunity* **44**, 116–130 (2016).
88. Inoue, T. *et al.* Exit from germinal center to become quiescent memory B cells depends on metabolic reprogramming and provision of a survival signal. *Journal of Experimental Medicine* **218**, (2021).
89. Mesin, L. *et al.* Restricted Clonality and Limited Germinal Center Reentry Characterize Memory B Cell Reactivation by Boosting. *Cell* **180**, 92 (2020).
90. Laidlaw, B. J. & Cyster, J. G. Transcriptional regulation of memory B cell differentiation. *Nat Rev Immunol* **21**, 329–343 (2020).

Chapter 2

System-level scenarios for the elucidation of T cell-mediated germinal center B cell differentiation

Niels J. M. Versteegen^{1,2}, Victor Ubels^{3,4}, Hans V. Westerhoff^{2,5}, S. Marieke van Ham^{1,2,†} and Matteo Barberis^{2,3,4,†}

Frontiers in Immunology 12:1-19 (2021)

1. Department of Immunopathology, Sanquin Research and Landsteiner Laboratory, Amsterdam University Medical Centers, University of Amsterdam, Amsterdam, The Netherlands
2. Synthetic Systems Biology and Nuclear Organization, Swammerdam Institute for Life Sciences, University of Amsterdam, Amsterdam, The Netherlands
3. Systems Biology, School of Biosciences and Medicine, Faculty of Health and Medical Sciences, University of Surrey, Guildford, United Kingdom
4. Centre for Mathematical and Computational Biology, CMCB, University of Surrey, Guildford, United Kingdom
5. Department of Molecular Cell Physiology, VU University Amsterdam, Amsterdam, The Netherlands

† These authors contributed equally to the study as last co-authors

ABSTRACT

Germinal center (GC) reactions are vital to the correct functioning of the adaptive immune system, through formation of high affinity, class switched antibodies. GCs are transient anatomical structures in secondary lymphoid organs where specific B cells, after recognition of antigen and with T cell help, undergo class switching. Subsequently, B cells cycle between zones of proliferation and somatic hypermutation and zones where renewed antigen acquisition and T cell help allows for selection of high affinity B cells (affinity maturation). Eventually GC B cells first differentiate into long-lived memory B cells (MBC) and finally into plasma cells (PC) that partially migrate to the bone marrow to encapsulate into long-lived survival niches. The regulation of GC reactions is a highly dynamically coordinated process that occurs between various cells and molecules that change in their signals. Here, we present a system-level perspective of T cell-mediated GC B cell differentiation, presenting and discussing the experimental and computational efforts on the regulation of the GCs. We aim to integrate Systems Biology with B cell biology, to advance elucidation of the regulation of high-affinity, class switched antibody formation, thus to shed light on the delicate functioning of the adaptive immune system. Specifically, we: i) review experimental findings of internal and external factors driving various GC dynamics, such as GC initiation, maturation and GCBC fate determination; ii) draw comparisons between experimental observations and mathematical modeling investigations; and iii) discuss and reflect on current strategies of modeling efforts, to elucidate B cell behavior during the GC tract. Finally, perspectives are specifically given on to the areas where a Systems Biology approach may be useful to predict novel GCBC-T cell interaction dynamics.

INTRODUCTION

Long lasting and effective humoral immunity depends on the generation of high-affinity, class switched memory B cells (MBC) and plasma cells (PC). Their differentiation occurs in germinal centers (GC), which are specialized structures that emerge in B cell follicles within secondary lymphoid organs after encounter of T cell-dependent antigen (Ag)¹. Each mature B cell expresses a transmembrane immunoglobulin, or antibody, which is also known as the B cell receptor (BCR). Immunoglobulins are composed of a heavy and a light chain that both contain a constant and a variable region. The immunoglobulin heavy chain constant region, also referred to as isotype, is classified in five main classes – the naive isotypes IgD and IgM and the class-switched isotypes IgG, IgA and IgE. Since these isotypes have different biochemical properties, the immunoglobulin isotypes also define the functional heterogeneity of these molecules²⁻⁴. In the course of a humoral immune response, B cells adapt their isotype in a process called class-switch recombination (CSR) so as to ultimately produce immunoglobulins with the effector function most appropriate to clear the specific infection. The variable region of the BCR confers the Ag-binding site. During GC reactions, Ag-specific B cells are subject to somatic hypermutation (SHM), which induces random mutations in the Ag-recognition domains of the variable regions. This results in cells that express slightly modified BCRs and thereby exhibit an altered affinity for the target Ag^{1,5}. GC B cells (GCBCs) that acquired an increased affinity for the target Ag are positively selected through interactions with the intact Ag retained by follicular dendritic cells (FDCs), and T follicular helper cells (Tfh cells)^{6,7}. Repeated cycles of proliferation, hypermutation and repeated Ag capture and T cell-mediated selection eventually ensure formation of high-affinity B cells in the maturing GCs. The dynamic extracellular signals directing the GC cycles activate intracellular signaling networks within the specific B cells. Together with cell intrinsic properties, these signaling networks control B cell differentiation and determine whether a GCBC will resume proliferation and continue in the GC cycle or will leave the cycle in favor of terminal differentiation into either MBC or PC. Although great progress has been made in experimentally identifying the signals that steer GCBC fate determination, it remains challenging to study how the dynamic extracellular signals synergize, let alone how changes in signaling strength may affect the system. In view of the positive feedbacks in the GC cycle, and distributed control in cell signaling⁸, it is to be expected that certain minor differences in signaling could make the difference between a proper and improper functioning of cellular immune networks⁹, whereas others may be ineffective due to homeostatic mechanisms.

Elucidation of some signaling flows through this multicomponent, temporally evolving dynamic system may be possible experimentally. Strategic experimentation, designed and informed by earlier experiments and from biochemical, biophysical, cell biology and genetic knowledge, is sought. The tremendous amount of information involved then requires a systematic way of containing the information in a predictive way. Therefore, other inter-disciplinary fields of research may be of substantial help to capture the information flows within the intracellular networks in terms of integrating process activities and the regulation thereof. To address such

dynamic processes, Systems Biology is on call to investigate how cellular functionality is achieved by integrating nonlinear molecular processes, employing computational, network-based approaches and detailed experimentation^{10,11}. Although it will remain a challenge to comprehend the complex dynamics of the GC reactions considering the experimental scenarios available, integration of data coming from new, targeted experiments in an appropriated computational framework of the GCs, should enable progression to more robust and predictive understanding. Methodologies have been developed that enable to assess the relative importance of various processes and components in an intracellular network to predict network functions, as well as to assess how such processes are being regulated^{12,13}. And, with the great advance of computing, an even larger variety of computational approaches has come about. In the present paper, we will examine Systems Biology approaches that integrate the concepts of regulation and mechanistic modeling in the context of quantitative experimental data. New with respect to immunology is this comprehensive systems biology angle. New to systems biology is the focus on the immunological phenomenon of GC maturation and the integration of intracellular and extracellular signaling.

We will examine which of these Systems Biology approaches and methodologies may be used to investigate intracellular networks that determine long lasting humoral immunity. Specifically, we will focus on the networks involving Ag and Tfh factors involved in GCBC fate determination. Therefore, we will i) identify intracellular networks that play a role in GCBCs fate determination, and ii) discuss how computational methodologies that have been developed may be integrated with current and new experimental scenarios. This will enable us to weigh the relative importance of Ag and Tfh factors, and hypothesize possible mechanistic explanations of the GCBCs differentiation process. This Systems Biology modeling has already lead to the elucidation of complex interconnected, highly non-linear networks or multiple redundant networks that regulate cellular differentiation, among which that of immune cells¹⁴. In another example, this type of systems biology modelling has suggested ways out of the apparently irreversible transition from transient to chronic inflammation¹⁵. In addition, these implementations of Systems Biology concepts may suggest missing factors or connections among factors. Prediction of functional networks and their regulators may be tested by design of additional, focused experimental strategies. Through iterative rounds of computational modeling and experimentation, hypotheses about functional mechanisms involved in the GC reactions may be predicted computationally and experimentally tested.

2 THE GERMINAL CENTER REACTION

2.1 Initiation of a Germinal Center

T cell-dependent B cell differentiation in response to so called thymus dependent Ags occurs in secondary lymphoid organs (SLOs). SLOs are populated by two lymphocyte populations – the B and T cells – that are largely segregated in two distinct areas through the action of multiple chemokine-receptor axes¹⁶. Once B cells enter the secondary lymphoid organs, they migrate

towards the CXC-chemokine ligand 13 (CXCL13) that is highly abundant in the B cell follicles. Instead, upon entry, T cells are directed to the surrounding T cell zone in response to the CC-chemokine ligands 19 (CCL19) and CCL21¹⁷. The follicles within the secondary lymphoid organs mostly include mature but Ag naive B cells, and are also populated by FDCs (**Figure 1A**). FDCs are non-migratory, long-lived stromal cells that derive from a mesenchymal precursor cell, and help to maintain primary follicles as B cell exclusive niches by secreting CXCL13¹⁸. Following passive influx or active transport of complement- and/or antibody-opsonized Ag into the follicle, the non-phagocytic FDCs bind and present the native Ag up to 12 months on the surface^{19–23}. Ag-specific B cells acquire intact Ag either by itself or after Ag-binding by FDC (**Figure 1A**)^{18,24–30}. Engagement with Ag results in BCR-mediated signaling and Ag internalization. This is followed by intracellular degradation, and the generation of peptides that are presented on the B cells surface through major histocompatibility complex class II molecules (pMHCII) (**Figure 1B**). This presentation enables B:CD4⁺ T cell interactions (**Figure 1A**). Ag-engaged B and activated CD4⁺ T cells interact at the T-B border after directed localization from their separate zones. This localization is mediated through upregulation of CCR7 on the activated B cell³¹ and through upregulation of CXCR5 and downregulation of CCR7 on the dendritic cell-activated CD4⁺ T cell (**Figure 1A**)³². After cognate interaction via the pMHCII and the specific T cell receptor (TCR) on the B and T cell, respectively, the CD4⁺ T cells confers additional signals mediated through co-stimulatory molecules and cytokines that together determine the fate of the activated B cells³³. Co-stimulation through CD40 on B cells induces anti-apoptotic programs in the BCR-activated B cells and allows B cell survival and proliferation. In addition, the T cell signals may allow B cells to migrate to extrafollicular sites within the secondary lymphoid organs, where they differentiate into short-lived PCs to produce the first wave of antibodies exhibiting relatively low-affinity (**Figure 1C**)^{34,35}. Alternatively, activated B cells acquire a GC-independent early MBC phenotype and enter the circulation (**Figure 1C**)^{36–38}. Finally, a limited number of B cells migrates back to the center of the B cell follicle after downregulation of CCR7 to start the GC reaction (**Figure 1C**)^{1,5,39,40}. For these B cells, the CSR inducing them into IgG B cells was recently found to already be initiated during the initial B:T cell interaction prior to GC entry⁴¹. Interestingly, whereas many individual naive B cells only produce one type of early effector cell, including short-lived plasma cells, GCBC and GC-independent MBCs, others were found to be able to take part in the various differentiation processes after initial B:T contact⁴². This suggests that both internal stochastic and externally regulated processes facilitate activated B cell fate determination.

2.2 Maturation of the Germinal Center

It is estimated for certain Ags that three fully activated Ag-specific B cells clones reach the center of the follicle and start to proliferate (**Figure 1C**). The cell cycle time of GCBCs is estimated to be approximately 6-12 hours, making these cells rank amongst the fastest dividing mammalian cells^{43,44}. Dividing GCBCs exhibit downregulated expression of the BCR, through which they

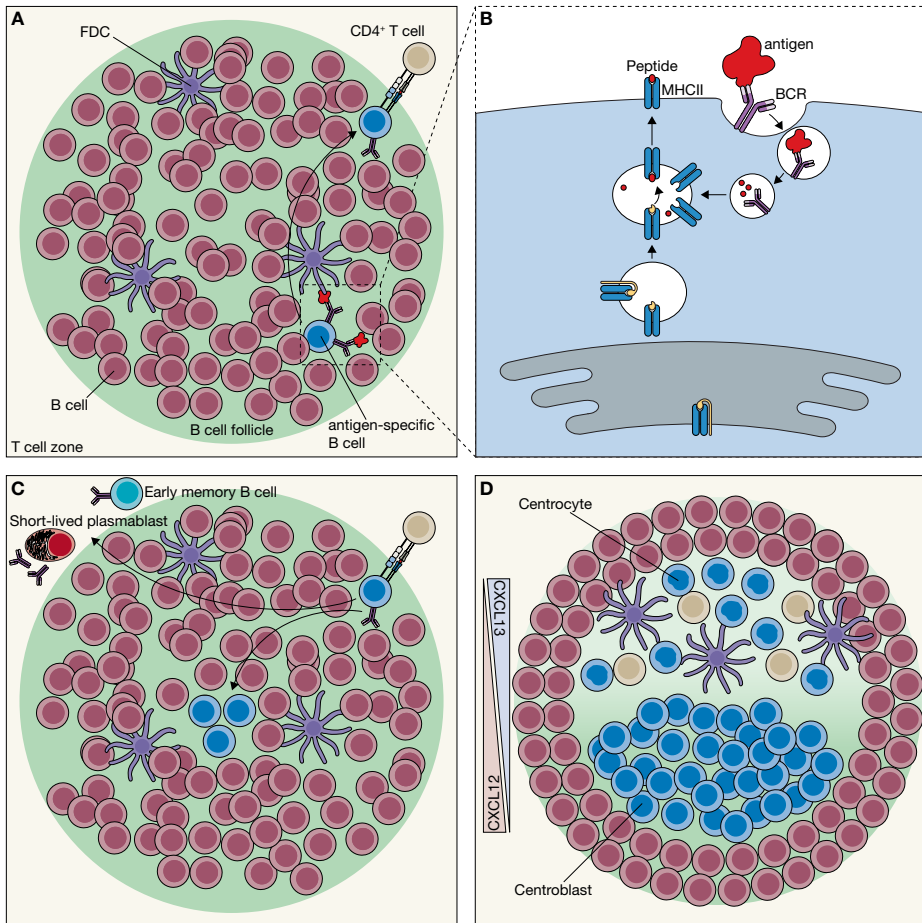


Figure 1 | Initiation of the germinal center (GC) network. (A) In the secondary lymphoid organs, B cells are located in the B cell follicle. Follicular B cells engage with an Antigen (Ag) via their B cell receptor (BCR). Most Ag in the follicle is presented by follicular dendritic cells (FDCs), which retain the Ag for extended periods. Ag engagement partly activates the follicular B cells; however, to become fully activated, it requires interaction with a CD4⁺ T cells. Ag-engaged follicular B cells localize to the border of the follicle to encounter CD4⁺ T cells with the same Ag specificity. (B) To interact with the CD4⁺ T cells, the B cell needs to present Ag-derived peptide fragments through the major histocompatibility complex class II (MHCII). Thereto, Ag engagement results in BCR-mediated endocytosis, followed by Ag degradation and presentation of resulting peptide fragments through MHCII. (C) At the border of the follicle, CD4⁺ T cells screen many Ag-specific B cells to find the B cell with the same Ag specificity. At the time the CD4⁺ T cell encounters a follicular B cell with a corresponding Ag specificity, it provides the B cell with help that in turn results in the differentiation towards either short-lived plasmablasts, early memory B cells or GC precursor B cells. GC precursor B cells migrate towards the center of the follicle and starts hyperproliferation. (D) Hyperproliferation drives the formation of the mantle zone, which contains non-activated B cells. As the GC expands the chemokine gradient, mediated by CXCL12 and CXCL13, GC differentiation occurs into two phenotypically distinct zones, the dark zone (DZ) and the light zone (LZ). The CXCL12⁺ DZ is almost entirely populated by hyperproliferating centroblasts, whereas the CXCL13⁺ LZ contains FDCs, T follicular helper (T_{fh}) cells and centrocytes.

are unreceptive to Ag during proliferation⁴⁵. The resident non-activated B cells that encircle the hyperproliferating GCBCs are pushed aside to form a mantle that surround the GC (**Figure 1D**)^{1,46}. After initiation of an early GC, GCBCs continue to clonally expand in the absence of mutations to reach a population size of about 1,500 B cells around day 7⁴⁶. Around the same time the GC start to polarize into two distinct zones, the dark zone (DZ) and the light zone (LZ), which were named as such based on their appearance using light microscopic analysis (**Figure 1D and Figure 2**)^{47,48}. The DZ is almost completely populated by clonally expanding densely packed GCBCs that have a high nucleus-to-cytoplasm ratio, which gives this zone its “dark” appearance (**Figure 1D and Figure 2**). The GCBCs in the LZ are surrounded by FDCs and Tfh cells, through which this zone appears to be “lighter” (**Figure 1D and Figure 2**)⁵. Hyperproliferating GCBCs, also called centroblasts (CBs), express the chemokine receptor CXCR4, which directs the migration towards the CXCL12-secreting reticular cells in the DZ (**Figure 1D and Figure 2**)^{49,50}. The importance of CXCR4 in GC organization was shown in CXCR4-deficient mice, which exhibited disrupted GC polarization compared to wild type, as shown by the exclusion of CBs from the DZ⁴⁹.

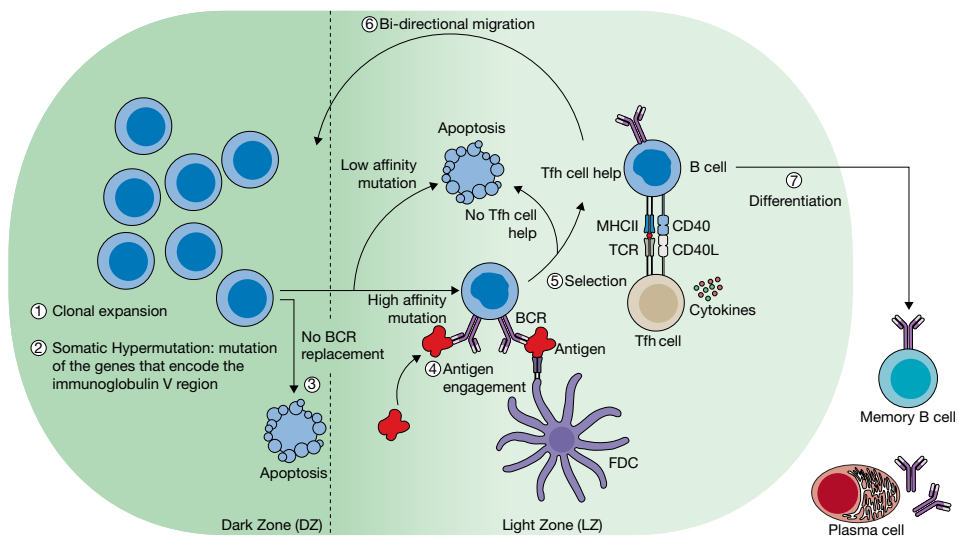


Figure 2 | The germinal center (GC) reactions. In the dark zone (DZ) of the GC, B cells undergo clonal expansion (1), which is accompanied by spontaneous point mutations in the gene that encodes for the variable domain of the B cell receptor (BCR) (2). GC B cells (GCBCs) with mutations that compromise BCR expression are removed through apoptosis (3). GCBCs with functional BCRs test the potentially altered affinity in the GC LZ through interactions with the antigen (4) and Tfh cells, which provide CD40L and cytokines (5). GCBCs that obtained a higher affinity BCR are expected to outcompete those with weaker affinity as a result of these interactions (4 and 5). Ultimately, positively selected B cells are the only ones to survive and either re-circulate to the DZ (6) or differentiate into either memory B cells (MBCs) or plasma cells (PCs) (7).

GCBCs in the DZ are subject to the activity of activation-induced cytidine deaminase (AID), an intracellular enzyme that mediates the introduction of random mutations (somatic hypermutation or SHM) in the Ag-binding domains (i.e. complementarity determining regions) of the BCR (and later secreted antibodies) (**Figure 2**)^{46,51,52}. As GCBCs downregulate expression of their initial BCR prior to SHM, these reactions yield Ag-specific B cells with altered affinities for their Ag⁵³. CBs that acquired damaging mutations – mostly mutations that induce a frameshift or a stop codon – and fail to replace surface BCR are removed by apoptosis in the DZ (**Figure 2**)^{53,54}. The CBs that post-SHM efficiently replace the BCR migrate to the LZ (**Figure 2**).

Migration to the LZ is initiated when CBs lose CXCR4 expression, which shifts the balance of chemokine receptor responsiveness in favor of CXCR5. It has been implied that this shift is regulated by a cell intrinsic “timer” or “counter” that controls the cellular localization of GCBCs⁵⁰. As a result of the shift in chemokine receptor responsiveness, CBs migrate towards the CXCR5 ligand, CXCL13, which is secreted by FDCs in the LZ (**Figure 1D**)²¹. The now non-proliferating LZ GCBCs, or centrocytes (CC), are then subject to the selective pressure of Ag and Tfh cell help. CC that successfully maintained or enhanced their affinity in the GC DZ acquire Ag and are selected after cognate help from Tfh cells (**Figure 2**)^{1,45}. Unless Ag is still present in excess, the CBs with lower Ag affinity will lose the competition with the cells with high affinity and succumb to apoptosis because they are not selected for survival. A CC that is selected for survival will either continue in the GC cycle and resume proliferation or will terminally differentiate into MBC or PC, which is regulated by the dynamic extracellular signals provided by antigen and Tfh cell interactions (**Figure 2; see below for details**). Alternating rounds of positive selection of high-affinity variants will progressively outcompete the CCs with low Ag affinity (**Figure 2**)⁵⁴. Eventually this process, coined affinity maturation, yields an Ag-specific B cell population with high affinity BCRs^{43,44,54,55}, unless Ag remains present in excess.

Systems Biology principles may be expected to be relevant here for proposing hypotheses. First, a multitude of processes determines the outcome of CCs with high affinity receptors producing high affinity antibodies. Suspecting analogies with other complex networks, it is unlikely that any single one of the factors involved is the rate limiting step for the production of B cells. It is more likely that many factors will control the process simultaneously and that, depending on the Ag load, different factors will be more in control. Second, with respect to the ultimate affinity of the antibodies, it may be expected that some factors will exert either an activatory or inhibitory effect. Third, there will be a difference depending on whether antigenic determinants are offered on a single macromolecular (or cellular) structure. In case they are offered on the same structure, high affinity antibodies should be developed only against one of the antigenic determinants, whilst if they are offered on separate structures, they should be developed against all. This should be relevant if the infectious agent is able to mutate its antigens. Fourth, since proteins are the ultimately functional molecules, the control of their effectiveness should be expected to reside as much at the level of transcription as at the level of post-translational processing.

3 GCBC SELECTION: RECYCLING VS. DIFFERENTIATION

3.1 Modeling the GCBC recycling process

Systems Biology helps to integrate information of different types in order to understand biological function. This does not imply that such activities were not already undertaken before Systems Biology took off as a discipline. In 1993 already Kepler and Perelson asked whether the proposed development of high affinity through mutation and selection in a single maturation step of B cells was consistent with established mutation rates. Their computational calculation determined that GCBCs should require a higher than physiologic mutation frequency during SHM if the affinities seen *in vivo* should be achieved through a single burst of mutations in the DZ⁵⁶. It was therefore suggested that, after LZ migration, GCBC should re-enter the GC DZ for further rounds of proliferation and SHM. Again typical for Systems Biology, the testing of this prediction required the development of a new experimentally methodology that allowed a prolonged tracking of GCBCs *in vivo*^{57,58}. Indeed, the emergence of two-photon microscopic imaging that allows the prolonged imaging of GCBCs *in vivo* was required to confirm that GCBCs re-enter in a proliferative state for further rounds of SHM⁵⁵.

However, although early computational predictions of the recycling probability of CCs indicated a recycling rate between 70-85%⁵⁹, recent mathematical and experimental investigations revealed that this value had been overestimated and in reality lies between 25-30%^{55,60}. The period during which CCs are recycled was mathematically predicted to last for no less than 42 hours, but not to exceed the 55-hour mark. During this time, all selected CCs were recycled at a variable rate and re-entered the phase of proliferation⁵⁹. High-affinity clones experienced a significantly lower recycling probability and a higher early GC exclusion rate as compared to their low-affinity counterparts^{59,61}. A mathematical model has been proposed where positively selected GCBCs localize to the DZ as they retain the Ag-derived peptides, which distributed asymmetrically during division between the two daughter cells. Based on this model, the daughter cell that acquired the Ag-derived peptide complexes differentiates to PCs and leaves the GC, whereas its sister GCBC, which did not acquire Ag, proliferates and localizes to the LZ⁶⁰. This computational prediction that early emigration of high-affinity GCBCs is a deterministic process, beneficial for affinity maturation and the early immune response, is in contrast to the earlier hypotheses that deemed this process to be of a stochastic nature⁶². But of course, stochastic is nothing but determinism by unidentified dynamic factors.

Numerous selection methods enabling GCBCs to re-enter or not the proliferative state have been propose by computer modeling throughout the past three decades, and almost as many have since been discarded by the scientific community as they are unable to reproduce experimentally verified aspects regarding general GC properties^{45,63,64}, efficiency of affinity maturation⁶⁵, robustness in FDC Ag-presenting site numbers^{66,67}, or output of high affinity GCBCs⁶⁸. Therefore, only the hypotheses that are still currently pursued are presented in this section.

First, stochastic modeling of GCBC DZ re-entry suggests that a single first survival signal – where CC selection is determined by the binding strength of the BCR to Ag provided by FDCs – suffices to reproduce the rate of affinity maturation that it resembles an *in vivo* environment (**Figure 3A**)⁶⁹. In this scenario, the number of FDC sites on which Ag is presented is the limiting factor, as the variety of clones would compete for Ag binding for their survival and GCBC DZ re-entry. It is possible to envision that both Tfh and FDC interaction with GCBCs may induce forkhead box O1 (FOXO1) expression. As activation of the FOXO1–CXCR4 pathway leads to GCBC DZ re-entry and not apoptosis, this activation may be considered a pro-survival signal. Therefore, GCBC DZ re-entry can conceivably be primarily instigated not only by Ag interaction with FDCs, as previously thought^{70,71}.

Second, an alternative method implements an increase in the refraction rate between CCs and FDCs (**Figure 3B**)^{72,73}. In this hypothesis, a theoretical mechanism that occurs as a consequence of IgM-independent interactions between CCs and FDCs is introduced, where GCBCs that fail to bind to an FDC survive for a ‘refractory’ period of time after which they have an opportunity to bind to the FDC again. This hypothesis is based on early experimental findings that LFA-1/ICAM-1 and VLA-4/VCAM-1 mediate adhesion of GCBCs to FDCs⁷⁴. However, a recent discovery showed that Ags displayed on FDCs do not remain membrane bound permanently⁷⁵, but are instead rapidly internalized whilst remaining intact within a nondegradative compartment, and are then cycled back to the FDC membrane surface as intact antigens where they are able to select Ag-specific GCBCs^{23,75}. As such, it may be envisioned that this process is the biological equivalent to the refractory period introduced *in silico*, with the specific time frame being the signal for apoptosis^{72,73}. The phenomenon should enable FDC and CC to dissociate from one other after selection of the latter and to enable the latter to move away and make way for another, not yet assessed, GCBC. By limiting the total number of encounters between CC and FDC, higher-affinity clones will be favored, as their binding occurs at an earlier time as a consequence of the continued selection pressure⁷².

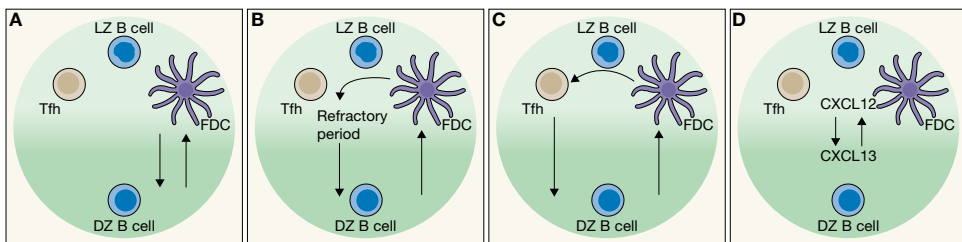


Figure 3 | Models of Germinal Center B cell (GCBC) recycling between the light (LZ) and the dark zone (DZ). (A) Centrocyte (CC) selection through binding strength of the BCR to an antigen provided by follicular dendritic cells (FDCs). CC then migrates to the DZ and become centroblast (CB). Black arrows indicate the GCBC migration. (B) Increase in the refraction rate between CCs and FDCs. (C) Verification step, where CCs are selected by Tfh cells after a first selection by FDCs. (D) Spontaneous oscillations of GCBC between CXCL12 (representing the LZ) and CXCL13 (representing the DZ).

Third, various models involve a validation by Tfh cells to ensure CC recycling to the DZ (**Figure 3C**). Initially, GCBCs must be selected by Ag retained by FDCs before a secondary interaction with Tfh cells would occur^{72,76,77}. As T cells constitute only the 5-10% of the GC cell population, this interaction may be highly competitive^{60,78}. The interaction time between GCBC:Tfh cells correlate positively with DZ re-entry and the number of divisions^{55,79}. The validation may even constitute a further selection: the Tfh cells are able to bind multiple CCs simultaneously, whereas only a single CC is polarized, i.e. the one with the highest binding affinity⁸⁰. Here the principle would be that dual consecutive selection (multiplying the probabilities) is more restrictive than additive selection. Furthermore, mathematical analyses predict that upon binding to the Tfh cell a high pMHCII density is vital to the GCBC divisions so that high MHC density on the membranes of the GCBC induces cell division whilst reducing the frequency of subsequent mutation⁶⁰. This suggests that GCBCs enter the S phase of the cell cycle when entering the LZ, but must reach the DZ prior to their entry into the G2/M phase⁶⁰. The mathematical models implement an additional control of CC and Tfh cells interaction, by introducing a predefined thresholds of minimal and maximal survival time that when exceeded induce apoptosis⁷². Affinity maturation in these models is strongest when Tfh cell count is minimal and can rescue a given Ag-presenting CC more specifically as compared to a larger subgroup of Tfh cells⁷²; multiple Tfh cells should increase the probability of GCBCs with other than the highest affinity to survive and be selected. This finding is in line with an *in vivo* scenario where Tfh cells recognize only a small set of Ag epitopes as opposed to being susceptible to a broad range of Ag presentation⁸⁰. This methodology allows for the highest affinity maturation where 60-70% of all output cells have a high affinity. Furthermore, methodologies that rely on T cell help can be robust to large variations in Ag availability in the event that Ag acquisition and FDCs interaction is uncompetitive⁷². This method has been tested both phenomenologically and including the impact of spatial cell distribution. Mathematical models that included the impact of spatial cell distribution did not find experimentally uncertain parameters that would change qualitative results⁷². The model has been experimentally validated, but the results do not exclude other mechanisms^{40,55}.

Finally, chemokine-driven receptor down-regulation is investigated as a potential alternative GCBC recycling mechanism, through a small sub-division of germinal center models (**Figure 3D**)⁸¹. Gaussian distributions in which CXCL12 represent the LZ and CXCL13 the DZ is used to establish a simple chemokine field. The robust oscillatory behavior is observed especially when CXCR4 and CXCR5 receptors are reciprocally regulated⁸¹, with a periodicity resembling the experimental observations. However, no indication is given about the extent to which such a mechanism contributes to GCBC recycling.

From the Systems Biology perspective, it is likely that various mechanisms play a role depending on the selection process of the antibodies. The fitness value of only generating antibodies with the highest affinity is limited, as it will take more time on average to reach the highest possible affinity and individual cells of the population may not have the ability to generate very high

affinity antibodies. In some conditions it may then be better to develop antibodies with lower specificity more quickly, especially if the target is a rapidly expanding pathogen. The occurrence of both IgM and IgG supports this consideration that biological fitness is served by a hierarchy of mechanisms that differ in both temporal and spatial acuteness. The ability of some antigens to evolve (or be selected) rapidly within the infected individual would call for fast and less specific antibodies, and then only produced in a short period, thereby accepting cross reactivity with 'self'. Dealing with tumor antigens, that are closer to 'self' would then require more selective and high affinity antibodies. This possibility may be relevant in the context of disease, where the frequency of tumor infiltrating B cells in the tumor microenvironment or in the tertiary lymphoid structures (TLS) is related to a positive outcome against cancer aggressiveness⁸²⁻⁸⁶. And then there is the cost of the system, which is much higher for the multi-stage process leading to the antibodies with highest affinity. More diversified studies are needed that take into consideration this variegated function of the immune system.

3.2 Effector B cells arise from Germinal Centers

In addition to engaging in Tfh cell-mediated selection for further rounds of DZ proliferation and BCR/antibody diversification, GCBCs differentiate into either long-living MBCs or, eventually, antibody-secreting cells^{44,55,87,88}. Two distinct categories of PCs can be found in the antibody-secreting cell compartment: short-lived proliferating PCs/plasmablast and non-proliferating PCs, which encapsulate into survival niches in the bone marrow where they can persist for decades to produce isotype-switched high-affinity antibodies^{89,90}. In contrast, MBCs recirculate through the blood and the lymphoid organs and may provide a rapid response upon recognition of the same Ag⁹¹⁻⁹⁴. Human peripheral blood primarily contains distinct GC-dependent MBC populations, mostly of the unswitched IgM⁺ and the switched IgG⁺ MBCs^{38,95,96}. Similar to humans, immunization with a T cell-dependent Ag results in development of unswitched and switched MBCs in mice^{97,98}. Upon re-recognition of the same Ag, switched MBCs differentiate into PCs, whereas unswitched MBCs induce proliferation and re-enter into a germinal center reaction^{97,98}.

The MBC and PC output from a GC is determined by a temporal switch⁹⁹. Effector cells are generated in a sequential order, starting with unswitched MBCs, followed by switched MBCs and then by a delayed appearance of long-lived PCs. Differentiation into the MBC or PC compartment was shown to be linked to the Ag affinity of the BCR, where GCBCs with high affinity end up in the PC compartment and GC-derived MBCs are generally of lower affinity, where switched MBCs have a higher mutation load as compared to the unswitched MBCs^{68,95,96,100}. Notably, GCBCs that receive signals in the LZ to undergo PC differentiation, first migrate back into the DZ to transit out of the GC via the DZ:T zone boundary^{7,60,101}. In contrast, MBCs leave the GC directly from the LZ. This suggests that the signals GCBCs receive to become PCs may resemble those that retain them in the GC.

Although the combined effort of computational prediction and experimental validation has

been shown to be of substantial use to elucidate the GC reaction, the dynamic regulation that determines terminal GCBC fate determination remains to be elucidated. To model GCBC fate determination, the different stages that LZ CCs endure should be defined. *In vitro* data suggests B cell fate to be determined stochastically with probabilities arrived from an as of yet unclear signaling pathway, independently from cell-cell contact or asymmetric division¹⁰². With the recent discovery that B cells divide asymmetrically three out of four times¹⁰³, this hypothesis becomes more appealing¹⁰⁴.

From the Systems Biology perspective, at ambient temperatures all actual processes are inherently stochastic. It is the relative magnitude of the dispersion and the nonlinearities of the processes involved that make this consequential. Because cell numbers (both FDC and Tfh) around the CCs are likely to be just a few at any point in time, and the cell proliferation processes are exponential and occur in bursts, if only due to the similarity of GC cycling time and cell cycle times at any point in space and time, the selection-process rates may readily vary by up to 100%, indeed predicting stochasticity to be actual. Fate determination starts with an extracellular signal, which is recognized and transmitted in the cell as a result of ligand-receptor interaction and subsequent intracellular signal transduction. For GCBCs, these extracellular signals are provided by Ag and Tfh cells. To understand how the integrated signals through these extracellular signals facilitate GC fate determination, insight into the transcriptional profiles corresponding to the three different fates – re-circulation to the DZ and differentiation into either MBC or PC – is relevant in order to identify and weight the interactions involved.

4 TRANSCRIPTION FACTOR NETWORK REGULATING GCBC FATE DETERMINATION

GC initiation, continuation and GCBC fate determination are regulated by a large signal transduction network (see **Figure 5 below**). The transduced signals regulate cell behavior, leading to the formation of cell phenotypes (identities) which serve dedicated functions (**Figure 4A**). The large network involves a complex and interconnected transcriptional network (**Figure 4B**). Follicular B cells express four transcription factors that put in place the signal transduction network responsible for their phenotype: paired box protein 5 (PAX5), BTB and CNC homologue 2 (BACH2), SPI-1 (also known as PU.1) and interferon-regulator factor 8 (IRF8). The latter two factors execute their function as heterodimer¹⁰⁵. PAX5 has been presented as the marker of B cell identity and positively regulates expression of BACH2, through which both factors are co-expressed throughout almost all mature B cell stages¹⁰⁶.

To differentiate into GCBC, naive B cells need to acquire expression of B cell lymphoma 6 (BCL6)¹⁰⁷. Upon activation, B cells start to express low levels of the transcription factor IRF4, which promotes GC fate through activation of BCL6 and PAX5^{89,108,109} (**Figure 4B**). PAX5 activates the IRF8 and PU.1 complex, which regulates GCBC development through the induction of BCL6 expression. The GCBC phenotype is preserved through transcriptional inhibition of the master regulator of PC differentiation, the B lymphocyte-induced maturation protein 1

(BLIMP1; also known as PRDM1) by BCL6¹¹⁰. To undergo further rounds of proliferation and SHM, the transcriptional profile of positively selected LZ GCBCs probably should not shift significantly from the GC profile stated above. Nevertheless, recent studies demonstrated that GC re-entry requires expression of MYC^{111,112}, a cell cycle regulator that is transcriptionally suppressed by BCL6^{113,114}. Further analyses on the MYC-expressing GCBCs indicated that IRF4 expression was induced in these cells^{111,112}. High levels of IRF4 transcriptionally suppress BCL6, whereas low levels could transcriptionally induce BCL6⁸⁹, suggesting that expression of IRF4 may be sufficiently high to repress BCL6 and to allow expression of MYC required for GC DZ re-enter (Figure 4B). Since BLIMP1 determines PC fate, and repression of MYC is required but not sufficient for terminal differentiation, these data indicate that MYC may determine whether a GCBC re-enters the GC or starts terminal PC-differentiation.

Terminal differentiation into the PC fate starts with the upregulation of IRF4. In addition to its inhibitory effect on BCL6, high levels of IRF4 induce BLIMP1, which itself represses

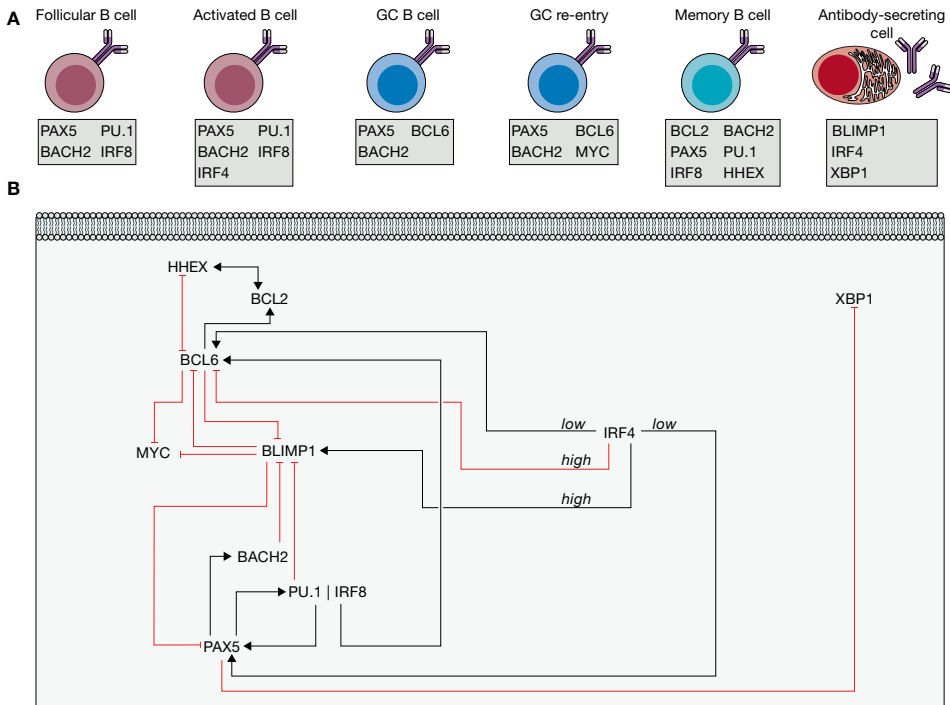


Figure 4 | Transcriptional control of the germinal center (GC) and differentiation. (A) Transcriptional profile of follicular B cells, activated follicular B cells, GC B cells, GC B cells that re-enter into the GC reaction, high-affinity memory B cells (MBCs) and antibody secreting plasma B cells in terms of their phenotype-specific marker genes. **(B)** Transcriptional regulation of GC continuation and differentiation. Activations (black lines with an arrow head) and inhibitions (red lines with a flattened head) among genes and some proteins are shown. Relevant ones are: BTB and CNC homologue 2 (BACH2), B cell lymphoma 2 (BCL2), BCL6, B lymphocyte-induced maturation protein-1 (BLIMP1), Haematopoietically-expressed homeobox (HHEX), interferon-regulator factor 4 (IRF4), IRF8, Paired box protein 5 (PAX5) and X-box-binding protein 1 (XBP1) (see text for details).

transcription of PAX5 and BCL6⁸⁹. Furthermore, PCs express high levels of X-box-binding protein 1 (XBP1). XBP1 is an important regulator of immunoglobulin secretion, activated by BLIMP1¹¹⁵ and suppressed by PAX5^{89,116–118}. In summary, a network involving high expression of IRF4, its repression of BCL6 and therewith activations of BLIMP1 and MYC is crucial for transition from GCBC into PC.

The identification of the transcriptional program of MBCs is less apparent than for the GCBC and the PC. As compared to activated B cells, MBC exhibit enhanced expression of the pro-survival factor BCL2^{119,120}. To enable BCL2 expression, cells would need to extinguish BCL6 expression, since BCL6 suppresses BCL2¹²¹. Indeed, loss of BCL6 was shown to be the main driver of a pre-MBC transcriptional program and required for formation of human MBCs *in vitro*^{122,123}. Recently, haematopoietically expressed homeobox (HHEX) was identified as a transcription factor regulating MBC differentiation through participation in downregulation of BCL6¹²⁴. Similarly to GCBCs, MBCs show co-expression of PAX5 and BACH2, but also express PU.1–IRF8^{89,125}. Since the transcription factor complex PU.1–IRF8 negatively regulates PC differentiation, it is suggested that this complex may facilitate MBC formation^{89,126}. However, no direct evidence supports this suggestion. Altogether, the aforementioned differences between the transcriptional profile facilitated by an Ag-mediated interaction and selection by Tfh cells are determinants of GCBC fate determination.

From the Systems Biology perspective, the signal transduction network (see **Figure 5 below**) and its transcriptional sub-network involved (**Figure 4B**) are not just manifold but also complex. For example, BLIMP1 represses PAX5 which induces PU.1–IRF8 and thereby suppresses BLIMP1. This is just one example of the many instances of circular causation in the network: a factor may cause itself and thereby be its own effect. Moreover, BACH2 is both a cause and an effect of PAX5, just as much as PAX5 is both an effect and a cause of BACH2. In such cases, the analysis of changes in expression levels with variation in extracellular signaling or differentiation type, may lead to correlations that do not contain sufficient information to infer the complex cause-effect patterns within the complex network. To approach these issues, the network needs to be analyzed as a function of time after inducing well-defined perturbations within the network, bringing the results of the perturbations together in a single quantitative model of the network. Binary perturbations of the network, such as by homozygous knock out mutations are likely to invoke equally strong homeostatic responses of the biology around the network and thereby change network make-up unrecognizably. Such experiments should therefore be accompanied by verification that the structure of the network, i.e. the identity of the cell type, is not destroyed.

5 REGULATION OF GCBC SELECTION

5.1 Antigen-mediated receptor stimulation

Following proliferation in the DZ and their localization to the LZ, the first signal that GCBCs receive is mediated by cross-linking of the re-expressed BCR by Ag. The different BCR-mediated

processes – including Ag capture, peptide presentation efficiency and BCR signaling – should be included as a functional module within the comprehensive model of GCBC fate determination. There has been intense debate whether Ag-mediated BCR signaling directly mediates positive selection and differentiation of B cells or whether Ag-binding is just needed to progress to pMHCII expression and attract Tfh cell help and that only the latter controls B cell differentiation^{68,100}. Ag capture is affected by the Ag concentration and the BCRs affinity. If the Ag concentration is too low, Ag-derived peptides are not presented by the GCBC and, consequently, will not receive help from Tfh cells; thus, the GCBCs initiate apoptosis and the GC collapses¹²⁷. In contrast, if the Ag concentration is too high, low affinity GCBCs will also be competent to be selected^{127,128}. Also, GCBCs regulate their own fate through an antibody-mediated feedback mechanism. The high-affinity antibodies secreted by the PCs generated during the GC reaction are able to block target Ag bound to the FDCs¹²⁹. As such, non-differentiated GCBCs with the same specificity are not able to capture and present the specific Ag through which the epitope specific reaction is terminated. An Ag either freely migrates through the GC or associates with FDCs, which have diverse expression of receptors that hold the Ag⁷⁵. The specific binding epitope on the Ag is either not recognized or already bound by a GCBC that previously localized to the LZ. Therefore, the ability to capture a specific Ag is dependent on both the Ag concentration and the competition for binding by other GCBCs. The affinity threshold of B cell activation has a K_A of ca. $10^6 - 10^{10} \text{ M}^{-1}$ in the case of Ag bound to a membrane¹³⁰. In addition to the affinity for Ag, the overall B cell activation is affected by the BCR density. The combined functions of Ag affinity and BCR density is better known as Ag avidity.

Canonically, BCR stimulation above the avidity threshold results in the formation of an immunological synapse (maybe explain), which facilitates Ag processing and presentation¹³¹. This synapse consists of BCR/Ag-FDC connection and associated protein micro-clusters, such as CD19 and LFA-1/ICAM-1 complexes^{132,133}. Many assumptions regarding B cell synapse formation derive from extensive studies of the T helper cell synapse formation. However, differences can be observed regarding receptor densities, ligand affinities, mechanical characteristics, and extracellular length of receptor-ligand complexes. Contrarily to T helper cell synapse formation, the B cell synapse can still be formed when both the BCR and active transport processes are impaired and Ag acquisition is compromised due to undirected diffusion of synapse zone accumulating proteins¹³⁴. As such, any BCR modeling must contain a basal activation rate of the B cell synapse formation independent of Ag recognition¹³⁴. Stochastic Monte Carlo-based computational models have elucidated that, in addition to BCR/Ag driving protein micro-cluster formation, a progression in the affinity of LFA-1 may be necessary to induce synapse formation under membrane deformation circumstances¹³⁵. This implies that upon the binding of the BCR to Ag, signaling cascades should be initiated that direct LFA-1 to assume a conformation with a higher affinity binding for ICAM-1¹³⁵. However, when BCR affinity exceeds a K_A value of 10^8 M^{-1} , this shift in LFA-1 affinity no longer suffices to induce synapse formation, indicating that still unknown synapse formation mechanisms must exist for

high BCR affinity and membrane deformation¹³⁵. The LFA-1 conformation change should lead to membrane deformation accommodating BCR/Ag complexes at their equilibrium bond length and, subsequently, the B cell synapse¹³⁵. This should then allow for synapse formation across the range of physiological BCR affinities.

Furthermore, detailed modeling efforts show that relocation of BCR/Ag complexes to the B synapse is likely facilitated by cytoskeleton-mediated transport¹³⁶. Mathematical models show that directed transport of BCR/Ag complexes to the center of the synapse is capable of forming canonical synapse patterns should mechanisms based on differences in bond properties between the B cell synapse protein complexes fail to do so¹³⁶. Cytoskeletal-mediated transport of B synapse formation contradicts with the mechanism of T cells' synapse formation. In T cells, the difference in the equilibrium bond length of TCR/MHCII and LFA-1/ICAM-1 is sufficient to induce segregation in the immunological synapse pattern^{137,138}. Whether this bond length difference-mediated synapse formation can be accomplished solely by diffusion or relies

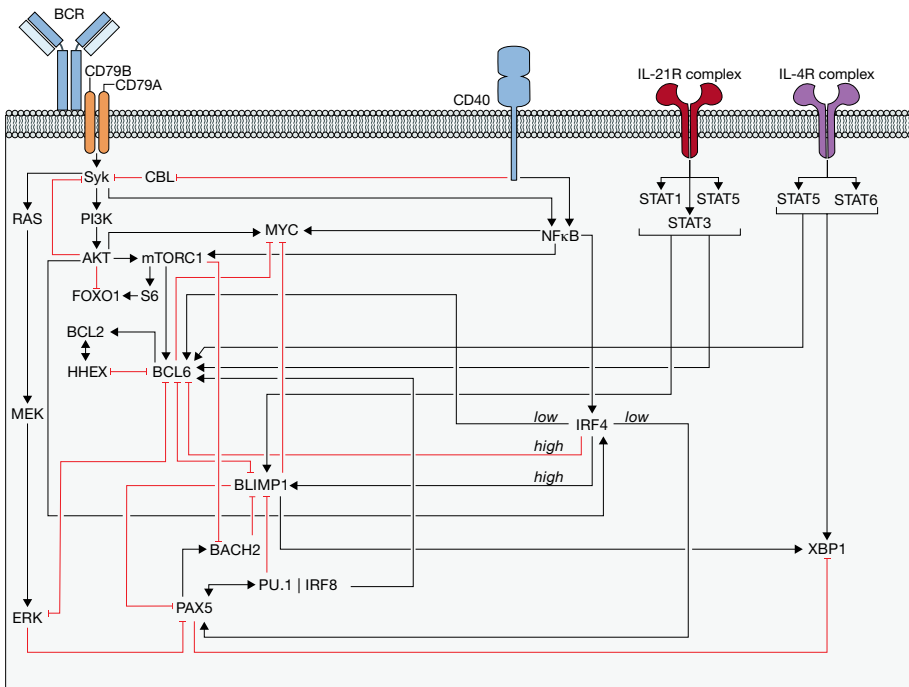


Figure 5 | Control of the germinal center (GC) and differentiation mediated through receptor stimulation. The regulation of GC continuation and differentiation mediated through the different receptors-mediated signal transductions is shown. Activations (black lines with an arrow head) and inhibitions (red lines with a flattened head) among genes and some proteins are shown. Relevant ones are: BTB and CNC homologue 2 (BACH2), B cell lymphoma 2 (BCL2), BCL6, B cell receptor (BCR), B lymphocyte-induced maturation protein-1 (BLIMP1), cluster of differentiation 40 (CD40), Extracellular signal-regulated kinases (ERK), Forkhead box protein O1 (FOXO1), Haematopoietically-expressed homeobox (HHEX), Interleukins 4 receptor (IL-4R), IL-21R, Interferon-regulator factor 4 (IRF4), IRF8, mammalian target of rapamycin complex 1 (mTORC1), Paired box protein 5 (PAX5), Phosphoinositide 3-kinases (PI3K), signal transducer and activator of transcription (STAT) and X-box-binding protein 1 (XBP1) (see text for details).

on activate transport of receptors remains unclear¹³⁵. Regardless, as the equilibrium bond length is identical between BCR/Ag and LFA-1/ICAM-1, in the B cell spontaneous segregation into the synapse formation is unlikely to occur^{136,139}.

Canonically, BCRs are cross-linked with Ags during the synapse formation, facilitating BCR-mediated signaling¹³². Indeed, selected CCs exhibit active BCR receptor signaling. However, in these cells, the signaling is markedly reduced as compared to activated B cells¹⁴⁰. Attenuated proximal BCR signaling is mediated by hyper-activated phosphatases^{141,142} and high expression of the E3 ubiquitin ligase Casitas B-lineage lymphoma (CBL), which, among others, tags a mediator of BCR signaling, Syk, for degradation through its ubiquitylation (**Figure 5**)^{143,144}. BCR ligation in GCBC results in a transient activation of Syk that rapidly decays¹⁴⁵. The rapid pulse of pSyk induces activation of the phosphoinositide 3-kinase (PI3K)-AKT pathway, which creates multiple negative feedback loops and dampens proximal BCR signaling in GCBC (**Figure 5**)¹⁴². Nevertheless, transient phosphorylation of AKT allows for an efficient inactivation of FOXO1¹⁴⁵, which controls GCBC proliferation and, by controlling the expression of CXCR4, allows DZ localization¹⁴⁶⁻¹⁴⁸. Considering that BCR signaling is directly linked to FOXO1 degradation, these data together indicate that DZ re-entry requires only limited BCR ligation to allow FOXO1 activity.

The cross-linking of the BCR increases the rate of internalization, whereas the intracellular trafficking to the MHCII loading compartments is not affected by the cross-link¹⁴⁹. It was observed that the Ag presentation efficiency of B cells is dependent on the affinity of B cells for the Ag¹⁵⁰. An Ag that binds the BCR with high affinity remains associated during the trafficking to the MHCII loading compartment, through which peptide presentation by high affinity GCBCs is more efficient as compared to low affinity GCBCs. As such, high affinity GCBCs internalize and present more pMHCII. The density of peptide presentation potentiates the recognition of the GCBCs by Tfh cells with the same Ag specificity. pMHCII can vary in length from 11-30 amino acids in length¹⁵¹. The internalized Ag is degraded intracellularly into a large number of possible peptides that may be loaded in the peptide binding pocket of MHCII and subsequently presented. Peptides with the highest binding affinity for the given MHCII allele will be preferentially expressed due to the peptide editing actions of HLA-DM and HLA-DO¹⁵²⁻¹⁵⁵. This whole process mediates binding of cognate Tfh cells through the peptide-specific TCR to the Ag-activated GCBC. The BCR signaling output is altered by extending the time over which the BCR is stimulated; as a consequence, GCBCs that have a prolonged interaction with an Ag obtain significantly higher activity of intracellular signaling transduction. In summary, Ag recognition does not only provide the GCBC with the first intracellular signal transduction that potentially prepares the cell for differentiation, but it also promotes the interaction with Tfh cells.

From the Systems Biology perspective, B cell activation may well cause bursts of transcription, through its dependence on the activation of multiple BCRs, and of transcriptional silencing, due to the intracellular cycling of the BCR antigen complexes. The functional consequence of

this decision making results in the cell exhibiting a phenotype switching to specific states of differentiation.

5.2 Tfh cells orchestrate GCBC fate determination

Before the discovery of the role of Tfh cells in the GC reactions, it was generally thought that only competition for Ag was responsible for GCBC selection. Nevertheless, it has been mathematically predicted, and recently experimentally validated, that selection of GCBCs is highly driven by competition for the pro-survival and mitogenic signals provided by the Tfh cells^{40,55,72,77}. Tfh cells are specialized CD4⁺ T cells, which differentiate from naive CD4⁺ T cells after being primed by Ag-presenting cells (APCs), such as dendritic cells (DCs) and stabilized for the Tfh phenotype by cognate B cell interaction during Tfh priming^{156,157}. Tfh cell differentiation is orchestrated by IL-6 and IL-21 in mice¹⁵⁸, and by IL-21, IL-12, IL-23 and TGF- β in human^{158,159}. The interplay between these signals promotes induction of the Tfh cell phenotype through expression of the Tfh-determining transcription factor BCL6, while simultaneously inhibiting differentiation into the canonical CD4⁺ T cell subtypes, Th1, Th2 and Th17 cells¹⁶⁰. Phenotypic hallmarks of Tfh cells are high expression of CXCR5 and CXCR4 and low expression of CCR7, important for their correct localization to the GC LZ¹⁶¹. In addition to Tfh, T follicular regulatory (Tfr) cells populate the GCs^{162,163}. Because Tfrs seem mainly involved in termination of GC responses, they fall beyond the scope of this paper.

Tfh cells migrate through the LZ and constantly screen surrounding GCBCs through short-lived interactions in search for cognate pMHCII. Tfh cells are able to distinguish the high-affinity from the low-affinity CCs. The selection of high-affinity CCs is likely mediated by the number of pMHCII they present; in fact, high-affinity interactions between the BCR and specific Ag results in a higher amount of peptide presentation as compared to low-affinity interactions. This implies that Tfh cells are somehow capable to count pMHCII. Information on the amount of pMHCII on the CCs is likely provided through mechanical forces, which is also used by GCBCs to discriminate Ag affinity¹⁶⁴. They do this through pulling-forces that mediate rupture of single low-affinity bounds, whereas high-affinity, multivalent BCR clusters remain connected. Such a mechanism could also be used by the Tfh cells to provide help to high-affinity GCBCs. Non-cognate B and Tfh cells show an average motility of 6.6 and 9 $\mu\text{m}/\text{min}$, respectively^{43,44,79}. Upon cognate TCR/pMHCII recognition, a stable synapse between GCBC and Tfh cell is formed, decreasing their average motility to 4.16 $\mu\text{m}/\text{min}$ ¹⁶⁵. The stable synapse formation now allows the additional Tfh signals needed to support further GCBC differentiation such as co-stimulation and cytokine secretion.

5.2.1 CD40 co-stimulation

An important interaction between GCBC and Tfh cell is mediated by the binding of CD40 to CD40 ligand (CD40L) (**Figure 2**). The CD40-CD40L pair is concentrated in the immunological synapse after cognate TCR/pMHCII recognition¹⁶⁶. The importance of CD40-CD40L

interaction in humoral responses to T cell-dependent antigens was identified in patients with a congenital CD40L deficiency that causes X-linked hyper-IgM syndrome^{167–171}. These patients are unable to undergo isotype switching *in vitro* and *in vivo*. In agreement with these findings, mice with targeted disruption of CD40 or CD40L genes exhibit a similar phenotype^{172,173}. Since patients and mice carry non-functional CD40L on all CD4⁺ T cells, it is not possible to determine which among the interactions at the B/T border or within the GC LZ is most critical. Administration of a CD40L blocking agent during the early phase of a T cell-dependent immune response abolished completely GC formation and reduced drastically serum antibodies, whereas its administration in the late phase almost completely dissolved the established GCs¹⁷⁴. Furthermore, late administration of the blocking agent decreased the affinity of the antibodies secreted by the PCs, as well as the amount of Ag-specific MBCs¹⁷⁵. These observations indicate that CD40L is required for the induction and continuation of the GC cycling, likely as a result of the incapability to inhibit the pro-apoptotic signals that GCBCs receive upon BCR ligation without being rescued by CD40 signaling. Recently it was demonstrated that interaction between the surface proteins Inducible T-cell co-stimulator (ICOS) and ICOS ligand (ICOSL) on the Tfh cells and GCBC, respectively, augmented CD40 signaling and promoted CD40L expression on Tfh cells; in turn, CD40-mediated signaling induced the up-regulation of ICOSL expression on the GCBCs¹⁷⁶. As such, ICOS and CD40 together facilitate an intercellular positive feedback loop that promotes GCBC-Tfh cell contacts.

CD40L-mediated clustering of CD40 promotes recruitment of tumor necrosis factor receptor (TNFR)-associated factor (TRAF) adaptor proteins^{177,178}, which promote the activation of canonical and non-canonical NF B pathways^{179,180} and facilitate activation of mitogen-activated protein kinase (MAPK) and PI3K (**Figure 5**)^{145,181–189}. Recently it was determined that attenuated proximal BCR signaling can be abolished by CD40-mediated degradation of CBL (**Figure 5**)¹⁴³. Removal of CBL should abolish the degradation of Syk, boosting BCR signaling intensity to the PI3K/AKT and extracellular signal-regulated kinases (ERK) pathways. Herewith, BCR and CD40 signaling synergistically induce expression of MYC and IRF4, and activate the AKT-mediated mammalian target of rapamycin complex 1 (mTORC1) pathway, which facilitates phosphorylation of the ribosomal protein S6 (**Figure 5**)^{7,112,145,190}. pS6 subsequently induces expression CXCR4 via FOXO1 to promote DZ re-entry, whereas MYC promotes the cell cycle progression. Active ERK inactivates BCL6 and PAX5, by rapidly degrading BCL6 through the ubiquitin/proteasome pathway and by repressing PAX5 activity (**Figure 5**)^{191,192}. Loss of functionally active BCL6 and PAX5 results in expression of BLIMP1, which in turn protects its transcriptionally active state through suppression of BCL6 and PAX5⁸⁹. Altogether, these observations indicate that BCR signaling and CD40 ligation are important for GCBC fate determination, notwithstanding additional signals provided by Tfh cell cytokines further supporting GC reactions.

5.2.2 Cytokine secretion by Tfh cells

IL-21 and IL-4 are the two main cytokines secreted by Tfh cells and promote the fate determination of positively selected GCBCs¹⁹³. Tfh cells progressively differentiate along with the GC cycling to fine tune humoral immunity^{194,195}. During the initiation of a GC, the first Tfh cells to emerge express IL-21. As the GC response progresses, Tfh cells gradually switch from IL-21 to IL-4 production. Interestingly, although the cytokines could be expressed simultaneously, secretion is limited to either IL-21 or IL-4. Within the GC, IL-21 Tfh cells are located on average more proximal to the DZ as compared to IL-4 Tfh cells¹⁹⁴. The cell-surface expression density of CD40L is significantly higher in Tfh cells that express IL-4 than in those that express IL-21 only¹⁹⁴. All of these differential characteristics suggest that cytokine-expressing GC Tfh cells have different roles in the GC.

IL-21 exerts its biological activities through interaction with the IL-21 receptor (IL-21R), whereas IL-4 can interact with two cell surface receptor complexes – the Type I IL-4 receptor and the Type II IL-4 receptor, which are both expressed by GCBCs. Receptor stimulation results in activation of Janus kinase–signal transducer and activator of transcription (STAT) signaling pathways¹⁹⁶. IL-21R signaling is predominantly mediated by STAT3, STAT1 and STAT5 (**Figure 5**)^{197,198}, whereas signaling through IL-4R is facilitated through STAT5 and STAT6 (**Figure 5**)^{199,200}.

In response to IL-4, GCBCs undergo a more pronounced isotype switching to IgG1 and differentiation into plasma cell, which may partly result from the enhanced CD40L expression in these different subsets¹⁹⁴. In contrast, IL-21 Tfh cells exhibit an increased rate of high-affinity mutations¹⁹⁴. IL-21 signaling was shown to play a large role in instructing the CC to CB transition¹⁹⁵, which is essential for the iterative rounds of SHM and affinity maturation. IL-21 induces the expression of both BLIMP1^{197,201} and BCL6 (**Figure 5**)^{201–206}. The balance between induction of either BCL6 or BLIMP1 may be mediated through the STAT signal transduction; STAT3 is important for the IL-21R-mediated induction of BLIMP1 expression¹⁹⁷, whereas both STAT3 and STAT1 induce BCL6²⁰⁷. Alternatively, the signals that GCBC receive prior to IL-21, such as BCR and CD40 signaling, could make them more prone to induce either BCL6 or BLIMP1. Considering that BCL6 and BLIMP1 antagonize each other's expression to help decide between GCBC and plasma cell differentiation, respectively, it is likely that, once a specific trait has initiated, IL-21 signaling is able to maintain it. This process may be observed early in the T-dependent Ag response. Here, high affinity B cells are predominantly observed in the extrafollicular plasma cells response, whereas clones with weaker Ag reactivity were primarily directed to GC reactions³⁵. As described above, prominent BCR and CD40 signaling responses induce high levels of IRF4 to enhance BLIMP1 and inhibit BCL6 expression. In this scenario, additional IL-21 signaling would synergize to complement the Ag-driven induction of BLIMP1. Conversely, weak BCR and CD40 signaling results in low IRF4 expression to enhance BCL6 and PAX5 expression, which both suppress BLIMP1 expression. In this way, IL-21 signaling would support BCL6 expression to promote GC retention, as observed¹⁹⁵, until the transcriptional

program shifts due to affinity maturation to then promote plasma cell differentiation.

The observation that GC Tfh cells, similar to GCBCs, mature phenotypically and transcriptionally throughout the GC response suggests a reciprocal relationship between GCBC and Tfh cells. Their contacts elicit transient and sustained increases in intracellular free calcium in Tfh cell that is associated to multi-functional Tfh cells and is driven by TCR/pMHCII interactions^{165,176}. Ag dose and BCR affinity, which change over time, affect TCR signaling strength and duration through the number of Ag-derived pMHCII molecules displayed by Ag-presenting B cells^{28,208–210}. The amount of TCR signaling can have qualitative effects on CD4⁺ T cell differentiation into the specialized effector cell lineage²¹¹, and may change the cytokines that are expressed by a specific lineage, such as IL-21 and IL-4 in Tfh cells, to achieve the required output response.

From the Systems Biology perspective, the interplay among the cytokines secreted by Tfh cells to promote GCBCs fate determination may well be non-linear, similarly to the regulations occurring in the GC signal transduction network (**Figure 5**) and its transcriptional sub-network (**Figure 4B**). Among the cytokines, IL-21 and IL-4 appears to play a major role in B cell differentiation, and a strategy that integrates predictive modeling to quantitative experimentation may point to the non-linear regulations occurring among the diverse cytokines involved in the process.

6 DISCUSSION

The molecular cross-talk provided through Ag and the physical, biochemical and expression-mediated interactions between GCBCs and Tfh cells in the GC LZ orchestrate GCBC fate determination. Great efforts have been made to characterize the complex intracellular signal transduction and gene expression networks that mediate these interactions. Characterization and integration of the cellular signaling pathways should help to elucidate how the extracellular signals transmitted through these interactions lead to GCBC re-circulation or differentiation. Nevertheless, since the system is coordinately regulated by multiple receptors which impinge on specific transcription factors involved in fate determination, it has been troublesome to comprehend the complexity of the GC reactions considering the available experimental scenarios that often focus on the analysis of the effects of one or a few components in a more or less static ‘on-off’ approach.

This is now changing with the development of sophisticated experimental methodologies such as single cell sequencing, in principle able to deliver a map of transcriptomes over the GC. With single cell analyses of the important regulators, this may soon advance to the protein level. But we are not quite there yet, as the massive data flows and detailed manipulation experiments with spatial resolution at the scale of the GC are still a matter of the, near, future. The shift to data driven biology is challenging, as the number of experiments needed in a completely data driven approach would be vast. For example, measuring all the *in vivo* parameters driving B cell development into different phenotypes. Where bioinformatics aids in clustering the data

according to defined criteria, dynamic methodologies are needed to simulate the implications of the data we obtain for the data we cannot obtain. This challenge then requires integration of predictive modelling with precise experimentation, what we have indicated here as Systems Biology. The application of principles developed and discovered in simpler networks could be of relevance for the understanding of how the GC works. Thus, modeling of its regulatory system may predict and elucidate how the fate of a GCBC is determined, followed by dedicated experimental testing.

One way to model an intracellular regulatory network is through a directed graph²¹², which visualizes the complex regulatory network that selects positively GCBCs. Such a graph can be translated into mathematical equations that, when simulated, may lead to the identification of temporal mechanisms of GCBC differentiation. We have recently illustrated this for the network underlying cell cycle control and reactive oxygen species (ROS) production where we discovered new regulatory patterns^{213,214}. The intracellular regulatory network involved in the positive selection of GCBCs should be modeled similarly as a multi-component, temporally evolving dynamic system. For such a model, sets of differential equations are applicable, which may include time and/or space dependent variables^{212,215}, where space may be divided into a limited number of representative compartments with transport in between.

Differential equations are divided into two main groups, the ordinary differential equations (ODEs) and the partial differential equations (PDEs)^{212,215}, whilst for each there are deterministic and stochastic types. ODEs are widely used and well-studied to analyze genetic, signal transduction and metabolic networks, by using concentration of components as a time-dependent variable. Nevertheless, in eukaryotes, cellular components rarely function in one single compartment; they rather shuttle between different compartments, and ODE equations may then be used to treat the dynamics of cellular components in different compartments separately, with additional rate equations for the transport processes between the compartments. When concentration gradients may exist within compartments, then the use of PDEs may be considered. In a PDE, a concentration is not only dependent on time, but also on three continuous space-dependent coordinates. As such, a PDE equation considers that molecules may behave differently in different areas of any same compartment. Although a PDE-based model more closely resembles biological realism, it requires increasing computing software as compared to ODEs, but worse, it requires more molecular information that is not always available. The use of an ODE-based over a PDE-based approach should be considered on a case-by-case basis. For the intracellular aspects of the GC, ODEs may well be suitable, as it has been recently shown in a computational model that recapitulated the switch from memory B cell to PC generation during the course of the GC reaction²¹⁶.

One of the relevant questions to be addressed regards the affinity, thus the quality, of different types of antibodies. The affinity-dependent selection serves the dual purpose of dealing with multiple novel antigenic determinants at relatively high concentration early on, and of subsequently removing the last few copies of more defined antigen. Affinity between

macromolecules is to a significant extent determined by the number of water molecules they exclude upon binding as well as by the surface area through which they interact energetically, and thereby by the extent to which their binding surfaces are complementary in shape and able to squeeze out all the water molecules between them. Early models^{59,217,218} thereto developed the concept of shape space as a way to comprehend Ag-antibody affinity. This complementary principle uses Ags to define where the antibody of maximum affinity is positioned in the shape space. This distance of the antibody to the theoretical optimal clone is defined in terms of the minimum number of mutations necessary for the shape of the optimal clone to be reached, as a measurement of antibody affinity to the Ag. Affinity is subsequently estimated using a Gaussian function with this distance as argument, the distribution being mapped by characterizing a number of known mutations. This principle fails to predict all the experimental information, thereby highlighting the inherent unreliability of using shape space alone to define antibody affinity⁷². In addition to shape, a network of other interactions dependent on electric charge, polarity, and hydrogen bridge formation of amino acid residues, will play a role.

Large scale systematic experimental data sets can be integrated into appropriate computational frameworks, to weigh the relative strengths and dynamics of the different signaling networks that control GC dynamics. To exemplify the necessity for systems-level approaches to the adaptive immune system, the interaction between Tfh cells, cytokines, and GCBCs to propagate the maturation process may be further investigated by training neural (artificial intelligence) networks on the data sets. This may generate a model that is able to predict the effects of changes in parameters. In addition, the neural network obtained may not heed laws of physics, chemistry or biology. The future is represented by neural networks trained on the experimental data sets as well as on artificial datasets produced by networks constructed on the basis of established physics, chemistry and biology.

Although, canonically, Tfh cells are presumed to have their lineage traced to Th1 and Th2 branches, recent studies show Tfh cells to have a distinct gene expression profile unlike Th1, Th2, Th17 or Treg cells²¹⁹. As cytokines have been confirmed to promote both T and B cell differentiation, understanding cytokine dynamics is vital, also when examining possible bistabilities of the |GC cycle, as it occurs in other immunology cycles⁹. Although details of the specific mechanisms through which these dynamics occur are beyond the scope of this paper, a few considerations may be the starting point of future research. Secretion of IL-21 and IL-4 has been confirmed, but the influence that other cytokines have on Tfh cells, apart from germinal center formation, is largely unexplored. Also, the reciprocal relationship between GCBC and Tfh cell is of substantial interest. GCBCs may influence their own fate via the amount of pMHCII that determines the cytokines that are secreted by Tfh cells. Limited qualitative work has been done to elucidate the effects that cytokines have on T and B cell differentiation, generally neglecting the influence of temporal factors and of T cells secreting uncommon or multi-phenotypical cytokine profiles. Furthermore, recent investigation have highlighted that the effectiveness of T cell functioning is qualitatively, quantitatively and temporally determined by cellular and

humoral signals such as cytokines²²⁰. Anticipating the need for a system-level analysis to dissect the mutual regulation between GCBC and T_{fh} cells, these scenarios may be investigated through detailed kinetic models that consider the regulatory, activatory and inhibitory interactions occurring among the various signals involved. Simulation of these computer models will then identify critical network components, as well as mechanistic explanations for both the T and B cell differentiation processes specifically through cytokines-mediated regulation. Modeling of this system may enable identification of the components that are most prone to biological intervention²²¹. It may also suggest improved vaccination strategies and therapeutic agents that can be employed for the treatment of B cell-mediated malignancy or auto-immunity.

FUNDING

This work was supported by the Systems Biology Grant of the University of Surrey to MB, and by the EU ERASMUS+ Traineeship Grant to MB (recipient VU).

REFERENCES

1. De Silva, N. S. & Klein, U. Dynamics of B cells in germinal centres. *Nat. Rev. Immunol.* **15**, 137–48 (2015).
2. Ravetch, J. V & Kinet, J. P. Fc Receptors. *Annu. Rev. Immunol.* **9**, 457–492 (1991).
3. Kubagawa, H. *et al.* Identity of the elusive IgM Fc receptor (FcμR) in humans. *J. Exp. Med.* **206**, 2779–2793 (2009).
4. Shibuya, A. *et al.* Fc alpha/mu receptor mediates endocytosis of IgM-coated microbes. *Nat. Immunol.* **1**, 441–6 (2000).
5. Victora, G. D. & Nussenzweig, M. C. Germinal Centers. *Annu. Rev. Immunol.* **30**, 429–457 (2012).
6. Jacob, J., Kelsoe, G., Rajewsky, K. & Weiss, U. Intraclonal generation of antibody mutants in germinal centres. *Nature* **354**, 389–92 (1991).
7. Kräutler, N. J. *et al.* Differentiation of germinal center B cells into plasma cells is initiated by high-affinity antigen and completed by Tfh cells. *J. Exp. Med.* **214**, 1259–1267 (2017).
8. Hornberg, J. J. *et al.* Principles behind the multifarious control of signal transduction. *FEBS J.* **272**, 244–258 (2004).
9. Abudukelimu, A. *et al.* Complex Stability and an Irreversible Transition Reverted by Peptide and Fibroblasts in a Dynamic Model of Innate Immunity. *Front. Immunol.* **10**, 3091 (2020).
10. Germain, R. N., Meier-Schellersheim, M., Nita-Lazar, A. & Fraser, I. D. C. Systems Biology in Immunology: A Computational Modeling Perspective. *Annu. Rev. Immunol.* **29**, 527–585 (2011).
11. Kidd, B. a, Peters, L. a, Schadt, E. E. & Dudley, J. T. Unifying immunology with informatics and multiscale biology. *Nat. Immunol.* **15**, 118–127 (2014).
12. Westerhoff, H. V. Signalling control strength. *J. Theor. Biol.* **252**, 555–567 (2008).
13. Mondeel, T. D. G. A., Ivanov, O., Westerhoff, H. V., Liebermeister, W. & Barberis, M. Clb3-centered regulations are recurrent across distinct parameter regions in minimal autonomous cell cycle oscillator designs. *npj Syst. Biol. Appl.* **6**, 8 (2020).
14. Puniya, B. L. *et al.* A Mechanistic Computational Model Reveals That Plasticity of CD4+ T Cell Differentiation Is a Function of Cytokine Composition and Dosage. *Front. Physiol.* **9**, 878 (2018).
15. Abudukelimu, A., Barberis, M., Redegeld, F. A., Sahin, N. & Westerhoff, H. V. Predictable Irreversible Switching Between Acute and Chronic Inflammation. *Front. Immunol.* **9**, 1596 (2018).
16. Girard, J.-P., Moussion, C. & Förster, R. HEVs, lymphatics and homeostatic immune cell trafficking in lymph nodes. *Nat. Rev. Immunol.* **12**, 762–73 (2012).
17. Müller, G., Höpken, U. E. & Lipp, M. The impact of CCR7 and CXCR5 on lymphoid organ development and systemic immunity. *Immunol. Rev.* **195**, 117–35 (2003).
18. Wang, X. *et al.* Follicular dendritic cells help establish follicle identity and promote B cell retention in germinal centers. *J. Exp. Med.* **208**, 2497–510 (2011).
19. Phan, T. G., Grigorova, I., Okada, T. & Cyster, J. G. Subcapsular encounter and complement-dependent transport of immune complexes by lymph node B cells. *Nat. Immunol.* **8**, 992–1000 (2007).
20. Phan, T. G., Green, J. A., Xu, Y. & Cyster, J. G. Immune complex relay by subcapsular sinus macrophages and noncognate B cells drives antibody affinity maturation. *Nat. Immunol.* **10**, 786–796 (2009).
21. Cyster, J. G. B cell follicles and antigen encounters of the third kind. *Nat. Immunol.* **11**, 989–996 (2010).
22. Kranich, J. & Krautler, N. J. How Follicular Dendritic Cells Shape the B-Cell Antigenome. *Front. Immunol.* **7**, 225 (2016).
23. Heesters, B. A. *et al.* Endocytosis and recycling of immune complexes by follicular dendritic cells enhances B cell antigen binding and activation. *Immunity* **38**, 1164–75 (2013).
24. Suzuki, K., Grigorova, I., Phan, T. G., Kelly, L. M. & Cyster, J. G. Visualizing B cell capture of cognate antigen from follicular dendritic cells. *J. Exp. Med.* **206**, 1485–1493 (2009).
25. Martínez-Riaño, A. *et al.* Antigen phagocytosis by B cells is required for a potent humoral response. *EMBO Rep.* **19**, 1–15 (2018).
26. Versteegen, N. J. M. *et al.* Human B Cells Engage the NCK/PI3K/RAC1 Axis to Internalize Large Particles via the IgM-BCR. *Front. Immunol.* **10**, 1–14 (2019).
27. Carrasco, Y. R. & Batista, F. D. B Cells Acquire Particulate Antigen in a Macrophage-Rich Area at the Boundary between the Follicle and the Subcapsular Sinus of the Lymph Node. *Immunity* **27**, 160–171 (2007).
28. Pape, K. A., Catron, D. M., Itano, A. A. & Jenkins, M. K. The humoral immune response is initiated in lymph nodes by B cells that acquire soluble antigen directly in the follicles. *Immunity* **26**, 491–502 (2007).

29. Souwer, Y. *et al.* B cell receptor-mediated internalization of salmonella: a novel pathway for autonomous B cell activation and antibody production. *J. Immunol.* **182**, 7473–81 (2009).
30. Shlomchik, M. J., Luo, W. & Weisel, F. Linking signaling and selection in the germinal center. *Immunol. Rev.* **288**, 49–63 (2019).
31. Förster, R. *et al.* CCR7 coordinates the primary immune response by establishing functional microenvironments in secondary lymphoid organs. *Cell* **99**, 23–33 (1999).
32. Ansel, K. M., McHeyzer-Williams, L. J., Ngo, V. N., McHeyzer-Williams, M. G. & Cyster, J. G. In vivo-activated CD4 T cells upregulate CXC chemokine receptor 5 and reprogram their response to lymphoid chemokines. *J. Exp. Med.* **190**, 1123–1134 (1999).
33. Reif, K. *et al.* Balanced responsiveness to chemoattractants from adjacent zones determines B-cell position. *Nature* **416**, 94–9 (2002).
34. O'Connor, B. P. *et al.* Imprinting the fate of antigen-reactive B cells through the affinity of the B cell receptor. *J. Immunol.* **177**, 7723–32 (2006).
35. Paus, D. *et al.* Antigen recognition strength regulates the choice between extrafollicular plasma cell and germinal center B cell differentiation. *J. Exp. Med.* **203**, 1081–91 (2006).
36. Taylor, J. J., Pape, K. A. & Jenkins, M. K. A germinal center-independent pathway generates unswitched memory B cells early in the primary response. *J. Exp. Med.* **209**, 597–606 (2012).
37. Toyama, H. *et al.* Memory B cells without somatic hypermutation are generated from Bcl6-deficient B cells. *Immunity* **17**, 329–39 (2002).
38. Berkowska, M. A. *et al.* Human memory B cells originate from three distinct germinal center-dependent and -independent maturation pathways. *Blood* **118**, 2150–2158 (2011).
39. Shlomchik, M. J. & Weisel, F. Germinal center selection and the development of memory B and plasma cells. *Immunol. Rev.* **247**, 52–63 (2012).
40. Schwickert, T. A. *et al.* A dynamic T cell-limited checkpoint regulates affinity-dependent B cell entry into the germinal center. *J. Exp. Med.* **208**, 1243–1252 (2011).
41. Roco, J. A. *et al.* Class-Switch Recombination Occurs Infrequently in Germinal Centers. *Immunity* **51**, 337–350. e7 (2019).
42. Taylor, J. J., Pape, K. A., Steach, H. R. & Jenkins, M. K. Apoptosis and antigen affinity limit effector cell differentiation of a single naive B cell. *Science (80-.)*. **347**, 784–787 (2015).
43. Allen, C. D. C., Okada, T., Tang, H. L. & Cyster, J. G. Imaging of germinal center selection events during affinity maturation. *Science (80-.)*. **315**, 528–531 (2007).
44. Hauser, A. E. *et al.* Definition of germinal-center B cell migration in vivo reveals predominant intrazonal circulation patterns. *Immunity* **26**, 655–67 (2007).
45. MacLennan, I. C. M. Germinal Centers. *Annu. Rev. Immunol.* **12**, 117–139 (1994).
46. Jacob, J., Przylepa, J., Miller, C. & Kelsoe, G. In situ studies of the primary immune response to (4-hydroxy-3-nitrophenyl)acetyl. III. The kinetics of V region mutation and selection in germinal center B cells. *J. Exp. Med.* **178**, 1293–307 (1993).
47. Cyster, J. G. *et al.* Follicular stromal cells and lymphocyte homing to follicles. *Immunol. Rev.* **176**, 181–193 (2000).
48. Nieuwenhuis, P. & Opstelten, D. Functional anatomy of germinal centers. *Am. J. Anat.* **170**, 421–435 (1984).
49. Allen, C. D. C. *et al.* Germinal center dark and light zone organization is mediated by CXCR4 and CXCR5. *Nat. Immunol.* **5**, 943–52 (2004).
50. Bannard, O. *et al.* Germinal center centroblasts transition to a centrocyte phenotype according to a timed program and depend on the dark zone for effective selection. *Immunity* **39**, 912–24 (2013).
51. Kallberg, E., Jainandunsing, S., Gray, D. & Leanderson, T. Somatic Mutation of Immunoglobulin V Genes in Vitro. *Science (80-.)*. **271**, 1285–1289 (1996).
52. Chua, K. F., Alt, F. W. & Manis, J. P. The Function of AID in Somatic Mutation and Class Switch Recombination. *J. Exp. Med.* **195**, F37–F41 (2002).
53. Stewart, I., Radtke, D., Phillips, B., McGowan, S. J. & Bannard, O. Germinal Center B Cells Replace Their Antigen Receptors in Dark Zones and Fail Light Zone Entry when Immunoglobulin Gene Mutations are Damaging. *Immunity* **49**, 477–489. e7 (2018).
54. Mayer, C. T. *et al.* The microanatomic segregation of selection by apoptosis in the germinal center. *Science (80-.)*. **358**, eaao2602 (2017).
55. Victora, G. D. *et al.* Germinal Center Dynamics Revealed by Multiphoton Microscopy with a Photoactivatable Fluorescent Reporter. *Cell* **143**, 592–605 (2010).

56. Kepler, T. B. & Perelson, A. S. Somatic hypermutation in B cells: an optimal control treatment. *J. Theor. Biol.* **164**, 37–64 (1993).
57. Figge, M. T. *et al.* Deriving a germinal center lymphocyte migration model from two-photon data. *J. Exp. Med.* **205**, 3019–29 (2008).
58. Meyer-Hermann, M., Figge, M. T. & Toellner, K.-M. Germinal centres seen through the mathematical eye: B-cell models on the catwalk. *Trends Immunol.* **30**, 157–64 (2009).
59. Meyer-Hermann, M., Deutsch, A. & Or-Guil, M. Recycling probability and dynamical properties of germinal center reactions. *J. Theor. Biol.* **210**, 265–85 (2001).
60. Meyer-Hermann, M. *et al.* A Theory of Germinal Center B Cell Selection, Division, and Exit. *Cell Rep.* **2**, 162–174 (2012).
61. Iber, D. & Maini, P. K. A mathematical model for germinal centre kinetics and affinity maturation. *J. Theor. Biol.* **219**, 153–75 (2002).
62. Radmacher, M. D., Kelsoe, G. & Kepler, T. B. Predicted and inferred waiting times for key mutations in the germinal centre reaction: Evidence for stochasticity in selection. *Immunol. Cell Biol.* **76**, 373–381 (1998).
63. Liu, Y.-J. & Arpin, C. Germinal center development. *Immunol. Rev.* **156**, 111–126 (1997).
64. Hollowood, K. & Macartney, J. Cell kinetics of the germinal center reaction - a stathmokinetic study. *Eur. J. Immunol.* **22**, 261–266 (1992).
65. Kepler, T. B. & Perelson, A. S. Cyclic re-entry of germinal center B cells and the efficiency of affinity maturation. *Immunol. Today* **14**, 412–415 (1993).
66. Vora, K. A., Ravetch, J. V & Manser, T. Amplified follicular immune complex deposition in mice lacking the Fc receptor gamma-chain does not alter maturation of the B cell response. *J. Immunol.* **159**, 2116–24 (1997).
67. Hannum, L. G., Haberman, A. M., Anderson, S. M. & Shlomchik, M. J. Germinal Center Initiation, Variable Gene Region Hypermutation, and Mutant B Cell Selection without Detectable Immune Complexes on Follicular Dendritic Cells. *J. Exp. Med.* **192**, 931–942 (2000).
68. Smith, K. G. C., Light, A., Nossal, G. J. & Tarlinton, D. M. The extent of affinity maturation differs between the memory and antibody-forming cell compartments in the primary immune response. *EMBO J.* **16**, 2996–3006 (1997).
69. Figge, M. T. Stochastic discrete event simulation of germinal center reactions. *Phys. Rev. E* **71**, 051907 (2005).
70. Wang, Y., Zhou, Y. & Graves, D. T. FOXO Transcription Factors: Their Clinical Significance and Regulation. *Biomed Res. Int.* **2014**, 1–13 (2014).
71. Cabrera-Ortega, A. A., Feinberg, D., Liang, Y., Rossa, C. & Graves, D. T. The Role of Forkhead Box 1 (FOXO1) in the Immune System: Dendritic Cells, T Cells, B Cells, and Hematopoietic Stem Cells. *Crit. Rev. Immunol.* **37**, 1–13 (2017).
72. Meyer-Hermann, M. E., Maini, P. K. & Iber, D. An analysis of B cell selection mechanisms in germinal centers. *Math. Med. Biol. A J. IMA* **23**, 255–277 (2006).
73. Yoshida, M., Fuchikami, K. & Uezu, T. Realization of immune response features by dynamical system models. *Math. Biosci. Eng.* **4**, 531–552 (2007).
74. Koopman, G. *et al.* Adhesion of human B cells to follicular dendritic cells involves both the lymphocyte function-associated antigen 1/intercellular adhesion molecule 1 and very late antigen 4/vascular cell adhesion molecule 1 pathways. *J. Exp. Med.* **173**, 1297–1304 (1991).
75. Heesters, B. A., Myers, R. C. & Carroll, M. C. Follicular dendritic cells: dynamic antigen libraries. *Nat. Rev. Immunol.* **14**, 495–504 (2014).
76. Keşmir, C. & De Boer, R. J. A mathematical model on germinal center kinetics and termination. *J. Immunol.* **163**, 2463–9 (1999).
77. Meyer-Hermann, M. E. A Concerted Action of B Cell Selection Mechanisms. *Adv. Complex Syst.* **10**, 557–580 (2007).
78. Kelsoe, G. The germinal center: a crucible for lymphocyte selection. *Semin. Immunol.* **8**, 179–184 (1996).
79. Gitlin, A. D., Shulman, Z. & Nussenzweig, M. C. Clonal selection in the germinal centre by regulated proliferation and hypermutation. *Nature* **509**, 637–40 (2014).
80. Kupfer, H., Monks, C. R. & Kupfer, A. Small splenic B cells that bind to antigen-specific T helper (Th) cells and face the site of cytokine production in the Th cells selectively proliferate: immunofluorescence microscopic studies of Th-B antigen-presenting cell interactions. *J. Exp. Med.* **179**, 1507–1515 (1994).
81. Chan, C. *et al.* A Model for Migratory B Cell Oscillations from Receptor Down-Regulation Induced by External Chemokine Fields. *Bull. Math. Biol.* **75**, 185–205 (2013).

82. Werner, F. *et al.* A Standardized Analysis of Tertiary Lymphoid Structures in Human Melanoma: Disease Progression- and Tumor Site-Associated Changes With Germinal Center Alteration. *Front. Immunol.* **12**, 675146 (2021).
83. Ruffin, A. T. *et al.* B cell signatures and tertiary lymphoid structures contribute to outcome in head and neck squamous cell carcinoma. *Nat. Commun.* **12**, 3349 (2021).
84. Alberts, E., Wall, I., Calado, D. P. & Grigoriadis, A. Immune Crosstalk Between Lymph Nodes and Breast Carcinomas, With a Focus on B Cells. *Front. Mol. Biosci.* **8**, 673051 (2021).
85. Aizik, L. *et al.* Antibody Repertoire Analysis of Tumor-Infiltrating B Cells Reveals Distinct Signatures and Distributions Across Tissues. *Front. Immunol.* **12**, 705381 (2021).
86. Harris, R. J. *et al.* Tumor-Infiltrating B Lymphocyte Profiling Identifies IgG-Biased, Clonally Expanded Prognostic Phenotypes in Triple-Negative Breast Cancer. *Cancer Res.* **81**, 4290–4304 (2021).
87. Tarlinton, D. & Good-Jacobson, K. Diversity among memory B cells: origin, consequences, and utility. *Science (80-.)*. **341**, 1205–1211 (2013).
88. Allen, C. D. C., Okada, T. & Cyster, J. G. Germinal-center organization and cellular dynamics. *Immunity* **27**, 190–202 (2007).
89. Nutt, S. L., Hodgkin, P. D., Tarlinton, D. M. & Corcoran, L. M. The generation of antibody-secreting plasma cells. *Nat. Rev. Immunol.* **15**, 160–71 (2015).
90. Khodadadi, L., Cheng, Q., Radbruch, A. & Hiepe, F. The Maintenance of Memory Plasma Cells. *Front. Immunol.* **10**, 721 (2019).
91. Kurosaki, T., Kometani, K. & Ise, W. Memory B cells. *Nat. Rev. Immunol.* **15**, 149–59 (2015).
92. Shlomchik, M. J. Do Memory B Cells Form Secondary Germinal Centers? Yes and No. *Cold Spring Harb. Perspect. Biol.* **10**, a029405 (2018).
93. McHeyzer-Williams, L. J., Dufaud, C. & McHeyzer-Williams, M. G. Do Memory B Cells Form Secondary Germinal Centers? Impact of Antibody Class and Quality of Memory T-Cell Help at Recall. *Cold Spring Harb. Perspect. Biol.* **10**, a028878 (2018).
94. Pape, K. A. & Jenkins, M. K. Do Memory B Cells Form Secondary Germinal Centers? It Depends. *Cold Spring Harb. Perspect. Biol.* **10**, a029116 (2018).
95. Seifert, M. & Küppers, R. Molecular footprints of a germinal center derivation of human IgM+(IgD+)CD27+ B cells and the dynamics of memory B cell generation. *J. Exp. Med.* **206**, 2659–69 (2009).
96. Seifert, M. *et al.* Functional capacities of human IgM memory B cells in early inflammatory responses and secondary germinal center reactions. *Proc. Natl. Acad. Sci. U. S. A.* **112**, E546–55 (2015).
97. Dogan, I. *et al.* Multiple layers of B cell memory with different effector functions. *Nat. Immunol.* **10**, 1292–9 (2009).
98. Pape, K. A., Taylor, J. J., Maul, R. W., Gearhart, P. J. & Jenkins, M. K. Different B cell populations mediate early and late memory during an endogenous immune response. *Science (80-.)*. **331**, 1203–1207 (2011).
99. Weisel, F. J., Zuccarino-Catania, G. V., Chikina, M. & Shlomchik, M. J. A Temporal Switch in the Germinal Center Determines Differential Output of Memory B and Plasma Cells. *Immunity* **44**, 116–130 (2016).
100. Phan, T. G. *et al.* High affinity germinal center B cells are actively selected into the plasma cell compartment. *J. Exp. Med.* **203**, 2419–24 (2006).
101. Zhang, Y. *et al.* Plasma cell output from germinal centers is regulated by signals from Tfh and stromal cells. *J. Exp. Med.* **215**, 1–17 (2018).
102. Duffy, K. R. *et al.* Activation-induced B cell fates are selected by intracellular stochastic competition. *Science (80-.)*. **335**, 338–341 (2012).
103. Thauinat, O. *et al.* Asymmetric segregation of polarized antigen on B cell division shapes presentation capacity. *Science (80-.)*. **335**, 475–479 (2012).
104. Barnett, B. E. *et al.* Asymmetric B cell division in the germinal center reaction. *Science (80-.)*. **335**, 342–344 (2012).
105. Kanno, Y., Levi, B.-Z., Tamura, T. & Ozato, K. Immune cell-specific amplification of interferon signaling by the IRF-4/8-PU.1 complex. *J. Interferon Cytokine Res.* **25**, 770–9 (2005).
106. Cobaleda, C., Schebesta, A., Delogu, A. & Busslinger, M. Pax5: the guardian of B cell identity and function. *Nat. Immunol.* **8**, 463–70 (2007).
107. Kitano, M. *et al.* Bcl6 protein expression shapes pre-germinal center B cell dynamics and follicular helper T cell heterogeneity. *Immunity* **34**, 961–72 (2011).
108. Ochiai, K. *et al.* Transcriptional regulation of germinal center B and plasma cell fates by dynamical control of IRF4. *Immunity* **38**, 918–29 (2013).

109. Sciammas, R. *et al.* Graded Expression of Interferon Regulatory Factor-4 Coordinates Isotype Switching with Plasma Cell Differentiation. *Immunity* **25**, 225–236 (2006).
110. Crotty, S., Johnston, R. J. & Schoenberger, S. P. Effectors and memories: Bcl-6 and Blimp-1 in T and B lymphocyte differentiation. *Nat. Immunol.* **11**, 114–20 (2010).
111. Calado, D. P. *et al.* The cell-cycle regulator c-Myc is essential for the formation and maintenance of germinal centers. *Nat. Immunol.* **13**, 1092–1100 (2012).
112. Dominguez-Sola, D. *et al.* The proto-oncogene MYC is required for selection in the germinal center and cyclic reentry. *Nat. Immunol.* **13**, 1083–91 (2012).
113. Ci, W. *et al.* The BCL6 transcriptional program features repression of multiple oncogenes in primary B cells and is deregulated in DLBCL. *Blood* **113**, 5536–5548 (2009).
114. Basso, K. *et al.* Integrated biochemical and computational approach identifies BCL6 direct target genes controlling multiple pathways in normal germinal center B cells. *Blood* **115**, 975–984 (2010).
115. Tellier, J. *et al.* Blimp-1 controls plasma cell function through the regulation of immunoglobulin secretion and the unfolded protein response. *Nat. Immunol.* **17**, 323–330 (2016).
116. Todd, D. J. *et al.* XBP1 governs late events in plasma cell differentiation and is not required for antigen-specific memory B cell development. *J. Exp. Med.* **206**, 2151–9 (2009).
117. Taubenheim, N. *et al.* High rate of antibody secretion is not integral to plasma cell differentiation as revealed by XBP-1 deficiency. *J. Immunol.* **189**, 3328–38 (2012).
118. Hu, C.-C. A., Dougan, S. K., McGehee, A. M., Love, J. C. & Ploegh, H. L. XBP-1 regulates signal transduction, transcription factors and bone marrow colonization in B cells. *EMBO J.* **28**, 1624–36 (2009).
119. Kaji, T. *et al.* Distinct cellular pathways select germline-encoded and somatically mutated antibodies into immunological memory. *J. Exp. Med.* **209**, 2079–97 (2012).
120. Takahashi, Y., Ohta, H. & Takemori, T. Fas is required for clonal selection in germinal centers and the subsequent establishment of the memory B cell repertoire. *Immunity* **14**, 181–92 (2001).
121. Saito, M. *et al.* BCL6 suppression of BCL2 via Miz1 and its disruption in diffuse large B cell lymphoma. *Proc. Natl. Acad. Sci. U. S. A.* **106**, 11294–9 (2009).
122. Laidlaw, B. J. *et al.* The Eph-related tyrosine kinase ligand Ephrin-B1 marks germinal center and memory precursor B cells. *J. Exp. Med.* **214**, 639–649 (2017).
123. Kuo, T. C. *et al.* Repression of BCL-6 is required for the formation of human memory B cells in vitro. *J. Exp. Med.* **204**, 819–30 (2007).
124. Laidlaw, B. J., Duan, L., Xu, Y., Vazquez, S. E. & Cyster, J. G. The transcription factor Hhex cooperates with the corepressor Tle3 to promote memory B cell development. *Nat. Immunol.* **21**, 1082–1093 (2020).
125. Shinnakasu, R. *et al.* Regulated selection of germinal-center cells into the memory B cell compartment. *Nat. Immunol.* **17**, 861–9 (2016).
126. Carotta, S. *et al.* The transcription factors IRF8 and PU.1 negatively regulate plasma cell differentiation. *J. Exp. Med.* **211**, 2169–81 (2014).
127. Wang, S. *et al.* Manipulating the Selection Forces during Affinity Maturation to Generate Cross-Reactive HIV Antibodies. *Cell* **160**, 785–797 (2015).
128. Goidl, E. A., Paul, W. E., Siskind, G. W. & Benacerraf, B. The effect of antigen dose and time after immunization on the amount and affinity of anti-hapten antibody. *J. Immunol.* **100**, 371–5 (1968).
129. Zhang, Y. *et al.* Germinal center B cells govern their own fate via antibody feedback. *J. Exp. Med.* **210**, 457–464 (2013).
130. Fleire, S. J. *et al.* B cell ligand discrimination through a spreading and contraction response. *Science (80-.).* **312**, 738–741 (2006).
131. Batista, F. D., Iber, D. & Neuberger, M. S. B cells acquire antigen from target cells after synapse formation. *Nature* **411**, 489–94 (2001).
132. Depoil, D. *et al.* CD19 is essential for B cell activation by promoting B cell receptor-antigen microcluster formation in response to membrane-bound ligand. *Nat. Immunol.* **9**, 63–72 (2008).
133. Carrasco, Y. R., Fleire, S. J., Cameron, T., Dustin, M. L. & Batista, F. D. LFA-1/ICAM-1 Interaction Lowers the Threshold of B Cell Activation by Facilitating B Cell Adhesion and Synapse Formation. *Immunity* **20**, 589–599 (2004).
134. Iber, D. Formation of the B cell synapse: retention or recruitment? *C. Cell. Mol. Life Sci.* **62**, 206–213 (2005).
135. Tsourkas, P. K., Baumgarth, N., Simon, S. I. & Raychaudhuri, S. Mechanisms of B-Cell Synapse Formation Predicted by Monte Carlo Simulation. *Biophys. J.* **92**, 4196–4208 (2007).

136. Tsourkas, P. K. & Raychaudhuri, S. Modeling of B cell Synapse Formation by Monte Carlo Simulation Shows That Directed Transport of Receptor Molecules Is a Potential Formation Mechanism. *Cell. Mol. Bioeng.* **3**, 256–268 (2010).
137. Qi, S. Y., Groves, J. T. & Chakraborty, A. K. Synaptic pattern formation during cellular recognition. *Proc. Natl. Acad. Sci.* **98**, 6548–6553 (2001).
138. Raychaudhuri, S., Chakraborty, A. K. & Kardar, M. Effective Membrane Model of the Immunological Synapse. *Phys. Rev. Lett.* **91**, 208101 (2003).
139. Burroughs, N. J. & Wülfing, C. Differential Segregation in a Cell-Cell Contact Interface: The Dynamics of the Immunological Synapse. *Biophys. J.* **83**, 1784–1796 (2002).
140. Mueller, J., Matloubian, M. & Zikherman, J. Cutting edge: An in vivo reporter reveals active B cell receptor signaling in the germinal center. *J. Immunol.* **194**, 2993–7 (2015).
141. Khalil, A. M., Cambier, J. C. & Shlomchik, M. J. B cell receptor signal transduction in the GC is short-circuited by high phosphatase activity. *Science (80-.)*. **336**, 1178–1181 (2012).
142. Luo, W. *et al.* The AKT kinase signaling network is rewired by PTEN to control proximal BCR signaling in germinal center B cells. *Nat. Immunol.* **20**, 736–746 (2019).
143. Li, X. *et al.* Cbl Ubiquitin Ligases Control B Cell Exit from the Germinal-Center Reaction. *Immunity* **48**, 530–541.e6 (2018).
144. Davidzohn, N. *et al.* Syk degradation restrains plasma cell formation and promotes zonal transitions in germinal centers. *J. Exp. Med.* **217**, (2020).
145. Luo, W., Weisel, F. & Shlomchik, M. J. B Cell Receptor and CD40 Signaling Are Rewired for Synergistic Induction of the c-Myc Transcription Factor in Germinal Center B Cells. *Immunity* **48**, 313–326.e5 (2018).
146. Sander, S. *et al.* PI3 Kinase and FOXO1 Transcription Factor Activity Differentially Control B Cells in the Germinal Center Light and Dark Zones. *Immunity* **43**, 1075–86 (2015).
147. Dominguez-Sola, D. *et al.* The FOXO1 Transcription Factor Instructs the Germinal Center Dark Zone Program. *Immunity* **43**, 1064–74 (2015).
148. Inoue, T. *et al.* The transcription factor Foxo1 controls germinal center B cell proliferation in response to T cell help. *J. Exp. Med.* **214**, 1181–1198 (2017).
149. Song, W., Cho, H., Cheng, P. & Pierce, S. K. Entry of B cell antigen receptor and antigen into class II peptide-loading compartment is independent of receptor cross-linking. *J. Immunol.* **155**, 4255–63 (1995).
150. Batista, F. D. & Neuberger, M. S. Affinity Dependence of the B Cell Response to Antigen: A Threshold, a Ceiling, and the Importance of Off-Rate. *Immunity* **8**, 751–759 (1998).
151. Rammensee, H.-G., Friede, T. & Stevanović, S. MHC ligands and peptide motifs: first listing. *Immunogenetics* **41**, 178–228 (1995).
152. Karlsson, L. DM and DO shape the repertoire of peptide–MHC–class-II complexes. *Curr. Opin. Immunol.* **17**, 65–70 (2005).
153. Schulze, M.-S. E. & Wucherpfennig, K. W. The mechanism of HLA-DM induced peptide exchange in the MHC class II antigen presentation pathway. *Curr. Opin. Immunol.* **24**, 105–111 (2012).
154. van Ham, S. M. *et al.* HLA-DO is a negative modulator of HLA-DM-mediated MHC class II peptide loading. *Curr. Biol.* **7**, 950–957 (1997).
155. van Ham, M. *et al.* Modulation of the Major Histocompatibility Complex Class II–Associated Peptide Repertoire by Human Histocompatibility Leukocyte Antigen (Hla)-Do. *J. Exp. Med.* **191**, 1127–1136 (2000).
156. Banchereau, J. & Steinman, R. M. Dendritic cells and the control of immunity. *Nature* **392**, 245–52 (1998).
157. Hong, S. *et al.* B Cells Are the Dominant Antigen-Presenting Cells that Activate Naive CD4+ T Cells upon Immunization with a Virus-Derived Nanoparticle Antigen. *Immunity* **49**, 695–708.e4 (2018).
158. Crotty, S. T follicular helper cell differentiation, function, and roles in disease. *Immunity* **41**, 529–42 (2014).
159. Schmitt, N. *et al.* The cytokine TGF- β co-opts signaling via STAT3-STAT4 to promote the differentiation of human TFH cells. *Nat. Immunol.* **15**, 856–65 (2014).
160. Nurieva, R. I. *et al.* Bcl6 mediates the development of T follicular helper cells. *Science (80-.)*. **325**, 1001–1005 (2009).
161. Yu, D. *et al.* The transcriptional repressor Bcl-6 directs T follicular helper cell lineage commitment. *Immunity* **31**, 457–68 (2009).
162. Sage, P. T. & Sharpe, A. H. T follicular regulatory cells. *Immunol. Rev.* **271**, 246–59 (2016).
163. Sage, P. T. & Sharpe, A. H. T follicular regulatory cells in the regulation of B cell responses. *Trends Immunol.* **36**, 410–8 (2015).

164. Natkanski, E. *et al.* B cells use mechanical energy to discriminate antigen affinities. *Science (80-.)*. **340**, 1587–1590 (2013).
165. Shulman, Z. *et al.* Dynamic signaling by T follicular helper cells during germinal center B cell selection. *Science (80-.)*. **345**, 1058–1062 (2014).
166. Boisvert, J., Edmondson, S. & Krummel, M. F. Immunological synapse formation licenses CD40-CD40L accumulations at T-APC contact sites. *J. Immunol.* **173**, 3647–52 (2004).
167. Allen, R. *et al.* CD40 ligand gene defects responsible for X-linked hyper-IgM syndrome. *Science (80-.)*. **259**, 990–993 (1993).
168. Aruffo, A. *et al.* The CD40 ligand, gp39, is defective in activated T cells from patients with X-linked hyper-IgM syndrome. *Cell* **72**, 291–300 (1993).
169. DiSanto, J. P. *et al.* CD40 ligand mutations in X-linked immunodeficiency with hyper-IgM. *Nature* **361**, 541–543 (1993).
170. Fuleihan, R. *et al.* Defective expression of the CD40 ligand in X chromosome-linked immunoglobulin deficiency with normal or elevated IgM. *Proc. Natl. Acad. Sci.* **90**, 2170–2173 (1993).
171. Korthäuer, U. *et al.* Defective expression of T-cell CD40 ligand causes X-linked immunodeficiency with hyper-IgM. *Nature* **361**, 539–41 (1993).
172. Xu, J. *et al.* Mice deficient for the CD40 ligand. *Immunity* **1**, 423–31 (1994).
173. Kawabe, T. *et al.* The immune responses in CD40-deficient mice: Impaired immunoglobulin class switching and germinal center formation. *Immunity* **1**, 167–178 (1994).
174. Han, S. *et al.* Cellular interaction in germinal centers. Roles of CD40 ligand and B7-2 in established germinal centers. *J. Immunol.* **155**, 556–67 (1995).
175. Foy, T. M. *et al.* gp39-CD40 interactions are essential for germinal center formation and the development of B cell memory. *J. Exp. Med.* **180**, 157–163 (1994).
176. Liu, D. *et al.* T-B-cell entanglement and ICOSL-driven feed-forward regulation of germinal centre reaction. *Nature* **517**, 214–8 (2015).
177. Pullen, S. S. *et al.* CD40–Tumor Necrosis Factor Receptor-Associated Factor (TRAF) Interactions: Regulation of CD40 Signaling through Multiple TRAF Binding Sites and TRAF Hetero-Oligomerization. *Biochemistry* **37**, 11836–11845 (1998).
178. Ahonen, C. *et al.* The CD40-TRAF6 axis controls affinity maturation and the generation of long-lived plasma cells. *Nat. Immunol.* **3**, 451–6 (2002).
179. Elgueta, R. *et al.* Molecular mechanism and function of CD40/CD40L engagement in the immune system. *Immunol. Rev.* **229**, 152–72 (2009).
180. Bishop, G. A., Moore, C. R., Xie, P., Stunz, L. L. & Kraus, Z. J. TRAF proteins in CD40 signaling. *Adv. Exp. Med. Biol.* **597**, 131–51 (2007).
181. Dadgostar, H. *et al.* Cooperation of multiple signaling pathways in CD40-regulated gene expression in B lymphocytes. *Proc. Natl. Acad. Sci.* **99**, 1497–1502 (2002).
182. Sutherland, C. L., Heath, A. W., Pelech, S. L., Young, P. R. & Gold, M. R. Differential activation of the ERK, JNK, and p38 mitogen-activated protein kinases by CD40 and the B cell antigen receptor. *J. Immunol.* **157**, 3381–90 (1996).
183. Hostager, B. S., Haxhinasto, S. A., Rowland, S. L. & Bishop, G. A. Tumor Necrosis Factor Receptor-associated Factor 2 (TRAF2)-deficient B Lymphocytes Reveal Novel Roles for TRAF2 in CD40 Signaling. *J. Biol. Chem.* **278**, 45382–45390 (2003).
184. Lee, S. Y. *et al.* TRAF2 Is Essential for JNK but Not NF- κ B Activation and Regulates Lymphocyte Proliferation and Survival. *Immunity* **7**, 703–713 (1997).
185. Gallagher, E. *et al.* Kinase MEKK1 is required for CD40-dependent activation of the kinases Jnk and p38, germinal center formation, B cell proliferation and antibody production. *Nat. Immunol.* **8**, 57–63 (2007).
186. Haxhinasto, S. A. & Bishop, G. A. Synergistic B Cell Activation by CD40 and the B Cell Antigen Receptor. *J. Biol. Chem.* **279**, 2575–2582 (2004).
187. Jabara, H. H. *et al.* The Binding Site for TRAF2 and TRAF3 but Not for TRAF6 Is Essential for CD40-Mediated Immunoglobulin Class Switching. *Immunity* **17**, 265–276 (2002).
188. Jabara, H. H., Weng, Y., Sannikova, T. & Geha, R. S. TRAF2 and TRAF3 independently mediate Ig class switching driven by CD40. *Int. Immunol.* **21**, 477–88 (2009).
189. Bishop, G. A., Warren, W. D. & Berton, M. T. Signaling via major histocompatibility complex class II molecules and antigen receptors enhances the B cell response to gp39/CD40 ligand. *Eur. J. Immunol.* **25**, 1230–8 (1995).

190. Ersching, J. *et al.* Germinal Center Selection and Affinity Maturation Require Dynamic Regulation of mTORC1 Kinase. *Immunity* **46**, 1045-1058.e6 (2017).
191. Niu, H., Ye, B. H. & Dalla-Favera, R. Antigen receptor signaling induces MAP kinase-mediated phosphorylation and degradation of the BCL-6 transcription factor. *Genes Dev.* **12**, 1953–61 (1998).
192. Yasuda, T. *et al.* B cell receptor-ERK1/2 signal cancels PAX5-dependent repression of BLIMP1 through PAX5 phosphorylation: a mechanism of antigen-triggering plasma cell differentiation. *J. Immunol.* **188**, 6127–34 (2012).
193. Crotty, S. Follicular Helper CD4 T Cells (T_{FH}). *Annu. Rev. Immunol.* **29**, 621–663 (2011).
194. Weinstein, J. S. *et al.* TFH cells progressively differentiate to regulate the germinal center response. *Nat. Immunol.* **17**, 1197–205 (2016).
195. Gonzalez, D. G. *et al.* Nonredundant Roles of IL-21 and IL-4 in the Phased Initiation of Germinal Center B Cells and Subsequent Self-Renewal Transitions. *J. Immunol.* **201**, 3569–3579 (2018).
196. Levy, D. E. & Darnell, J. E. Stats: transcriptional control and biological impact. *Nat. Rev. Mol. Cell Biol.* **3**, 651–62 (2002).
197. Avery, D. T. *et al.* B cell-intrinsic signaling through IL-21 receptor and STAT3 is required for establishing long-lived antibody responses in humans. *J. Exp. Med.* **207**, 155–71 (2010).
198. Deenick, E. K. *et al.* Naive and memory human B cells have distinct requirements for STAT3 activation to differentiate into antibody-secreting plasma cells. *J. Exp. Med.* **210**, 2739–53 (2013).
199. Lischke, A. *et al.* The Interleukin-4 Receptor Activates STAT5 by a Mechanism That Relies upon Common γ -Chain. *J. Biol. Chem.* **273**, 31222–31229 (1998).
200. Rolling, C., Treton, D., Pellegrini, S., Galanaud, P. & Richard, Y. IL4 and IL13 receptors share the γ c chain and activate STAT6, STAT3 and STAT5 proteins in normal human B cells. *FEBS Lett.* **393**, 53–56 (1996).
201. Ding, B. B., Bi, E., Chen, H., Yu, J. J. & Ye, B. H. IL-21 and CD40L synergistically promote plasma cell differentiation through upregulation of Blimp-1 in human B cells. *J. Immunol.* **190**, 1827–36 (2013).
202. Ettinger, R. *et al.* IL-21 induces differentiation of human naive and memory B cells into antibody-secreting plasma cells. *J. Immunol.* **175**, 7867–79 (2005).
203. Ozaki, K. *et al.* Regulation of B cell differentiation and plasma cell generation by IL-21, a novel inducer of Blimp-1 and Bcl-6. *J. Immunol.* **173**, 5361–71 (2004).
204. Zotos, D. *et al.* IL-21 regulates germinal center B cell differentiation and proliferation through a B cell-intrinsic mechanism. *J. Exp. Med.* **207**, 365–78 (2010).
205. Linterman, M. A. *et al.* IL-21 acts directly on B cells to regulate Bcl-6 expression and germinal center responses. *J. Exp. Med.* **207**, 353–363 (2010).
206. Bryant, V. L. *et al.* Cytokine-mediated regulation of human B cell differentiation into Ig-secreting cells: predominant role of IL-21 produced by CXCR5+ T follicular helper cells. *J. Immunol.* **179**, 8180–90 (2007).
207. Scheeren, F. A. *et al.* STAT5 regulates the self-renewal capacity and differentiation of human memory B cells and controls Bcl-6 expression. *Nat. Immunol.* **6**, 303–13 (2005).
208. Baumjohann, D. *et al.* Persistent antigen and germinal center B cells sustain T follicular helper cell responses and phenotype. *Immunity* **38**, 596–605 (2013).
209. Deenick, E. K. *et al.* Follicular helper T cell differentiation requires continuous antigen presentation that is independent of unique B cell signaling. *Immunity* **33**, 241–53 (2010).
210. Tubo, N. J. *et al.* Single Naive CD4+ T Cells from a Diverse Repertoire Produce Different Effector Cell Types during Infection. *Cell* **153**, 785–796 (2013).
211. Tubo, N. J. & Jenkins, M. K. TCR signal quantity and quality in CD4+ T cell differentiation. *Trends Immunol.* **35**, 591–596 (2014).
212. de Jong, H. Modeling and simulation of genetic regulatory systems: a literature review. *J. Comput. Biol.* **9**, 67–103 (2002).
213. Linke, C. *et al.* A Clb/Cdk1-mediated regulation of Fkh2 synchronizes CLB expression in the budding yeast cell cycle. *npj Syst. Biol. Appl.* **3**, 7 (2017).
214. N. Kolodkin, A. *et al.* ROS networks: designs, aging, Parkinson's disease and precision therapies. *npj Syst. Biol. Appl.* **6**, 34 (2020).
215. Ay, A. & Arnosti, D. N. Mathematical modeling of gene expression: a guide for the perplexed biologist. *Crit. Rev. Biochem. Mol. Biol.* **46**, 137–151 (2011).
216. Merino Tejero, E. *et al.* Multiscale Modeling of Germinal Center Recapitulates the Temporal Transition From Memory B Cells to Plasma Cells Differentiation as Regulated by Antigen Affinity-Based Tfh Cell Help. *Front. Immunol.* **11**, 1–15 (2021).

217. Meyer-Hermann, M. Does recycling in germinal centres exist? *Immunol. Cell Biol.* **80**, 30–35 (2002).
218. Meyer-Hermann, M. A mathematical model for the germinal center morphology and affinity maturation. *J. Theor. Biol.* **216**, 273–300 (2002).
219. Chtanova, T. *et al.* T Follicular Helper Cells Express a Distinctive Transcriptional Profile, Reflecting Their Role as Non-Th1/Th2 Effector Cells That Provide Help for B Cells. *J. Immunol.* **173**, 68–78 (2004).
220. Barberis, M., Helikar, T. & Verbruggen, P. Simulation of Stimulation: Cytokine Dosage and Cell Cycle Crosstalk Driving Timing-Dependent T Cell Differentiation. *Front. Physiol.* **9**, 879 (2018).
221. Puniya, B. L. *et al.* Integrative computational approach identifies drug targets in CD4+ T-cell-mediated immune disorders. *npj Syst. Biol. Appl.* **7**, 4 (2021).

Chapter 3

Human B cells engage the NCK/PI3K/RAC1 axis to internalize large particles via the IgM-BCR

Niels J.M. Verstegen^{1,3,†}, Peter-Paul A. Unger^{1,†}, Julia Z. Walker¹, Benoit P. Nicolet¹, Tineke Jorritsma¹, Jos van Rijssel², Robbert M. Spaapen¹, Jelle de Wit¹, Jaap D. van Buul², Anja ten Brinke¹, and S. Marieke van Ham^{1,4}

Frontiers in Immunology 10:1-14 (2019)

1. Department of Immunopathology, Sanquin Research and Landsteiner Laboratory, Amsterdam University Medical Centers, University of Amsterdam, Amsterdam, The Netherlands
2. Molecular Cell Biology, Sanquin Research, Amsterdam, The Netherlands, and Landsteiner Laboratory, Amsterdam UMC, University of Amsterdam, Amsterdam, The Netherlands.
3. Synthetic Systems Biology and Nuclear Organization, Swammerdam Institute for Life Sciences, University of Amsterdam, Amsterdam, The Netherlands.
4. Swammerdam Institute for Life Sciences, University of Amsterdam, Amsterdam, The Netherlands.

† Both authors contributed equally

ABSTRACT

Growing evidence indicates that large antigen-containing particles induce potent T cell-dependent high-affinity antibody responses. These responses require large particle internalization after recognition by the B cell receptor (BCR) on B cells. However, the molecular mechanisms governing BCR-mediated internalization remain unclear. Here we use a high-throughput quantitative image analysis approach to discriminate between B cell particle binding and internalization. We systematically show, using small molecule inhibitors, that human B cells require a SYK-dependent IgM-BCR signaling transduction via PI3K to efficiently internalize large anti-IgM-coated particles. IgM-BCR-mediated activation of PI3K involves both the adaptor protein NCK and the co-receptor CD19. Interestingly, we here reveal a strong NCK-dependence without profound requirement of the co-receptor CD19 in B cell responses to large particles. Furthermore, we demonstrate that the IgM-BCR/NCK signaling event facilitates RAC1 activation to promote actin cytoskeleton remodeling necessary for particle engulfment. Thus, we establish NCK/PI3K/RAC1 as an attractive IgM-BCR signaling axis for biological intervention to prevent undesired antibody responses to large particles.

INTRODUCTION

The first step in induction of antibody production is binding of external antigen to the B cell receptor (BCR) on naive B cells. BCR ligation by antigen results in BCR-mediated transmembrane signaling and antigen internalization, followed by proteolytic degradation and presentation of antigen-derived peptides through major histocompatibility complex class II (MHCII) molecules on the B cell plasma membrane¹⁻³. MHCII/antigen complexes are recognized by antigen-specific T cell receptors expressed by CD4⁺ T cells⁴. After formation of a stable antigen-specific interaction, B cells receive help from CD4⁺ T cells via co-stimulatory molecules and soluble cytokines to promote B cell differentiation into high-affinity antibody-producing plasma cells during germinal center (GC) reactions in secondary lymphoid organs.

The BCR consists of a membrane-bound immunoglobulin associated with a CD79a and CD79b heterodimer containing intracellular immunoreceptor tyrosine activation motifs (ITAMs)⁵. Upon cognate antigen recognition, phosphorylation of the ITAMs is initiated by the SRC family kinase LYN and spleen tyrosine kinase (SYK)⁶⁻⁸. These phosphorylated motifs recruit several adaptor and effector proteins that make up the signalosome, containing SYK, B cell linker (BLNK), bruton's tyrosine kinase (BTK), phospholipase C- γ 2 (PLC γ 2) and the co-receptor CD19. The signalosome drives activation of multiple downstream effector pathways to amplify the signal from the BCR that results in changes in cell metabolism, gene expression, and cytoskeletal organization. Many of proteins required for transmembrane signaling are also involved in antigen internalization and the subsequent intracellular trafficking of the antigen-BCR complex⁹. Most studies describing signaling components and molecular mechanisms that control BCR-mediated antigen internalization use small soluble antigens or antigen tethered to planer lipid bilayer surfaces or plasma membrane sheets that is extracted though force-dependent extraction or enzymatic liberation¹⁰⁻¹³. B cells are, however, also able to internalize large particles. This ability has long been disregarded, but in recent years, multiple groups, including our own, have demonstrated the existence of this cell biological process for internalization of large particles including anti-IgM-coated bacteria and beads¹⁴⁻¹⁷. The physiological importance of this pathway was recently demonstrated by showing that internalization of large particles by follicular B cells resulted in a strong GC response and the generation of high-affinity class-switched antibodies in mice¹⁶. Of added importance in large particle uptake is the process of epitope spreading. Epitope spreading is a process in which antigens distinct from the antigen that was recognized by the antigen-specific BCR are presented on the B cells plasma membrane¹⁸⁻²⁰. As such, B cells and CD4⁺ T cells with different specificity can interact to drive the ongoing immune response. This process is highly desirable if it targets foreign antigens during infection to broadening the B cell response. In contrast, in cases of self-reactivity in autoimmune reactions or alloimmunization against transfused blood products, epitope spreading is a clinical problem in much need of targeted therapy.

Here we investigated the molecular mechanisms that mediate internalization and antigen presentation of large particles in human B cells. A high-throughput quantitative image analysis

approach was employed using inactivated anti-IgM-coated *Salmonella typhimurium* as a model particle to quantify IgM-BCR-mediated internalization. We show that phosphoinositide-3 kinase (PI3K) is the main driver of actin-dependent large particle acquisition by human B cells. IgM-BCR-mediated activation of PI3K involves both the adaptor protein NCK and the co-receptor CD19²¹⁻²⁴. We demonstrate that the IgM-BCR/NCK axis is required for internalization of large particles in human B cells. This axis drives internalization via activation of the actin cytoskeleton modulator RAC1. Collectively, our data reveal that the NCK-PI3K-RAC1 axis is essential to mount a humoral immune response to large particles.

MATERIALS AND METHODS

Purification of CD19⁺ B and CD4⁺ T cells

Human buffy coats were obtained from healthy blood donors after informed consent, in accordance with the protocol of the local institutional review board, the Medical Ethics Committee of Sanquin Blood Supply, and conforms to the principles of the Declaration of Helsinki. Peripheral blood mononuclear cells (PBMCs) were isolated through standard gradient centrifugation using Ficoll-lymphoprep (Axis-Shield). CD19⁺ B cells and CD4⁺ T cells were purified from PBMCs with anti-CD19 and anti-CD4 Dynabeads, respectively, and DETACHaBEAD (Invitrogen) following the manufacturer's instructions. Purity was typically greater than 98% as assessed by flow cytometry.

Cell cultures

HEK293T cells were grown in IMDM (Lonza) supplemented with 10% fetal calf serum (FCS; Bodinco), 100 U/ml penicillin and 100 µg/ml streptomycin (Thermo Fisher Scientific). Ramos B cells were grown in B cell medium that consists of RPMI 1640 medium (Life Technologies) supplemented with 5% FCS, 100 U/ml penicillin and 100 µg/ml streptomycin, 2 mM L-glutamine (Invitrogen), 50 µM β-mercaptoethanol (Sigma) and 20 µg/ml human apotransferrin (Sigma; depleted for human IgG with protein G Sepharose (Amersham Biosciences)). The HLA-DOβ-GFP Ramos cell line has been described before¹⁷ and was cultured in B cell medium in the presence of 2 mg/ml G418 (Life Technologies).

gRNA design and plasmids

Guide sequences with homology to CD19 (5'-AAGCGGGACTCCCCGAGACC-3'), NCK1 (5'-GGTCATAGAGACGTTCCCCT-3') and NCK2 (5'-CGGTACATAGCCCGTCCTGT-3') were designed using CRISPR design, and subsequently cloned into the lentiCRISPRv2 backbone containing puromycin resistance gene²⁵. The Lifeact-GFP and DORA RAC1-sensor constructs in a lentiviral backbone have been described before^{26,27}.

Lentiviral vector construction

Lentiviral vectors were produced by co-transfecting HEK293T cells with the lentiviral transfer plasmids gRNA/Cas9-expressing lentiCRISPRv2, Lifeact-GFP or DORA RAC1-sensor, and the packaging plasmids pVSVg, psPAX2 and pAdv^{28,29} using polyethylenimine (PEI, Polysciences). Virus-containing supernatant was harvested 48 and 72 hours after transfection, then frozen and stored in -80 °C.

Cell lines and transduction

Transduction of lentiviral vector into Ramos B cells was performed with 8 µg/ml protamine sulfate (Sigma). CRISPR-mediated knockout cells were enriched by culturing in B cell medium supplemented with 1-2 µg/ml puromycin (Invitrogen). CD19 knockout Ramos B cells were purified using a FACSAria II (BD Bioscience). For this, cells were washed and then stained with anti-CD19 APC (clone SJ25-C1; BD Bioscience) in phosphate buffered saline (PBS; Fresenius Kabi) supplemented with 0.1% bovine serum albumin (BSA; Sigma). The NCK1/2 double-knockout cell line was obtained by single cell sorting using a FACSAria II (BD Bioscience). After clonal expansion, cells were screened for complete knockout using an immunoblot assay (as described below). Ramos B cells that stably expressed Lifeact-GFP or RAC1 biosensor were sorted by flow cytometry-based sorting using a FACSAria II (BD Bioscience).

Serum preparation

Blood samples were drawn from healthy volunteers after informed consent (Sanquin). Serum was obtained by collecting blood, allowing it to clot for 1 hour at room temperature (RT) and collecting the supernatant after centrifugation at 3,000 rpm for 15 minutes. Serum of sixteen healthy donors was mixed and stored in small aliquots at -80 °C to avoid repetitive freeze/thawing.

Labeling of antibodies and beads

Mouse monoclonal anti-human IgG (MH16-1; Sanquin Reagents), mouse monoclonal anti-human C3d (C3-19; Sanquin Reagents) and mouse monoclonal anti-human IgM (MH15-1, Sanquin Reagents) were labeled with DyLight 650, DyLight 488 or DyLight 405, respectively, according to manufacturer's instructions (Thermo Fisher Scientific). To get rid of excess dye, the antibodies were washed extensively using an Amicon Ultra centrifugal filter (10K; Merck Milipore). The labeling rate was around 7 fluorochromes per antibody, as determined by UV-VIS spectroscopy on a Nanodrop ND1000 spectrophotometer (Thermo Scientific).

Goat-anti-mouse IgG (Fc) polystyrene beads (3µm, Spherotech) were washed twice with PBS containing 0.1% BSA and labeled overnight with anti-human IgM-DyLight405. The beads were stored at 4 °C until further use. Before use, the beads were washed twice with PBS supplemented with 0.1% normal mouse serum (in house), and once with PBS supplemented with 0.1% BSA.

Bacterial strains

Salmonella typhimurium SL1344 has been described before³⁰. *S. typhimurium* SL1344 that constitutively express the dsRed protein were generated by electroporating bacteria with a pMW211 plasmid. Bacteria were grown overnight shaking at 37 °C in Luria-Bertani (LB) medium broth with 50 µg/ml carbenicillin (Invitrogen). To reach mid-log growth phase, the overnight grown bacteria were diluted 1/33 in fresh LB medium and incubated at 37 °C for 3 hours while shaking. Subsequently, bacteria were washed twice with PBS and inactivated through incubation at 65 °C for 15 minutes, or through incubation with 4% paraformaldehyde (PFA; Sigma) in PBS for 20 minutes. To block the free aldehyde groups of PFA, bacteria were incubated with 0.02 M glycine (Merck). Mouse monoclonal anti-human IgM (Fc) (clone MH15-1; Sanquin) or mouse monoclonal anti-human CD19 (clone LT19; Miltenyi Biotec) was mixed with mouse monoclonal anti-*S. typhimurium* LPS (clone 1E6; Bidesign International) and rat anti-mouse IgG1 (clone RM161-1; Sanquin) to generate anti-LPS/IgM^{17,31–33} or anti-LPS/CD19 antibody complexes. Inactivated bacteria were coated with these antibody complexes in the dark for 30 minutes, while rotating. Subsequently, the bacteria were washed with PBS and kept at 4 °C until further use.

For complement/antibody opsonization, *S. typhimurium* was incubated with 10% freshly thawed or heat-inactivated serum in PBS supplemented with 10 mM CaCl₂ and 2 mM MgCl₂ at 37 °C for 30 minutes. Heat-inactivation of the serum was performed by incubation at 56 °C for 30 minutes. After incubation, bacteria were washed thoroughly with PBS to wash away all non-bound serum components. To assess *S. typhimurium*-reactive antibody and complement opsonization, bacteria were washed and stained with anti-human IgG-DyLight650 and anti-human C3d-DyLight488 in PBS supplemented with 0.1% BSA for 20 minutes in the dark at RT and measured on a FACSCanto II (BD Bioscience). The acquired data was analyzed using FlowJo Software version 10 (Tree Star).

Soluble anti-IgM or large particle challenge

Primary human B cells or Ramos B cells were left untreated or incubated with vehicle (DMSO) or small molecule inhibitors (Supplementary Table 1) in B cell medium without antibiotics for 15 minutes at 37 °C. Subsequently, cells were incubated with soluble anti-IgM (5 µg/ml), uncoated or antibody complex-coated PFA-inactivated *S. typhimurium*, or anti-IgM-coated 3µm polystyrene beads for 30 minutes at 37 °C. Ice cold PBS was added to halt internalization. Alternatively, B cells were incubated with anti-IgM-coated PFA-inactivated *S. typhimurium* for 30 minutes in B cell medium without antibiotics on ice to allow particle binding but not internalization (**Figures 3F-G; Figures 5G and 5H**). Subsequently, the B cells were washed extensively to remove unbound particles, then incubated at 37 °C for the time indicated, after which ice cold PBS was added to halt internalization.

ImageStream^x analysis

Cells were stained with anti-HLA-DR APC (clone L243; BD Bioscience) in PBS supplemented with 0.1% BSA for 30 minutes in the dark on ice and fixed for 20 minutes in PBS with 4% PFA. Primary human B cells or Ramos B cells were washed and 4',6'-diamidino-2-phenylindole (DAPI; Sigma) was added to stain the cell nucleus. Large particle internalization by human B cells was evaluated on an ImageStream^x mark II imaging flow cytometer (Merck). The acquired data was analyzed using IDEAS V6.2 Software (Merck) and FlowJo Software version 10 (**Supplementary Figure 1A; Supplementary Figure 4**).

CD4⁺ T cell proliferation assay

Primary human B cells were incubated with vehicle (DMSO) or small molecule inhibitors (Supplementary Table 1) for 15 minutes at 37 °C before being challenged with uncoated (control) or anti-IgM-coated heat-inactivated *S. typhimurium*. Heat-inactivated *S. typhimurium* was used instead of PFA-inactivated *S. typhimurium* to allow antigenic peptide presentation. B cells were primed with *S. typhimurium* for 30 minutes at 37 °C and then washed in medium containing 100 µg/ml gentamicin (Invitrogen) to eliminate non-internalized bacteria¹⁷. To allow antigenic peptide presentation, cells were cultured in B cell medium with 10 µg/ml gentamicin, supplemented with small molecule inhibitors (Supplementary Table 1) for 20 hours at 37 °C/5% CO₂. Subsequently, *S. typhimurium*-primed B cells were washed extensively and irradiated with 60 Gy to halt antigen processing before incubation with autologous CD4⁺ T cells that were labelled with Cell Trace CFSE according to manufacturer's instructions (Invitrogen). 10x10⁴ B cells and 5x10⁴ CD4⁺ T cells were cocultured in 200 µl B cell medium at 37 °C/5% CO₂ in 96-well round-bottom plates (Greiner Bio-One) for 6 days. Cells were then stained with anti-CD4 APC (clone SK3; BD Bioscience) to separate CD4⁺ T cells from the remaining CD19⁺ B cells and CD4⁺ T cell proliferation was measured on a FACSLSR II (BD Bioscience). DAPI was added to exclude dead cells. The acquired data was analyzed using FlowJo Software version 10.

Lifeact-imaging

For confocal laser scanning microscopy analysis, Lab-Tec 8-well chamber slides (Thermo Fisher Scientific) were coated with 1 mg/ml poly-lysine (Sigma) for 1 hour, washed thoroughly with Aquadest and air-dried. Ramos B cells expressing Lifeact-GFP were allowed to bind to the coated slides for 15 minutes at 37 °C before being challenged with anti-human IgM-coated polystyrene beads (3 µm). For real-time imaging a LEICA TCS SP8 confocal microscope system equipped with a 63 x 1.4 NA oil objective and 405 nm diode, 488 nm argon, 594 nm HeNe and 633 nm HeNe laser, was used. Images were processed using ImageJ software (National Institutes of Health).

Fluorescence Resonance Energy Transfer (FRET)-based biosensor analysis

RAC1 activity was measured in Ramos B cells after stimulation with anti-IgM-coated *S. typhimurium* by monitoring yellow fluorescent protein (YFP) FRET over donor cyan fluorescent protein (CFP) intensities as described before²⁷. Lab-Tec 8-well chamber slides were prepared as described above. A Zeiss Observer Z1 microscope equipped with a 63x NA1.3 oil immersion objective, an HXP 120-V excitation light source, a Chroma 510 DCSP dichroic splitter, and two Hamamatsu ORCA-R2 digital charge-coupled device cameras was used for simultaneous monitoring Cerulean3 and Venus emission. Zeiss Zen 2012 microscope software was used to control the system. Offline ratio analyses between Cerulean3 and Venus images were processed using the ImageJ software. Image stacks were background corrected, stacks were aligned, and a smooth filter was applied to both image stacks to improve image quality by reducing noise. FRET ratios were bleed-through corrected (62%) for the CFP leakage into the YFP channel. An image threshold was applied exclusively to the Venus image stack, converting background pixels to 'not a number' (NaN) allowing elimination of artifacts in ratio image stemming from the background noise. Finally, the Venus/Cerulean3 ratio was calculated and the Parrot-2 look-up table (created by dr. J. Goedhart) was applied to generate a heatmap.

Immunoblot analysis

Ramos B cells (10×10^6) were lysed in 50 mM Tris, pH 7.6, 20 mM $MgCl_2$, 150 mM NaCl, 1% (v/v) Triton X-100, 0.5% (w/v) deoxycholic acid (DOC) and 0.1% (w/v) SDS supplemented with a phosphatase inhibitor cocktail (Sigma) and fresh protease-inhibitor-mixture tablets (Roche Applied Science). Cell lysates were then centrifuged at 14,000 rpm for 15 minutes at 4 °C, and supernatants were recovered and boiled in SDS sample buffer containing 4% β -mercaptoethanol. Samples were analyzed using 12.5% SDS-Page. Proteins were transferred onto a 0.2 μ m nitrocellulose membrane (Whatman), subsequently membranes were blocked with 5% (w/v) BSA (**Figure 2E; Figure 3K**) or 5% (w/v) milk powder (**Figure 3B; Figure 5G**) in Tris-buffered saline with Tween 20 (TBST). The nitrocellulose membrane was incubated for 1 hour at RT with mouse monoclonal anti-NCK (clone 108; BD Bioscience), rabbit polyclonal anti-cofilin (cat #ab42823; Abcam), rabbit polyclonal anti-pAKT (Ser473) (cat #9271; Cell Signaling Technology) or rabbit monoclonal anti-AKT (pan) (clone C67E7; Cell Signaling Technology), followed by incubation for 1 hour at RT with HRP-conjugated rat monoclonal anti-mouse kappa (RM-19; Sanquin Reagents) or HRP-conjugated goat anti-rabbit IgG (cat #ab205718; Abcam) in TBST. Between the incubation steps, the membranes were washed with TBST. Antibody staining was visualized with the Pierce enhanced chemiluminescence (ECL) 2 Western Blotting substrate kit (Thermo Fisher Scientific) according to manufacturer's instructions and analyzed using ChemiDoc MP System (BioRad). Brightness/contrast parameters were adjusted globally across the entire image using Image Lab software (BioRad).

RacGTP pulldown assay

Cells were lysed in 50 mM Tris, pH 7.6, 20 mM MgCl₂, 150 mM NaCl, 1% (v/v) Triton X-100, 0.5% (w/v) DOC and 0.1% (w/v) SDS supplemented with protease inhibitors. Cell lysates were then centrifuged at 14,000 rpm for 15 minutes at 4 °C. Supernatants were recovered and GTP-bound RAC1 was isolated by rotating supernatants at 4 °C for 30 minutes with 5 µg biotinylated PAK-CRIB peptide coupled to streptavidin agarose as described before²⁷. Beads were centrifuged at 5,000 rpm for 20 seconds at 4 °C, washed five times in 50 mM Tris, pH 7.6, 10 mM MgCl₂, 150 mM NaCl, 1% (v/v) Triton X-100 and boiled in SDS-sample buffer containing 4% β-mercaptoethanol. Samples were then analyzed by 12.5% SDS-Page as described in the immunoblot section above using mouse monoclonal anti-RAC1 (clone 102; BD Transduction Laboratories) and HRP-conjugated rat monoclonal anti-mouse kappa (RM-19; Sanquin Reagents).

Statistical analyses

Statistical analyses were performed using Prism 7 (Graphpad). The statistical tests used are indicated in the figure descriptions. Differences were considered statistically significant when $p \leq 0.05$.

RESULTS

Internalization of large particles by primary human B cells is mediated via the IgM-B cell receptor (BCR) and not by antibody and complement receptors

To evaluate internalization of large particles by primary human B cells, a high-throughput quantitative image analyses approach was established using ImageStream^x, as this combines visual analysis with the statistical power of flow cytometry. Inactivated *Salmonella typhimurium* was used as a model particle. Primary human B cells isolated from blood displayed a low proportion of B cells associating with our model particle (**Figure 1A**), in line with the low numbers of primary human B cells expressing a BCR that specifically binds *S. typhimurium*, as observed before¹⁷. *S. typhimurium* was coated with a monoclonal antibody specific for immunoglobulin M (anti-IgM) allowing association irrespective of the B cells antigen specificity. Indeed, anti-IgM coating markedly enhanced particle binding as compared with uncoated control (**Figure 1A**). Subsequently, a custom feature was generated to quantify the relative particle internalization distance into B cells, only taking cells into account in which both particle and B cell were imaged in the same focal plane (**Figures 1B and 1C; Supplementary Figures 1A and 1B**). This allowed us to distinguish between B cells having membrane-bound particles from B cells that completely internalized the particles (**Figures 1C and 1D**). Using this approach, we demonstrated that IgM-BCR-mediated internalization of large antigen-coated particles occurred within 30 minutes of incubation with primary human B cells (**Figure 1E**), confirming earlier observations^{17,31}. To validate this property of the IgM-BCR in large particle internalization, particles were opsonized

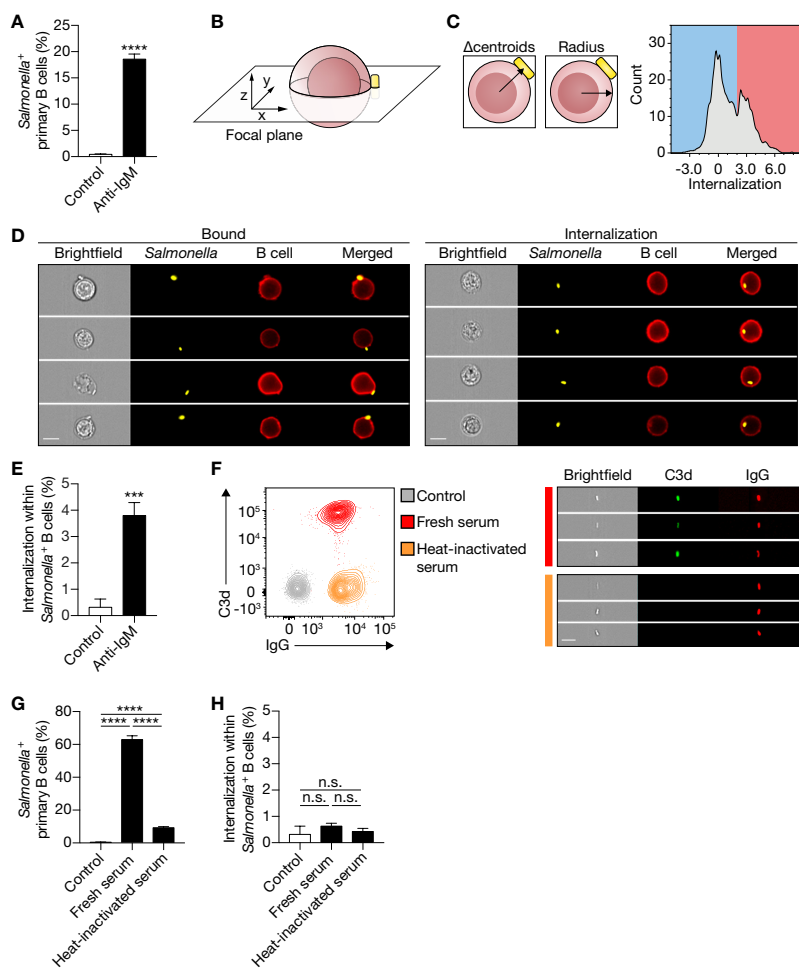


Figure 1 | IgM-BCR stimulation specifically promotes large particle internalization. (A) Proportion of primary human B cells interacting with control or anti-IgM-coated *S. typhimurium* ($n = 9$). (B) Schematics of a B cell:*S. typhimurium* interaction. Internalization was assessed using a high-throughput quantitative image analysis approach for *S. typhimurium* located in the same focal plane as the human B cell only. (C) To discriminate between bound and internalized *S. typhimurium*, analysis masks were generated to determine the center of both the B cell and *S. typhimurium*. Internalization was defined as the distance between the two centroids (left) after correction for the B cell radius as a measure for the cell size (middle). Internalization was plotted against the event count (right). The red/blue shadings behind the plot indicate the portion of cells that bound (blue) or internalized (red) large particles. Events that had a calculated value similar to or greater than 2 were defined as being internalized. (D) Representative images of primary human B cells containing bound (left) or internalized (right) *S. typhimurium*. Bar, 7mm. (E) Proportion of internalization of control or anti-IgM-coated *S. typhimurium* within Salmonella⁺ primary human B cells ($n = 9$). (F) Representative plots (left) and images (right) of *S. typhimurium* opsonized with antibodies (IgG) or together with complement (C3d) derived from human serum. Bar, 7mm. (G-H) Proportion of primary human B cells that interacted with (G) and internalized (H) serum-opsonized *S. typhimurium* ($n = 9$). Bars depict mean values and error bars are SEM. ***, $P < 0.001$; ****, $P < 0.0001$; n.s., not significantly different by paired t test (A, E) or repeated-measures one-way ANOVA with Sidak post-test (G-H).

with serum derived complement and/or antibodies to bind complement- and Fc γ receptors expressed by primary human B cells, respectively (**Figure 1F**; **Supplementary Figure 2**). Interestingly, complement and antibody opsonization both mediate particle binding (**Figure 1G**), but did not facilitate internalization (**Figure 1H**). Together, these data demonstrate that large particle internalization by human B cells is specifically induced after IgM-BCR-mediated particle binding.

SYK and PI3K are important signaling components to mediate IgM-BCR-mediated particle internalization

To understand the mechanism by which human B cells facilitate IgM-BCR-mediated internalization of large particles, small molecule inhibitors that decrease activity of signaling proteins downstream of the IgM-BCR were used. Two major players in the signaling cascade downstream of the IgM-BCR include SRC-family protein tyrosine kinase LYN and SYK, which both mediate phosphorylation of conserved ITAMs contained within the cytoplasmic domains of CD79a and CD79b associated with the IgM-BCR^{34,35}. The LYN inhibitor SU6656 did not affect internalization by primary human B cells (**Figure 2A**), whereas the SYK inhibitor piceatannol significantly reduced internalization (**Figure 2B**), suggesting that large particle uptake is SYK-dependent. A well-known signaling protein that becomes activated after SYK recruitment to the IgM-BCR is PI3K³⁶. The PI3K inhibitors PI103 and LY294002 significantly reduced internalization of large anti-IgM-coated particles in both primary and Ramos B cells (**Figures 2C and 2D**). In line with the fact that PI3K drives AKT phosphorylation³⁷, inhibition of SYK or PI3K abrogated phosphorylation of AKT at S473 after stimulation with anti-IgM-coated *S. typhimurium* (**Figure 2E**). In contrast, inhibition of AKT did not affect large particle internalization, indicating that although being activated AKT is not essential for internalization (**Figures 2D and 2F**). In addition, inhibition of BTK known to amplify the signal from the IgM-BCR also did not affect large particle internalization, both in primary B cells and in the Ramos B cell line (**Figures 2D and 2G**). To assess potential involvement of bacterial virulence factors or pathogen associated molecular patterns (PAMPs) that may engage additional receptors to affect IgM-BCR signaling pathways, inert polystyrene beads were coated with anti-IgM. Anti-IgM-coated polystyrene beads were internalized by Ramos B cells similar to anti-IgM-coated *S. typhimurium* (**Figure 2D**). Additionally, internalization of polystyrene beads was equally dependent on SYK and PI3K as compared to anti-IgM-coated *S. typhimurium* indicative of a shared mechanism underlying large particle internalization (**Figure 2D**). Together, these data systematically show that IgM-BCR-mediated uptake of large particles by human B cells is initiated by SYK and requires activation of PI3K irrespective of downstream signaling through AKT or BTK.

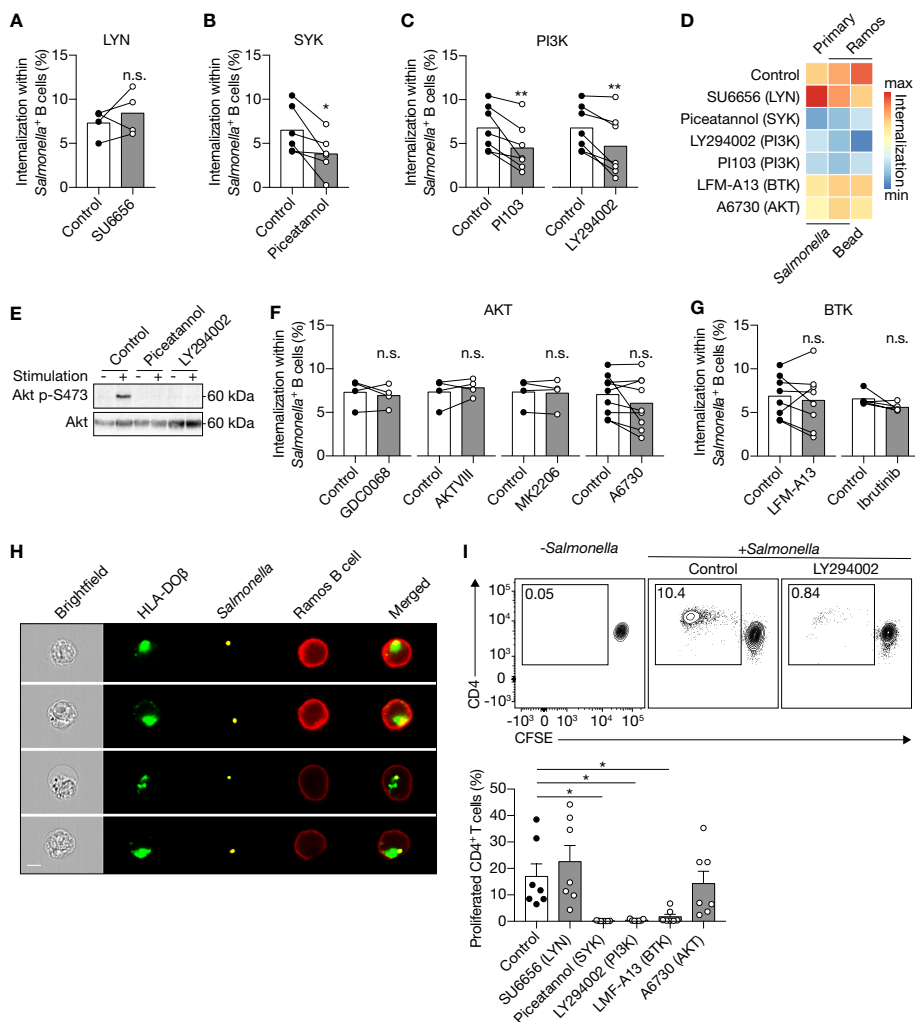


Figure 2 | IgM-BCR-mediated signaling through SYK and PI3K facilitate large particle internalization. (A–C) Proportion of internalization within *S. typhimurium*+ primary human B cells after treatment with inhibitors of LYN (A; n = 4), SYK (B; n = 6) or PI3K (C; n = 7). (D) Heatmap of the mean proportion of internalization within *S. typhimurium*+ or 3 μ m polystyrene bead+ primary human B cells and Ramos B cells after treatment with inhibitors of LYN, SYK, PI3K, BTK or AKT. Heatmap colors indicate effect on internalization. (E) Immunoblot of whole cell extracts from Ramos B cells that were unstimulated (-) or stimulated (+) with *S. typhimurium* after incubation with inhibitors of SYK (Piceatannol) or PI3K (LY294002). The blots were probed with specific antibodies for pAKT at S473 and AKT. (F–G) Proportion of internalization within *S. typhimurium*+ primary human B cells after treatment with inhibitors of AKT (F; n = 4 and 9) or BTK (G; n = 8 and 5). (H) Representative images of Ramos B cells expressing GFP-tagged HLA-DO β having internalized *S. typhimurium*. *S. typhimurium*-containing phagosomes localize to the HLA-DO β -containing MHC class II-antigen loading compartments. Bar, 7 μ m. (I) Representative plots (top) and quantification (bottom) of the proportion of proliferated CD4+ T cells after co-culture with *S. typhimurium*-primed autologous primary human B cells that were treated with inhibitors (n = 7). All data points represent the mean of an individual experiment with duplicate measurements. Error bars indicate SEM. *, P < 0.05; **, P < 0.01; n.s., not significantly different by paired t test (A, B, C, F, G) or repeated-measures one-way ANOVA with Dunnett's post-test (I).

Inhibition of large particle uptake impairs presentation to CD4⁺ T cells

Visualization of internalization of large particles by Ramos B cells revealed that after uptake the particle-containing phagosomes colocalized with HLA-DOB-containing MHC class II antigen-loading compartments (**Figure 2H**). To establish whether large particle internalization by primary human B cells led to MHC class II antigen-derived peptide loading and presentation, we assessed their capacity to stimulate autologous CD4⁺ T cells. Particle-primed, but not control primary human B cells induced CD4⁺ T cell proliferation (**Figure 2I**). Consistent with the effects on large particle internalization, inhibition of SYK and PI3K, in contrast to LYN and AKT in primary human B cells diminished the ability of particle-primed B cells to activate CD4⁺ T cells (**Figure 2I**). Of note, while BTK inhibition did not affect antigenic particle internalization (**Figure 2G**), it did significantly abolish CD4⁺ T cells activation (**Figure 2I**), suggesting that BTK is involved in antigen presentation after large particle internalization.

Large particle induced IgM-BCR activation of PI3K strongly depends on the adaptor protein NCK

PI3K can be activated through two pathways after IgM-BCR-mediated recognition of antigen. Direct signaling downstream of the IgM-BCR is propagated by the adaptor protein NCK via B cell adaptor for PI3K (BCAP) bound to PI3K²¹. Alternatively, the activation of PI3K has been shown to be mediated by CD19 as part of the IgM-BCR co-receptor complex²²⁻²⁴. To determine which pathway is involved in PI3K-driven uptake of large anti-IgM-coated particles by B cells, CD19 and NCK knockout (KO) Ramos B cells were generated using CRISPR-Cas9 (**Figures 3A and 3B**). Plasma membrane IgM expression was not affected upon CD19 or NCK KO (**Figure 3C**). Targeting of the large particle to the co-receptor CD19 did not induce internalization (**Supplementary Figures 3A and 3B**). Remarkably, deletion of NCK and not CD19 significantly decreased IgM-BCR-mediated uptake of large anti-IgM-coated particles as compared to wild type control Ramos B cells (**Figures 3D and 3E**). To further assess the role of CD19 and NCK in the dynamics of large particle internalization, internalization of IgM-BCR-bound particles was analyzed in time. In confirmation, absence of NCK strongly and significantly reduced internalization of large anti-IgM-coated particles in Ramos B cells at different time points after particle binding, whereas absence of CD19 did not significantly affect internalization efficiency, although an inhibitory trend was visible (**Figures 3F and 3G**). In line with the efficient uptake of large anti-IgM-coated particles in absence of CD19, inhibition of PI3K still significantly decreased internalization in the CD19 KO Ramos B cells, demonstrating a continued dependence on PI3K in the absence of CD19 similar to wild type control (**Figures 3H and 3I**). In contrast, inhibition of PI3K along with NCK KO had no significant effect on large anti-IgM-coated particle internalization, suggesting that the adaptor protein NCK is responsible for the recruitment of PI3K into the signalosome to drive large particle internalization (**Figure 3J**). Indeed, NCK KO, but not CD19 KO Ramos B cells exhibit a lack of phosphorylation of AKT at S473 following stimulation with large particles, which is

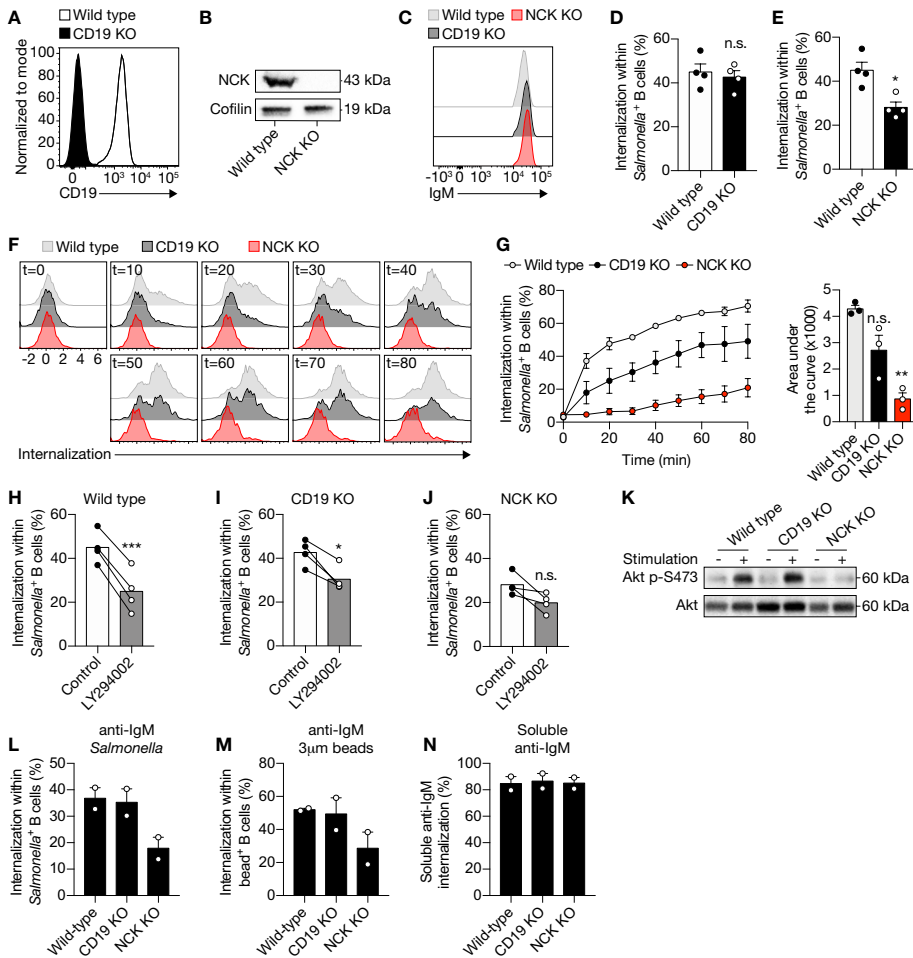
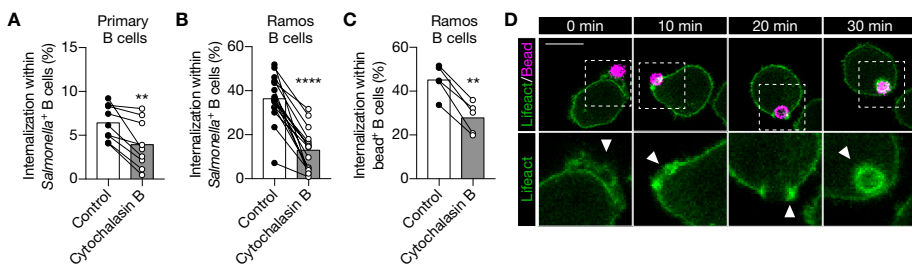


Figure 3 | The adaptor protein NCK is required for PI3K activity to facilitate IgM-BCR-induced internalization of large particles. (A) Representative histogram of CD19 expression in wild type and CD19 KO Ramos B cells. (B) Immunoblot of whole cell extracts from wild type and NCK KO Ramos B cells probed with NCK- or cofilin-specific (loading control) antibodies. (C) Representative histogram of surface IgM expression in wild type, CD19 KO and NCK KO Ramos B cells. (D–E) Proportion of internalization within *S. typhimurium*⁺ CD19 KO (D) and NCK KO (E) Ramos B cells compared with wild type (n = 4). (F–G) Representative histograms (F) and quantification (G; left) of the proportion of internalization within *S. typhimurium*⁺ wild type, CD19 KO and NCK KO Ramos B cells in time (n = 3). The area under the curve was obtained to quantify internalization in time (G; right). (H–J) Proportion of internalization within *S. typhimurium*⁺ wild type (H), CD19 KO (I) and NCK KO (J) Ramos B cells after treatment with a PI3K inhibitor (n = 4). (K) Immunoblot of whole cell extracts from wild type, CD19 KO and NCK KO Ramos B cells that were unstimulated (-) or stimulated (+) with *S. typhimurium*. The blots were probed with specific antibodies against pAKT at S473 and AKT. (L–N) Proportion of internalization within *S. typhimurium*⁺ (L), 3µm polystyrene bead⁺ (M) and soluble anti-IgM⁺ (N) wild type, CD19 KO and NCK KO Ramos B cells (n = 2). Each data point represents the mean of an individual experiment with duplicate measurements. Error bars indicate SEM. *, P < 0.05; **, P < 0.01; ***, P < 0.001; n.s., not significantly different by paired t test (B, D, G, H, I) or repeated-measures one-way ANOVA with Dunnett's post-test (F).

indicative of diminished PI3K activity (**Figure 3K**). To determine whether the adaptor protein NCK is required for internalization of large particle in general, the internalization efficiency of anti-IgM-coated *S. typhimurium*, inert anti-IgM-coated polystyrene beads and soluble anti-IgM were compared. Interestingly, absence of NCK strongly reduced internalization of both anti-IgM-coated particles, whereas internalization of soluble anti-IgM was unaffected (**Figures 3L-M; Supplementary Figure 4**). Altogether, these data demonstrate that uptake of large anti-IgM-coated particles, and not soluble anti-IgM, by the IgM-BCR requires the adaptor protein NCK.

Actin polymerization drives IgM-BCR-mediated large particle internalization

We then asked how PI3K induces internalization of large anti-IgM-coated particles. PI3K is a modulator of actin cytoskeleton rearrangement, which is important for BCR mobility and micro cluster formation^{12,38–42}. Although disruption of the actin cytoskeleton by cytochalasin B did not alter membrane IgM expression (**Supplementary Figures 5A-C**), it did significantly decreased internalization of large anti-IgM-coated particles in primary human B cells and in the Ramos B cell line (**Figures 4A-C**). To further assess the role of the actin cytoskeleton, Ramos B cells expressing Lifeact-GFP were used to effectively visualize actin cytoskeleton remodeling during large particle internalization. Formation of F-actin containing pod-like structure that extends the plasma membrane and surrounds the particle immediately upon contact were visualized using anti-IgM-coated polystyrene beads. F-actin further accumulated during uptake and encircled the particle-containing phagosome long after antigen uptake, which suggests that actin mediates intracellular antigen trafficking (**Figure 4D**). These data show that BCR-induced internalization of large particles is dependent on actin polymerization.



NCK facilitates RAC1 activity during internalization of large anti-IgM-coated particles

We established that NCK/PI3K signaling is required for IgM-BCR-mediated internalization of large particles, which is further propagated irrespective of BTK and AKT. How does PI3K then promote downstream signaling transduction to facilitate actin-dependent internalization? The potential involvement of RAC1 was investigated as RAC1 is a key regulator of the actin cytoskeleton organization in mammalian cells, and its activity is modulated by various guanine nucleotide exchange factors (GEFs) and GTPase-activating proteins (GAPs) that are recruited to phosphorylated lipids produced by PI3K⁴³⁻⁴⁵. Internalization of large anti-IgM-coated particles was significantly affected in both primary and Ramos B cells upon inhibition of RAC1 activity (**Figures 5A and 5B**). To further elucidate the role of RAC1 in internalization, a DORA-based RAC1 biosensor was used to visualize RAC1 activity during internalization (**Figure 5C**). This revealed enhanced RAC1 activity near the particle binding site during particle engulfment, which faded once the particle was fully internalized (**Figures 5D-F**). In contrast, RAC1 activity in the cytosol was largely unaffected (**Figures 5D-F**). To establish further a mechanistic link between upstream NCK-dependent PI3K recruitment and downstream RAC1 activity to modulate actin organization, we performed a pull-down assay with the biotinylated CDC42/RAC1-interactive binding (CRIB) domain of PAK1 that binds activated RAC1 from stimulated cells. This analysis validated upregulation of RAC1 activity upon stimulation with large anti-IgM-coated particles in wild type Ramos B cells (**Figures 5G and 5H**). In contrast, RAC1 activity was markedly decreased after stimulation of NCK KO Ramos B cells (**Figures 5G and 5H**). Together, these data demonstrate a requirement for NCK-mediated signaling in BCR-induced activation of RAC1 during large particle engulfment by human B cells.

DISCUSSION

BCR engagement with antigen initiates two critical cellular processes in B cells. On the one hand, triggering of the signaling receptor induces B cell activation. On the other hand, antigen encounter promotes internalization and efficient antigen-derived peptide presentation to facilitate an interaction with CD4⁺ T cell help. Over the past decades it has become evident that CD4⁺ T cell help is essential to the development of high affinity, class switched IgG antibody responses⁴⁶⁻⁵².

In the current study, we aimed to identify the molecular mechanisms that govern internalization of large particles and bacteria by human B cells, as this process enables B cells that recognize one antigen to attract broad T cell help directed against other antigens in the particle, and yields broad undesired antibody responses in autoimmunity and blood transfusion. We present data that demonstrate that human B cells take up large particles via the IgM-BCR-induced NCK/PI3K/RAC1 axis to drive actin cytoskeleton modulation, without a requirement for the co-receptor CD19 (**Figure 6**). Using our high-throughput quantitative image analysis approach, we established that complement and antibodies opsonization both induce large particle binding,

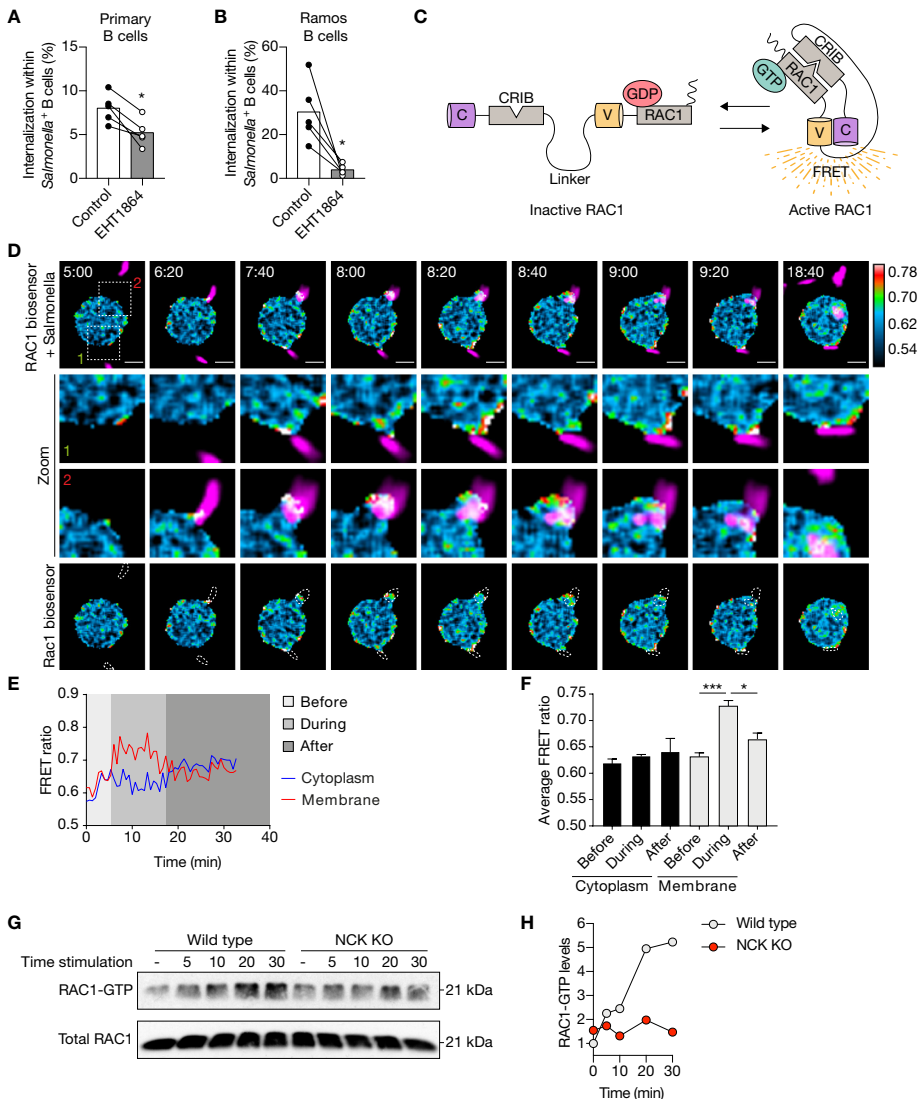


Figure 5 | NCK facilitates IgM-BCR-mediated activation of RAC1 subsequent large particle binding. (A–B) Proportion of internalization within *S. typhimurium*+ primary human B cells (A) and Ramos B cells (B) after treatment with a RAC1 inhibitor (n = 5). (C) Schematic illustration of the Cerulean3-CRIB-Venus-RAC1 FRET sensor. Inactive GDP-bound RAC1 results in a large distance between the two fluorescent proteins without a FRET signal. Active GTP-bound RAC1 binds the CDC42/RAC1-interactive binding (CRIB) motif of PAK1, which brings the two fluorescent proteins into close proximity resulting in high FRET efficiency. (D) Time-lapse Venus/Cerulean3 ratio images of the RAC1 DORA biosensor showing spatiotemporal RAC1 activation upon stimulation with anti-IgM-coated *S. typhimurium* expressing dsRed (magenta). Bar, 5mm. The boxed region at the upper panel is enlarged at the middle panels. Lower panels show RAC1 biosensor FRET ratio images with dashed lines marking *S. typhimurium* localization. Time indicated in minutes. Calibration bar shows RAC1 activation (red) relative to basal RAC1 activity (blue). (E–F) Representative activation ratio (E) and quantification (F) of the RAC1 biosensor in time. The activation ratio was assessed at the membrane as compared to the cytoplasm in close proximity to the particle contact area before, during and after *S. typhimurium* internalization (n = 3 independent experiments). (G–H) Immunoblot and quantification of GTP-RAC1 levels. (legend continues on next page)

- bound RAC1 precipitated from whole cell extracts of wild type and NCK KO Ramos B cells that were unstimulated (-) or stimulated with anti-IgM-coated *S. typhimurium* for 5, 10, 20 and 30 minutes. Total Rac1 levels from whole cell extracts were determined to control precipitation input (representative of n = 2 independent experiments). Bars depict mean values and error bars are SEM. Each data point represents the mean of an individual experiment with duplicate measurements. *, P < 0.05; **, P < 0.01; ****, P < 0.0001 by paired t test.

whereas particle internalization was exclusively achieved when the IgM-BCR is engaged. The ability to bind complement and/or antibody-opsonized particles is likely used for antigen transfer. Indeed, non-cognate B cells carry complement-opsonized antigen on their plasma membrane in a CR2-dependent manner to transfer and deposit these antigens onto follicular dendritic cells (FDC)⁵³. In confirmation with previous observations, we here demonstrate that IgM-BCR-mediated large particle internalization is highly dependent on active transmembrane signaling, which reflects a need for functional intracellular immunoreceptor tyrosine activation motifs (ITAMs)^{16,54}. By using small molecule inhibitors, we demonstrate that the signaling protein SYK, and not LYN, is required for large particle internalization. The observation that LYN is not essential in IgM-BCR signaling has been made previously in B cells from *lyn*^{-/-} mice that were found to be hyperresponsive to BCR ligation⁵⁵. As strength of the initial BCR signaling correlates with the stability of clustered antigenic receptor molecules, our data suggest that upon proper cross-linking of the IgM-BCR by large particles, signaling can be transmitted independent of LYN, whereas SYK, the protein required for the initiation of the multimolecular signalosome that activates distinct and inter-related signaling pathways, cannot be bypassed⁴². BTK inhibition did not affect internalization of large particles, whereas it greatly inhibited particle-dependent CD4⁺ T cell proliferation. This suggests that BTK regulates other intracellular processes that are necessary to mount a proper CD4⁺ T cell response. Indeed, BTK was found to promote the rate of BCR internalization and the movement of the internalized antigen-BCR complex to late endosomes and peptide presentation in splenic mouse B cells⁵⁶. This suggests that small soluble antigen and large particles require distinct molecular pathways downstream of the BCR to be internalized, but once internalized similar molecular events are activated, that are dependent on BTK and regulate antigen processing and presentation.

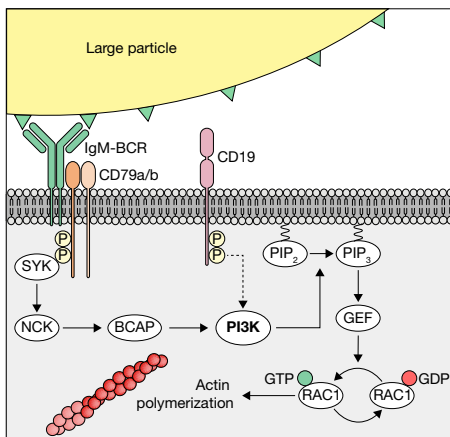


Figure 6 | Schematic of IgM-BCR-induced PI3K-driven internalization of large particles. Human B cells internalize large particles though IgM-BCR activation of PI3K via NCK without profound requirement of the co-receptor CD19 (dotted arrow). PI3K facilitates internalization though the conversion of phosphatidylinositol 4,5-biphosphate (PIP₂) to phosphatidylinositol 3,4,5-triphosphate (PIP₃) to recruit guanine nucleotide exchange factors (GEFs) that modulate RAC1-dependent activation of the actin cytoskeleton.

The involvement of the co-receptor CD19 in PI3K recruitment and its central role in BCR signaling are well known^{57,58}. Since PI3K activity was key in the internalization process, the finding that PI3K activity was not profoundly dependent on CD19 was unexpected. It has been observed before that CD19 does not fully account for PI3K translocation to the BCR since PI3K activity is still present in B cells from CD19^{-/-} mice after BCR stimulation⁵⁹, as also determined in the current study. Previously, it was shown that BCR signaling in response to small soluble antigen is independent of the co-receptor, whereas CD19 is essential in potentiation BCR-mediated signaling transduction in response to membrane-bound antigen stimulation⁴². This may suggest that the co-receptor CD19 is only required for antigen internalization when the antigen is linked to a membrane. Here we demonstrate that PI3K-dependent internalization of large anti-IgM-coated particles is strongly promoted by the adaptor protein NCK, in line with the recent finding that NCK can also propagate BCR-mediated activation of PI3K²¹. Although, NCK can be recruited to participate in BCR signaling through the BLNK complex in B cells⁶⁰, Castello and colleagues demonstrate that NCK is recruited to a non-ITAM phosphorylated tyrosine on the BCR-associated Iga to participate in BCR signaling in a BTK- and SYK-independent manner. As large particle internalization is dependent on SYK, this may suggest that NCK recruitment is facilitated by the SYK-dependent BLNK route.

It has been described previously that actin cytoskeleton rearrangements are required for internalization of soluble antigen⁵⁶. We have extended on this observation by showing that internalization of large particles by human B cells is mediated by the actin cytoskeleton, as also observed for murine follicular B cells¹⁶. Furthermore, we show that actin cytoskeleton rearrangements are modulated by IgM-BCR-induced NCK-PI3K axis via the small GTPase RAC1. PI3K facilitates RAC1 activation through the generation of lipids that can bind and recruit PH-domain-containing guanine nucleotide exchange factors (GEFs) that control RAC1 activation⁶¹. A well-known GEF that might be the bridge between PI3K and RAC1 is VAV, which was shown to activate RAC1 and regulate cytoskeletal structures after BCR activation^{34,62}. VAV would be of particular interest since it is the predominant RAC1 GEF expressed in B cells⁶³. In addition, other PI3K dependent adaptors such as Bam32 have been shown to be an important regulator for RAC1 activation and actin remodeling, warranting future research⁶⁴.

In conclusion, we provide evidence for the first time that internalization of large anti-IgM-coated particles by human B cells occurs via the SYK/NCK/PI3K/RAC1-actin axis, which may be susceptible to regulation. SYK and PI3K are both targets of clinically-approved inhibitors that are currently used in clinical trials against autoimmune thrombocytopenia (ITP), leukemia and lymphomas^{65,66}. It is important to realize that these patients may be more susceptible to microbial infections due to reduced B cell humoral immune response against microbes as a result of the affected ability to internalize large particles and to attract the CD4⁺ T cell help required for class switching, somatic hypermutation and plasma cell differentiation.

ACKNOWLEDGEMENTS

We thank M.L.M. Jongsma for assistance on the generation of CRISPR/Cas9 induced knockout cells; M. Fernandez-Borja for kindly providing the Lifeact-GFP construct; G. Marsman and Y.E. Bar-Ephraïm for titrating the small molecule inhibitors; Y. Wu (UConn Health, Farmington, CT) for longstanding collaboration on the DORA sensor; and E.P.J. Mul, M. Hoogenboezem and S. Tol for technical support.

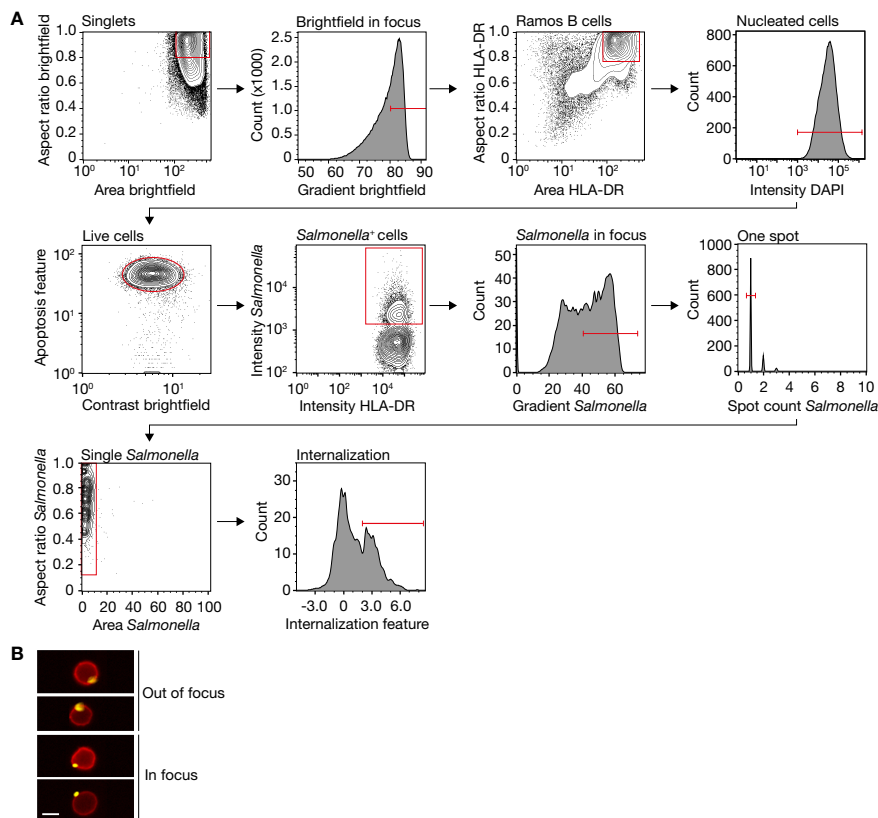
REFERENCES

1. Tulp, A., Verwoerd, D., Dobberstein, B., Ploegh, H. L. & Pieters, J. Isolation and characterization of the intracellular MHC class II compartment. *Nature* **369**, 120–6 (1994).
2. Qiu, Y., Xu, X., Wandinger-Ness, A., Dalke, D. P. & Pierce, S. K. Separation of subcellular compartments containing distinct functional forms of MHC class II. *J. Cell Biol.* **125**, 595–605 (1994).
3. Amigorena, S., Drake, J. R., Webster, P. & Mellman, I. Transient accumulation of new class II MHC molecules in a novel endocytic compartment in B lymphocytes. *Nature* **369**, 113–20 (1994).
4. Lanzavecchia, A. Antigen-specific interaction between T and B cells. *Nature* **314**, 537–539 (1985).
5. Reth, M. Antigen receptor tail clue. *Nature* **338**, 383–4 (1989).
6. Dal Porto, J. M. *et al.* B cell antigen receptor signaling 101. *Mol. Immunol.* **41**, 599–613 (2004).
7. Kuokkanen, E., Šuštar, V. & Mattila, P. K. Molecular control of B cell activation and immunological synapse formation. *Traffic* **16**, 311–26 (2015).
8. Woyach, J. A., Johnson, A. J. & Byrd, J. C. The B-cell receptor signaling pathway as a therapeutic target in CLL. *Blood* **120**, 1175–1184 (2012).
9. Hoogeboom, R. & Tolar, P. Molecular mechanisms of B cell antigen gathering and endocytosis. *Curr. Top. Microbiol. Immunol.* **393**, 45–63 (2015).
10. Tolar, P., Sohn, H. W., Liu, W. & Pierce, S. K. The molecular assembly and organization of signaling active B-cell receptor oligomers. *Immunol. Rev.* **232**, 34–41 (2009).
11. Spillane, K. M. & Tolar, P. B cell antigen extraction is regulated by physical properties of antigen-presenting cells. *J. Cell Biol.* **216**, 217–230 (2017).
12. Natkanski, E. *et al.* B cells use mechanical energy to discriminate antigen affinities. *Science (80-.).* **340**, 1587–1590 (2013).
13. Nowosad, C. R., Spillane, K. M. & Tolar, P. Germinal center B cells recognize antigen through a specialized immune synapse architecture. *Nat. Immunol.* **17**, 870–877 (2016).
14. Gao, J. *et al.* Novel functions of murine B1 cells: active phagocytic and microbicidal abilities. *Eur. J. Immunol.* **42**, 982–92 (2012).
15. Parra, D. *et al.* Pivotal advance: peritoneal cavity B-1 B cells have phagocytic and microbicidal capacities and present phagocytosed antigen to CD4+ T cells. *J. Leukoc. Biol.* **91**, 525–36 (2012).
16. Martínez-Riaño, A. *et al.* Antigen phagocytosis by B cells is required for a potent humoral response. *EMBO Rep.* **19**, 1–15 (2018).
17. Souver, Y. *et al.* B cell receptor-mediated internalization of salmonella: a novel pathway for autonomous B cell activation and antibody production. *J. Immunol.* **182**, 7473–81 (2009).
18. Vanderglugt, C. J. & Miller, S. D. Epitope spreading. *Curr. Opin. Immunol.* **8**, 831–836 (1996).
19. Cornaby, C. *et al.* B cell epitope spreading: mechanisms and contribution to autoimmune diseases. *Immunol. Lett.* **163**, 56–68 (2015).
20. Degn, S. E. *et al.* Clonal Evolution of Autoreactive Germinal Centers. *Cell* **170**, 913–926.e19 (2017).
21. Castello, A. *et al.* Nck-mediated recruitment of BCAP to the BCR regulates the PI(3)K-Akt pathway in B cells. *Nat. Immunol.* **14**, 966–975 (2013).
22. Beckwith, M., Jorgensen, G. & Longo, D. L. The protein product of the proto-oncogene c-cbl forms a complex with phosphatidylinositol 3-kinase p85 and CD19 in anti-IgM-stimulated human B-lymphoma cells. *Blood* **88**, 3502–3507 (1996).
23. Weng, W. K., Jarvis, L. & LeBien, T. W. Signaling through CD19 activates Vav/mitogen-activated protein kinase pathway and induces formation of a CD19/Vav/phosphatidylinositol 3-kinase complex in human B cell precursors. *J. Biol. Chem.* **269**, 32514–21 (1994).
24. Tuveson, D., Carter, R., Soltoff, S. & Fearon, D. CD19 of B cells as a surrogate kinase insert region to bind phosphatidylinositol 3-kinase. *Science (80-.).* **260**, 986–989 (1993).
25. Sanjana, N. E., Shalem, O. & Zhang, F. Improved vectors and genome-wide libraries for CRISPR screening. *Nat. Methods* **11**, 783–784 (2014).
26. Riedl, J. *et al.* Lifeact: a versatile marker to visualize F-actin. *Nat. Methods* **5**, 605–607 (2008).
27. Timmerman, I. *et al.* A local VE-cadherin and Trio-based signaling complex stabilizes endothelial junctions through Rac1. *J. Cell Sci.* **128**, 3041–54 (2015).
28. Carette, J. E. *et al.* Haploid genetic screens in human cells identify host factors used by pathogens. *Science (80-.).* **326**, 1231–1235 (2009).

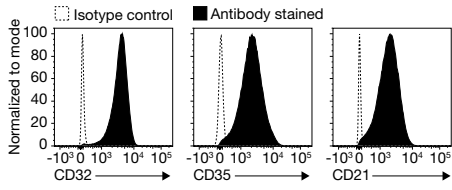
29. Shalem, O. *et al.* Genome-scale CRISPR-Cas9 knockout screening in human cells. *Science (80-.)*. **343**, 84–87 (2014).
30. Martínez-Lorenzo, M. J., Méresse, S., de Chastellier, C. & Gorvel, J.-P. Unusual intracellular trafficking of Salmonella typhimurium in human melanoma cells. *Cell. Microbiol.* **3**, 407–416 (2001).
31. Souwer, Y. *et al.* Selective Infection of Antigen-Specific B Lymphocytes by Salmonella Mediates Bacterial Survival and Systemic Spreading of Infection. *PLoS One* **7**, e50667 (2012).
32. de Wit, J. *et al.* Antigen-Specific B Cells Reactivate an Effective Cytotoxic T Cell Response against Phagocytosed Salmonella through Cross-Presentation. *PLoS One* **5**, e13016 (2010).
33. de Wit, J. *et al.* Human B cells promote T-cell plasticity to optimize antibody response by inducing coexpression of TH1/TFH signatures. *J. Allergy Clin. Immunol.* **135**, 1053–60 (2015).
34. Niiri, H. & Clark, E. A. Regulation of B-cell fate by antigen-receptor signals. *Nat. Rev. Immunol.* **2**, 945–56 (2002).
35. Rolli, V. *et al.* Amplification of B cell antigen receptor signaling by a Syk/ITAM positive feedback loop. *Mol. Cell* **10**, 1057–69 (2002).
36. Beitz, L. O., Fruman, D. A., Kurosaki, T., Cantley, L. C. & Scharenberg, A. M. SYK is upstream of phosphoinositide 3-kinase in B cell receptor signaling. *J. Biol. Chem.* **274**, 32662–6 (1999).
37. Hamman, B. D., Pollok, B. A., Bennett, T., Allen, J. & Heim, R. Binding of a Pleckstrin homology domain protein to phosphoinositide in membranes: a miniaturized FRET-based assay for drug screening. *J. Biomol. Screen.* **7**, 45–55 (2002).
38. Schlam, D. *et al.* Phosphoinositide 3-kinase enables phagocytosis of large particles by terminating actin assembly through Rac/Cdc42 GTPase-activating proteins. *Nat. Commun.* **6**, 8623 (2015).
39. Tolar, P., Hanna, J., Krueger, P. D. & Pierce, S. K. The constant region of the membrane immunoglobulin mediates B cell-receptor clustering and signaling in response to membrane antigens. *Immunity* **30**, 44–55 (2009).
40. Liu, W., Won Sohn, H., Tolar, P., Meckel, T. & Pierce, S. K. Antigen-induced oligomerization of the B cell receptor is an early target of Fc gamma RIIB inhibition. *J. Immunol.* **184**, 1977–89 (2010).
41. Treanor, B. *et al.* The Membrane Skeleton Controls Diffusion Dynamics and Signaling through the B Cell Receptor. *Immunity* **32**, 187–199 (2010).
42. Depoil, D. *et al.* CD19 is essential for B cell activation by promoting B cell receptor-antigen microcluster formation in response to membrane-bound ligand. *Nat. Immunol.* **9**, 63–72 (2008).
43. Campa, C. C., Ciralo, E., Ghigo, A., Germena, G. & Hirsch, E. Crossroads of PI3K and Rac pathways. *Small GTPases* **6**, 71–80 (2015).
44. Guo, F., Debidda, M., Yang, L., Williams, D. A. & Zheng, Y. Genetic deletion of Rac1 GTPase reveals its critical role in actin stress fiber formation and focal adhesion complex assembly. *J. Biol. Chem.* **281**, 18652–9 (2006).
45. Welch, H. C. E., Coadwell, W. J., Stephens, L. R. & Hawkins, P. T. Phosphoinositide 3-kinase-dependent activation of Rac. *FEBS Lett.* **546**, 93–7 (2003).
46. Shulman, Z. *et al.* T follicular helper cell dynamics in germinal centers. *Science (80-.)*. **341**, 673–677 (2013).
47. Gitlin, A. D., Shulman, Z. & Nussenzweig, M. C. Clonal selection in the germinal centre by regulated proliferation and hypermutation. *Nature* **509**, 637–40 (2014).
48. Shulman, Z. *et al.* Dynamic signaling by T follicular helper cells during germinal center B cell selection. *Science (80-.)*. **345**, 1058–1062 (2014).
49. Gitlin, A. D. *et al.* T cell help controls the speed of the cell cycle in germinal center B cells. *Science (80-.)*. **349**, 643–646 (2015).
50. Kräutler, N. J. *et al.* Differentiation of germinal center B cells into plasma cells is initiated by high-affinity antigen and completed by Tfh cells. *J. Exp. Med.* **214**, 1259–1267 (2017).
51. Allen, C. D. C. *et al.* Germinal center dark and light zone organization is mediated by CXCR4 and CXCR5. *Nat. Immunol.* **5**, 943–52 (2004).
52. Mesin, L., Ersching, J. & Victora, G. D. Germinal Center B Cell Dynamics. *Immunity* **45**, 471–82 (2016).
53. Phan, T. G., Grigorova, I., Okada, T. & Cyster, J. G. Subcapsular encounter and complement-dependent transport of immune complexes by lymph node B cells. *Nat. Immunol.* **8**, 992–1000 (2007).
54. Batista, F. D. & Neuberger, M. S. B cells extract and present immobilized antigen: implications for affinity discrimination. *EMBO J.* **19**, 513–20 (2000).
55. Xu, Y., Harder, K. W., Huntington, N. D., Hibbs, M. L. & Tarlinton, D. M. Lyn tyrosine kinase: Accentuating the positive and the negative. *Immunity* **22**, 9–18 (2005).
56. Sharma, S., Orlowski, G. & Song, W. Btk regulates B cell receptor-mediated antigen processing and presentation by controlling actin cytoskeleton dynamics in B cells. *J. Immunol.* **182**, 329–39 (2009).

57. Fearon, D. T. & Carroll, M. C. Regulation of B lymphocyte responses to foreign and self-antigens by the CD19/CD21 complex. *Annu. Rev. Immunol.* **18**, 393–422 (2000).
58. Tedder, T. F., Inaoki, M. & Sato, S. The CD19-CD21 complex regulates signal transduction thresholds governing humoral immunity and autoimmunity. *Immunity* **6**, 107–18 (1997).
59. Otero, D. C., Omori, S. A. & Rickert, R. C. CD19-dependent Activation of Akt Kinase in B-lymphocytes. *J. Biol. Chem.* **276**, 1474–1478 (2001).
60. Cannons, J. L., Zhao, F. & Schwartzberg, P. L. Ncking BCR-mediated PI3K activation. *EMBO Rep.* **14**, 852–3 (2013).
61. Jellusova, J. & Rickert, R. C. The PI3K pathway in B cell metabolism. *Crit. Rev. Biochem. Mol. Biol.* **51**, 359–378 (2016).
62. Malhotra, S., Kovats, S., Zhang, W. & Coggeshall, K. M. B cell antigen receptor endocytosis and antigen presentation to T cells require Vav and dynamin. *J. Biol. Chem.* **284**, 24088–97 (2009).
63. Turner, M. & Billadeau, D. D. VAV proteins as signal integrators for multi-subunit immune-recognition receptors. *Nat. Rev. Immunol.* **2**, 476–86 (2002).
64. Allam, A., Niiro, H., Clark, E. A. & Marshall, A. J. The adaptor protein Bam32 regulates Rac1 activation and actin remodeling through a phosphorylation-dependent mechanism. *J. Biol. Chem.* **279**, 39775–82 (2004).
65. Podolanczuk, A., Lazarus, A. H., Crow, A. R., Grossbard, E. & Bussel, J. B. Of mice and men: an open-label pilot study for treatment of immune thrombocytopenic purpura by an inhibitor of Syk. *Blood* **113**, 3154–3160 (2009).
66. Okkenhaug, K., Graupera, M. & Vanhaesebroeck, B. Targeting PI3K in Cancer: Impact on Tumor Cells, Their Protective Stroma, Angiogenesis, and Immunotherapy. *Cancer Discov.* **6**, 1090–1105 (2016).

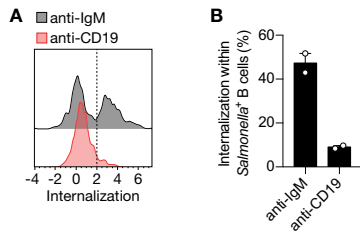
SUPPLEMENTARY INFORMATION



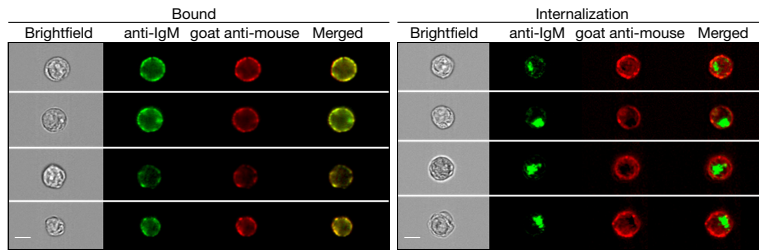
Supplementary Figure 1 | Gating strategy to quantify particulate antigen internalization by human B cells. (A) Single cells were gated from total collected cells using size and morphology parameters of the brightfield channel. Subsequently, focused cells were selected by use of the gradient parameter of the brightfield channel. Another single cell gate was set using size and morphology parameters of the plasma membrane mask based on HLA-DR staining. Nucleated cells were gated using the intensity of the DAPI stain. DAPI was added after fixation of the cells, therefore all nucleated cells are DAPI positive. The IDEAS V6.2 software apoptosis feature was used to define apoptotic cells. B cells interacting with dsRed-expressing *S. typhimurium* were gated using the intensity of *S. typhimurium* fluorescent tag. The gradient of the *S. typhimurium* channel was used to define particles in the same focal plane as the human B cell (example in B). Single *S. typhimurium*-positive B cells were defined using a spot count together with the particle size and morphology parameters. Finally, internalization was assessed as described (see Figure 1C). **(B)** Representative pictures of *S. typhimurium* interacting with a human B cell either outside or inside the same focal plane as the B cell. Bar, 7 μ m.



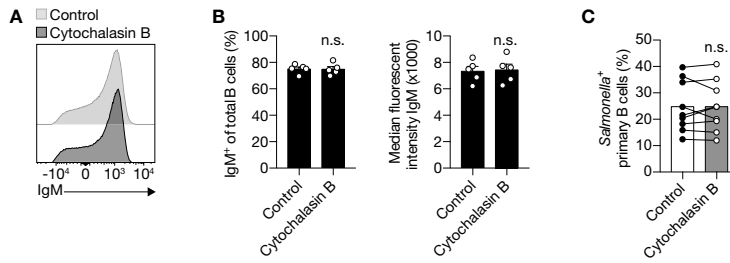
Supplementary Figure 2 | Expression of complement and antibody receptors on primary human B cells. Representative plots of plasma membrane FcγRIIB (CD32), complement receptor 1 (CR1; CD35) and complement receptor 2 (CR2; CD21) expression by primary human B cells. Dotted line represents a sample stained with an isotype control antibody.



Supplementary Figure 3 | Targeting large particles to the co-receptor CD19 does not facilitate internalization. (A–B) Representative histogram (A) and proportion (B) of Ramos B cells that internalized anti-IgM- or anti-CD19-coated *S. typhimurium*. Each data point represents the mean of an individual experiment with duplicate measurements. Error bars indicate SEM.



Supplementary Figure 4 | Visualization of soluble anti-IgM internalization. Representative images of Ramos B cells containing bound (left) or internalized (right) anti-IgM. Bar, 10 μ m. Soluble anti-IgM internalization was assessed by using the IDEAS V6.2 software colocalization feature. Colocalization was determined using the mouse anti-human IgM and the goat anti-mouse IgG image.



Supplementary Figure 5 | Inhibition of actin polymerization by cytochalasin B does not affect IgM-BCR expression. (A–B) Representative histogram (A) and quantification (B) of surface IgM-BCR expression in total peripheral B cells after incubation with vehicle (DMSO) or cytochalasin B ($n = 5$). (C) Proportion of primary human B cells interacting with anti-IgM-coated *S. typhimurium* after incubation with vehicle (DMSO) or cytochalasin B ($n = 9$). All data points represent the mean of an individual experiment with duplicate measurements. Error bars indicate SEM. n.s., not significantly different by paired t test.

Supplementary Table 1 | Small molecule compounds that decrease activity of signaling proteins downstream of the BCR.

Name	Inhibitor of	Concentration (μM)	Manufacturer
SU6656	LYN	0.1	Sigma
Pinacetannol	SYK	0.1	Sigma
LFM-A13	BTK	200	Sigma
Ibrutinib	BTK	1	Medkoo
PI103	PI3K	5	Selleckchem
LY294002	PI3K	50	Sigma
A6730	AKT 1/2	1	Sigma
MK-2206	AKT 1/2	5	Selleckchem
GDC-0068	AKT 1/2/3	0.5	Selleckchem
VIII	AKT 1/2/3	1	Merck
Cytochalasin B	Actin polymerization	10	Sigma
EHT1864	RAC1	50	Sigma

All inhibitors were titrated and added in a concentration that did not induce cell death of primary human B cells and Ramos B cells. DMSO was used as a negative control.

Chapter 4

TCR signal strength regulates plastic co-expression of IL-4 and IFN- γ by Tfh-like cells

Niels J. M. Verstegen^{1,2}, Tineke Jorritsma¹, Matteo Barberis^{2,3,4}, Anja ten Brinke¹ and S. Marieke van Ham^{1,5}

Manuscript in preparation

1. Department of Immunopathology, Sanquin Research and Landsteiner Laboratory, Amsterdam University Medical Centers, University of Amsterdam, Amsterdam, The Netherlands
2. Synthetic Systems Biology and Nuclear Organization, Swammerdam Institute for Life Sciences, University of Amsterdam, Amsterdam, The Netherlands
3. Systems Biology, School of Biosciences and Medicine, Faculty of Health and Medical Sciences, University of Surrey, Guildford, United Kingdom
4. Centre for Mathematical and Computational Biology, CMCB, University of Surrey, Guildford, United Kingdom
5. Swammerdam Institute for Life Sciences, University of Amsterdam, Amsterdam, The Netherlands

ABSTRACT

In the germinal center (GC), B cells undergo affinity selection and differentiation into effector B cells and antibody-secreting cells, which rely on interactions with T follicular helper (Tfh) cells. Tfh cells secrete IL-21 and can coexpress IL-4 and IFN- γ to modulate the antigen-specific B cell response. IL-21 is necessary for GC reactions and antibody-secreting cell (ASC) formation, while IL-4 promotes the formation of memory B cells and IFN- γ induces the appropriate bone marrow homing receptors. T cell receptor (TCR) signaling, costimulation, and the antigen-presenting cell (APC)-derived cytokine environment are all important in regulating the formation of Tfh cells. It is not fully understood how these stimuli integrate to control plastic expression of the effector cytokines that regulate the GC reactions and their output; however, the availability of antigens likely plays a role. We investigate the contribution of TCR signaling strength (signal 1) to human Tfh differentiation and cytokine expression and demonstrate that CD3-TCR stimulation of naive CD4⁺ T cells led to a dose-dependent induction of IL-21 expression that peaked relatively early after stimulation, and IL-21-secreting cells had a Tfh-like phenotype characterized by expression of CXCR5 and PD1. Induced IL-21 enhanced proliferation and differentiation of IL-21-producing CD4⁺ T cells in an autocrine or paracrine manner. IL-21-producing Tfh-like cells could also coexpress IL-4 and IFN- γ , with low CD3-TCR stimulation resulting in production of IL-4, while high CD3-TCR stimulation yielding in coexpression of IFN- γ . The coexpression of these cytokines was modulated by exogenous IL-21 or IL-4, leading to different ranges of coexpression depending on the strength of CD3 background. These findings provide new insights into the signal 1-dependent plasticity of Tfh-like cells and provide further clues on how antigen availability is involved in Tfh-dependent B cell differentiation during the dynamic evolution of the GC reactions.

INTRODUCTION

CD4⁺ T cells are key components of the adaptive immune response, the body's specific response to a pathogen or other foreign substance. When a pathogen enters the body, dendritic cells (DCs) take up antigens, process it, and present them to the immune system in the form of antigen-derived peptides displayed on their cell membrane via major histocompatibility complex II (MHCII). DCs then move to secondary lymphoid organs, such as lymph nodes, to activate naive CD4⁺ T cells, which recognize the peptide-MHCII complexes using their antigen-specific T cell receptors (TCRs)¹. When a naive CD4⁺ T cell encounters an antigen-presenting DC, it becomes activated and divides and differentiates into different T helper (Th) cells guided by additional cues provided by the DCs^{2,3}. Traditionally, Th cell subsets were believed to be distinct and did not overlap. However, it is now widely accepted that there is significant plasticity between these subsets, which indicates that Th cells can adapt and respond to various immune challenges⁴⁻⁹.

One of the subtypes of CD4⁺ T cells that can be induced by DC activation is the pre-T follicular helper (Tfh) cell¹⁰. Pre-Tfh cells are a transient stage in differentiating naive CD4⁺ T cells into Tfh cells, specialized cells that help B cells during the immune response¹¹. After activation by DCs, pre-Tfh cells migrate to the border of the B cell zone, where they interact with activated, antigen-presenting B cells¹². This interaction between pre-Tfh cells and activated B cells is essential for differentiation of pre-Tfh cells into Tfh cells¹³. Tfh cells are characterized by expression of certain surface markers, such as CXCR5 and PD1, which allow them to move into the germinal center (GC)¹⁴. During the GC reaction, B cells rapidly divide, mutate their antibody genes, and undergo affinity-based selection facilitated by productive interactions with Tfh cells. Tfh cells select the GC B cells for cyclic reentry or support formation of memory B cells and plasma cells. The regulation of this choice is not fully understood, but it is thought that Tfh-derived cytokines may play a role, particularly IL-21, IL-4, and IFN- γ . Disruptions in the signaling pathways of these cytokine leads to impaired humoral responses. It is known that IL-21 is one of the most potent inducers of plasma cell differentiation *in vitro*^{15,16}, and that absence of IL-21 or its receptor will result in a lack of antibody responses and GC responses^{17,18}. It was demonstrated that helminth stimulation induces IL-4 secretion in Tfh cells and that these undergo progressive differentiation from IL-21 to IL-4 production as they mature, allowing them to fine-tune their regulatory functions within the GC¹⁹. IL-4 promotes B cell activation and immunoglobulin class switching to IgG1 and IgE²⁰. Recently, it was demonstrated that scavenging IL-4 from germinal centers by follicular dendritic cells fosters generation of memory B cells²¹. Furthermore, human Tfh cells might plastically coexpress the Th1 cytokine IFN- γ ²², which can direct chemokine expression during B cell differentiation.

This raises the question of how the plasticity of Tfh cells is regulated. While much research has been conducted on the mechanisms that regulate B cell selection in the GC, much less is understood about the dynamic behavior of Tfh cells. One possibility is that the supply of antigens may influence this regulation. It is known that interactions between Tfh and GC B cells increase intracellular calcium concentration within Tfh cells and the production of B cell-

stimulating cytokines²³. In addition, an increased antigen presentation by GC B cells leads to increased proliferation of Tfh cells that exhibit enhanced expression of genes downstream of the TCR²⁴. The symbiotic interactions between GC B cells and Tfh cells in the GC may also regulate cytokine production plasticity. In the classical Th1/Th2 polarization dogma, the outcome of Th1/Th2 polarization is influenced by the amount of antigen available and strength of TCR signaling and costimulation^{25–28}. Strong TCR signaling and costimulation facilitate IFN- γ (Th1) polarization, while weak TCR signaling and costimulation direct IL-4 (Th2) polarization. These observations were extended after the discovery of Tfh cells, which initially demonstrated that strong TCR-signaling was necessary for Tfh cell development, but recent research suggests that Tfh cells can develop within a range of TCR signal strengths^{29–36}. The current research is focused on understanding how TCR signaling strength regulates the plastic coexpression of IL-4 and IFN- γ in IL-21-producing Tfh-like cells.

MATERIALS AND METHODS

Purification of CD4⁺ T cells

Human peripheral blood mononuclear cells (PBMC) were isolated through standard gradient centrifugation using Ficoll-lymphoprep (Axis-Shield) from buffy coats obtained from healthy blood donors (Sanquin Blood Supply). All donors provided written informed consent following the protocol of the local institutional review board, the Medical Ethics Committee of Sanquin Blood Supply, and the Medical Ethics Committee of Sanquin approved the study. Subsequently, CD4⁺ T cells were purified from PBMCs with anti-CD4 Dynabeads and DETACHaBEAD (Invitrogen) following the manufacturer's instructions. Naive CD4⁺ T cells were obtained through magnetic-activated cell sorting (MACS) using CD45RO-PE (BD Biosciences) and anti-PE beads (Miltenyi Biotech). Cells were cryopreserved in liquid nitrogen. Purity was typically greater than 98%, as assessed by flow cytometry.

Naive CD4⁺ T cell stimulation

Naive CD4⁺ T cells labeled with Cell Trace CFSE according to manufacturer's instructions (Invitrogen) were cultured in 96-round bottom well plates at a density 2.5×10^3 /well in a total volume of 200 μ l complete RPMI 1640 medium (Invitrogen), supplemented with 5% FCS (Bodinco), 100 U/ml penicillin (Invitrogen), 100 μ g/ml streptomycin (Invitrogen), 2 mM L-glutamine (Invitrogen), 50 μ M 2-ME (Sigma) and 20 μ g/ml human apotransferrin (Sigma; depleted for human IgG with protein G Sepharose (Amersham Biosciences)). Cells were activated with anti-CD3 (clone 1XE; Sanquin) and anti-CD28 (clone 15E8; Sanquin) with or without IL-21 (Invitrogen), IL-4 (Cellgro), and IFN- γ (Peprotech).

Flow cytometry analysis

Surface markers and intracellular cytokines were detected by the following FACS anti-human

antibodies: CD4 (clone SK3; BD Biosciences); IL-21 (clone 3A3-N2; eBiosciences); IFN- γ (clone B27; BD Biosciences); and IL-4 (clone 3010.211; BD Biosciences). Before FACS staining, cells were incubated in a complete medium with 0.1 mg/ml phorbol 12-myristate 13-acetate (PMA; Sigma), 1 mg/ml ionomycin (Sigma), and 10 mg/ml brefeldin A (Sigma) for 5 hours. To exclude dead cells, samples were washed twice with PBS and stained with a Fixable Near-IR Dead Cell Stain Kit (Invitrogen). Subsequently, cells were fixed with 4% paraformaldehyde (PFA; Sigma) for 15 minutes, permeabilized with 0.5% saponin (Calbiochem) in PBS containing 1% BSA (Sigma) and incubated with fluorescent antibodies for 30 minutes at room temperature. Samples were collected on an LSRII flow cytometer (BD Bioscience), and single live cells were analyzed with FACSDiva software (BD) and FlowJo version 10 (Treestar).

RNA isolation and qRT-PCR

RT-PCR has been described before³⁷. In short, RNA was reverse transcribed to cDNA using random hexamers in combination with Superscript II and a RNase H-reverse transcriptase kit. Primers for 18S rRNA, IL-21, and CXCR5, were developed to span exon-intron junctions to prevent amplification of genomic DNA (primer sets in **Supplementary Table 1**). Primers were validated on cDNA of total CD4⁺ T cells. The product specificity of each primer set was verified by agarose gel electrophoresis and sequence analysis of the amplified PCR product. Gene expression levels were measured in triplicate reactions for each sample in StepOnePlus (Applied Biosystems) using the SYBR green method (Applied Biosystems). All results were normalized to the internal control 18S rRNA.

Statistical analysis

Statistical analyses were performed using Prism 9 (Graphpad). The statistical tests used are indicated in the figure descriptions. Data show the mean of multiple donors, and error bars represent mean \pm SEM.

RESULTS AND DISCUSSION

High CD3-TCR stimulation facilitates the induction of IL-21-expressing Tfh-like cells

To investigate whether strength of TCR stimulation influences differentiation of naive (CD45RA⁺CD45RO⁻) CD4⁺ T cells into IL-21-secreting Tfh-like cells, human naive CD4⁺ T cells were isolated and stimulated for various periods with varying amounts of CD3-stimulating antibodies (signal 1) in presence of optimal CD28-stimulation (signal 2). In line with previous findings^{24,38,39}, increasing CD3-TCR stimulation leads to enhanced proliferation of CD4⁺ T cells and an increase in the number of live cells, of which the effect is mainly presented at later time points (**Figure 1b-c**). Analysis of IL-21 production after 3, 5, and 11 days of CD3-TCR stimulation and 5 hours PMA/Ionomycin restimulation showed that CD3-TCR stimulation

leads to a dose-dependent induction of IL-21 expression that peaks relatively early after stimulation (**Figure 1d-f**). By staining CFSE-labeled cells intracellularly after restimulation, the relationship between IL-21 production and cell division was assessed. IL-21 secretion occurred early during cell division and did not significantly increase with increasing divisions, indicating that IL-21 is produced early in response to CD3-TCR stimulation (**Figure 1g**). IL-21 plays an important role in the development and function of T follicular helper (Tfh) cells⁴⁰. To determine whether the IL-21-expressing cells have a Tfh-like phenotype, expression of Tfh cell-associated markers CXCR5 and PD1 was analyzed (**Figure 1h**). PMA/Ionomycin stimulation and addition of Brefeldin A significantly negatively affected CXCR5 expression (data not shown), in line with earlier observations⁴¹. To still evaluate IL-21 expression and other Tfh characteristics, CXCR5⁺PD1⁻ and CXCR5⁺PD1⁺ populations were sorted at the peak of IL-21 production (3 days) induced by high CD3-TCR stimulation, and expression of CXCR5 and IL-21 mRNA was determined in both populations. As expected, mRNA expression of CXCR5 and IL-21 was higher in CXCR5⁺PD1⁺ than in CXCR5⁺PD1⁻ CD4⁺ T cells, indicating that IL-21-secreting cells have a phenotype related to Tfh-like cells (**Figure 1h**). Tfh cell formation is dependent on a CD4⁺ T cell-intrinsic requirement for IL-21⁴⁰. To determine potential autocrine or paracrine effects of IL-21 during CD4⁺ T cell differentiation, exogenous IL-21 was added. IL-21 increased the percentage of proliferating cells and the division rate, resulting in more CD4⁺ T cells at later stages (**Figure 1i**). This effect was particularly prominent when CD3-TCR stimulation was low, possibly due to the significantly lower percentage of cells that secrete endogenous IL-21 after low CD3-TCR stimulation. Similarly, the magnitude of TCR signaling defined the ability of additional exogenous IL-21 to enhance the differentiation of IL-21-producing CD4⁺ T cells. It appears that the percentage of IL-21-producing cells induced by TCR stimulation reached a plateau above which additional IL-21 did not further enhance differentiation (**Figure 1j**). Altogether, these data show that especially high levels of CD3-TCR stimulation of naive CD4⁺ T cells induce IL-21 in Tfh-like cells. Low CD3-TCR stimulation yields less IL-21 induction, but autocrine or paracrine feed-forward signals of IL-21 can enhance IL-21 production in the Tfh-like cells under those conditions.

The plastic coexpression of IL-4 and IFN- γ by IL-21-producing Tfh cells requires a delicate balance in CD3-TCR stimulation

It is unclear how Tfh cells plastically express cytokines that have different effects on the dynamics of the GC responses and formation of memory B cells or antibody-secreting cells. Effects of CD3 strength signal were investigated on IFN- γ and IL-4 expression. Consistent with the current understanding of the Th1 and Th2 dogma²⁵⁻²⁸, low-intensity CD3-TCR stimulation facilitated production of IL-4 at day 5 after stimulation, which then gradually decreased (Supplementary figure 1a-b). It is worth noting that intermediate and high CD3-TCR stimulation initially resulted in less IL-4-producing cell induction than low stimulation and that the proportion increases later (**Supplementary Figure 1a-b**). Strong stimulation resulted in a more profound production of

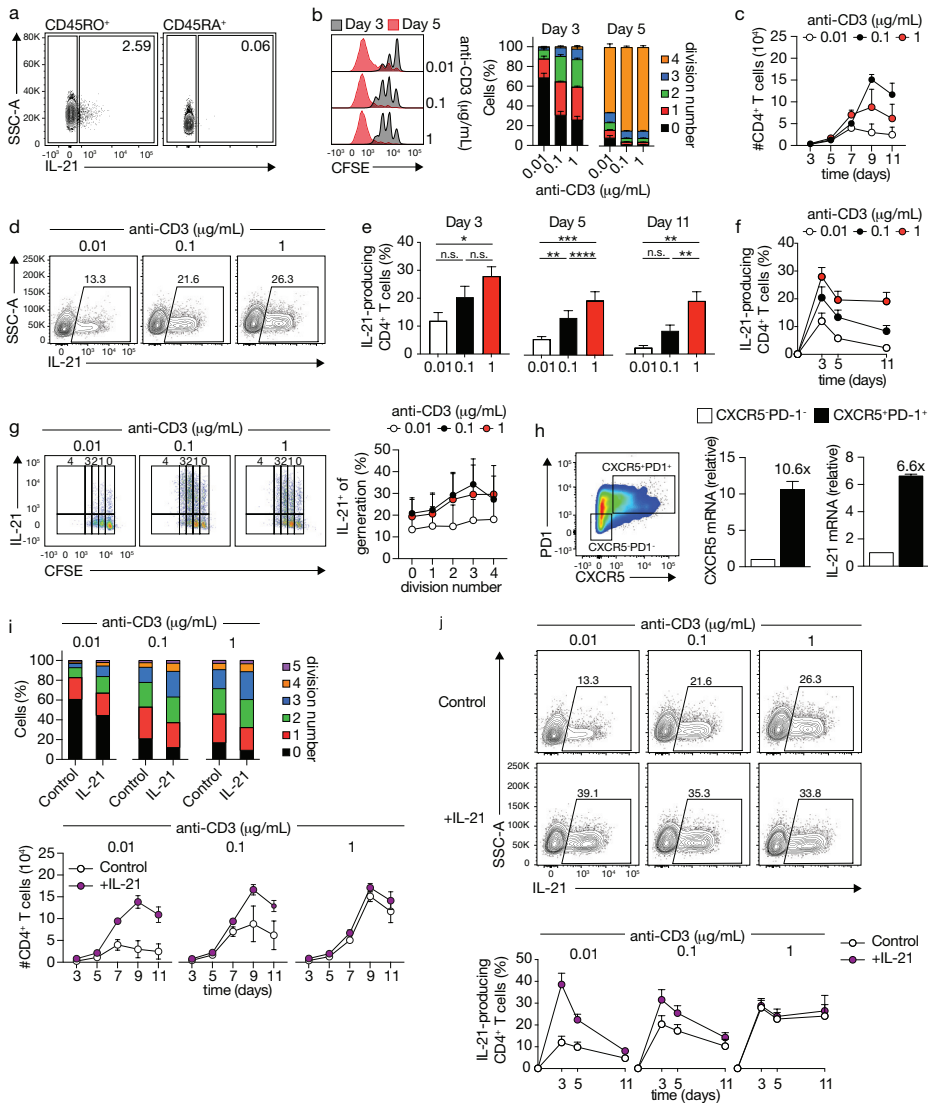


Figure 1 | CD4⁺ T cells produce IL-21 and acquire a Tfh-like phenotype upon increasing CD3-TCR stimulations.

(a) Flow cytometry of IL-21 expression in human memory (CD45RA⁺CD45RO⁻) and naive (CD45RA⁻CD45RO⁺) CD4⁺ T cells. (b) Flow cytometry of CFSE-labeled CD4⁺ T cells stimulated with varying concentrations of CD3-TCR stimulating antibodies (anti-CD3) for 3 or 5 days (left) and summary of the fraction within each division (right). (c) The number of live CD4⁺ events after culture with anti-CD3 for the indicated time points. (d) Flow cytometry of IL-21 expression after anti-CD3 stimulation for 5 days. Numbers in the gate indicate the percentage of cells. (e-f) Quantification of IL-21 production after anti-CD3 stimulation for 3 (n=6), 5 (n=17), and 11 (n=6) days. (g) Flow cytometry (left) of CFSE-labeled CD4⁺ T cells stimulated with anti-CD3 for 3 days and a summary of the fraction of IL-21-positive CD4⁺ T cells at each division (right). (h) Flow cytometry CD4⁺ T cells at day 3 after stimulation with 1 μg/mL anti-CD3. Outlined areas indicate CXCR5⁺PD1⁻ and CXCR5⁺PD1⁺ cells that were sorted and analyzed for CXCR5 and IL-21 mRNA expression (right; n=2). (i) Summary of the fraction of CD4⁺ T cells within each division after anti-CD3 and recombinant IL-21 (rIL-21) stimulation for 3 days (top) and the number of live CD4⁺ events as measured at

(legend continues on next page)

- ◀ the indicated time points (bottom; n=3). (j) Flow cytometry of IL-21 expression after anti-CD3 and rIL-21 stimulation for 5 days (top). Numbers in the gate indicate the percent cells. (bottom) quantification of IL-21 production after anti-CD3 and rIL-21 stimulation for 3 (n=6), 5 (n=17) and 11 (n=6) days. Data were analyzed by (e) repeated-measures one-way ANOVA with Sidak post-test; *p < 0.05, **p < 0.01, ***p < 0.001, ****p < 0.0001, n.s., not significantly different. Stacked bars show mean (n=3) individual donors.

IFN- γ (**Supplementary Figure 1c-d**). In contrast to IL-21, IL-4 and IFN- γ secretion was strongly related to cell division number, with levels increasing progressively over consecutive divisions (**Supplementary Figure 2e-f**). Exogenous IL-4 and IFN- γ provided positive feedforward signals on themselves (**Supplementary Figure 1g-h**), which was particularly pronounced for IL-4 when CD3-TCR stimulation was low (**Supplementary Figure 1g**), while suppressing expression of each other (**Supplementary Figure 1i-j**).

We then examined whether IL-21-producing Tfh-like cells can coexpress IL-4 and IFN- γ through variation in strength of TCR signaling (**Figure 2a-d**). Naive CD4⁺ T cell priming mainly yielded cells either expressing IL-4 or IL-21 (**Figure 2a-b**), with only a small fraction of cells coexpressing both along the entire range of CD3-TCR stimulations (**Figure 2b**). The inhibitory effects of IL-21 and IL-4 on their reciprocal expression (**Supplementary Figure 1k-l**) may contribute to the observed results. Exogenous IL-21 prominently suppressed IL-4 secretion after low and intermediate CD3-TCR stimulation (**Supplementary Figure 1k**), while exogenous IL-4 suppressed IL-21 mainly after high stimulations (**Supplementary Figure 1l**). In contrast, variation in CD3 signaling induced more coexpression of IL-21 and IFN- γ of (**Figure 2c-d**). Although most cells that produce IFN- γ did not simultaneously express IL-21, a significant portion of the cells that express IL-21 also expressed IFN- γ (**Figure 2c-d**). Strong CD3-TCR stimulation yielded relatively more IL-21 and IFN- γ coexpression than cells expressing only IL-21 (**Figure 2c-d**). To evaluate cytokine coexpression by IL-21-producing Tfh-like cells in more detail, IL-21-producing cells were selected, and IL-4 and IFN- γ production and potential triple expression were analyzed after CD3-TCR stimulation (**Figure 2e-f**). We found that on day 3 of priming, most Tfh-like cells produced only IL-21 across a range of CD3-TCR stimulations (red; **Figure 2e-f**). Coexpression of IFN- γ was observed in a significant proportion of IL-21-producing CD4⁺ T cells, especially when CD3-TCR stimulation was high (**Figure 2e-f**). From day 5 on, the number of IL-21-producing Tfh-like cells that coexpressed IL-4 increased, particularly when CD3-TCR stimulation was low (**Figure 2e-f**). In these conditions, most cells coexpressing IL-4 also expressed IFN- γ (**Figure 2e-f**). Coexpression of IL-4 alone was mainly observed with low CD3-TCR stimulation, potentially due to positive feedforward signaling by IL-4 and limited secretion of IFN- γ and IL-21. These results indicate that the cytokines within the CD4⁺ T cell network interact and regulate each other in a complex manner, with both positive and negative feedback loops playing a role. Whereas single IL-21 expression is observed early after naive CD4⁺ T cell priming, plastic coexpression of IL-4 and IFN- γ occurs later, with especially restricted IL-21 and IL-4 coexpression upon low TCR stimulation.

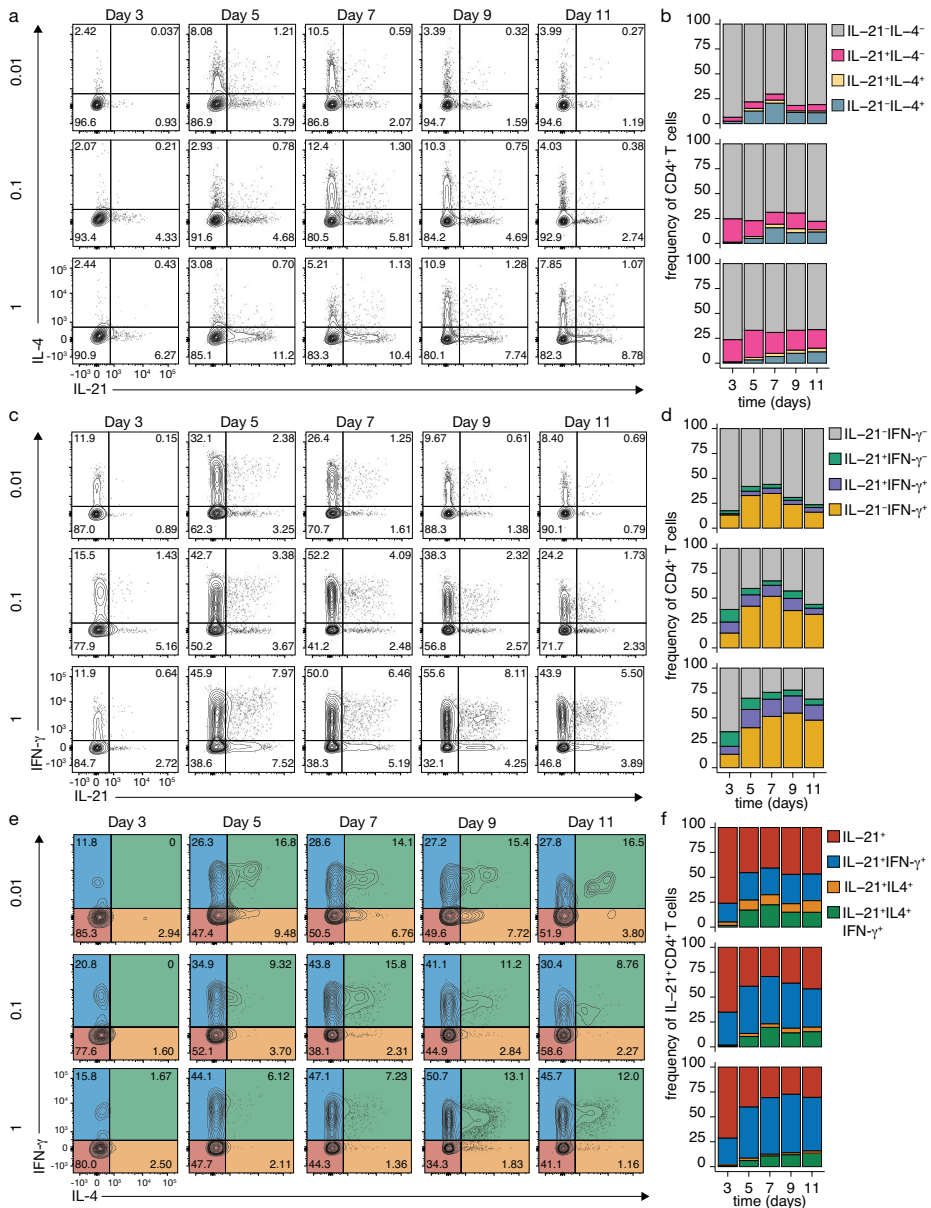


Figure 2 | CD3-TCR stimulation induces dynamic expression of IL-21, IL-4 and IFN- γ . (a, c) Flow cytometry of IL-4 and IL-21 (a) or IFN- γ and IL-21 (c) (co-)expression in CD4⁺ T cells. Numbers in the gate indicate the percentage of cells after 0.01 (top), 0.1 (middle), or 1 (bottom) μ g/mL anti-CD3 stimulation for the indicated days. (b, d) Quantification of IL-4 and IL-21 (b) or IFN- γ and IL-21 (d) (co-)expression in CD4⁺ T cells after variable anti-CD3 stimulation for the indicated days. (e) Flow cytometry of IL-4 and IFN- γ coexpression in IL-21-producing Tfh-like cells after 0.01 (top), 0.1 (middle), or 1 (bottom) μ g/mL anti-CD3 stimulation for the indicated days. Outlined areas indicate IL-21⁺IL-4⁻IFN- γ ⁻ (red), IL-21⁺IL-4⁺IFN- γ ⁻ (blue), IL-21⁺IL-4⁻IFN- γ ⁺ (green) and IL-21⁻IL-4⁺IFN- γ ⁻ (orange). (f) Quantification of IL-4 and IFN- γ coexpression in IL-21-producing Tfh-like cells after variable anti-CD3 stimulation for the indicated days. Stacked bars show mean (n=3) individual donors.

Exogenous cytokines IL-21 and IL-4 regulate plastic coexpression of IL-4 and IFN- γ in IL-21-producing Tfh-like cells

Next, effects of IL-21 and IL-4 on plastic coexpression of IL-4 and IFN- γ in IL-21-producing Tfh cells were investigated (**Supplementary Figure 2 and 3**), with a particular focus on effective range of these exogenous cytokines: low CD3-TCR stimulation for IL-4 and high for IL-21 (**Figure 3**). Exogenous IL-4 or IL-21 profoundly affected the coexpression of IL-21 and IL-4 (**Figure 3a**). Exogenous IL-4 induced IL-4 (**Figure 3a-b versus Figure 2a-b**, top rows), while addition of IL-21 induced IL-21 production without coexpression of IL-4 (**Figure 3a-b versus Figure 2a-b**, bottom rows). Interestingly, exogenous IL-21 induced coexpression of IL-21 and IL-4 double-positive cells (**Figure 3a versus Figure 2a-b**, bottom rows). Exogenous IL-4 or IL-21 had a notable effect on the coexpression of IL-21 and IFN- γ (**Figure 3c-d**). Coexpression was limited after CD3-TCR stimulation alone (**Figure 2c-d**) but was significantly enhanced with exogenous IL-21 (**Figure 3c-d and Supplementary Figure 2c-d**). Exogenous IL-4 mainly repressed cells that produce IFN- γ only (**Figure 3c-d and Supplementary Figure 3c-d**). To further evaluate cytokine coexpression by IL-21-producing Tfh-like cells, IL-21-producing cells were selected, and production of IL-4 and IFN- γ was analyzed (**Figure 3e-f, Supplementary Figure 2e-f, and Supplementary Figure 3e-f**). Exogenous IL-4 greatly increased the population of IL-21-producing Tfh-like cells coexpressing IL-4 either alone or in combination with IFN- γ , particularly but not exclusively after low stimulation (**Figure 3e-f and Supplementary Figure 3e-f versus Figure 2e-f, top rows**). Exogenous IL-21 did not significantly change coexpression of IL-4 and IFN- γ by IL-21-producing cells, at most, it slightly enhanced the IL-21⁺IFN- γ ⁺ population (**Figure 3e-f versus Figure 2e-f, bottom rows**). Thus, to induce major coexpression of IL-4 by IL-21-producing Tfh cells, excess IL-4 needs to be present that may act beyond the immunological synapse in which it is released, as has been shown for IL-21⁴².

Concluding remarks

This manuscript's data demonstrate that the intensity of TCR signaling (as a proxy for antigenic stimulation) significantly impacts activation and differentiation of naive CD4⁺ T cells into Tfh-like cells, with high TCR signaling leading to production of IL-21 and IFN- γ and low TCR signaling facilitating production of IL-4. Coexpression of these cytokines is regulated by TCR signaling strength and can be modulated by exogenous IL-21 or IL-4. This research provides new insights into the plasticity of Tfh-like cells and the complex regulatory mechanisms that govern their cytokine production. This is especially important for the regulation of the B cell response. As these data show that strength of signal 1 co-regulates Tfh cell plasticity, these data may indicate that *in vivo* variation in antigen availability regulates Tfh cell plasticity. As these data show that with limited signal 1 coexpression of IL-21 and IL-4 is induced, it may suggest that limited antigen *in vivo* may favor induction of the GC reactions and later subsequent B memory formation. In contrast, the here observed repression of IL-4 in situations of strong signal 1 and subsequent predominance of IL-21⁺ cells either or not coexpressing IFN- γ , may suggest

that high antigen availability *in vivo* favors a switch towards plasma cell formation⁴³. These data warrant a more in-depth *in vivo* investigation on the effects of variation of antigen availability by using cytokine reporter mice^{44,45} and or detailed *ex vivo* analyses of antigen-specific Tfh cells in lymph node biopsies upon a human antigenic challenge over time.

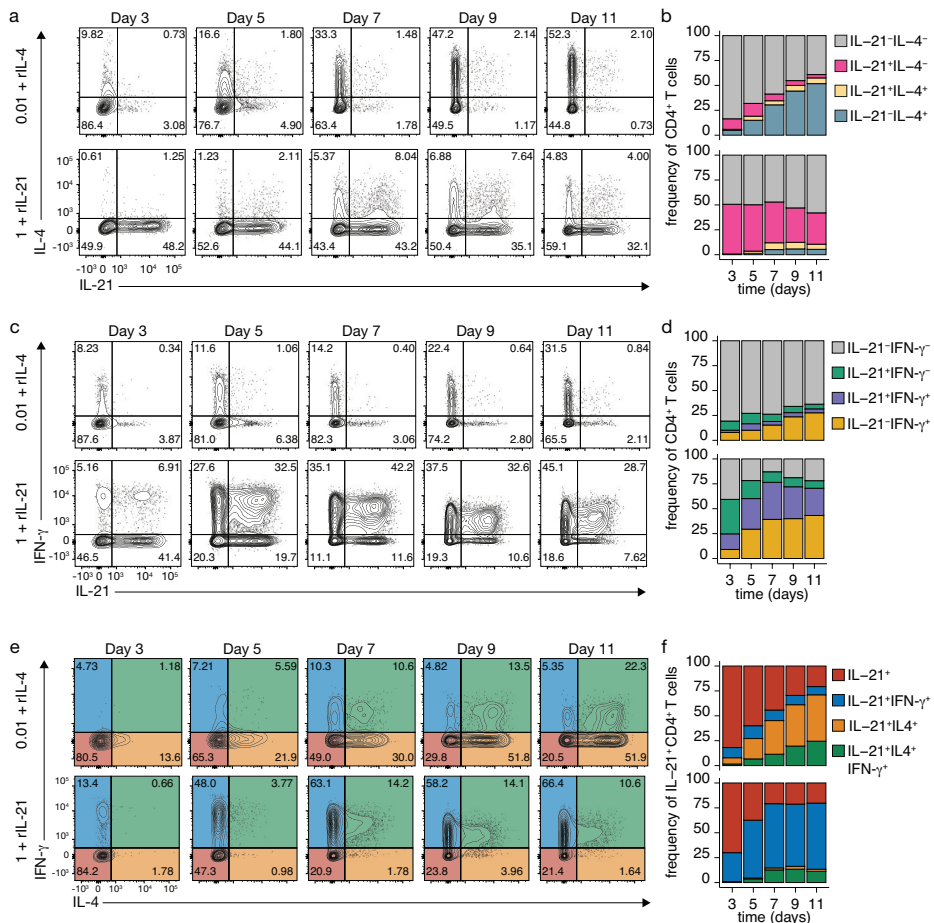


Figure 3 | Recombinant IL-21 and IL-4 affect CD3-TCR-induced dynamic expression of IL-21, IL-4, and IFN- γ . (a, c) Flow cytometry of IL-4 and IL-21 (a) or IFN- γ and IL-21 (c) (co-)expression in CD4⁺ T cells. Numbers in the gate indicate the percent of cells after 0.01 μ g/mL anti-CD3 stimulation with recombinant IL-4 (rIL-4; top) or 1 μ g/mL anti-CD3 stimulation with rIL-21 (bottom) for the indicated days. (b, d) Quantification of IL-4 and IL-21 (b) or IFN- γ and IL-21(d) (co-)expression in CD4⁺ T cells after 0.01 or 1 μ g/mL anti-CD3 together with rIL-4 or rIL-21, respectively, for the indicated days. (e) Flow cytometry of IL-4 and IFN- γ coexpression in IL-21-producing Tfh-like cells after 0.01 μ g/mL anti-CD3 stimulation with recombinant IL-4 (rIL-4; top) or 1 μ g/mL anti-CD3 stimulation with rIL-21 (bottom) for the indicated days. Outlined areas indicate IL-21⁺IL-4⁻IFN- γ ⁻ (red), IL-21⁺IL-4⁻IFN- γ ⁺ (blue), IL-21⁺IL-4⁺IFN- γ ⁺ (green) and IL-21⁻IL-4⁺IFN- γ ⁻ (orange). (f) Quantification of IL-4 and IFN- γ coexpression in IL-21-producing Tfh-like cells after 0.01 or 1 μ g/mL anti-CD3 together with rIL-4 or rIL-21, respectively, for the indicated days. Stacked bars show mean (n=3) individual donors.

ACKNOWLEDGMENTS

We thank E.P.J. Mul, M. Hoogenboezem, and S. Tol for their technical support.

DECLARATION OF INTEREST

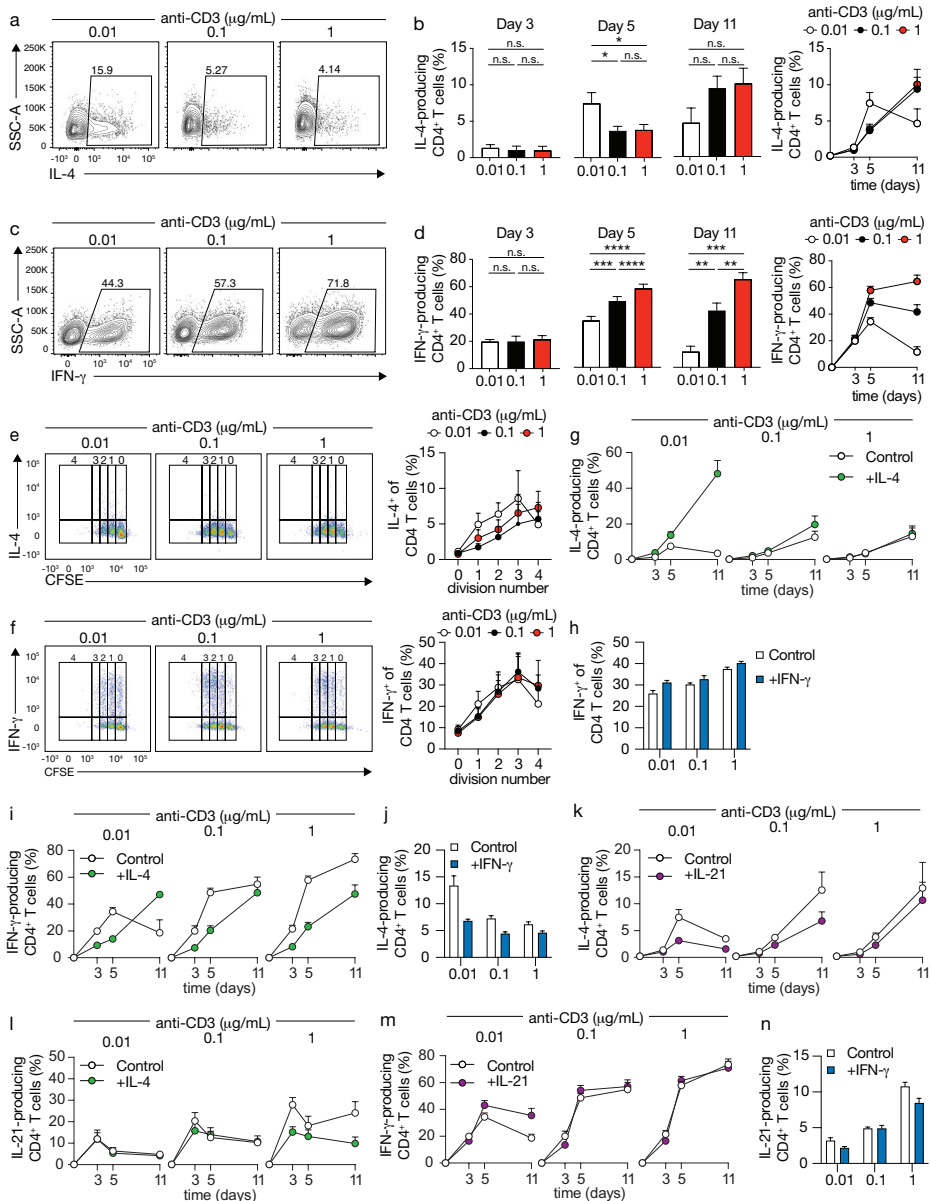
The authors declare that they have no conflict of interest.

REFERENCES

1. Randolph, G. J., Angeli, V. & Swartz, M. A. Dendritic-cell trafficking to lymph nodes through lymphatic vessels. *Nat Rev Immunol* **5**, 617–28 (2005).
2. Kaliński, P., Hilkens, C. M. U., Wierenga, E. A. & Kapsenberg, M. L. T-cell priming by type-1 and type-2 polarized dendritic cells: The concept of a third signal. *Immunol Today* **20**, 561–567 (1999).
3. Kapsenberg, M. L. Dendritic-cell control of pathogen-driven T-cell polarization. *Nat Rev Immunol* **3**, 984–993 (2003).
4. O’Shea, J. J., Hunter, C. A. & Germain, R. N. T cell heterogeneity: firmly fixed, predominantly plastic or merely malleable? *Nat Immunol* **9**, 450–3 (2008).
5. Nakayamada, S., Takahashi, H., Kanno, Y. & O’Shea, J. J. Helper T cell diversity and plasticity. *Curr Opin Immunol* **24**, 297–302 (2012).
6. Geginat, J. *et al.* Plasticity of human CD4 T cell subsets. *Front Immunol* **5**, 630 (2014).
7. Zhu, J. & Paul, W. E. Heterogeneity and plasticity of T helper cells. *Cell Research* **20**, 4–12 (2009).
8. Zhu, J. T Helper Cell Differentiation, Heterogeneity, and Plasticity. *Cold Spring Harb Perspect Biol* **10**, a030338 (2018).
9. Bonelli, M. *et al.* Helper T cell plasticity: impact of extrinsic and intrinsic signals on transcriptomes and epigenomes. *Curr Top Microbiol Immunol* **381**, 279–326 (2014).
10. Krishnaswamy, J. K., Alsén, S., Yrlid, U., Eisenbarth, S. C. & Williams, A. Determination of T Follicular Helper Cell Fate by Dendritic Cells. *Front Immunol* **9**, 2169 (2018).
11. Mintz, M. A. & Cyster, J. G. T follicular helper cells in germinal center B cell selection and lymphomagenesis. *Immunol Rev* **296**, 48–61 (2020).
12. Kerfoot, S. M. *et al.* Germinal center B cell and T follicular helper cell development initiates in the interfollicular zone. *Immunity* **34**, 947–60 (2011).
13. Crotty, S. T follicular helper cell differentiation, function, and roles in disease. *Immunity* **41**, 529–42 (2014).
14. Crotty, S. Follicular helper CD4 T cells (TFH). *Annu Rev Immunol* **29**, 621–63 (2011).
15. Unger, P.-P. A. *et al.* Minimalistic In Vitro Culture to Drive Human Naive B Cell Differentiation into Antibody-Secreting Cells. *Cells* **10**, 1183 (2021).
16. Marsman, C. *et al.* Termination of CD40L co-stimulation promotes human B cell differentiation into antibody-secreting cells. *Eur J Immunol* 1–14 (2022) doi:10.1002/eji.202249972.
17. Kotlarz, D., Ziętara, N., Milner, J. D. & Klein, C. Human IL-21 and IL-21R deficiencies: two novel entities of primary immunodeficiency. *Curr Opin Pediatr* **26**, 704–12 (2014).
18. Ozaki, K. *et al.* A critical role for IL-21 in regulating immunoglobulin production. *Science* **298**, 1630–1634 (2002).
19. Weinstein, J. S. *et al.* TFH cells progressively differentiate to regulate the germinal center response. *Nat Immunol* **17**, 1197–205 (2016).
20. Snapper, C. M., Finkelman, F. D. & Paul, W. E. Regulation of IgG1 and IgE Production by Interleukin 4. *Immunol Rev* **102**, 51–75 (1988).
21. Duan, L. *et al.* Follicular dendritic cells restrict interleukin-4 availability in germinal centers and foster memory B cell generation. *Immunity* **54**, 2256–2272.e6 (2021).
22. Yu, S. *et al.* IL-12 induced the generation of IL-21-and IFN- γ -co-expressing poly-functional CD4+ T cells from human naive CD4+ T cells. *Cell Cycle* **14**, 3362–3372 (2015).
23. Shulman, Z. *et al.* Dynamic signaling by T follicular helper cells during germinal center B cell selection. *Science* **345**, 1058–1062 (2014).
24. Merckenschlager, J. *et al.* Dynamic regulation of TFH selection during the germinal centre reaction. *Nature* 1–6 (2021) doi:10.1038/s41586-021-03187-x.
25. Rogers, P. R. & Croft, M. Peptide dose, affinity, and time of differentiation can contribute to the Th1/Th2 cytokine balance. *J Immunol* **163**, 1205–13 (1999).
26. Constant, S., Pfeiffer, C., Woodard, A., Pasqualini, T. & Bottomly, K. Extent of T cell receptor ligation can determine the functional differentiation of naive CD4+ T cells. *J Exp Med* **182**, 1591–6 (1995).
27. Corse, E., Gottschalk, R. A. & Allison, J. P. Strength of TCR-peptide/MHC interactions and in vivo T cell responses. *J Immunol* **186**, 5039–45 (2011).
28. Tao, X., Constant, S., Jorritsma, P. & Bottomly, K. Strength of TCR signal determines the costimulatory requirements for Th1 and Th2 CD4+ T cell differentiation. *J Immunol* **159**, 5956–63 (1997).

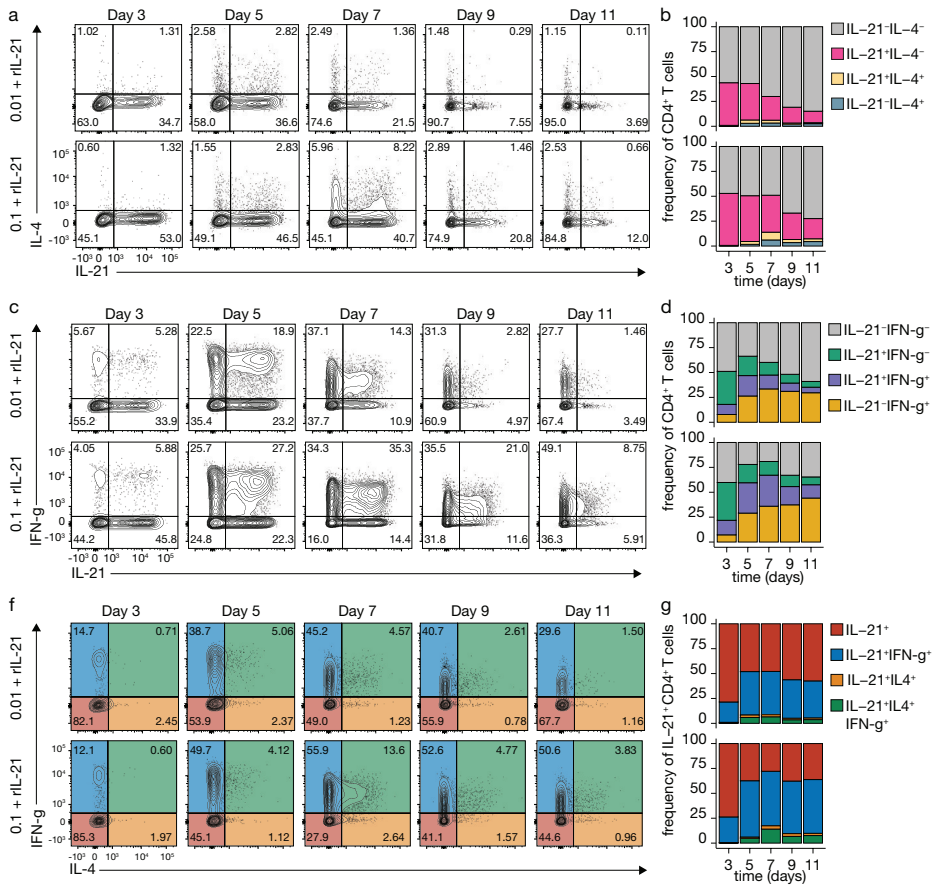
29. Keck, S. *et al.* Antigen affinity and antigen dose exert distinct influences on CD4⁺ T-cell differentiation. *Proc Natl Acad Sci U S A* **111**, 14852–7 (2014).
30. Kotorov, D. I. *et al.* TCR Affinity Biases Th Cell Differentiation by Regulating CD25, Eef1e1, and Gbp2. *The Journal of Immunology* **202**, 2535–2545 (2019).
31. Snook, J. P., Kim, C. & Williams, M. A. TCR signal strength controls the differentiation of CD4⁺ effector and memory T cells. *Sci Immunol* **3**, eaas9103 (2018).
32. Ditoro, D. *et al.* Differential IL-2 expression defines developmental fates of follicular versus nonfollicular helper T cells. *Science (1979)* **361**, (2018).
33. Krishnamoorthy, V. *et al.* The IRF4 Gene Regulatory Module Functions as a Read-Write Integrator to Dynamically Coordinate T Helper Cell Fate. *Immunity* **47**, 481–497.e7 (2017).
34. Tubo, N. J. *et al.* Single Naive CD4⁺ T Cells from a Diverse Repertoire Produce Different Effector Cell Types during Infection. *Cell* **153**, 785–796 (2013).
35. Ploquin, M. J.-Y., Eksmond, U. & Kassiotis, G. B Cells and TCR Avidity Determine Distinct Functions of CD4⁺ T Cells in Retroviral Infection. *The Journal of Immunology* **187**, 3321–3330 (2011).
36. Fazilleau, N., McHeyzer-Williams, L. J., Rosen, H. & McHeyzer-Williams, M. G. The function of follicular helper T cells is regulated by the strength of T cell antigen receptor binding. *Nat Immunol* **10**, 375–384 (2009).
37. Souwer, Y. *et al.* B cell receptor-mediated internalization of salmonella: a novel pathway for autonomous B cell activation and antibody production. *J Immunol* **182**, 7473–81 (2009).
38. Guy, C. S. *et al.* Distinct TCR signaling pathways drive proliferation and cytokine production in T cells. *Nat Immunol* **14**, 262–270 (2013).
39. Liu, J. *et al.* Enhanced CD4⁺ T Cell Proliferation and Th2 Cytokine Production in DR6-Deficient Mice. *Immunity* **15**, 23–34 (2001).
40. Vogelzang, A. *et al.* A Fundamental Role for Interleukin-21 in the Generation of T Follicular Helper Cells. *Immunity* **29**, 127–137 (2008).
41. Fishman, P. H. & Curran, P. K. Brefeldin A inhibits protein synthesis in cultured cells. *FEBS Lett* **314**, 371–374 (1992).
42. Quast, I. *et al.* Interleukin-21, acting beyond the immunological synapse, independently controls T follicular helper and germinal center B cells. *Immunity* 1–22 (2022) doi:10.1016/j.immuni.2022.06.020.
43. Weisel, F. J., Zuccarino-Catania, G. v., Chikina, M. & Shlomchik, M. J. A Temporal Switch in the Germinal Center Determines Differential Output of Memory B and Plasma Cells. *Immunity* **44**, 116–130 (2016).
44. Mohrs, K., Wakil, A. E., Killeen, N., Locksley, R. M. & Mohrs, M. A Two-Step Process for Cytokine Production Revealed by IL-4 Dual-Reporter Mice. *Immunity* **23**, 419 (2005).
45. Lüthje, K. *et al.* The development and fate of follicular helper T cells defined by an IL-21 reporter mouse. *Nat Immunol* **13**, 491–498 (2012).

SUPPLEMENTARY INFORMATION

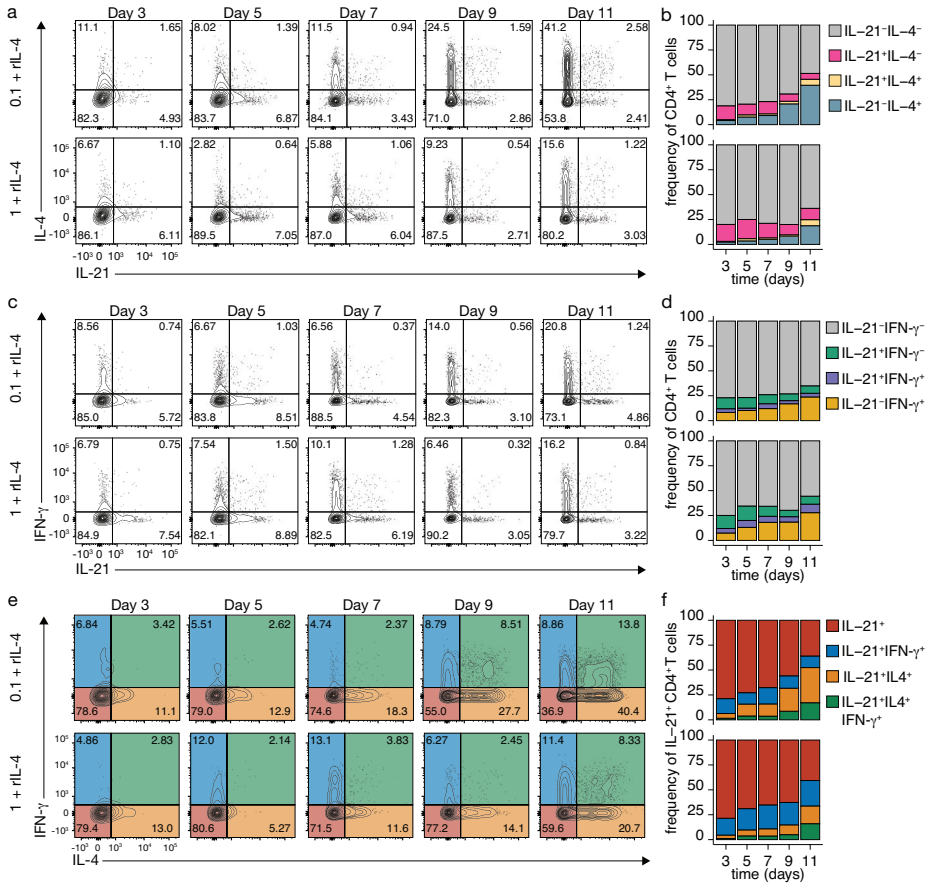


Supplementary Figure 1 | Dynamic modulating effects of Th1, Th2, and Tfh cell cytokines. (a) Flow cytometry of IL-4 expression after anti-CD3 stimulation for 5 days. Numbers in the gate indicate the percent cells. (b) Quantification of IL-4 production after anti-CD3 stimulation for 3 (n=6), 5 (n=17) and 11 (n=6) days. (c) Flow cytometry of IFN- γ expression after anti-CD3 stimulation for 5 days. Numbers in the gate indicate the percentage of cells. (d) Quantification of IFN- γ production after anti-CD3 stimulation for 3 (n=6), 5 (n=17) and 11 (n=6) days. (e-f) Flow cytometry (left) (legend continues on next page)

- ◀ of CFSE-labeled CD4⁺ T cells stimulated with anti-CD3 for 3 days and a summary of the fraction of IL-4-positive (e) or IFN- γ -positive (f) CD4⁺ T cells at each division (right). (g) Quantification of IL-4 production after anti-CD3 and recombinant IL-4 (rIL-4) stimulation for 3 (n=6), 5 (n=17) and 11 (n=6) days. (h) Quantification of IFN- γ production after anti-CD3 and rIFN- γ stimulation for 5 days (n=3). (i) Quantification of IFN- γ production after anti-CD3 and rIL-4 stimulation for 3 (n=6), 5 (n=17) and 11 (n=6) days. (j) Quantification of IL-4 production after anti-CD3 and rIFN- γ stimulation for 5 days (n=3). (k) Quantification of IL-4 production after anti-CD3 and rIL-21 stimulation for 3 (n=6), 5 (n=17) and 11 (n=6) days. (l) Quantification of IL-21 production after anti-CD3 and rIL-4 stimulation for 3 (n=6), 5 (n=17) and 11 (n=6) days. (m) Quantification of IFN- γ production after anti-CD3 and rIL-21 stimulation for 3 (n=6), 5 (n=17) and 11 (n=6) days. (n) Quantification of IL-21 production after anti-CD3 and rIFN- γ stimulation for 5 days (n=3). Data were analyzed by (b and d) repeated-measures one-way ANOVA with Sidak post-test; *p < 0.05, **p < 0.01, ***p < 0.001, ****P < 0.0001, n.s., not significantly different.



Supplementary Figure 2 | Recombinant IL-21 (rIL-21) affect CD3-TCR-induced dynamic expression of IL-21, IL-4, and IFN- γ . (a, c) Flow cytometry of IL-4 and IL-21 (a) or IFN- γ and IL-21 (c) (co-)expression in CD4⁺ T cells. Numbers in the gate indicate the percentage of cells after 0.01 (top) or 0.1 (bottom) $\mu\text{g}/\text{mL}$ anti-CD3 stimulation with rIL-21 for the indicated days. (b, d) Quantification of IL-4 and IL-21 (b) or IFN- γ and IL-21(d) (co-)expression in CD4⁺ T cells after 0.01 (top) or 0.1 (bottom) $\mu\text{g}/\text{mL}$ anti-CD3 stimulation with rIL-21 for the indicated days. (e) Flow cytometry of IL-4 and IFN- γ coexpression in IL-21-producing Tfh-like cells after 0.01 (top) or 0.1 (bottom) $\mu\text{g}/\text{mL}$ anti-CD3 stimulation with rIL-21 for the indicated days. Outlined areas indicate IL-21⁺IL-4⁺IFN- γ ⁻ (red), IL-21⁺IL-4⁺IFN- γ ⁺ (blue), IL-21⁺IL-4⁻IFN- γ ⁻ (green) and IL-21⁺IL-4⁻IFN- γ ⁺ (orange). (f) Quantification of IL-4 and IFN- γ coexpression in IL-21-producing Tfh-like cells after 0.01 (top) or 0.1 (bottom) $\mu\text{g}/\text{mL}$ anti-CD3 stimulation with rIL-21 for the indicated days. Stacked bars show mean (n=3) individual donors.



Supplementary Figure 3 | Recombinant IL-4 (rIL-4) affect CD3-TCR-induced dynamic expression of IL-21, IL-4, and IFN- γ . (a, c) Flow cytometry of IL-4 and IL-21 (a) or IFN- γ and IL-21 (c) (co-expression) in CD4⁺ T cells. Numbers in the gate indicate the percentage of cells after 0.1 (top) or 1 (bottom) $\mu\text{g}/\text{mL}$ anti-CD3 stimulation with rIL-4 for the indicated days. (b, d) Quantification of IL-4 and IL-21 (b) or IFN- γ and IL-21 (d) (co-expression) in CD4⁺ T cells after 0.1 (top) or 1 (bottom) $\mu\text{g}/\text{mL}$ anti-CD3 stimulation with rIL-4 for the indicated days. (e) Flow cytometry of IL-4 and IFN- γ coexpression in IL-21-producing Tfh-like cells after 0.1 (top) or 1 (bottom) $\mu\text{g}/\text{mL}$ anti-CD3 stimulation with rIL-4 for the indicated days. Outlined areas indicate IL-21⁺IL-4⁻IFN- γ ⁻ (red), IL-21⁺IL-4⁻IFN- γ ⁺ (blue), IL-21⁺IL-4⁺IFN- γ ⁻ (green) and IL-21⁺IL-4⁺IFN- γ ⁺ (orange). (f) Quantification of IL-4 and IFN- γ coexpression in IL-21-producing Tfh-like cells after 0.1 (top) or 1 (bottom) $\mu\text{g}/\text{mL}$ anti-CD3 stimulation with rIL-4 for the indicated days. Stacked bars show mean (n=3) individual donors.

Supplementary Table 1 | Primer sequences.

Genes		Sequence (5'-3')
<i>18S-rRNA</i>	Forward	CGGCTACCACATCCAAGGAA
	Reverse	GCTGGAATTACCGCGGCT
<i>IL-21</i>	Forward	GTCATCTGTCTGATGGTCATC
	Reverse	CCACTCACAGTTTGTCTCTAC
<i>CXCR5</i>	Forward	CCGCTAACGCTGGAAATGGAC
	Reverse	GCAAAGGGCAAGATGAAGACC

Chapter 5

Minimalistic *in vitro* culture to drive human naive B cell differentiation into antibody-secreting cells

Niels J. M. Versteegen^{1,2,†}, Peter-Paul A. Unger^{1,†}, Casper Marsman¹, Tineke Jorritsma¹, Theo Rispens¹, Anja ten Brinke¹ and S. Marieke van Ham^{1,3}

Cells 10:1183 (2021)

1. Department of Immunopathology, Sanquin Research and Landsteiner Laboratory, Amsterdam University Medical Centers, University of Amsterdam, Amsterdam, The Netherlands
2. Synthetic Systems Biology and Nuclear Organization, Swammerdam Institute for Life Sciences, University of Amsterdam, Amsterdam, The Netherlands
3. Swammerdam Institute for Life Sciences, University of Amsterdam, Amsterdam, The Netherlands

† These authors contributed equally to this work.

ABSTRACT

High-affinity antibody-secreting cells (ASC) arise from terminal differentiation of B-cells after coordinated interactions with T follicular helper (Tfh) cells in germinal centers (GC). Elucidation of cues promoting human naive B-cells to progress into ASCs is challenging, as this process is notoriously difficult to induce *in vitro* while maintaining enough cell numbers to investigate the differentiation route(s). Here, we describe a minimalistic *in vitro* culture system that supports efficient differentiation of human naive B-cells into antibody-secreting cells. Upon initial stimulations, the interplay between level of CD40 costimulation and the Tfh cell-associated cytokines IL-21 and IL-4 determined the magnitude of B-cell expansion, immunoglobulin class-switching and expression of ASC regulator *PRDM1*. In contrast, the B-cell-specific transcriptional program was maintained, and efficient ASC formation was hampered. Renewed CD40 costimulation and Tfh cytokines exposure induced rapid secondary STAT3 signaling and extensive ASC differentiation, accompanied by repression of B-cell identity factors *PAX5*, *BACH2* and *IRF8* and further induction of *PRDM1*. Our work shows that, like *in vivo*, renewed CD40L costimulation also induces efficient terminal ASC differentiation after initial B-cell expansion *in vitro*. This culture system for efficient differentiation of human naive B-cells into ASCs, while also maintaining high cell numbers, may form an important tool in dissecting human naive B-cell differentiation, thereby enabling identification of novel transcriptional regulators and biomarkers for desired and detrimental antibody formation in humans.

INTRODUCTION

Production of high-affinity antibodies by long-lived plasma cells (PC) and the generation of long-lived memory B-cells (MBC) are essential characteristics of T-cell-dependent humoral immunity to combat invading pathogens and protect upon pathogen re-encounter. On the downside, undesired antibody responses result in pathologies, such as alloimmunity^{1,2} and autoimmunity³⁻⁶. Generation of class-switched high-affinity PCs and MBCs upon antigen encounter of B-cells also requires CD40 costimulation and cytokines, like IL-21 and IL-4, provided by T follicular helper (Tfh) cells in germinal center (GC) reactions in secondary lymphoid organs⁷⁻¹³. A GC contains two distinct morphological regions, the dark zone (DZ) and the light zone (LZ). In the DZ, GC B-cells (GCBC) undergo expansion and hypermutation of the genes that encode the immunoglobulin V region that affect antigen binding. GCBC that acquired B-cell receptor (BCR) mutants with increased affinity preferentially bind intact antigen displayed on the surface of follicular dendritic cells (FDC) in the LZ, which results in antigen internalization and presentation of antigen-derived peptides via major histocompatibility complex class II molecules (pMHCII) on the B-cell surface¹⁴. Subsequently, Tfh cells in the LZ engage in cognate interaction with GCBC necessary for GCBC selection. GCBC frequently migrate between DZ/LZ, which ultimately leads to the differentiation of GCBC with the highest affinity into the effector populations¹⁵. *In vivo*, GCBC thus repeatedly receive Tfh signals before terminal differentiation into antibody-secreting cells (ASCs), which consist of short-lived plasmablasts (PB) and long-lived PCs.

Insight into the factors that determine the actual fate decision of GCBC to become either MBC or ASC is being gained. Antibody-mediated inhibition and genetically manipulated mouse models have demonstrated an essential requirement for CD40L^{16,17} and IL-21 signaling^{18,19}, but also a contribution of inducible T cell costimulatory (ICOSL)²⁰, complement receptor (CR) 1 and 2²¹, programmed cell death protein 1 (PD1) and its ligands²², and CD80²³ in long-lived PC fate decision have been indicated. CD40 stimulation of naive B-cells combined with cytokines induces efficient proliferation, isotype switching and formation of a CD27⁺ B-cell population *in vitro*. In contrast, ASC formation is only observed in cultures with very limited B-cell numbers, which do not allow elucidation of the ASC differentiation process^{10,24}. This demonstrates that the current *in vitro* culture systems do not reflect the *in vivo* situation well enough. Previous research has demonstrated that strong CD40 signaling facilitates stable GCBC:Tfh cell interactions to drive the generation of ASC²⁵. In addition, graded levels of CD40-CD40L interactions in total B-cells regulated expansion and differentiation in the presence of IL-2, IL-4 and IL-10 *in vitro*²⁶. However, this study did not elucidate the effects of CD40 costimulation on naive B-cell differentiation.

An *in vitro* system that allows efficient naive B-cell differentiation into the ASCs is highly desired to (i) unravel the process(es) involved in ASC formation, (ii) identify the factors that control the fate decision of differentiating B-cells into ASCs and find targets to modulate antibody formation *in vivo* and (iii) identify membrane markers associated with the distinct

stages of B-cell to ASC formation with diagnostic potential for (early) assessment of undesired short-lived or long-lived antibody formation. Therefore, we established an *in vitro* culture system for human naive B-cell differentiation into ASCs by varying the level and frequency of CD40 costimulation. We demonstrate that high CD40 costimulation and IL-21 signaling induce naive B-cell expansion but do not allow full ASC formation due to maintenance of B-cell-specific transcription factors, *PAX5*, *IRF8* and *BACH2*. Renewed CD40 costimulation and IL-21 allowed effective ASC differentiation by extinguishing the B-cell transcriptional program, which correlated with the re-induction of STAT3 signaling.

MATERIALS AND METHODS

Cell lines

NIH3T3 fibroblast cells (3T3) were stably transfected with Fsp I linearized human CD40L plasmid (a kind gift from G. Freeman)^{27,28} and Pvu I linearized pcDNA3-neomycin plasmid in 3T3 medium (IMDM (Lonza, Basel, Switzerland) containing 10% FCS (Bodinco, Alkmaar, the Netherlands), 100 U/mL penicillin (Invitrogen, Carlsbad, CA, USA), 100 µg/mL streptomycin (Invitrogen, Carlsbad, CA, USA), 2 mM L-glutamine (Invitrogen, Carlsbad, CA, USA) and 50 µM β-mercaptoethanol (Sigma Aldrich, St. Louis, MO, USA) using the Lipofectamine 2000 DNA transfection reagent protocol (Invitrogen, Carlsbad, CA, USA). After three days, transfectants were cultured in 3T3 medium supplemented with 500 µg/mL G418 (Life Technologies, Carlsbad, CA, USA). Transfectants were sorted four times based on their CD40L expression using flow cytometry (anti-CD154; clone TRAP1; BD Bioscience) to select subclones stably expressing low (CD40L⁺) and intermediate (CD40L⁺⁺) CD40L levels than the already available NIH3T3 fibroblasts expressed high (CD40L⁺⁺⁺) human CD40L levels²⁷. Comparison of CD40L levels between the 3T3 cells expressing low, intermediate and high CD40L levels was done via flow cytometry after trypsinization. These cells were also cultured in 3T3 medium supplemented with 500 µg/mL G418.

Isolation of B cells from human healthy donors

Buffy coats were collected from voluntary, non-remunerated, adult healthy blood donors (Sanquin Blood Supply, Amsterdam, the Netherlands), who provided written informed consent for the use of remainders of their donation for research as part of routine donor selection and blood collection procedures. Peripheral blood mononucleated cells (PBMCs) were isolated from buffy coats using a Lymphoprep (Axis-Shield PoC AS, Dundee, Scotland) density gradient. Afterward, CD19⁺ B-cells were separated using magnetic anti-CD19 Dynabeads and DETACHaBEAD (Invitrogen, Carlsbad, CA, USA) according to manufacturer's instructions with purity >99%.

In vitro naive B cell differentiation cultures

3T3 WT and/or CD40L-expressing 3T3 cells were harvested and irradiated with 30 Gy.

Equal numbers (1×10^4) WT or CD40L-expressing (+, ++ or +++) 3T3 cells or, alternatively, 9:1 WT to CD40L⁺⁺⁺-expressing 3T3 cell ratio were seeded in B-cell medium (RPMI 1640 (Gibco, Dublin, Ireland) without phenol red containing 5% FCS, 100 U/mL penicillin, 100 µg/mL streptomycin, 2 mM L-glutamine, 50 µM β-mercaptoethanol and 20 µg/mL human apotransferrin (Sigma Aldrich, St. Louis, MO, USA; depleted for human IgG with protein G sepharose)) in 96-well flat-bottom Nunc plates (Thermo Fisher Scientific, Waltham, MA, USA) to allow adherence overnight.

The next day, CD19⁺CD27⁻IgG⁻ naive B-cells, to prevent BCR-mediated activation, were sorted on a FACS Aria II. To assess proliferation, FACS-sorted naive B-cells were labeled with 0.5 µM CFSE (Invitrogen, Carlsbad, CA, USA) in PBS for 15 min at room temperature. Labeling was stopped by adding B-cell medium. Immediately after labeling, 2.5×10^4 naive B-cells were cultured on the irradiated CD40L-expressing 3T3 fibroblasts in the presence of optimal concentrations (data not shown) of IL-21 (50 ng/mL; Invitrogen, Carlsbad, CA, USA) and/or IL-4 (100 ng/mL; CellGenix, Freiburg im Breisgau, Germany) for six and eleven days, without refreshing medium during these cultures, to assess IgG B-cell formation, antibody-secreting cell (ASC) differentiation and Ig secretion in the culture supernatants.

For secondary cultures, six-day stimulated B-cells were collected, washed and 2.5×10^4 cells were re-cultured in fresh medium on irradiated CD40L-expressing 3T3 fibroblasts (as described above), including cytokines as in the primary cultures for 5 days.

B-cell receptor stimulations were performed as previously described using soluble anti-IgM antibodies or anti-IgM-coated 3 µm polystyrene beads (Spherotech, Lake Forest, IL, USA)²⁹. For soluble antibody stimulation, B-cells were first incubated with 10 µg/mL mouse anti-human IgM (clone MH15-1; Sanquin Reagents, Amsterdam, the Netherlands) for 15 min. Excess non-bound antibodies were washed, and conditions were incubated with 10 µg/mL rat anti-mouse IgG1 antibodies for 15 min to crosslink all bound anti-IgM. Excess non-bound antibodies were washed, and 2.5×10^4 naive B-cells were cultured on irradiated CD40L-expressing 3T3 fibroblasts as described above. For stimulation with anti-IgM-coated beads (coated according to manufacturer's instructions), B-cells were pre-incubated with beads in a B:bead ratio of 1:2 for 30 min at 37 °C before putting the cells in co-culture with the irradiated CD40L-expressing 3T3 fibroblasts as described above.

Flow cytometry

Cells were first washed with PBS and stained with LIVE/DEAD fixable near-IR (dead cell stain kit, Invitrogen, Carlsbad, CA, USA) for 30 min at room temperature in the dark. Then, cells were washed with PBS supplemented with 1% bovine serum albumin. Extracellular staining was performed by incubating the cells for 30 min at room temperature in the dark with the following antibodies: Anti-CD19 (clone SJ25-C1, BD Bioscience, Franklin Lakes, NJ, USA), anti-CD20 (clone L27, BD Bioscience, Franklin Lakes, NJ, USA), anti-CD27 (clone L128, BD Bioscience, Franklin Lakes, NJ, USA; clone O323, eBioscience, San Diego, CA, USA), anti-CD38 (clone

HB7, BD Bioscience, Franklin Lakes, NJ, USA) and anti-IgG (clone G18-145, BD Bioscience, Franklin Lakes, NJ, USA or clone MH16-1, Sanquin Reagents, Amsterdam, the Netherlands). Samples were measured on a FACSCanto, FACSLSR II or FACSLSR Fortessa (BD Bioscience, Franklin Lakes, NJ, USA) and analyzed using FlowJo software version 10 (Treestar, Ashland, OR, USA).

Analysis of STAT phosphorylation

A total of 2×10^5 naive B-cells were cultured with 0.8×10^5 CD40L⁺⁺⁺-expressing 3T3 cells in a 24-well Nunc plate (Thermo Fisher Scientific, Waltham, MA, USA) in the absence or presence of IL-21 for 6, 36, 72, 144, 150, 180 and 216 h. IL-21 stimulated B-cells were harvested after 144 h, and secondary cultures were initiated with irradiated 0.8×10^5 CD40L⁺⁺⁺-expressing 3T3 cells in the absence or presence of IL-21 for 6, 36 and 72 h. Subsequently, the cells were harvested, stained with LIVE/DEAD Fixable Near-IR and anti-CD19 for 15 min on ice, fixed in 4% paraformaldehyde (Sigma Aldrich, St. Louis, MO, USA) for 10 min at 37 °C and permeabilized with ice-cold methanol (90%) for 30 min on ice. The cells were then stained with BD Phosflow anti-pSTAT3 (clone 4/P-STAT3) for 30 min at room temperature. Samples were measured on FACSLSR II and analyzed using FlowJo software version 10 (Treestar, Ashland, OR, USA).

IgM and IgG ELISA of culture supernatants

IgM and IgG levels in supernatants were measured as previously described³⁰. In short, plates were coated with monoclonal anti-IgM or anti-IgG (2 µg/mL; clone MH15-1 and MH16-1, respectively; Sanquin Reagents, Amsterdam, the Netherlands) and for detection, horseradish peroxidase-conjugated mouse-anti-human-IgM or mouse-anti-human-IgG (1 µg/mL in HPE; clone MH15-1 and MH16-1, respectively; Sanquin Reagents, Amsterdam, the Netherlands) were used. The ELISA was developed with 100 µg/mL tetramethylbenzidine in 0.11 mol/L sodium acetate (pH 5.5) containing 0.003% (v/v) H₂O₂. The reaction was stopped with 2 M H₂SO₄. Absorption at 450 and 540 nm was measured with a Synergy 2 microplate reader (Biotek, Winooski, VT, USA). Results were related to a titration curve of a serum pool in each plate. The lower-limit detection levels of IgM and IgG ELISA were 5 ng/mL and 2 ng/mL, respectively.

3T3 cell-specific BCR/antibody assay

3T3 WT cells were harvested, and 2×10^5 3T3 cells were incubated with culture supernatants that contain secreted antibodies of unswitched (IgM) and class-switched (IgG) isotypes or with 4 µg/mL normal human immunoglobulin (Nanogram 5%; Sanquin Reagents, Amsterdam, the Netherlands) for 30 min at 4 °C in the dark. After incubation, cells were washed with PBS supplemented with 1% bovine serum albumin and subsequently incubated with mouse anti-human IgM (clone MH15-1; Sanquin Reagents, Amsterdam, the Netherlands) and mouse anti-human IgG (clone MH16-1; Sanquin Reagents, Amsterdam, the Netherlands) for 30 min at 4 °C in the dark. Samples were measured on a FACSCanto (BD Bioscience, Franklin Lakes, NJ,

USA) and analyzed using FlowJo software version 10 (Treestar, Ashland, OR, USA).

Wide-field microscopy

WT and human CD40L-expressing 3T3 cells were harvested and irradiated with 30 Gy. CD40L⁺⁺⁺-expressing 3T3 cells were labeled with 5.88 μ M PKH26 (PKH26 Fluorescent Cell Linker Mini Kit for General Cell Membrane Labeling; Sigma Aldrich, St. Louis, MO, USA) in Diluent C for 5 min at room temperature. Labeling was stopped by adding B-cell medium. Equal numbers (2.1×10^4) WT or CD40L⁺⁺⁺-expressing 3T3 cells or, alternatively, 9:1 WT to CD40L⁺⁺⁺-expressing 3T3 cell ratio were seeded in B-cell medium on Nunc Lab-Tek II Chamber Slide 8 well glass slides (Thermo Fisher Scientific, Waltham, MA, USA) to allow adherence overnight. The next day 5.2×10^4 naive B-cells labeled with 0.5 μ M CFSE (Invitrogen, Carlsbad, CA, USA) were added and imaged every 10 min for 48 h on a Zeiss Observer Z1.

Real-time semi-quantitative RT-PCR

Different B-cell subsets (as indicated) were sorted. After sorting, RT-PCR was performed as described before³⁰. Primers were developed to span exon-intron junctions and then validated (**Table S1**). Gene expression levels were measured in duplicate reactions for each sample in StepOnePlus (Applied Biosystems, Foster City, CA, USA) using the SYBR green method (Applied Biosystems, Foster City, CA, USA).

Statistical analysis

Statistical analysis was performed using Prism 7 (GraphPad, San Diego, CA, USA). The statistical tests used are indicated in figure descriptions. Differences were considered statistically significant when $p \leq 0.05$.

RESULTS

The level of CD40 costimulation cooperates with IL-21 and/or IL-4 signaling to regulate human naive B cell expansion and IgG isotype switching

The first step in establishing an *in vitro* human naive B-cell differentiation system was to investigate how variation in CD40 costimulation regulates naive B-cell responses as graded levels of CD40-CD40L interactions regulated expansion and differentiation of total B-cells *in vitro*²⁶. Therefore, 3T3 mouse fibroblasts expressing varying levels of human CD40L were generated (**Figure 1A**). CD19⁺CD27⁻IgG⁻ human naive B-cells were cultured on WT (=CD40L-negative) or CD40L-expressing cells. The Tfh cell-associated cytokines IL-21 and/or IL-4 were either or not added as it has been shown that *in vivo* Tfh cells extinguish IL-21 production to switch to IL-4 production, including a transitory IL-21⁺/IL-4⁺ double-positive phase that allowed secretion of either one⁷. In line with a previous report³¹, the expansion of naive B-cells was highly reliant on costimulation by CD40L (**Figures 1B and S1A**). Although the proliferation of the naive B-cell

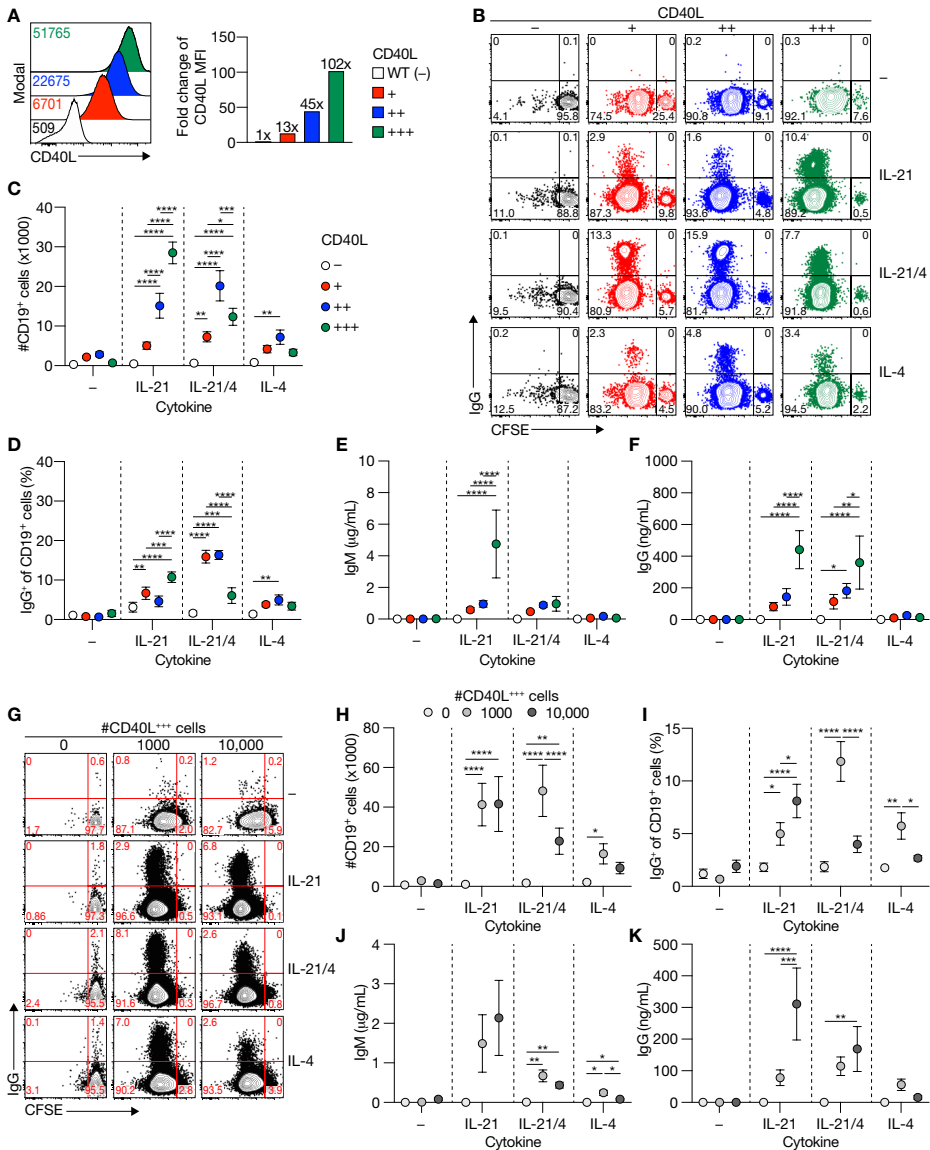


Figure 1 | Level of CD40L expression and number of CD40L feeder cells supports human naive B-cell expansion and IgG class switching. (A) Representative histograms (left) of human CD40L expression stably transfected 3T3 fibroblasts expressing various amounts of human CD40L (+, ++ or +++) compared to non-transfected 3T3 cells (WT; -). Numbers indicate the mean fluorescence intensity (MFI) of CD40L expression. Fold changes compared to WT controls of CD40L MFI are shown in the right panel (data shown represent three separate experiments). (B–D) Human CFSE-labeled naive B-cells were cultured on 3T3 cells expressing varying levels of CD40L with or without IL-21 and/or IL-4 for 6 days and analyzed for proliferation and class switching to surface IgG (B; representative plots). The number of live CD19⁺ B-cells (C) and surface IgG-expression (D) was quantified after the cultures by flow cytometry analysis (n = 6). (E–F) Cumulative secretion of IgM (E; n = 9) and IgG (F; n = 8) measured in culture supernatants after 11 days. (G) Representative plots of CFSE-labeled human naive B-cells cultured on 0/1000/10,000 CD40L⁺⁺⁺-expressing 3T3 cells (supplemented to 10,000 with WT 3T3 cells) with or without IL-21 and/or IL-4 for 6 days. (H–I) Number of CD19⁺ cells (H) and IgG secretion (I) quantified after 11 days. (J–K) IgM secretion (J) and IgG secretion (K) quantified after 11 days. *(legend continues on next page)*

- ◀ of live CD19⁺ events (C; n = 9) and the frequency of IgG⁺ cells (D; n = 7) after culture on 0/1000/10,000 CD40L⁺⁺⁺-expressing 3T3 cells, and cytokines for 6 days. (J–K) Cumulative IgM (F; n = 7) and IgG (G; n = 7) levels measured in culture supernatants after 11 days. Data are shown as mean ± SEM of independent experiments. Single experiments were conducted in triplicate. Data were analyzed by a two-way ANOVA followed by Tukey's multiple comparison test. * $P \leq 0.05$, ** $P \leq 0.01$, *** $P \leq 0.001$, **** $P \leq 0.0001$.

population was detected upon CD40 ligation, the number of living cells retrieved 6 days after culture remained low (**Figure 1C**). This indicates that CD40 ligation is essential for naive B-cell proliferation but that the level of expansion requires additional signals. Indeed, especially in the presence of IL-21, higher CD40 costimulation enhanced B-cell numbers and B-cell proliferation after 6 days in culture (**Figure 1B,C and S1B**). The addition of IL-4 to the culture system supported CD40-mediated B-cell expansion but provided a threshold for the maximum level of CD40 stimulation that could support B-cell proliferation and live B-cell numbers (**Figure 1B,C and S1B**). These data indicate that, especially in the presence of IL-21, costimulation via CD40 controls maximal expansion and maintenance of human naive B-cells in an intensity-dependent manner *in vitro*.

Analysis of effects of the levels of CD40 costimulation on B-cell differentiation showed that the level of CD40 costimulation positively correlated with BCR class switch recombination (CSR) from IgM to IgG in the presence of IL-21 after 6 days of culture (**Figure 1B,D**). Again, the addition of IL-4 in the system introduced a maximum threshold for the positive effect of CD40 costimulation, although IL-4 did enhance CSR in conditions where low and intermediate levels of CD40L costimulation were provided than IL-21 alone (**Figure 1D**). Human BCRs did not recognize 3T3 cell antigens (**Figure S3**), neither did BCR-ligation using soluble anti-IgM antibodies or anti-IgM-coated particles further affect BCR class switching induced by CD40 ligation and IL-21 and/or IL-4 signaling (**Figure S2A**). Varying levels of CD40 costimulation demonstrated that secretion of IgM and IgG antibodies depended on the strength of costimulation, with the highest level of costimulation being especially supportive for IgM and IgG secretion in the presence of IL-21 (**Figure 1E,F**). Interestingly, the introduction of IL-4 in the system downmodulated IgM secretion at high CD40 costimulation, but the less affecting secretion of IgG (**Figure 1E,F**). Correlation between frequency of IgG cells on day 6 and secreted IgG on day 11 was moderate (**Figure S4**), indicating that part, but not all IgG cells after six days of culture, will survive and differentiate between secreting IgG antibodies. These data indicate that *in vitro*-induced BCR isotype switching from IgM to IgG and immunoglobulin secretion is determined by the level of CD40 costimulation in the presence of a supporting cytokine environment.

As an alternative to our in-house generated cell lines with variable expression of human CD40L, we cultured human naive B-cells on varying numbers of NIH3T3 cells expressing high CD40L levels²⁷. Live imaging of these *in vitro* cultures demonstrated that the number of B-cells that interact with a CD40L-expressing cell significantly increased when only limited CD40L-expressing cells are available (**Figure S5A,B**). This suggests that *in vitro* B-cells only generate stable interaction with cells expressing CD40L. Similar to stimulation of naive B-cells with

feeder cells expressing variable levels of CD40L per cell, the proliferation of naive B-cells was not affected by a reduced number of CD40L-expressing cells (**Figure S6A**) but was increased by both cytokines IL-21 and IL-4 (**Figure S6B**). Confirming the observations using cell lines with different expression levels of CD40L, reducing the number of CD40L-expressing feeder cells also altered the number of viable B-cells after 6 days of culture (**Figure 1G,H**). In IL-4 conditions, B-cell expansion and maintenance were enhanced when the number of CD40L-expressing feeder cells was reduced 9-fold, whereas, in the presence of IL-21 varying, the number of CD40L-expressing feeders did not affect B-cell expansion and maintenance (**Figure 1G,H**). BCR isotype switching mainly occurred with highly abundant CD40L-expressing feeder cells in the presence of IL-21 (**Figure 1G,I**). Like stimulations with feeder cells with low and intermediate expression levels of CD40L, the frequency of BCR isotype switching to IgG cells was increased with the lower number of CD40L-expressing cells in the presence of IL-4. Isotype switching is regulated by activation-induced cytidine deaminase (*AICDA*)³². Expression of *AICDA* was increased by increasing the number of CD40L-expressing cells in the presence of IL-21 and/or IL-4, with a maximum of *AICDA* expression when only IL-21 was present (**Figure S6C**). While IgM and IgG antibody secretion increased with higher amounts of CD40L-expressing cells and IL-21, IgG antibody-secretion in a micro-environment that included IL-4 showed a maximal beneficial effect of the number of CD40L-expressing cells (**Figure 1J,K**). This was in line with the observations made when naive B-cells were stimulated with feeder cells exhibiting varying expression levels of CD40L (**Figure 1E,F**). Altogether these data demonstrate that CD40L expression levels and the number of CD40L-expressing cells both regulate naive B-cell survival, IgG isotype switching, and immunoglobulin secretion.

The level of CD40 costimulation in crosstalk with IL-4/IL-21 signaling regulates differentiation of human naive B cells into CD27⁺CD38⁻ B cells and antibody-secreting cells

To investigate how variation in CD40 costimulation regulates naive B-cell differentiation into CD27⁺CD38⁻ B-cells, a B-cells phenotype observed in human MBCs in blood and in activated B-cells, and CD27⁺CD38⁺ antibody-secreting cells (ASCs), human naive B-cells were cultured on 3T3s expressing varying levels of human CD40L for 11 days. Naive B-cell differentiation into CD27⁺CD38⁻ B-cells was highly induced in conditions that included IL-4 and low CD40 costimulation (**Figure 2A,B**). Strikingly, increased levels of CD40L costimulation decreased the formation of the CD27⁺CD38⁻ B-cell population (**Figure 2B**). IL-21 repressed differentiation into CD27⁺CD38⁻ B-cells in the presence of IL-4 and a low-level of CD40 costimulation (**Figure 2A,B**). Analysis of CD27⁺CD38⁺ ASC differentiation showed a significant induction, although frequencies were low (to around 3%), and only in the presence of IL-21 (**Figure 2C**). Interestingly, additional B-cell receptor (BCR) triggering did not affect this differentiation process *in vitro* (**Figure S2B,C**).

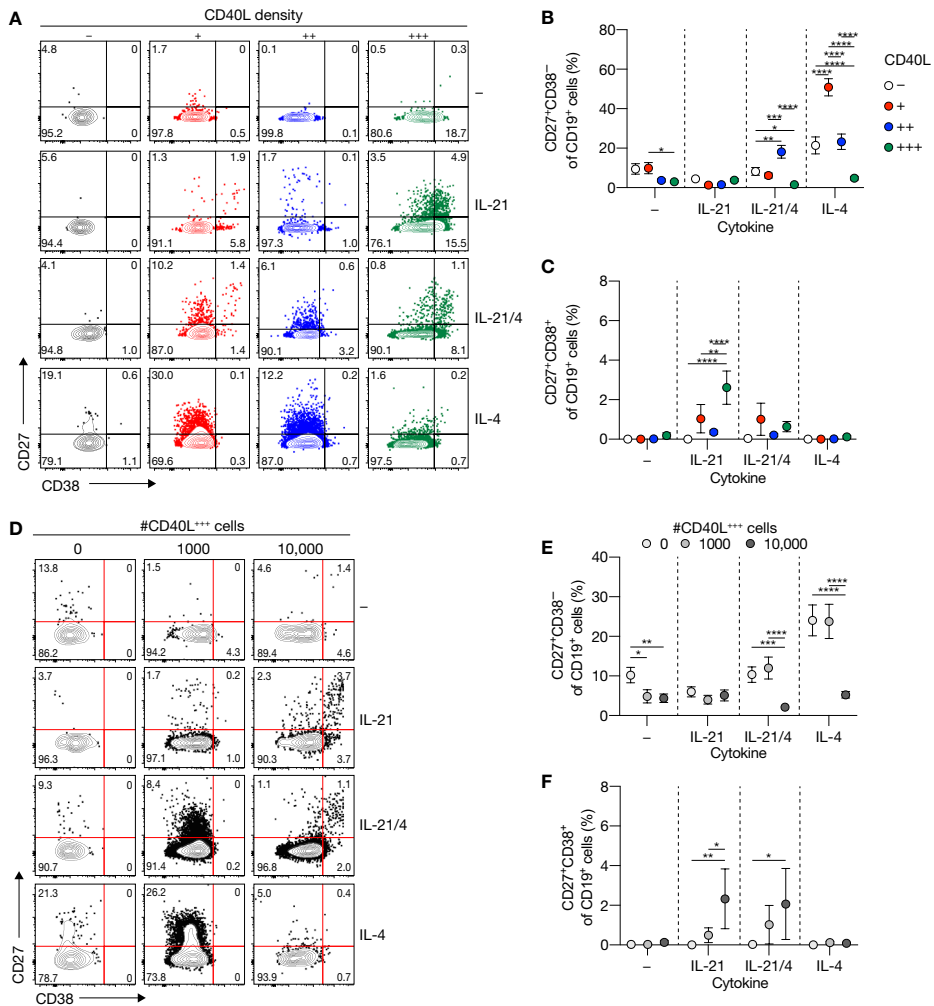


Figure 2 | Level of CD40L expression and number of CD40L feeder cells regulates differentiation of human naive B-cell into CD27⁺CD38⁻ B-cells and CD27⁺CD38⁺ antibody-secreting cells. (A) Representative of FACS plot showing CD27 and CD38 expression among human naive B-cells cultured on CD40L-expressing 3T3 cells (as in Figure 1A) with or without IL-21 and/or IL-4 for 11 days. (B–C) The frequency of CD27⁺CD38⁻ (B) and CD27⁺CD38⁺ (C) populations were analyzed 11 days after culture on CD40L-expressing 3T3 cells and cytokines. (D) Representative plots of human naive B-cells cultured on 0/1000/10,000 CD40L⁺⁺⁺-expressing 3T3 cells (as in Figure 1A) supplemented to 10,000 with WT with or without IL-21 and/or IL-4 for 11 days. (E–F) The frequency of CD27⁺CD38⁻ (E) and CD27⁺CD38⁺ (F) cells 11 days after culture on different numbers of CD40L⁺⁺⁺-expressing 3T3 cells and cytokines. Data are shown as the mean ± SEM. (n = 6 (A–C) and n = 7 (D–F) independent experiments). Single experiments were conducted in triplicate. Data were analyzed by a two-way ANOVA followed by Tukey’s multiple comparison test. * $P \leq 0.05$, ** $P \leq 0.01$, *** $P \leq 0.001$, **** $P \leq 0.0001$.

Next, we assessed whether B-cell differentiation was regulated by the amount of CD40L-expressing feeder cells. Interestingly, the number of CD40L-expressing cells attenuated IL-4-dependent induction of CD27⁺CD38⁻ B-cells, which was decreased by IL-21 (**Figure 2D,E**). Similar to stimulations with feeder cells that exhibit variation in CD40L surface densities, ASC differentiation occurred to a minimal extent (~0.5–3%), mainly in the presence of IL-21 with highly abundant CD40L-expressing cells (**Figure 2D,F**).

These data demonstrate that specifically lower CD40 costimulation in the presence of IL-4 supports naive B-cell differentiation into CD27⁺CD38⁻ B-cells *in vitro*, albeit with low numbers of live CD19⁺ cells. In contrast, higher CD40 costimulation in the presence of IL-21 promotes naive B-cell differentiation into CD27⁺CD38⁺ ASCs.

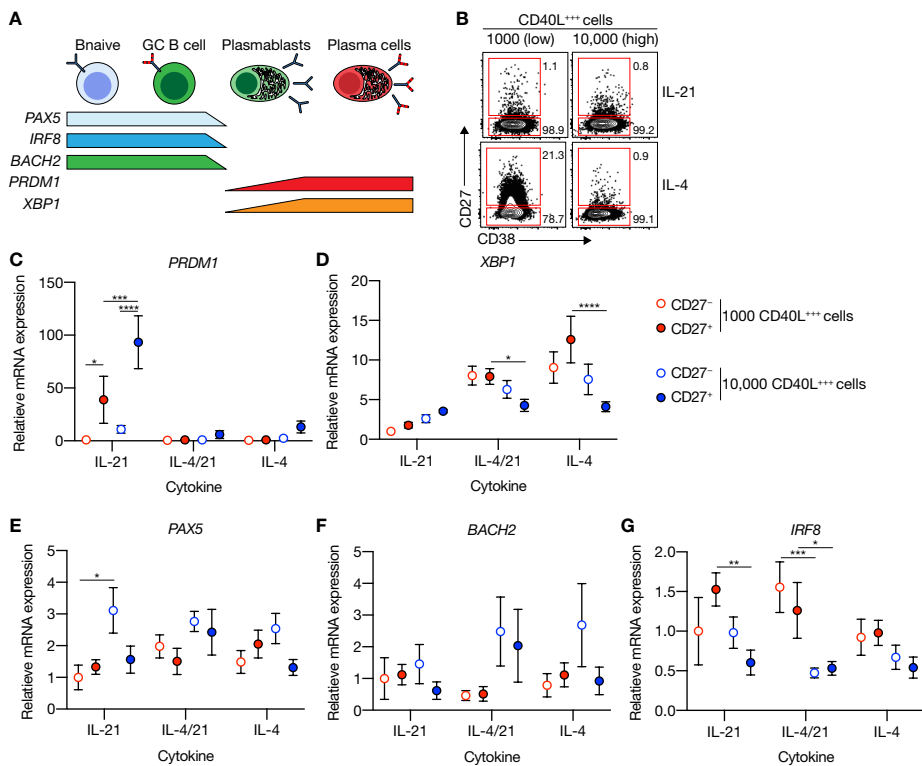


Figure 3 | CD40 costimulation together with IL-21 signaling induces PRDM1 expression and does not extinguish the B-cell lineage transcriptional program. (A) Schematic overview of the cellular stages and important transcription factors involved in B-cells differentiation from naive to antibody-secreting plasma cell (GC = germinal center). (B) Representative plots of human naive B-cells cultured on 1000 (low; supplemented with 9000 WT 3T3 cells) or 10,000 (high) CD40L⁺⁺⁺-expressing 3T3 cells (as in Figure 1A) with or without IL-21 and/or IL-4 for 9 days. Subsequently, CD27⁻CD38⁻ (CD27⁻) and CD27⁺CD38⁻ (CD27⁺) cells were purified by cell sorting. (C–G) Expression of *PRDM1* (C), *XBP1* (D), *PAX5* (E), *BACH2* (F) and *IRF8* (G) mRNA in the sorted populations were analyzed by qPCR and related to levels present in the CD27⁻ cells that were cultured on 1000 (low) CD40L⁺⁺⁺-expressing 3T3 cells together with IL-21. Data are shown as mean ± SEM. (n = 5 independent experiments). Single experiments were conducted in triplicate. Data were analyzed by a two-way ANOVA followed by Tukey's multiple comparison test. * $P \leq 0.05$, ** $P \leq 0.01$, *** $P \leq 0.001$, **** $P \leq 0.0001$.

High CD40 costimulation in the presence of IL-21 induces *PRDM1* (BLIMP1) expression, but does not extinguish B cell lineage program

To elucidate why only limited ASC differentiation was induced after 11 days of culture in the presence of highly abundant CD40L and IL-21, expression of transcriptional regulators of the B-cell and ASC fate was assessed at day 9 (**Figure 3A**). Comparing FACS-sorted differentiated (CD27⁺CD38⁻) and undifferentiated (CD27⁻CD38⁻) cells after 9 days in culture (**Figure 3B**) showed that CD40L-expressing cells in the presence of IL-21 significantly induced *PRDM1* mRNA levels in the differentiated subsets, whereas the addition of IL-4 fully abolished *PRDM1* expression (**Figure 3C**). In contrast, *XBP1*, critical for the development of ASCs, was highly induced in conditions with IL-4 and limited CD40L-expressing cells (**Figure 3D**). Despite significant induction of the ASC regulator *PRDM1*, the B-cell-specific regulators, *PAX5*, *BACH2* and *IRF8*, were not significantly changed in the CD27⁺ subset compared to CD27⁻ subset (**Figure 3E–G**). These data show that *in vitro* stimulated naive B-cells that do not show strong ASC formation become transcriptionally primed for ASC differentiation via upregulation of CD40L/IL-21-mediated *PRDM1* gene expression but still maintain the B-cell identity program.

Secondary cultures including CD40L/IL-21 drive optimal ASC differentiation

Next, we assessed which essential cues were lacking in our minimal *in vitro* culture system to promote substantial terminal ASC differentiation upon naive B-cell stimulation. *In vivo*, differentiation of B-cells is dependent on repeated interactions and signals provided by Tfh cells in mature GCs that are formed 5 to 7 days after immunization¹⁵. To achieve a closer simulation of the *in vivo* situation, cells were harvested 6 days after starting the primary culture and re-cultured in a secondary culture with CD40L-expressing feeder cells and cytokines (**Figure 4A**). Remarkably, re-culturing under high CD40 costimulatory conditions in the presence of IL-21 induced prominent and significantly more CD27⁺CD38⁺ cells than initial culture only (**Figure 4B,C**). Renewed culture with low CD40 costimulation also induced ASC differentiation in the presence of IL-21 and IL-4 (and significantly increased the number of live CD19⁺ cells; **Figure S7**), but not with IL-21 alone. The extensive ASC differentiation after initial expansion resulted in a profound population of ASC (**Figure 4D**). Remarkably, a more detailed analysis revealed an induction of CD138⁺ PCs upon renewed costimulation/cytokine culture during naive B-cell differentiation (**Figure 4E,F**). Moreover, the secretion of IgM and IgG was profoundly enhanced in the secondary cultures (5 days cumulative) than the primary cultures (11 days cumulative) and was mediated by IL-21 (**Figure 4G,H**). These data demonstrate that renewed culture with CD40L and the cytokines IL-21 and IL-4 are required to finalize the differentiation of human naive B-cells into CD138⁺ PCs *in vitro*.

Second round of *in vitro* stimulation switches off the B cell lineage program and induces rapid re-induction of pSTAT3

ASC differentiation is controlled by a complex interplay of multiple interconnecting

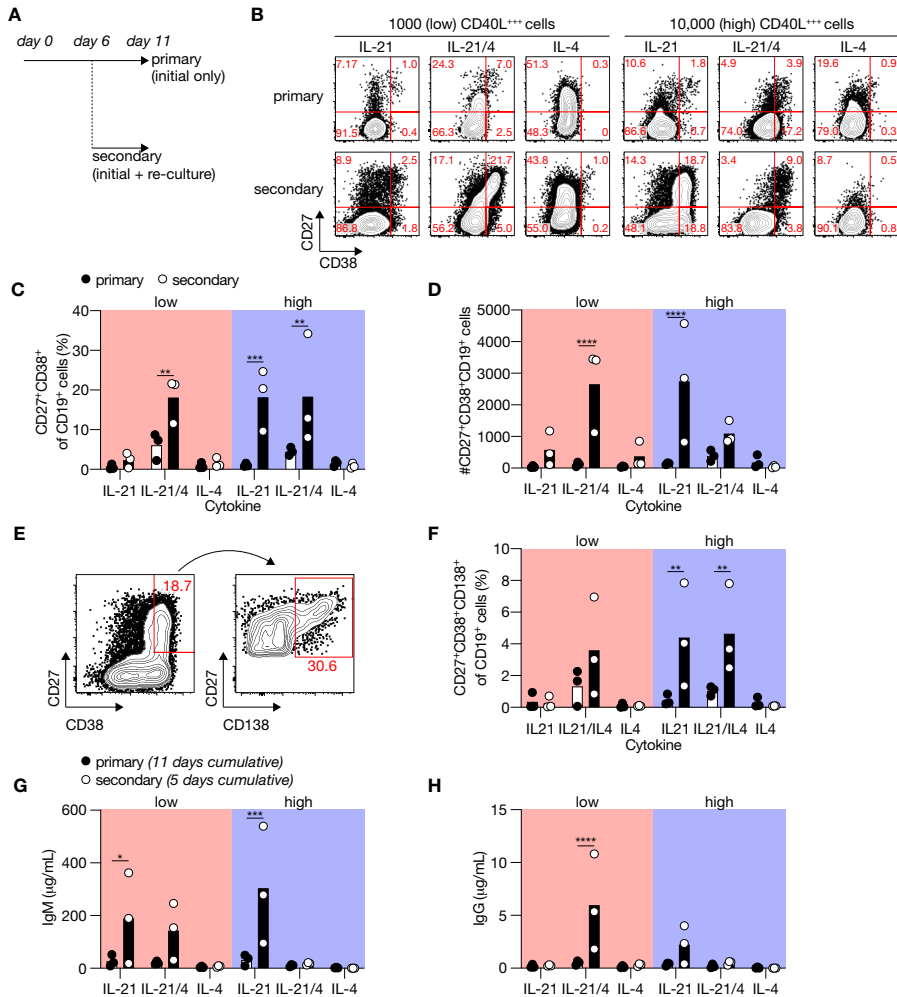


Figure 4 | Renewed CD40 costimulation and Tfh cytokines induce in vitro differentiation of human naive B-cells into antibody-secreting cells (ASCs). (A) Human B-cells cultured on 1000 (low; supplemented with 9000 WT 3T3 cells) or 10,000 (high) CD40L⁺-expressing 3T3 cells (as in Figure 1A) with or without IL-21 and/or IL-4 for 11 days (primary—initial only stimulation). Alternatively, primary cultures were harvested after 6 days, and secondary cultures were initiated for 5 days with the same number of CD40L⁺-expressing 3T3 cells and similar cytokine environments as in the primary culture. (B) Representative of FACS plots showing CD27 and CD38 expression among human B-cells cultured as in A. (C–D) The frequency (C) and number (D) of CD27⁺CD38⁺ cells were analyzed 11 days after initial only, or initial + secondary culture. (E) Representative plots of CD138 expression within the CD27⁺CD28⁺ ASC population. (F) The frequencies of CD138⁺ plasma cells were determined 11 days after initial only or initial + secondary culture. (G–H) Cumulative secretion of IgM (G) and IgG (H) measured in culture supernatants 11 days after initial only or 5 days after initial + secondary culture. Each data point represents the mean of an individual experiment (n = 3) with triplicate measurements. Mean values are represented as bars. *p*-values were calculated using multiple *t*-tests. * *P* ≤ 0.05, ** *P* ≤ 0.01, *** *P* ≤ 0.001, **** *P* ≤ 0.0001.

transcription factors (**Figure 5A**). In short, differentiation involves induction of gene expression of the ASC regulator *PRDM1*, which subsequently represses various important pathways that define the B-cell lineage (*PAX5*, *BACH2* and *IRF8*). Further characterization of the effects of renewed costimulation and Tfh-cytokine cultures revealed that mRNA levels of ASC-defining transcription factors *PRDM1* were not further increased in the FACS-sorted differentiated cells (CD27⁺CD38⁺ and CD27⁺CD38⁻ ASCs; **Figure 5B**) than the CD27⁻CD38⁻ B-cells (**Figure 5B**) after five days into the secondary culture (**Figure 5C**). In contrast, mRNA levels of *XBPI* were significantly higher in CD27⁺CD38⁺ ASCs than in the other populations (**Figure 5D**). Additionally, compared to naive CD27⁻CD38⁻ cells derived from primary cultures, *PRDM1* mRNA levels were significantly increased, whereas no increase is observed for *XBPI* (**Figure 5S**). Interestingly, the mRNA levels of B-cell-defining transcription factors *PAX5*, *BACH2* and *IRF8* were significantly decreased in both differentiating populations with the lowest expression in CD27⁺CD38⁺ ASCs and already profoundly reduced in the undifferentiated cells from secondary cultures than initial culture only (**Figure 5E–G and 5S**). These data demonstrate that re-culture with CD40 costimulation and IL-21 yields full extinguishment of the B-cell transcriptional program and induction of full ASC differentiation of naive B-cells.

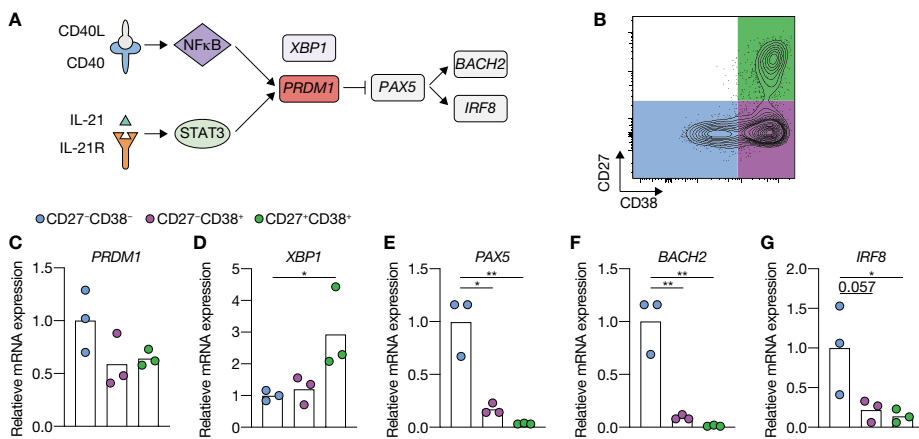


Figure 5 | Renewed CD40 costimulation and IL-21 signaling drives antibody-secreting cell (ASC) differentiation and represses transcriptional program related to the B-cell fate. (A) Schematic representation of BLIMP1 activation upon CD40 and IL-21 receptor (IL-21R) signaling. STAT3, together with NFκB, regulates BLIMP1 expression. BLIMP1 downregulates *PAX5* expression and, consequently, its downstream targets *BACH2* and *IRF8*. (B–G) Human naive B-cells were cultured on 10,000 (high) CD40L⁺-expressing 3T3 cells (as in Figure 1A) for 6 days with IL-21. After 6 days, secondary cultures were initiated for 5 days with the initial stimuli. (B) Subsequently, CD27⁻CD38⁻, CD27⁺CD38⁻ and CD27⁺CD38⁺ cell populations were sort purified. (C–G) Expression of *PRMD1* (C), *XBPI* (D), *PAX5* (E), *BACH2* (F) and *IRF8* (G) mRNA in sorted populations were analyzed by qPCR and related to levels present in CD27⁻CD38⁻ cells. Each data point represents the mean of an individual experiment (n = 3) with triplicate measurements. Mean values are represented as bars. *p* values were calculated using RM one-way ANOVA followed by Tukey’s multiple comparison test. * *P* ≤ 0.05, ** *P* ≤ 0.01.

5

To address further the link between the extracellular signals provided and the induction of a transcriptional program that efficiently induces ASC differentiation, we investigated the kinetics of phosphorylation of STAT3 (pSTAT3; **Figure 6A**), the signaling molecule positively regulating *PRDM1* expression and consequently negatively regulating the B-cell transcriptional program (**Figure 5A**). In line with previous data³³, the presence of IL-21 induced a strong expression of pSTAT3. At the start of culture, pSTAT3 levels in the presence of IL-21 steadily increased and reached maximum levels after 3 days, before return to baseline 3 days later (**Figure 6B,C**). IL-21 signaling in renewed costimulation cultures induced rapid re-phosphorylation of STAT3 and remained high for at least 3 days (**Figure 6D,E**). CD27⁺CD38⁺ cells were observed in the secondary cultures in the presence of IL-21 starting from 3 days and rose to around 15% after 5 days (**Figure S9**). These data demonstrate that re-stimulation cultures with CD40L/IL-21 result in rapid re-phosphorylation of STAT3 correlated with efficient naive B-cell differentiation into ASC formation.

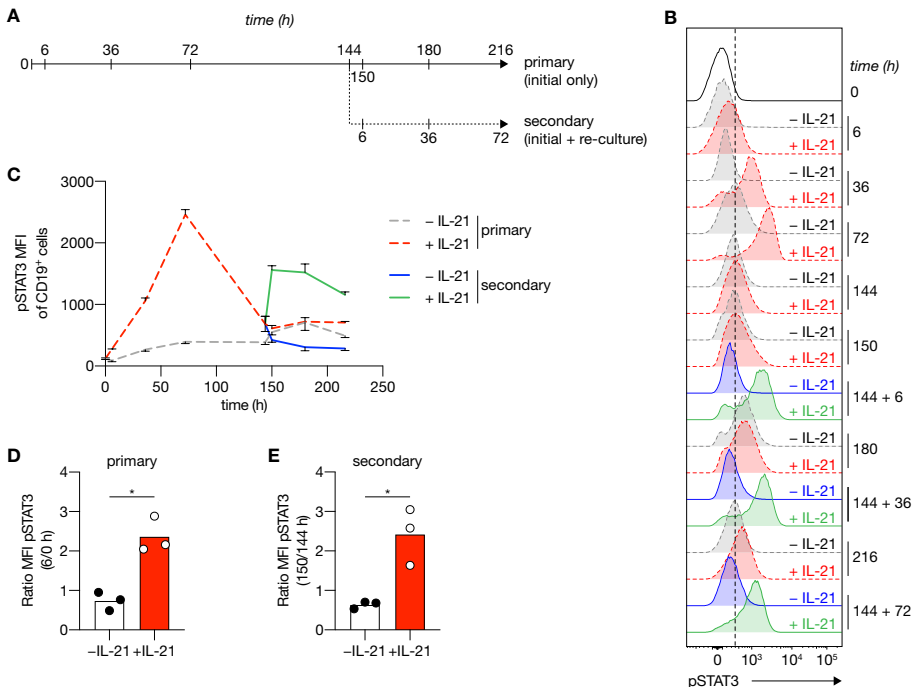


Figure 6 | STAT3 is rapidly re-phosphorylated upon re-stimulation using CD40 costimulation and IL-21 signaling. (A) Overview of the time points sampled from primary and secondary human B-cell cultures. Human naive B-cells were cultured on 10,000 CD40L⁺-expressing 3T3 cells (as in Figure 1A) with or without IL-21 for 6 days. After 6 days, secondary cultures were initiated for 3 days with 10,000 CD40L⁺-expressing 3T3 cells with(out) IL-21 ($n = 3$). (B–C) Representative plot of pSTAT3 levels (B) and quantification (C) at baseline and 6, 36, 72, 144, 150, 180 and 216 h in primary culture (dotted gray w/o IL-21 and red lines with IL-21); and 6, 36 and 72 in secondary culture (solid blue w/o IL-21 and green lines with IL-21). Data are shown as mean \pm SEM ($n = 3$ independent experiments). Single experiments were conducted in triplicate. (D–E) Fold induction of pSTAT3 6 h in primary (D) and secondary (E) cultures relative to time point 0 or 144 h. Each data point represents the mean of an individual experiment ($n = 3$) with triplicate measurements. Mean values are represented as bars. p values were calculated using paired t -test. * $P \leq 0.05$.

DISCUSSION

In this study, we established an *in vitro* culture system that could efficiently differentiate human peripheral blood naive B-cells into ASCs. We demonstrate that naive B-cell survival, abundance and differentiation are dependent on CD40L expression levels by the feeder cells used in the *in vitro* culture system and on the cytokine environment provided. We also show that renewed costimulation greatly enhanced ASC differentiation. Low CD40 costimulation in the presence of IL-4 prominently induces CD27⁺CD38⁻ cells, compared to high costimulation. CD27 is used as a discriminate marker for human MBCs in blood, raising the possibility that our observed CD27⁺CD38⁻ cells represent the development of the MBCs. However, current discussions in the field attribute the appearance of CD27 to the status of activation, especially *in vitro*, and not necessarily the formation of long-lived MBCs (reviewed in³⁴). Therefore, we cannot make any firm conclusions on MBC formation in our system. Survival of human B-cells under high CD40 costimulatory conditions *in vitro* was superior in the presence of IL-21. Additionally, these stimulatory conditions made human naive B-cells more prone to differentiate into CD27⁺CD38⁺ ASCs even though the magnitude of ASC formation was low. Although *PRDM1* was upregulated in the culture, the B-cell lineage program was unaltered, possibly contributing to the low magnitude of ASC formation *in vitro*. However, similar observations have been made in mice in a subset of proliferating dark zone GC B-cells that have low expression of *BLIMP1*³⁵. These GC B-cells were also not fully committed to PC differentiation but may be more prone to differentiation via that route.

During GC reactions *in vivo*, GC B-cells repeatedly interact over several cycles, with Tfh cells that provide, among others, CD40 costimulation, IL-21 and IL-4 to the interacting B-cells. Therefore, to mimic the *in vivo* GC reactions, we utilized secondary cultures, including CD40 costimulation and cytokine stimulation succeeding initial stimulation. Renewed CD40 costimulation in the presence of IL-21 prominently induced ASC formation and concomitantly decreased expression of B-cell-defining transcription factors *PAX5*, *BACH2* and *IRF8*. This demonstrates that also *in vitro* human naive B-cells, after initial proliferation, require renewed Tfh cell signals to transcend a minimal signaling threshold required for effective differentiation into ASCs. We did observe discrepancies between the expression levels of *PRDM1* and *XBPI*, two transcription factors important in ASC differentiation and function. In secondary cultures, *PRDM1* levels were already increased in the undifferentiated CD27⁻CD38⁻ population and remained constant in the differentiated populations, whereas *XBPI* levels only increased in the fully differentiated CD27⁺CD38⁺ ASC. This indicates that *PRDM1* is important before the fate transition to really drive differentiation, whereas *XBPI* is relevant for the large production of antibodies.

Previous studies using murine naive B-cells reported that CD40L stimulation, with or without BAFF stimulation, together with phasic (re-)stimulation of IL-21 and IL-4, resulted in significant expansion and induction of GC-like cells and differentiation into CD138⁺ cells. These cells required an adoptive transfer model to fully mature into long-lived PCs^{36,37}. We

here show that for human *in vitro* naive B-cell differentiation, renewed costimulation and Tfh-cytokines during the B-cell priming phase induce potent plasmablast (PB) and PCs formation from CD40L-stimulated naive B-cells in the presence of IL-21 $-/+$ IL-4. Whether these are long-lived PCs as observed in the adoptive transfer model³⁷ remains to be determined. Other groups have demonstrated *in vitro* differentiation of human MBCs into long-lived PCs using an intricate 3-step culture system, in which stromal cell factors, mimicking the bone marrow environment, prolonged the survival of the *in vitro*-generated PCs^{38,39}. This could be the next step in our human naive B-cell culture system to assess the longevity of our induced ASCs.

Renewed CD40 costimulation of human naive B-cells *in vitro* with high CD40L levels in the presence of IL-21 rapidly re-induced STAT3 activation, an IL-21 receptor signaling protein. Individuals with STAT3 mutations and mice deficient for IL-21 or IL-21 receptor have shown that STAT3 is essential in GC formation and maintenance, PC differentiation and immunoglobulin secretion^{18,19,40–42}. Furthermore, IL-21 synergizes with CD40L stimulation to induce expression of the ASC-defining transcription factors *PRDM1* and *IRF4* in human B-cells⁴³. Altogether, the observed rapid re-induction of STAT3 in the secondary *in vitro* cultures could explain the more prominent ASC induction and suggests that dynamic reexpression of STAT3 is important in ASC differentiation.

The establishment of this minimalistic *in vitro* culture system that supports efficient differentiation of human naive B-cells into antibody-secreting cells while also maintaining high cell numbers to investigate the differentiation pathways may form an important step for the much-desired in-depth dissection of human B-cell terminal differentiation. It may eventually prove beneficial in devising new strategies and targets for treating antibody/ASC-mediated inflammatory and auto-immune diseases and might prove invaluable for monitoring vaccination efficiency.

FUNDING

This research was made possible thanks to the financial support of the Landsteiner Foundation for Blood Transfusion Research, grant 1609 to S.M. van Ham (for C. Marsman), Sanquin Innovation Grant 2020–45 to S.M. van Ham (for T. Jorritsma) and Sanquin Product/process-development project PPOC-17-34 to S.M. van Ham (for P.-P. Unger).

INSTITUTIONAL REVIEW BOARD STATEMENT

The study was conducted following the protocol of the local institutional review board, the Medical Ethics Committee of Sanquin Blood Supply, and conforms to the principles of the Declaration of Helsinki.

INFORMED CONSENT STATEMENT

Informed consent was obtained from all subjects involved in the study.

ACKNOWLEDGEMENTS

We thank Erik Mul, Simon Tol, Floris van Alphen and Mark Hoogenboezem for sorting naive B-cells using flow cytometry. We thank Gordon J. Freeman of the DFCI, Harvard, for kindly providing us with the human CD40L plasmid ^{27,28}.

CONFLICTS OF INTEREST

The authors declare no conflicts of interest. The funders had no role in the design of the study; in the collection, analyses or interpretation of data; in the writing of the manuscript; or in the decision to publish the results.

REFERENCES

1. Zimring, J.C.; Stowell, S.R.; Johnsen, J.M.; Hendrickson, J.E. Effects of genetic, epigenetic, and environmental factors on alloimmunization to transfused antigens: Current paradigms and future considerations. *Transfus. Clin. Biol.* **2012**, *19*, 125–131, doi:10.1016/j.tracli.2012.03.002.
2. Zimring, J.C.; Hudson, K.E. Cellular immune responses in red blood cell alloimmunization. *Hematology* **2016**, *2016*, 452–456, doi:10.1182/asheducation-2016.1.452.
3. Laffitte, E.; Skaria, M.; Jaunin, F.; Tamm, K.; Saurat, J.-H.; Favre, B.; Borradori, L. Autoantibodies to the extracellular and intracellular domain of bullous pemphigoid 180, the putative key autoantigen in bullous pemphigoid, belong predominantly to the IgG1 and IgG4 subclasses. *Br. J. Dermatol.* **2001**, *144*, 760–768, doi:10.1046/j.1365-2133.2001.04130.x.
4. Gilhus, N.E.; Skeie, G.O.; Romi, F.; Lazaridis, K.; Zisimopoulou, P.; Tzartos, S. Myasthenia gravis—Autoantibody characteristics and their implications for therapy. *Nat. Rev. Neurol.* **2016**, *12*, 259–268, doi:10.1038/nrneuro.2016.44.
5. Berentsen, S.; Sundic, T. Red Blood Cell Destruction in Autoimmune Hemolytic Anemia: Role of Complement and Potential New Targets for Therapy. *BioMed Res. Int.* **2015**, *2015*, 363278, doi:10.1155/2015/363278.
6. Pos, W.; Luken, B.M.; Sorvillo, N.; Kremer Hovinga, J.A.; Voorberg, J. Humoral immune response to ADAMTS13 in acquired thrombotic thrombocytopenic purpura. *J. Thromb. Haemost.* **2011**, *9*, 1285–1291, doi:10.1111/j.1538-7836.2011.04307.x.
7. Weinstein, J.S.; Herman, E.I.; Lainez, B.; Licona-Limón, P.; Esplugues, E.; Flavell, R.; Craft, J. TFH cells progressively differentiate to regulate the germinal center response. *Nat. Immunol.* **2016**, *17*, 1197–1205, doi:10.1038/ni.3554.
8. King, C.; Tangye, S.G.; Mackay, C.R. T Follicular Helper (T FH) Cells in Normal and Dysregulated Immune Responses. *Annu. Rev. Immunol.* **2008**, *26*, 741–766, doi:10.1146/annurev.immunol.26.021607.090344.
9. Zaretsky, A.G.; Taylor, J.J.; King, I.L.; Marshall, F.A.; Mohrs, M.; Pearce, E.J. T follicular helper cells differentiate from Th2 cells in response to helminth antigens. *J. Exp. Med.* **2009**, *206*, 991–999, doi:10.1084/jem.20090303.
10. Bryant, V.L.; Ma, C.S.; Avery, D.T.; Li, Y.; Good, K.L.; Corcoran, L.M.; de Waal Malefyt, R.; Tangye, S.G. Cytokine-mediated regulation of human B cell differentiation into Ig-secreting cells: Predominant role of IL-21 produced by CXCR5+ T follicular helper cells. *J. Immunol.* **2007**, *179*, 8180–8190, doi:10.4049/jimmunol.179.12.8180.
11. Reinhardt, R.L.; Liang, H.-E.; Locksley, R.M. Cytokine-secreting follicular T cells shape the antibody repertoire. *Nat. Immunol.* **2009**, *10*, 385–393, doi:10.1038/ni.1715.
12. King, I.L.; Mohrs, M. IL-4-producing CD4+ T cells in reactive lymph nodes during helminth infection are T follicular helper cells. *J. Exp. Med.* **2009**, *206*, 1001–1007, doi:10.1084/jem.20090313.
13. Yusuf, I.; Kageyama, R.; Monticelli, L.; Johnston, R.J.; Ditoro, D.; Hansen, K.; Barnett, B.; Crotty, S. Germinal center T follicular helper cell IL-4 production is dependent on signaling lymphocytic activation molecule receptor (CD150). *J. Immunol.* **2010**, *185*, 190–202, doi:10.4049/jimmunol.0903505.
14. Victora, G.D.; Nussenzweig, M.C. Germinal Centers. *Annu. Rev. Immunol.* **2012**, *30*, 429–457, doi:10.1146/annurev-immunol-020711-075032.
15. De Silva, N.S.; Klein, U. Dynamics of B cells in germinal centres. *Nat. Rev. Immunol.* **2015**, *15*, 137–148, doi:10.1038/nri3804.
16. Takahashi, Y.; Dutta, P.R.; Cerasoli, D.M.; Kelsoe, G. In situ studies of the primary immune response to (4-hydroxy-3-nitrophenyl)acetyl. V. Affinity maturation develops in two stages of clonal selection. *J. Exp. Med.* **1998**, *187*, 885–895, doi:10.1084/jem.187.6.885.
17. Weisel, F.J.; Zuccarino-Catania, G.V.; Chikina, M.; Shlomchik, M.J. A Temporal Switch in the Germinal Center Determines Differential Output of Memory B and Plasma Cells. *Immunity* **2016**, *44*, 116–130, doi:10.1016/j.immuni.2015.12.004.
18. Linterman, M.A.; Beaton, L.; Yu, D.; Ramiscal, R.R.; Srivastava, M.; Hogan, J.J.; Verma, N.K.; Smyth, M.J.; Rigby, R.J.; Vinuesa, C.G. IL-21 acts directly on B cells to regulate Bcl-6 expression and germinal center responses. *J. Exp. Med.* **2010**, *207*, 353–363, doi:10.1084/jem.20091738.
19. Zotos, D.; Coquet, J.M.; Zhang, Y.; Light, A.; D’Costa, K.; Kallies, A.; Corcoran, L.M.; Godfrey, D.I.; Toellner, K.-M.; Smyth, M.J.; et al. IL-21 regulates germinal center B cell differentiation and proliferation through a B cell-intrinsic mechanism. *J. Exp. Med.* **2010**, *207*, 365–378, doi:10.1084/jem.20091777.
20. Mak, T.W.; Shahinian, A.; Yoshinaga, S.K.; Wakeham, A.; Boucher, L.-M.; Pintilie, M.; Duncan, G.; Gajewska, B.U.; Gronski, M.; Eriksson, U.; et al. Costimulation through the inducible costimulator ligand is essential

- for both T helper and B cell functions in T cell-dependent B cell responses. *Nat. Immunol.* **2003**, *4*, 765–772, doi:10.1038/ni947.
21. Gatto, D.; Pfister, T.; Jegerlehner, A.; Martin, S.W.; Kopf, M.; Bachmann, M.F. Complement receptors regulate differentiation of bone marrow plasma cell precursors expressing transcription factors Blimp-1 and XBP-1. *J. Exp. Med.* **2005**, *201*, 993–1005, doi:10.1084/jem.20042239.
 22. Good-Jacobson, K.L.; Szumilas, C.G.; Chen, L.; Sharpe, A.H.; Tomayko, M.M.; Shlomchik, M.J. PD-1 regulates germinal center B cell survival and the formation and affinity of long-lived plasma cells. *Nat. Immunol.* **2010**, *11*, 535–542, doi:10.1038/ni.1877.
 23. Good-Jacobson, K.L.; Song, E.; Anderson, S.; Sharpe, A.H.; Shlomchik, M.J. CD80 expression on B cells regulates murine T follicular helper development, germinal center B cell survival, and plasma cell generation. *J. Immunol.* **2012**, *188*, 4217–4225, doi:10.4049/jimmunol.1102885.
 24. Deenick, E.K.; Avery, D.T.; Chan, A.; Berglund, L.J.; Ives, M.L.; Moens, L.; Stoddard, J.L.; Bustamante, J.; Boisson-Dupuis, S.; Tsumura, M.; et al. Naive and memory human B cells have distinct requirements for STAT3 activation to differentiate into antibody-secreting plasma cells. *J. Exp. Med.* **2013**, *210*, 2739–2753, doi:10.1084/jem.20130323.
 25. Ise, W.; Fujii, K.; Shiroguchi, K.; Ito, A.; Kometani, K.; Takeda, K.; Kawakami, E.; Yamashita, K.; Suzuki, K.; Okada, T.; et al. T Follicular Helper Cell-Germinal Center B Cell Interaction Strength Regulates Entry into Plasma Cell or Recycling Germinal Center Cell Fate. *Immunity* **2018**, *48*, 702–715.e4, doi:10.1016/j.immuni.2018.03.027.
 26. Néron, S.; Racine, C.; Roy, A.; Guérin, M. Differential responses of human B-lymphocyte subpopulations to graded levels of CD40-CD154 interaction. *Immunology* **2005**, *116*, 454–463, doi:10.1111/j.1365-2567.2005.02244.x.
 27. Urashima, M.; Chauhan, D.; Uchiyama, H.; Freeman, G.; Anderson, K. CD40 ligand triggered interleukin-6 secretion in multiple myeloma. *Blood* **1995**, *85*, 1903–1912, doi:10.1182/blood.V85.7.1903.bloodjournal8571903.
 28. Schultze, J.L.; Cardoso, A.A.; Freeman, G.J.; Seamon, M.J.; Daley, J.; Pinkus, G.S.; Gribben, J.G.; Nadler, L.M. Follicular lymphomas can be induced to present alloantigen efficiently: A conceptual model to improve their tumor immunogenicity. *Proc. Natl. Acad. Sci. USA* **1995**, *92*, 8200–8204, doi:10.1073/pnas.92.18.8200.
 29. Versteegen, N.J.M.; Unger, P.-P.A.; Walker, J.Z.; Nicolet, B.P.; Jorritsma, T.; van Rijssel, J.; Spaapen, R.M.; de Wit, J.; van Buul, J.D.; ten Brinke, A.; et al. Human B Cells Engage the NCK/PI3K/RAC1 Axis to Internalize Large Particles via the IgM-BCR. *Front. Immunol.* **2019**, *10*, 1–14, doi:10.3389/fimmu.2019.00415.
 30. Souwer, Y.; Griekspoor, A.; Jorritsma, T.; de Wit, J.; Janssen, H.; Neefjes, J.; van Ham, S.M. B cell receptor-mediated internalization of salmonella: A novel pathway for autonomous B cell activation and antibody production. *J. Immunol.* **2009**, *182*, 7473–7481, doi:10.4049/jimmunol.0802831.
 31. Avery, D.T.; Bryant, V.L.; Ma, C.S.; de Waal Malefyt, R.; Tangye, S.G. IL-21-induced isotype switching to IgG and IgA by human naive B cells is differentially regulated by IL-4. *J. Immunol.* **2008**, *181*, 1767–1779, doi:10.1189/j.1767-1779.2008.011111.x.
 32. Muramatsu, M.; Kinoshita, K.; Fagarasan, S.; Yamada, S.; Shinkai, Y.; Honjo, T. Class Switch Recombination and Hypermutation Require Activation-Induced Cytidine Deaminase (AID), a Potential RNA Editing Enzyme. *Cell* **2000**, *102*, 553–563, doi:10.1016/S0092-8674(00)00078-7.
 33. Marsman, C.; Jorritsma, T.; ten Brinke, A.; van Ham, S.M. Flow Cytometric Methods for the Detection of Intracellular Signaling Proteins and Transcription Factors Reveal Heterogeneity in Differentiating Human B Cell Subsets. *Cells* **2020**, *9*, 2633, doi:10.3390/cells9122633.
 34. Weisel, F.; Shlomchik, M. Memory B Cells of Mice and Humans. *Annu. Rev. Immunol.* **2017**, *35*, 255–284, doi:10.1146/annurev-immunol-041015-055531.
 35. Radtke, D.; Bannard, O. Expression of the Plasma Cell Transcriptional Regulator Blimp-1 by Dark Zone Germinal Center B Cells During Periods of Proliferation. *Front. Immunol.* **2019**, *9*, 1–16, doi:10.3389/fimmu.2018.03106.
 36. Robinson, M.J.; Pitt, C.; Brodie, E.J.; Valk, A.M.; O'Donnell, K.; Nitschke, L.; Jones, S.; Tarlinton, D.M. BAFF, IL-4 and IL-21 separably program germinal center-like phenotype acquisition, BCL6 expression, proliferation and survival of CD40L-activated B cells in vitro. *Immunol. Cell Biol.* **2019**, *97*, 826–839, doi:10.1111/imcb.12283.
 37. Nojima, T.; Haniuda, K.; Moutai, T.; Matsudaira, M.; Mizokawa, S.; Shiratori, I.; Azuma, T.; Kitamura, D. In-vitro derived germinal centre B cells differentially generate memory B or plasma cells in vivo. *Nat. Commun.* **2011**, *2*, 465, doi:10.1038/ncomms1475.
 38. Cocco, M.; Stephenson, S.; Care, M.A.; Newton, D.; Barnes, N.A.; Davison, A.; Rawstron, A.; Westhead, D.R.

- Doody, G.M.; Tooze, R.M. In vitro generation of long-lived human plasma cells. *J. Immunol.* **2012**, *189*, 5773–5785, doi:10.4049/jimmunol.1103720.
39. Jourdan, M.; Caraux, A.; De Vos, J.; Fiol, G.; Larroque, M.; Cognot, C.; Bret, C.; Duperray, C.; Hose, D.; Klein, B. An in vitro model of differentiation of memory B cells into plasmablasts and plasma cells including detailed phenotypic and molecular characterization. *Blood* **2009**, *114*, 5173–5181, doi:10.1182/blood-2009-07-235960.
40. Avery, D.T.; Deenick, E.K.; Ma, C.S.; Suryani, S.; Simpson, N.; Chew, G.Y.; Chan, T.D.; Palendira, U.; Bustamante, J.; Boisson-Dupuis, S.; et al. B cell-intrinsic signaling through IL-21 receptor and STAT3 is required for establishing long-lived antibody responses in humans. *J. Exp. Med.* **2010**, *207*, 155–171, doi:10.1084/jem.20091706.
41. McGuire, H.M.; Vogelzang, A.; Warren, J.; Loetsch, C.; Natividad, K.D.; Chan, T.D.; Brink, R.; Batten, M.; King, C. IL-21 and IL-4 Collaborate to Shape T-Dependent Antibody Responses. *J. Immunol.* **2015**, *195*, 5123–5135, doi:10.4049/jimmunol.1501463.
42. Veen, W.; Krätz, C.E.; McKenzie, C.I.; Aui, P.M.; Neumann, J.; Noesel, C.J.M.; Wirz, O.F.; Hagl, B.; Kröner, C.; Spielberger, B.D.; et al. Impaired memory B-cell development and antibody maturation with a skewing toward IgE in patients with STAT3 hyper-IgE syndrome. *Allergy* **2019**, *74*, 2394–2405, doi:10.1111/all.13969.
43. Ding, B.B.; Bi, E.; Chen, H.; Yu, J.J.; Ye, B.H. IL-21 and CD40L synergistically promote plasma cell differentiation through upregulation of Blimp-1 in human B cells. *J. Immunol.* **2013**, *190*, 1827–1836, doi:10.4049/jimmunol.1201678.

SUPPLEMENTARY INFORMATION

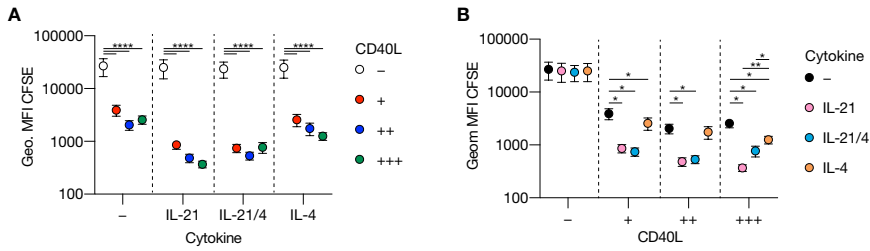


Figure S1 | Level of CD40L expression affects expansion of six day stimulated naive B cells. (A–B) Human naive B cells were cultured on WT or CD40L-expressing 3T3 cells (as in Figure. 1A) with or without IL-21 and/or IL-4 for 6 days. Geometric mean fluorescent intensity (Geo. MFI) of the proliferation-dye CFSE of live CD19⁺ cells was measured using flow cytometry. Data are shown as mean \pm SEM (n=6 independent experiments). Single experiments were conducted in triplicate. Data were analyzed by a two-way ANOVA followed by Tukey's multiple comparison test. * $P \leq 0.05$, ** $P \leq 0.01$, *** $P \leq 0.001$, **** $P \leq 0.0001$.

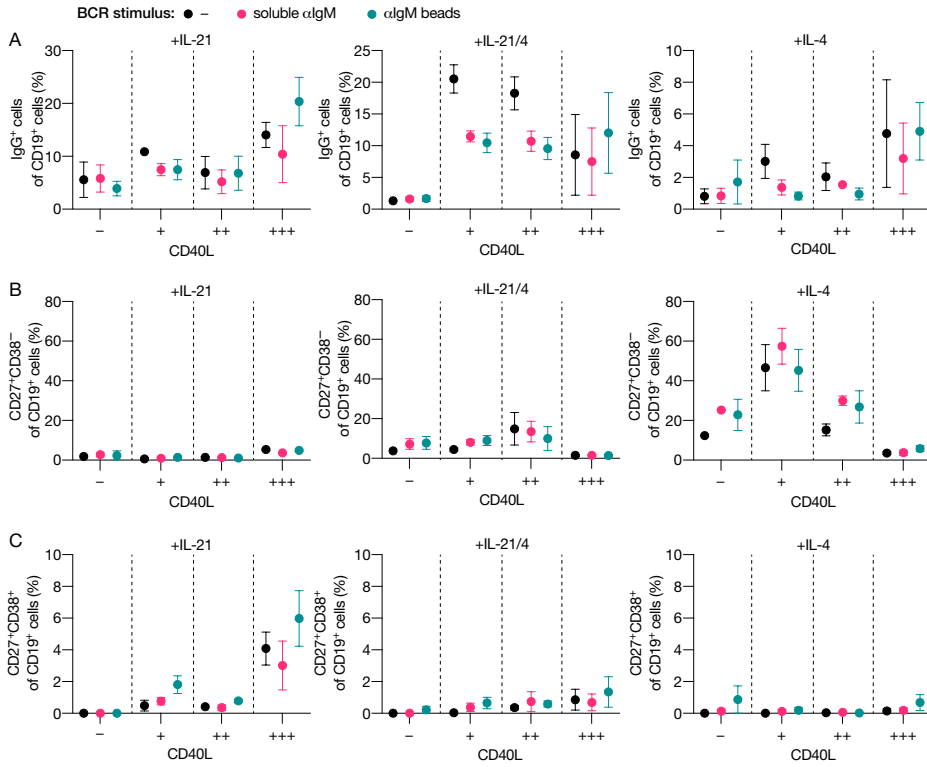


Figure S2 | BCR ligation does not affect human naive B cell differentiation upon CD40 co-stimulation. (A–C) Human naive B cells were cultured on 3T3 cells either or not expressing CD40L (as in Figure 1A) with or without IL-21 and/or IL-4 for 6 (A) and 11 days (B–C). B cell receptors were ligated using soluble anti-IgM antibodies or anti-IgM coated polystyrene beads. (A–C) Frequencies of IgG⁺ B cells (A), CD27⁺CD38⁻ cells (B) and CD27⁺CD38⁺ cells (C) were measured using flow cytometry. Data are shown as mean \pm SEM (n=2 independent experiments). Single experiments were conducted in triplicate. Data were analyzed by a two-way ANOVA followed by Tukey's multiple comparison test.

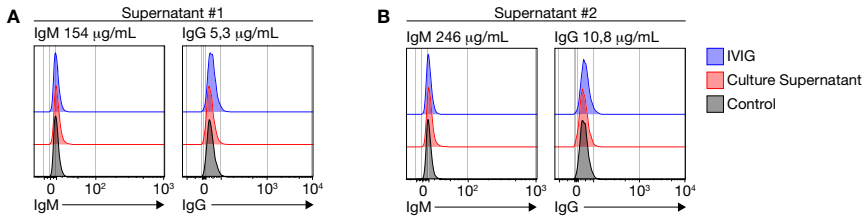


Figure S3 | Secreted antibodies do not recognize 3T3 cells. (A–B) Culture supernatants that contain vast amounts of secreted antibodies of unswitched (IgM) and class-switched (IgG) isotypes were incubated with 3T3 cells in suspension. Intravenous immunoglobulin (IVIg) that contains a wide range of antibodies was used to determine cross-reactivity.

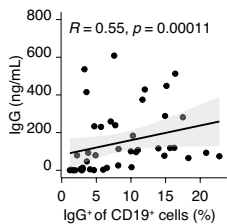


Figure S4 | Moderate correlation between the frequency of IgG cells and secreted IgG. Human naive B cells were cultured on 3T3 cells expressing varying levels of CD40L with or without IL-21 and/or IL-4 and analyzed for class switching to surface IgG after 6 days and cumulative secretion of IgG after 11 days. Spearman's rank correlation coefficient was used to describe the association between frequency of IgG cells and secreted IgG.

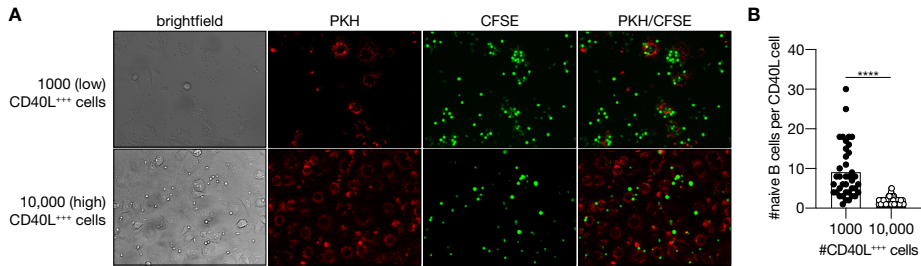


Figure S5 | Naive B cells compete for CD40L-expressing cells. (A–B) CFSE-labeled naive B cells (green) cultured on 1000 (supplemented with 9000 WT 3T3 cells) or 10,000 CD40L⁺-expressing PKH-labeled 3T3 cells (red). Cultures were imaged every 10 minutes during the time course of 48 hours. Representative images are shown of conditions at 9 hours after start of co-culture (A) and quantification (B) was performed after 4, 9, 20 and 38 hours. Data were analyzed by an unpaired t test. **** P ≤ 0.0001.

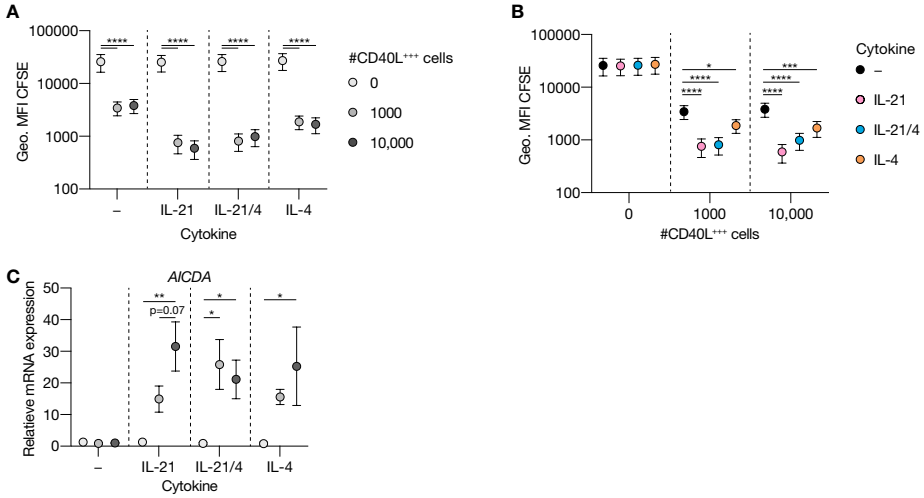


Figure S6 | The number of CD40L-expressing cells affects naive B cell expansion and AICDA mRNA expression. (A–B) Human naive B cells were cultured on a ratio WT: CD40L⁺-expressing 3T3 cells (10:0, 9:1 or 0:10) with or without IL-21 and/or IL-4 for 6 days (n=7). Geometric mean fluorescent intensity (Geo. MFI) of the proliferation-dye CFSE of live CD19⁺ cells was measured using flow cytometry. (C) *AICDA* mRNA expression after 3 days of culture on 0/1000/10,000 CD40L⁺-expressing 3T3 cells with or without cytokines (n=3). *AICDA* mRNA levels were expressed relative to expression levels in B cells stimulated for three days with 10,000 CD40L⁺-expressing 3T3 cells without cytokines. Data are shown as mean ± SEM of independent experiments. Single experiments were conducted in triplicate. Data were analyzed by a two-way ANOVA followed by Tukey’s multiple comparison test. * P ≤ 0.05, ** P ≤ 0.01, *** P ≤ 0.001, **** P ≤ 0.0001.

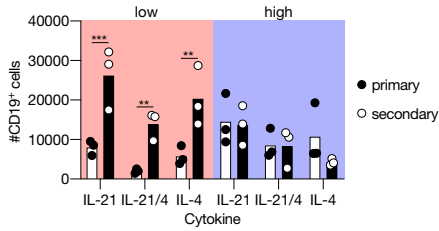


Figure S7 | Re-stimulation via CD40 and Tfh cytokine signaling minimally affects number of live CD19+ cells. Human B cells cultured on 1000 (supplemented with 9000 WT 3T3 cells; low) or 10,000 (high) CD40L⁺⁺⁺-expressing 3T3 cells (as in Figure 1A) with or without IL-21 and/or IL-4 for 11 days (primary - initial only stimulation). Alternatively, primary cultures were harvested after 6 days and secondary cultures were initiated for 5 days with the same number of CD40L⁺⁺⁺-expressing 3T3 cells and similar cytokine environments as in the primary culture. The number of live CD19⁺ events were assessed 11 days in primary or secondary culture using flow cytometry. Each data point represents the mean of an individual experiment (n=3) with triplicate measurements. Mean values are represented as bars. p-values were calculated using multiple t-test. * P ≤ 0.05, ** P ≤ 0.01, *** P ≤ 0.001.

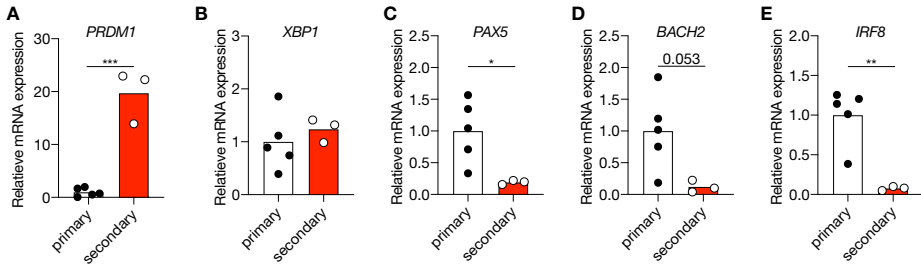


Figure S8 | B cells are transcriptionally prepared before transition into the antibody-secreting cell fate. Human naïve B cells were cultured on 10,000 CD40L⁺⁺⁺-expressing 3T3 cells (as in Figure 1A) and IL-21 for 9 days. Alternatively, primary cultures were harvested after 6 days and secondary cultures were initiated for 5 days with 10,000 CD40L⁺⁺⁺-expressing 3T3 cells and IL-21 (n=3). Subsequently, the CD27⁺CD38⁻ cell population was purified by cell sorting. (A–E) Expression of *PRDM1* (A), *XBP1* (B), *PAX5* (C), *BACH2* (D) and *IRF8* (E) mRNA in the CD27⁺CD38⁻ cell population was analyzed by qPCR relative to levels present in the CD27⁺CD38⁻ cell population after 9 days in primary culture. Each data point represents the mean of an individual experiment (n=5 for primary culture and n=3 for secondary culture) with triplicate measurements. Mean values are represented as bars. p-values were calculated using unpaired t-test. * P ≤ 0.05, ** P ≤ 0.01, *** P ≤ 0.001.

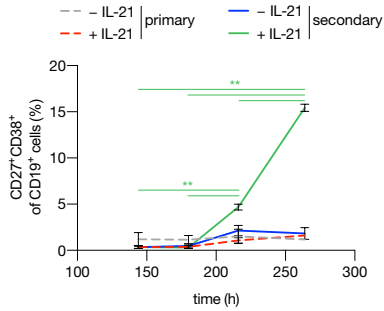


Figure S9 | Re-stimulation via CD40 and IL-21 signaling efficiently promotes B cell fate transition into CD27⁺CD38⁺ antibody-secreting cells. Human naive B cells were cultured on 10,000 CD40L⁺-expressing 3T3 cells (as in Figure 1A) with or without IL-21 for 6 days. After 6 days, primary cultures were harvested and secondary cultures were initiated for 5 days with 10,000 CD40L⁺-expressing 3T3 cells with or without IL-21 (n=3). The frequency of CD27⁺CD38⁺ cells was analyzed at 144, 180, 216 and 264 hours (h) in primary culture (dotted lines); and 36, 72 and 120 h in secondary culture (solid lines) using flow cytometry. Data are shown as mean ± SEM (n=3 independent experiments). Single experiments were conducted in triplicate. Data were analyzed by a two-way ANOVA followed by Tukey's multiple comparison test. ** P ≤ 0.01.

Table S1 | Primer sequences.

Genes		Sequence (5'-3')
<i>18S-rRNA</i>	Forward	CGGCTACCACATCCAAGGAA
	Reverse	GCTGGAATTACCGCGGCT
<i>AICDA</i>	Forward	GACTTTGGTTATCTTCGCAATAAGA
	Reverse	GGTCCCAGTCCGAGATGTA
<i>PRDM1</i>	Forward	AACGTGTGGGTACGACCTTG
	Reverse	ATTTTCATGGTCCCCTTGGT
<i>XBP1</i>	Forward	CCGCAGCACTCAGACTACG
	Reverse	TGCCAACAGGATATCAGACT
<i>PAX5</i>	Forward	ACGCTGACAGGGATGGTG
	Reverse	CCTCCAGGAGTCGTTGTACG
<i>BACH2</i>	Forward	TTCCTGAGGAGGTCACAG
	Reverse	ACAGGCCATCCTCACTGTTC
<i>IRF8</i>	Forward	AACTGGACATTTCCGAGCCA
	Reverse	AATCGTCCACAGAAGGCTCC

Chapter 6

Single-cell analysis reveals dynamics of human B cell differentiation and identifies novel B and antibody-secreting cell intermediates

Niels J.M. Verstegen^{1,2,†}, Sabrina Pollastro^{1,†}, Peter-Paul A. Unger¹, Casper Marsman¹, George Elias¹, Tineke Jorritsma¹, Marij Streutker¹, Kevin Baßler³, Kristian Händler^{3,4}, Theo Rispens¹, Joachim L. Schultze^{3,4}, Anja ten Brinke¹, Marc Beyer^{3,4,5}, S. Marieke van Ham^{1,6}

In press, eLife

1. Department of Immunopathology, Sanquin Research and Landsteiner Laboratory, Amsterdam University Medical Centers, University of Amsterdam, Amsterdam, The Netherlands
 2. Synthetic Systems Biology and Nuclear Organization, Swammerdam Institute for Life Sciences, University of Amsterdam, The Netherlands
 3. Genomics and Immunoregulation, LIMES Institute, University of Bonn, Bonn, Germany
 4. Platform for Single Cell Genomics and Epigenomics, German Center for Neurodegenerative Diseases (DZNE) and University of Bonn, Bonn, Germany
 5. Immunogenomics & Neurodegeneration, German Center for Neurodegenerative Diseases (DZNE), Bonn, Germany
 6. Swammerdam Institute for Life Sciences, University of Amsterdam, The Netherlands
- † These authors contributed equally to this work.

ABSTRACT

Differentiation of B cells into antibody-secreting cells (ASCs) is a key process to generate protective humoral immunity. A detailed understanding of the cues controlling ASC differentiation is important to devise strategies to modulate antibody formation. Here, we dissected differentiation trajectories of human naive B cells into ASCs using single-cell RNA sequencing. By comparing transcriptomes of B cells at different stages of differentiation from an *in vitro* model with *ex vivo* B cells and ASCs, we uncovered a novel pre-ASC population present *ex vivo* in lymphoid tissues. For the first time, a germinal-center-like population is identified *in vitro* from human naive B cells and possibly progresses into a memory B cell population through an alternative route of differentiation, thus recapitulating *in vivo* human GC reactions. Our work allows further detailed characterization of human B cell differentiation into ASCs or memory B cells in both healthy and diseased conditions.

INTRODUCTION

Protection from invading pathogens is, in part, provided by antibody-secreting cells (ASCs) that secrete high-affinity class-switched antibodies. Antibody formation, however, can also be highly undesired. This is the case for detrimental autoantibodies in autoimmune disorders, for alloantibodies that react with donor blood cells after a blood transfusion, or for antibodies that are formed against therapeutic biologics and that interfere with their therapeutic efficacy. Plasma cells secreting high-affinity antibodies are generated from naive B cells that, upon foreign antigen recognition by the antigen-specific B cell receptor (BCR) get activated and after CD4 T cell help can start a germinal center (GC) reaction. Here, B cells differentiate into GC B cells and begin to cycle between the GC dark zone (DZ) and the GC light zone (LZ). In the former, GC B cells undergo several rounds of cell cycle and receptor editing processes, such as somatic hypermutation and class-switching. In the latter, B cells need to reacquire antigen and present antigenic peptides to cognate antigen-specific CD4 T follicular helper (T_{fh}) cells to receive the required co-stimulatory, survival, and differentiation signals¹⁻⁶. After several rounds of DZ to LZ cycling, this process results in the selection of high affinity, class-switched B cells (reviewed in⁷). While early memory B cell and early plasmablast formation occur before GC establishment⁸, the GC reactions give rise to a later stage, higher affinity memory B cell formation followed by the eventual formation of high affinity, antibody-secreting cells (plasmablasts and plasma cells)⁹. Migration of plasma cells to the bone marrow and incorporation into bone marrow survival niches establishes long-lived plasma cells that may secrete antibodies for decades¹⁰⁻¹².

The transition of B cell into ASC is tightly regulated on the molecular level by a complex network of transcription factors that control the switch from the B cell stage to the ASC stage (reviewed in¹³). The ASC-specific transcription factors IRF4, XBP1, and BLIMP1 are upregulated only once the B cell-specific transcription factors PAX5, IRF8, and BACH2 are downregulated. These transcriptional changes are then followed by surface expression of stage-specific cellular markers, such as CD27, CD38, and CD138 on ASCs, with simultaneous downregulation of the B cell markers CD19 and CD20¹⁴⁻¹⁸.

Although these transcription factors associated with plasma cell differentiation and plasma cell markers have been well-studied, the differentiation trajectories of naive B cells into short-lived and long-lived ASCs and the regulators that control transition at the different stages of human B cell differentiation remain largely unknown. Bulk RNA sequencing on sorted B cells *ex vivo* has identified differences between naive B cells, GC B cells, memory B cells, plasmablasts, and plasma cells¹⁹⁻²¹, but does not allow delineation of the actual differentiation process and the various stages through which B cells transition to becoming ASCs. The development of single-cell sequencing techniques circumvents this problem and allows for the discovery of new cellular subsets and cells that are transitioning from one cellular differentiation state to another. To date, single-cell sequencing has been used, among others, to identify B cell subsets in the immune landscape of tumor-infiltrating lymphocytes²², to delineate malignant B cells in follicular lymphomas²³, and to identify transiting bone marrow progenitor cell populations that commit to

the B cell lineage^{24,25}. In addition, software to reconstruct B cell receptor sequences from single-cell RNA sequencing data has been developed in recent years^{26–29}. In-depth characterization of the differentiation process of mature naive B cells into ASCs has been investigated by focusing on parts of this differentiation process, for example, GC LZ to DZ migration^{30–32}. Although this contributed to new insights into GC reactions, it remains unclear how differentiation into plasma cells occurs and is regulated. More insight into this differentiation process might uncover targets to regulate B cell differentiation into ASC at an early stage and to intervene in the generation of undesired antibodies in disease.

We previously established a minimalistic *in vitro* culture system that uniquely supports efficient *in vitro* differentiation of human naive B cells into CD27⁺CD38⁺ ASCs while also maintaining high cell numbers along the differentiation stages³³. Here, we applied in-depth single-cell transcriptomics, B cell receptor reconstruction and trajectory inference on the *in vitro* generated ASCs and combined analyses with data from publicly available single-cell datasets of *ex vivo* obtained B cells and ASCs from different human tissues. Our data demonstrate that *in vitro* generated ASCs are highly comparable to their *ex vivo* counterparts. The differentiation trajectories uncover a hitherto unknown pre-ASC cellular stage that is detected also *ex vivo* in lymphoid tissue with active ASC differentiation processes. For the first time, germinal center-like B cells are identified *in vitro* from human naive B cells and possibly progress through an alternative route of differentiation into memory B cells. In addition to known regulatory transcription factors and cell surface markers, potential novel transcriptional regulators and plasma membrane markers are identified that may control or, respectively, mark the process of human plasma cell differentiation.

MATERIALS AND METHODS

Cell culture

NIH3T3 WT fibroblast cells (3T3) and human CD40L-expressing 3T3³⁴ were cultured in IMDM (Lonza) containing 10% FCS (Bodinco), 100 U/ml penicillin (Invitrogen), 100 µg/ml streptomycin (Invitrogen), 2 mM L-glutamine (Invitrogen), 50 µM β-mercaptoethanol (Sigma Aldrich) and 500 µg/ml G418 (Life Technologies).

Isolation of peripheral blood B cells from human healthy donors

Buffy coats of healthy human donors were obtained from Sanquin Blood Supply. All healthy donors provided written informed consent following the protocol of the local institutional review board, the Medical Ethics Committee of Sanquin Blood Supply, and conforms to the principles of the Declaration of Helsinki. Peripheral blood mononucleated cells (PBMCs) were isolated from buffy coats using a Lymphoprep (Axis-Shield PoC AS) density gradient. Afterward, CD19⁺ B cells were separated using magnetic Dynabeads (Invitrogen) according to the manufacturer's instructions.

***In vitro* naive B cell differentiation cultures**

CD40L-expressing 3T3 cells were harvested, irradiated with 30 Gy, and 1×10^4 CD40L-expressing 3T3 cells were seeded in B cell medium (RPMI 1640 (Gibco) without phenol red containing 5% FCS, 100 U/ml penicillin, 100 μ g/ml streptomycin, 2 mM L-glutamine, 50 μ M β -mercaptoethanol and 20 μ g/ml human apotransferrin (Sigma Aldrich; depleted for human IgG with protein G sepharose)) in 96-well flat-bottom plates (NUNC) to allow adherence overnight. The next day, 2.5×10^4 human naive (CD19⁺CD27⁻IgG-IgD⁺) B cells were sorted on a FACS Aria and activated using the irradiated CD40L-expressing 3T3 cells in the presence of IL-4 (100 ng/ml; Cellgenix) for six days.

After six days, activated B cells were collected and co-cultured with 1×10^4 CD40L-expressing 3T3 cells or 1×10^4 WT together with CD40L-expressing 3T3 cells (ratio 9:1) that were irradiated and seeded one day in advance (as described above), together with IL-4 (100 ng/ml) and IL-21 (50 ng/ml; Invitrogen) for five days.

Flow cytometry and sorting

Cells were first washed with PBS and stained with LIVE/DEAD Fixable Near-IR (Dead cell stain kit, Invitrogen) for 30 minutes at room temperature in the dark. Then, cells were washed with PBS supplemented with 1% bovine serum albumin. Extracellular staining was performed by incubating the cells for 30 minutes on ice in the dark with the following antibodies: Anti-CD19 (clone SJ25-C1, BD Bioscience), anti-CD27 (clone L128, BD Bioscience; clone O323, eBioscience), anti-CD38 (clone HB7, BD Bioscience), anti-CD138 (clone MI15; BD Bioscience) and anti-IgG (clone G18-145, BD Bioscience; clone MH16-1, Sanquin Reagents). Samples were measured on LSRII and analyzed using Flowjo software (Treestar).

For FACS sorting for single-cell RNA-sequencing, samples were stained as described previously with LIVE/DEAD Fixable Near-IR (Invitrogen) and the following antibodies: anti-CD19 (clone SJ25-C1, BD Bioscience), anti-CD27 (clone O323, eBioscience), anti-CD38 (clone HB7, BD Bioscience), anti-CD138 (clone MI15; BD Bioscience). Sorting was performed on Aria IIIu with FACSDiva software v7 optimized for indexed cell sorting. Single cells were sorted by gating CD27/CD38 subpopulations of the living cell compartment. Cells were sorted in 384-well twin.tec plates (Eppendorf) containing 2.3 μ l of lysis buffer per well. Lysis buffer consisted of 2.5 μ M oligo-dT30 VN primers, 2.5 μ M dNTP mix, 0.2% Triton X-100, and 1 U RNase inhibitor. After sorting, plates were centrifuged, snap-frozen on dry ice, and stored at -80°C until further processing.

Real-time semi-quantitative RT-PCR

Different B-cell subsets (as indicated) were sorted. After sorting, RT-PCR was performed as described before³⁵. Primers were developed to span exon-intron junctions and then validated (**Supplementary file 1**). Gene expression levels were measured in duplicate reactions for each sample in StepOnePlus (Applied Biosystems, Foster City, CA, USA) using the SYBR green

method (Applied Biosystems, Foster City, CA, USA).

CRISPR–Cas9-mediated gene deletion of primary B cells

CRISPR-targeting RNA (crRNAs) were designed with the InDelphi (<https://indelfi.giffordlab.mit.edu>), benchling (<https://www.benchling.com>), and Integrated DNA Technologies design tools (<http://www.idtdna.com>). Designed crRNAs were synthesized by Integrated DNA Technologies as Alt-R CRISPR/Cas9 crRNAs. crRNA sequences used in the study were as follows: crCD19, 5'-TCCCTCGGTGGGAGACACGG-3'; crPRDM1#1, 5'-CATTAAAGCCGTCAATGAAG-3'; crPRDM1#2, 5'-TGCTCCCGGGGAGAGTGTGC-3'; crPRDM1#3, 5'-GAAGTGGTGAAGCTCCCCTC-3'.

crRNA and trans-activating CRISPR RNA (tracrRNA; Integrated DNA Technologies) were duplexed by heating at 95 °C for 5 minutes. crRNA–tracrRNA duplexes were mixed with Cas9 protein (TrueCut v2; ThermoFisher) for 10 minutes at room temperature to form stable ribonucleoprotein (RNP) complexes. 2.5×10^4 primary human naive (CD19⁺CD27⁻IgG-IgD⁻) B cells were activated for 3 days with 1×10^4 irradiated CD40L-expressing 3T3 cells in the presence of IL-21 (50 ng/ml). After 3 days cells were harvested and resuspended in P3 buffer (Lonza), mixed with RNP complexes, added to nucleofector cuvettes (Lonza), and electroporated with Amaxa 4D Nucleofector (Lonza) using program EH-115. Activated and electroporated B cells were then resuspended in a pre-warmed B cell medium and 2.5×10^4 cells were plated in wells pre-seeded with 1×10^4 irradiated CD40L-expressing 3T3 cells in the presence of IL-21 (50 ng/ml). After 3 days, B cells were harvested and put on freshly irradiated CD40L-expressing 3T3 cells in the presence of IL-21 (50 ng/ml) for 5 days.

Preparation of cDNA libraries and sequencing

Sorted cells were processed using the Smart-seq2 protocol³⁶ adjusted for 384-well plates. In short, 384-well plates containing single cells were thawed and cells were lysed and mRNA denatured by incubating the plates at 95°C for 3 minutes and put back on ice. Subsequently, 2.7 µl of first-strand cDNA reagent mix, containing 1x First-strand buffer, 5 mM DTT, 1 M betaine, 14 mM MgCl₂, 5 U RNase inhibitor, 25 U Superscript II Reverse Transcriptase, and 1 µM Template-Switching oligonucleotides in nuclease-free water, was added to each well. Plates were incubated at 42°C for 90 minutes, 70°C for 15 minutes, and kept on hold at 4°C. Afterward, 7.5 µl of the pre-amplification mix, consisting of 1x KAPA HiFi HotStart Readymix and 0.12 µM ISPCR primers in nuclease-free water, was added to each well. Plates were then incubated as followed: 98°C for 3 minutes, 23 cycles of 98°C for 20 seconds; 67°C for 15 seconds; and 72°C for 6 minutes, then at 72°C for 5 minutes and kept on hold at 4°C. Purification of the resulting cDNA was performed using SeraMag SpeedBeads containing 19% w/v PEG 8,000 and a 1:0.8 ratio of cDNA/beads was used for cDNA precipitation. Purified cDNA was eluted in 14 µl of nuclease-free water. The quality of cDNA was randomly checked in 5% of the wells using the TapeStation High-Sensitivity D5000 assay. For the tagmentation reaction, 0.5 µl of 50-150

pg cDNA was mixed with a 1.5 μ l Tagmentation mix containing 1x Tagment DNA buffer and Amplicon Tagment mix (Nextera XT DNA sample preparation kit). Plates were incubated at 55°C for 8 minutes and kept on hold at 4°C. 0.5 μ l Neutralize Tagment buffer was added and incubated at room temperature for 5 minutes to inactivate Tn5. PCR amplification of adapter-ligated cDNA fragments was performed in a final volume of 5 μ l containing the two index primers (Nextera XT Index kit) in a 1:5 dilution and Nextera PCR master mix. Plates were then incubated as followed: 72°C for 3 minutes, 95°C for 30 seconds, then 14-15 cycles of 95°C for 10 seconds; 55°C for 30 seconds; and 72°C for 30 seconds, then 72°C for 5 minutes and kept on hold at 4°C. 384 wells (the entire plate, including negative controls) were pooled in a single 2 ml tube (Eppendorf). Purification of cDNA was performed by adding 400 μ l of cDNA in a 1:1 ratio with SeraMag SpeedBeads in 19% w/v PEG 8,000 in a 1.5 ml LoBind tube. Beads were washed with 1 ml of 80% ethanol. Purified cDNA was eluted in 200 μ l of nuclease-free water. The concentration of the library was measured by Qubit according to the manufacturer's instructions. The size distribution of the library was measured using the TapeStation High-Sensitivity D1000 or D5000 assay. The cDNA library pool was stored at -20°C until ready for sequencing.

cDNA library pool was diluted to 2 nM and prepared for sequencing using the NextSeq 500 High Output Kit v2 (75 cycles) according to the manufacturer's instructions. Sequencing was performed on an Illumina NextSeq 500 instrument.

Pre-processing of single-cell RNA sequencing data

The quality of the retrieved sequencing data was assessed using FastQC³⁷. Reads were pseudo-aligned to the human transcriptome (gencode version v27) using kallisto³⁸. Quantification of gene expression was obtained by gene-level summarization of transcripts abundance using the R package tximport³⁹, without any scaling (countsFromAbundance option set to "no"). Counts were then normalized using the Transcript per Million (TPM) method⁴⁰ with the following approach: a) gene length scaling, b) removal of all immunoglobulins genes and pseudogenes, and c) sequencing depth scaling (**Figure1—figure supplement 1a**). Removal of immunoglobulin genes at this stage prevented the artificial skewing of other genes expressed in the antibody-secreting cell clusters, due to the high content of immunoglobulins RNA present in this cell type. The scaled TPM matrix was used for downstream analysis.

Single-cell RNA sequencing data analysis

Gene expression was analyzed using the Seurat package in R⁴¹. The scaled TPM matrix and metadata information were used to create a Seurat object with the following specifications: min.cell = 3, min.feature = 200. Putative low-quality cells and doublets were removed based on the distribution of genes per cell⁴². Cells were then checked for alignment to the human genome (GRCh38) and the fraction of mitochondrial genes as a measure of cell stress. Quality control criteria for cell exclusion were set as follows: percentage of mitochondrial genes >20%, percentage of aligned reads <60%, and the number of total genes expressed within 5,000 and 10,000 (**Figure1—**

figure supplement 1b-c). 276 cells passed quality control and did not affect the distribution of the four CD27/38 populations, indicating that all populations were of equal quality, and could be used for further analysis (**Figure1—figure supplement 1d**). Gene expression values were then transformed to $\log_2 \text{TPM}+1$ and these values were used for all downstream analyses. Before performing dimensional reduction, the *FindVariableFeatures* function was applied to retrieve the top 2000 high variable genes followed by a global data scaling using the *ScaleData* function. Principal component analysis (PCA) was chosen as a linear dimensionality reduction technique using the previously selected 2,000 high variable genes as input and allowing 50 components. PCA-based cell clustering was performed by applying the *FindNeighbors* function on the first 10 PCAs followed by the *FindClusters* function with 0.5 resolution and the Leiden algorithm. For visualization purposes, a second non-linear dimensionality reduction was performed using the *RunUMAP* function on the first 10 PCAs (**Figure1—figure supplement 1e**).

Differential expression analysis

Differential expression analysis was performed on all genes using the wilcoxauc method from *presto*⁴³. Gene Set Enrichment Analysis (GSEA) was performed using the *clusterProfiler* package in R on 17,716 genes ranked based on $\log_{\text{FC}} * \text{adjusted p-value}$ using the Gene Ontology (GO) and the hallmark human gene sets obtained from MsigDB⁴⁴. For visualization, hierarchical clustering of GSEA results was performed using the *pairwise_termsim* function from *enrichplot* with an adjusted p-value < 0.05 and then plotted using the *emapplot* function.

Publicly available (sc)RNAseq datasets

For the analysis of the publicly available scRNA-seq dataset of B cells from different human tissues^{45–47}, processed gene expression matrixes were downloaded and cells were annotated as provided by the authors. For similarity and enrichment score analyses, the publicly available genes set GSE12366 which includes gene sets from up- and downregulated genes found in sorted naive B cells, memory B cells, GC B cells, and plasma cells were used⁴⁸. The similarity score was then calculated using *AddModuleScore* from Seurat. For the analysis of similarity score over differentiation as reported in **Figure 41**, the upregulated gene sets were compared and genes that were uniquely expressed by one population were used to calculate the similarity score to that population.

Trajectory inference

Pseudotemporal ordering of the differentiating B cells trajectory, a partition-based graph abstraction (PAGA)⁴⁹ was performed for the transcriptionally distinct cell clusters using the *tl.paga* function in *scanpy*. Velocity-based pseudotime reconstruction was performed using RNA velocity. To obtain the spliced and unspliced matrix for RNA velocity analysis, original fastq files were re-aligned using STAR (v2.7.7). Obtained .sam files were converted to sorted .bam files using *samtools* (v1.11). Sorted .bam files were fed into *velocity* (v0.17.17) using the run-

smartseq2 option. The obtained *loom* file containing the spliced and unspliced count matrix was imported into python and then merged with the Seurat object after conversion to *annData* format (*convertFormat* function from the *sceasy* R package). RNA velocity analysis was then performed using the *scVelo* (v0.2.2) package in python.

B cell receptor analysis

Reconstruction of the rearranged B cell receptor sequences was performed using BraCeR²⁹ on the cells that passed quality control. The functions *assemble* and *summarise* were run to obtain respectively all possible BCR rearrangements and only the functional BCR rearrangements per cell. For every cell, one functional heavy chain and one functional light chain BCR rearrangements were selected based on the highest expression. These sequences were then submitted to the HighV-quest portal of the International ImMunoGeneTics information system website (<http://www.imgt.org>) for further BCR characterization. Further analysis of the BCR rearrangements was performed using the tools from the Immcantation portal (<https://immcantation.readthedocs.io/en/stable/>). In particular, *Change-O* was used to perform clonal clustering and *Alakazam* was used for the analysis of somatic hypermutation.

RESULTS

Single-cell transcriptomic analysis of *in vitro* differentiated antibody-secreting cells

We previously described a minimalistic *in vitro* system that effectively differentiates human naive B cells into antibody-secreting cells (ASCs) while also maintaining high cell numbers at the various stages of B cell differentiation³³. Briefly, human naive B cells (CD19⁺CD27-IgG-IgD⁺) are sorted from healthy donor PBMCs and cultured on a feeder layer of human CD40L-expressing mouse fibroblasts and restimulated after six days. Cytokines typically expressed by follicular T cells (Tfh) (IL-21, IL-4) are added to mimic Tfh help for B cell differentiation. Restimulation with CD40 costimulation and Tfh cytokines *in vitro* was demonstrated to be needed to drive efficient ASC differentiation, in line with *in vivo* GC reactions (**Figure 1a**). To assess the transition of naive B cells (CD27⁻CD38⁻) into ASCs (CD27⁺⁺CD38⁺⁺), cells from the four CD27/CD38 quadrants were sorted on day 11 and the expression of master regulators of B cells to ASCs differentiation was analyzed (**Figure 1b**)¹³. CD27⁻CD38⁻ cells gradually lose expression of B cell signature genes *PAX5* and *BACH2* upon acquisition of CD27 and/or CD38 expression with CD27⁺⁺CD38⁺⁺ cells showing the most downregulated expression of *PAX5* and *BACH2* and upregulation of ASC signature genes *IRF4*, *XBPI1*, and *PRDM1* (**Figure 1c-g**). In line with this, CRISPR-Cas9-mediated knockout of *PRDM1* on day 3 strongly suppressed the formation of CD27⁺CD38⁺ cells on day 11 compared to control and *CD19* knockout (**Figure 1h**).

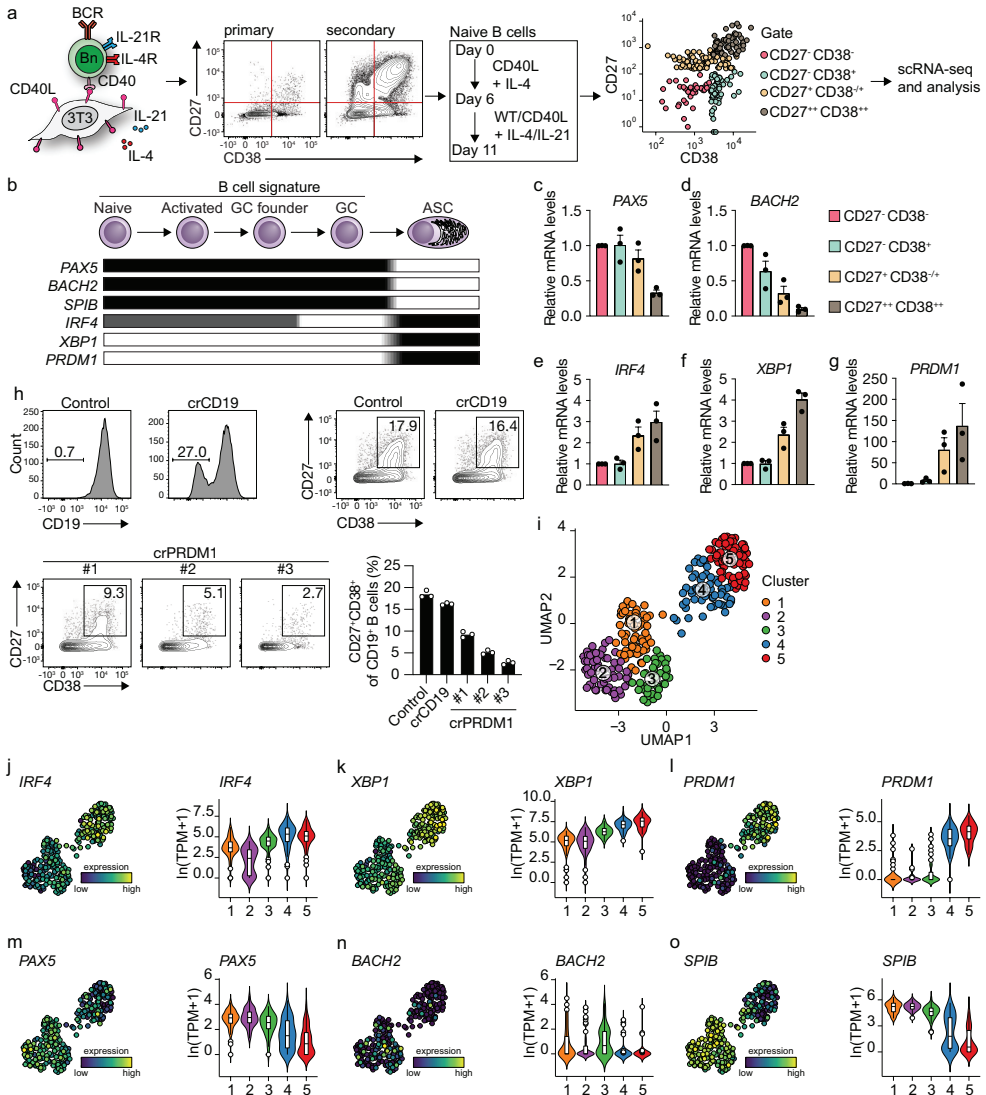


Figure 1 | Unbiased analysis of *in vitro* induced human naive B cell differentiation by scRNA-seq reveals five transcriptionally distinct B cell clusters. **a**, Overview of the scRNA-seq experiment in short human naive B cells were isolated and cultured with a human CD40L-expressing mouse fibroblast (3T3) cell line and recombinant IL-4 and IL-21. Secondary cultures were initiated on day 6 as this was necessary to induce substantial differentiation into the CD27⁺CD38⁺ ASC subset. On day 11, 384 cells were single-cell sorted based on the expression of CD27 and CD38 and sequenced using the Smart-seq2 method. **b**, Overview of the cellular stages and important transcription factors involved in B cells differentiation from naive to antibody-secreting cell (GC = Germinal Center and ASC = Antibody-Secreting Cell). **c-g**, Expression of *PAX5* (c), *BACH2* (d), *IRF4* (e), *XBP1* (f), and *PRDM1* (g) mRNA in sorted populations were analyzed by qPCR and related to levels present in CD27⁺CD38⁺ cells. Each data point represents the mean of an individual experiment (n=3) with triplicate measurements. Mean values are represented as bars. **h**, FACS analysis of surface CD19 levels (top left) and ASC differentiation (top right) in cultured primary human B cells expressing the indicated control or CD19-targeting RNP. FACS analysis of ASC differentiation (bottom left) and quantification (bottom right) in cultured primary human B cells expressing the indicated control or three different *PRDM1*-targeting RNP (*legend continues on next page*)

- ◀ RNPs. Representative of three independent experiments with triplicate measurements. **i**, UMAP projection of single-cell transcriptomes of *in vitro* differentiated human naive B cells (276 high-quality cells). Each point represents one cell, and colors indicate graph-based cluster assignments. **j–o**, UMAP projection as in **i** colored by the transcriptional regulators *IRF4* (**j**), *XBP1* (**k**) and *PRDM1* (**l**), *PAX5* (**m**), *BACH2* (**n**), *SPIB* (**o**), which are important in B cell differentiation (left graph of each panel), along with corresponding distribution of average expression levels ($\ln(\text{TPM}+1)$) across the B cell clusters (1, 2 and 3) and the ASC clusters (4 and 5) (right graph of each panel).

Since the minimalistic *in vitro* system efficiently drives differentiation of primary human naive B cells into ASCs and follows the *in vivo* observed transitions of the master regulators of transcription, the dynamics of human naive B cell differentiation were investigated in detail by single-cell RNA sequencing. Cultured cells were single-cell sorted on day 11 based on the expression of CD27 and CD38 to obtain a faithful representation of cells at varying stages of B cell to ASC differentiation. Next, cells were processed for single-cell RNA sequencing using the SMARTseq2 method. After raw data processing and quality control, a total of 275 (out of 382 sorted cells) high-quality cells that together express 17,716 genes were included in the final dataset (**Figure 1—figure supplement 1a–e**). Cells were assigned to one of three phases of the cell cycle (G1, G2/M, S) as determined by scores calculated based on the expression of G2/M and S phase genes (**Figure 1—figure supplement 1f**). As the cell cycle is an essential component of germinal center (GC) reactions, data were analyzed with and without regressing cell cycle heterogeneity. When the cell cycle was not regressed out, cells were clustered based on cell cycle scores, and most differentially expressed genes were related to the cell cycle (**Figure 1—figure supplement 1g**). Cell cycle heterogeneity was regressed out in the final dataset to primarily focus our analysis on factors influencing B cells differentiation apart from the cell cycle (**Figure 1—figure supplement 1h, i**).

Unsupervised hierarchical clustering and visualization with Uniform Manifold Approximation and Projection (UMAP) identified five clusters of differentiating cells (**Figure 1i and Figure 1—figure supplement 1j**). Clusters 4 and 5 showed a clear ASCs gene signature with a prominent expression of known ASC-specific genes *IRF4*, *XBP1*, and *PRDM1* (**Figure 1j–l**). Of note, 99% of CD27⁺CD38⁺ double-positive sorted cells were represented in clusters 4 and 5 (**Figure 1—figure supplement 2a–b**). The other three clusters, (clusters 1–3) still showed a pronounced B cell signature with higher expression of genes known to repress the ASCs state such as *PAX5*, *BACH2*, and *SPIB* (**Figure 1m–o**). Thus, upon 11 days of culture with CD40 costimulation and IL-21/IL-4, human naive B cells differentiate into distinct B cells and ASC clusters based on overall gene signatures.

***In vitro* generated ASCs are highly comparable with *ex vivo* obtained ASCs from different human tissues**

To further characterize *in vitro* generated ASCs, transcribed immunoglobulin genes were reconstructed from the single-cell transcriptomic data using *BraCeR*, and transcription levels and properties of immunoglobulin genes were compared between B cell and ASC clusters. A functional B cell receptor heavy chain rearrangement was successfully reconstructed for 255 out of

276 cells analyzed. Expression of the reconstructed B cell receptor (BCR) genes in clusters 4 and 5 were up to 10 times higher compared to clusters 1-3, demonstrating a very high transcriptional activity of immunoglobulin genes in the ASCs clusters (**Figure 2a**). Isotype analysis of the reconstructed BCR heavy chains revealed a homogeneous distribution of isotypes in the different clusters (**Figure 2b and Figure 2—figure supplement 1a-b**). When combining data for B cell and ASC clusters, the percentage of cells expressing immunoglobulin of the IgM isotype was lower in clusters 4 and 5 compared to clusters 1-3 (clusters 4 and 5: 36.6% vs. clusters 1-3: 50.3%; p -value < 0.01), while the opposite was true for expression of immunoglobulins of the

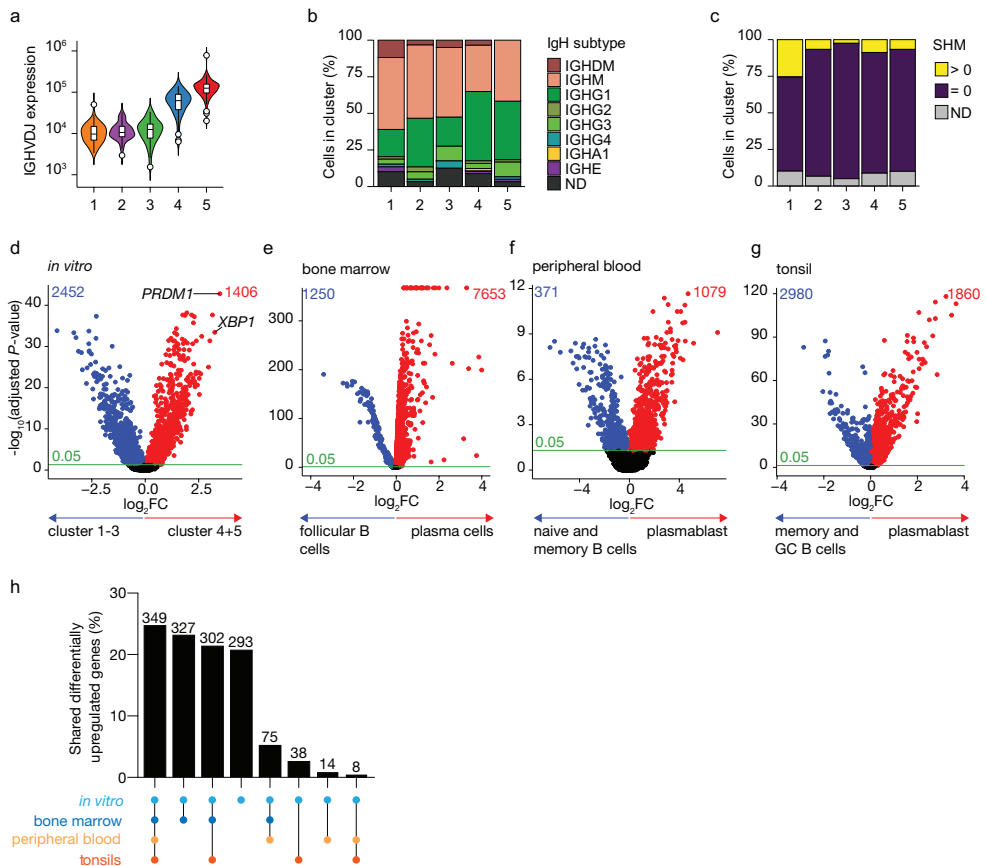


Figure 2 | Identification of antibody-secreting cells with substantial gene expression overlap as compared to *ex vivo* derived plasmablast/plasma cells among the *in vitro* differentiated human naive B cells. **a**, Violin plot of the reconstructed B cell receptor immunoglobulins gene expression as determined by BraCeR within each B cell cluster. **b**, Stacked bars denotes the frequency of isotype analysis of the reconstructed immunoglobulin heavy chain within each cluster. **c**, Stacked bars showing the percentage of cells with a given B cell receptor mutation count within each B cell cluster. **d–g**, Volcano plot depicting significantly (adjusted p -value < 0.05) down- and up-regulated genes. (d) *in vitro* generated antibody-secreting cells (clusters 4 and 5), *ex vivo* bone marrow-derived plasma cells (e), *ex vivo* peripheral blood-derived plasmablast (f), and *ex vivo* tonsil-derived plasmablast/plasma cells (g) were compared to each specific B cell counterparts. **h**, UpSetR plot depicts the intersection among all up-regulated genes identified in *in vitro* and *ex vivo* antibody-secreting cells.

IgG1 isotype (cluster 4 and 5: 43.7% vs. cluster 1-3: 24.6%; p-value <0.001). In addition, 87% (226/255) of all the reconstructed BCR heavy genes were identical to the germline sequence, i.e. not somatically hypermutated, independently of their cluster origin (**Figure 2c**). Thus, *in vitro* generated ASCs express a high load of, mostly, IgG1 class-switched but no significant mutated immunoglobulin genes.

To assess how the transcriptional profile of the *in vitro* generated ASCs was representative of the *in vivo* situation the specific gene signature of the *in vitro*-generated ASCs was first identified by performing differential expression analysis in the ASCs clusters 4 and 5 compared to the B cell clusters 1-3 (**Figure 2d**). A total of 3,858 genes were differentially expressed in the ASCs clusters, with 1,406 over-expressed among which *PRDM1* and *XBPI* were top hits. Next, publicly available scRNA-seq datasets from bone marrow from the Human Cell Atlas Data Coordination Portal ‘Census of Immune Cells’ project (<https://data.humancellatlas.org/explore/projects/cc95ff89-2e68-4a08-a234-480eca21ce79>) (**Figure 2—figure supplement 2**), human peripheral blood⁴⁵ (**Figure 2—figure supplement 3**), and tonsils⁴⁶ (**Figure 2—figure supplement 4**) were used to perform differential expression analysis in which each tissue-specific ASCs cluster was compared to its tissue-specific B cell counterpart. A total of 7653, 1079, and 1860 genes were up-regulated in *ex vivo* obtained ASCs from bone marrow, peripheral blood, and tonsils, respectively (**Figure 2e-g**). Analysis of the overlap between the identified up-regulated genes selected in *in vitro* and *ex vivo* data revealed that out of the 1406 upregulated genes found in *in vitro* generated ASCs, 1113 (79%) were shared with at least one *ex vivo* ASCs population, of which 349 (25%) were shared with all populations (**Figure 2h**). The remaining 293 (21%) genes were uniquely upregulated in *in vitro* generated ASCs, indicating that these genes might be linked to *in vitro* culture rather than be general for ASCs. Taken together these data show that the *in vitro* generated ASCs have highly similar transcriptional profiles compared to *ex vivo* obtained ASCs.

A novel B cell to ASC intermediate cellular stage is identified as a precursor of terminally differentiated ASCs

In our dataset, cells with a prominent ASCs gene signature were separated into two distinct transcriptional clusters. The cells in these clusters also show a slightly different expression of the ASCs phenotypic markers CD27 and CD38, with cells in cluster 5 being predominantly CD27⁺⁺CD38⁺⁺, while cluster 4 also includes CD27⁺CD38⁺ cells (**Figure 1—figure supplement 2a**). When performing clustering analysis on the dataset without cell cycle regression, again cells from clusters 4 and 5 separated from the B cells clusters. Interestingly, the two former ASC clusters now separated into two new clusters, whereby the cell cycle stage became the major common denominator between the two clusters (**Figure 1—figure supplement 1j**). This shows that original clusters 4 and 5 contain both cells in the cell cycle and cells that are out of the cell cycle. To further investigate the differences between cells in cluster 4 and 5, the similarity and the enrichment score for ASCs gene signature was analyzed for both clusters (**Figure 3a, b**). Cells in cluster 4 scored lower than cells in cluster 5 for both ASCs similarity and enrichment, indicating a

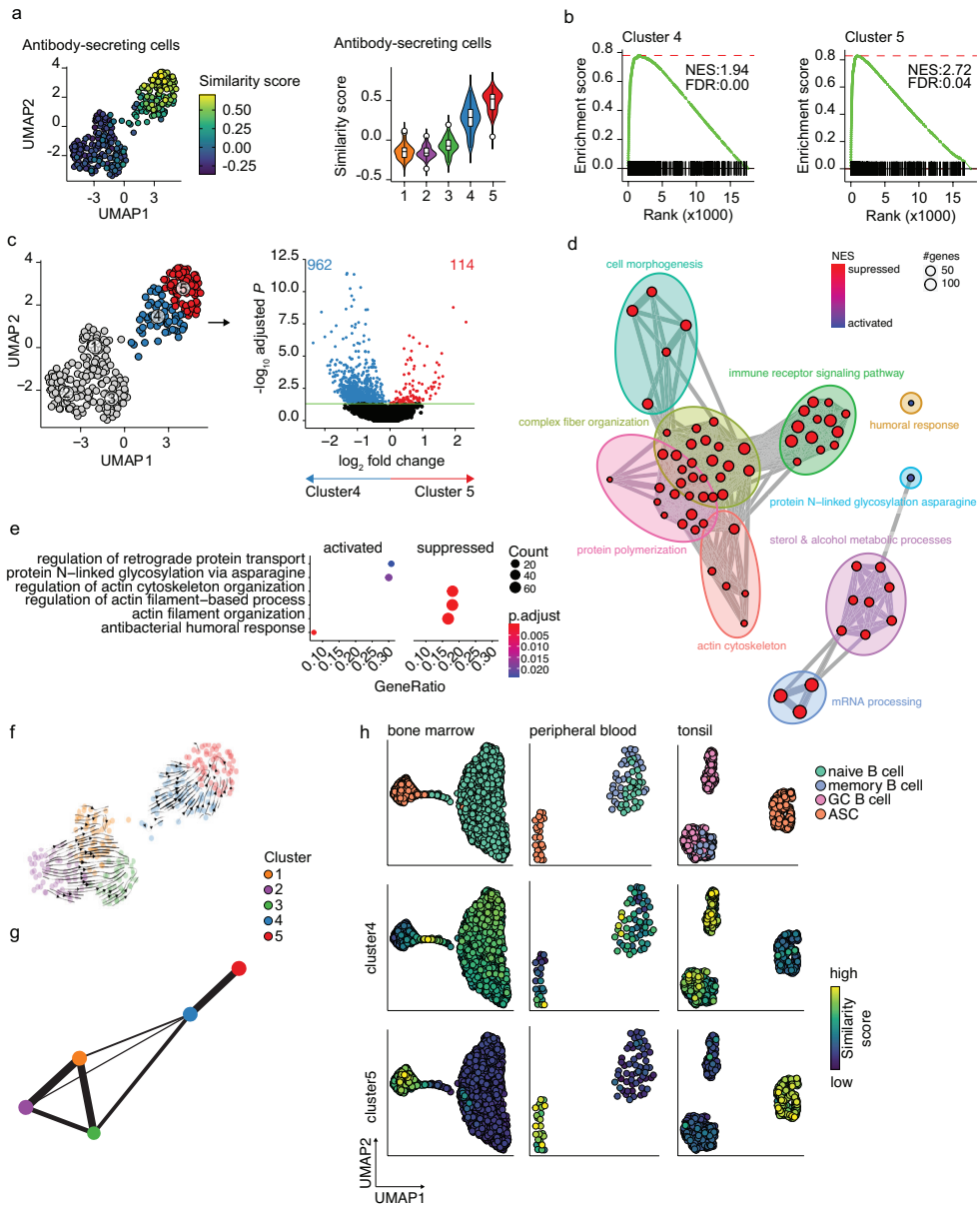


Figure 3 | Pre- and terminally differentiated ASCs separated in different clusters. **a**, UMAP projection colored by antibody-secreting cells (ASC) similarity score (left), along with corresponding distribution of the similar score within each cluster (right). **b**, GSEA enrichment plots for ASC gene signature in cells from clusters 4 (left) and 5 (right) as compared to the other clusters (NES: Normalized Enrichment Score; FDR: False Discovery Rate). **c**, UMAP projection as in *figure 1i* colored by cluster 4 and 5 membership (left) and Volcano plot depicting significantly (adjusted p-value <0.05) down- and up-regulated genes in cluster 5 as compared to cluster 4. **d**, Functional grouping network diagram of gene set enrichment analysis comparing clusters 4 and 5. The dot size and the dot color represent the number of genes in the pathway and the NES, respectively. **e**, The top 3 most significantly differentially activated pathways as determined by GO enrichment analysis comparing clusters 4 and 5. The dot size and the dot color represent the number of genes in (legend continues on next page)

- ◀ the pathway and the adjusted p-value, respectively. **f**, Velocyto force field showing the average differentiation trajectories (velocity) for cells located in different parts of the UMAP plot. Arrow size conveys the strength of predicted directionality. **g**, PAGA graph showing the connectivity between the clusters. Each node corresponds to each of the clusters identified using Seurat. The most probable path connecting the clusters is plotted with thicker edges. **h**, UMAP projection of *ex vivo* B cells and ASC derived from bone marrow, peripheral blood, and tonsil colored by clusters 4 and 5 similarity score.

less dominant ASCs gene signature in this cluster. Differential expression analysis between clusters 4 and 5 identified a total of 1076 differentially expressed genes, with 114 and 962 genes up- and down-regulated in cluster 5, respectively (**Figure 3c**). Network analysis of Gene Set Enrichment Analysis (GSEA) results for the differentially expressed genes revealed a predominant enrichment for terms concerning cytoskeleton organization, including supramolecular fiber organization, immune cell receptor signaling, and metabolism of steroids (**Figure 3d and Figure 3—figure supplement 1**). Of note, among the enriched terms concerning cytoskeleton organization, we found “*Arp2/3 complex-mediated actin nucleation*”, recently shown to be important in immune synapses formation^{50,51}, BCR signaling and B cell activation, together with other terms involved in antigen uptake and processing (**Figure 3—figure supplement 1**). The majority of the processes indicated by the predominantly enriched terms were suppressed in cluster 5 compared to cluster 4, while specifically activated processes in cluster 5 were “*protein N-linked glycosylation*” and “*retrograde protein transport*” (**Figure 3e**). Thus, cells in cluster 4 are still active in antigen presentation and processing, BCR signaling, and fatty acid metabolism, while such processes are being shut down in cells from cluster 5 that conversely up-regulate genes involved in protein glycosylation and protein transport.

To assess whether cluster 4 is a precursor population of cluster 5, we applied two algorithms for analyzing respectively the connectivity and the dynamics between clusters in scRNA-seq datasets, namely Partition-based graph abstraction (PAGA)⁴⁹ and RNA velocity⁵². Projection of the RNA velocity vectors on the UMAP representation revealed an area of increased velocity in cluster 4 in the direction of cluster 5, indicating that cells in cluster 4 are rapidly transitioning towards the transcriptomic signature of cells in cluster 5 (**Figure 3f**). At the top right extremity of cluster 5, where most of the non-cycling cells are located, no velocity vectors are projected. This implies that no subsequent cellular stage could be appointed, suggesting an endpoint of differentiation here. In line with this, results of PAGA showed increased connectivity among clusters 4 and 5 (**Figure 3g**). Interestingly, only cluster 4 and not cluster 5 were shown to be connected with all three B cell clusters, with cluster 3 being the most pronounced connection followed by cluster 1. This indicates that cluster 4 is more similar to the B cell clusters than cluster 5.

To confirm that cluster 4 represents a previously overseen intermediate B cell to ASCs population, we obtain a set of hallmark genes for cluster 4 and tested them on the publicly available scRNA-seq dataset from bone marrow, tonsil, and peripheral blood (**Figure 3h**). In the bone marrow dataset, the highest similarity score with the cluster 4 hallmark genes was observed in the cells connecting naive B cells to plasma cells. Interestingly, the GC B cells in the tonsil dataset, both non-cycling light zone (LZ) and cycling dark zone (DZ) GC B cells, showed the

highest similarity score with cluster 4 cells, while in the peripheral blood dataset few cells in the naive/memory cluster showed increased similarity. Of note, when performing the same analysis with the hallmark genes from cluster 5, the highest similarity was observed in each tissue-specific ASC population, as expected.

Thus, taken together these results show that cluster 5 represents a terminally differentiated ASCs population and that cluster 4 represents a novel B cell to ASC intermediate cellular stage, a precursor of terminally differentiated ASCs. This population can also be found *ex vivo*, mainly in lymphoid tissues with active ASCs differentiation.

Differentiating B cells transit through a germinal-center-like and early memory phenotype

To analyze the earlier stage of naive B cell to ASC differentiation, differential expression analysis among the three B cell clusters was performed to identify cluster-specific gene signatures (**Figure 4a**). Interestingly, genes that mark a germinal center (GC) B cells phenotype, such as *IRF8*, *BCL6*, *CD22*, and *CD83* were among the top 30 differentially expressed genes in cluster 2^{14,53-55}. When performing GSEA using hallmark gene sets on the differentially expressed genes in cluster 2, *MYC*^{56,57} and *E2F58* targets, known to promote GC B cell differentiation, were the top 3 significantly enriched gene sets and, in fact, *MYC* was expressed at its highest in cluster 2 compared to the other clusters (**Figure 4b-c**). Finally, the similarity score with *ex vivo* sorted human GC B cells was the highest in cluster 2, followed by cluster 3 (**Figure 4d**). Thus, we concluded that cells in cluster 2 represent GC-like B cells.

For cells in cluster 3, no definite phenotypic signature could be appointed based on the cluster-specific gene signature. However, given the intermediate similarity with both GC B cells and ASCs gene signatures (**Figure 4b and Figure 3a**) and the higher connectivity indicated by PAGA with the pre-ASCs cluster 4 compared to the other B cell cluster, we hypothesize that cluster 3 might represent a post-GC population primed to become ASCs.

Among the top differentially expressed genes of cluster 1, we found *BANK1*, recently identified as a marker of a pre-memory B cell stage⁵⁹ together with *CCR6* which was also expressed at the highest in cluster 1 (**Figure 4e-f**). Of note, *MZB1*, identified in the same study as a marker of pre-ASCs, is expressed at its lowest in cluster 1 (**Figure 4g**). Interestingly, *ITGAX* (CD11c) was indicated as differentially expressed in cluster 1 (**Figure 4h**). This gene defines a heterogeneous population of, mostly, memory B cells initially discovered in the context of aging and autoimmune disease, called atypical memory B cells or age-associated B cells (ABCs) that are thought to be generated through an alternative extra-follicular pathway^{60,61}. Likewise, the expression of other genes associated with the CD11c⁺ phenotype, such as *SIGLEC6* and *FCRL5*, were increased in cluster 1 (**Figure 4i-j**) while *CR2* (CD21), *TBX21* (T-bet), *FCRL4*, and *CXCR3* were not expressed in our dataset (data not shown). Finally, *HHEX*, recently shown to direct B cells away from the GC reaction into memory differentiation⁶², was also increased in cluster 1 (**Figure 4k**). Together, these data suggest that cells in cluster 1 are committed to becoming

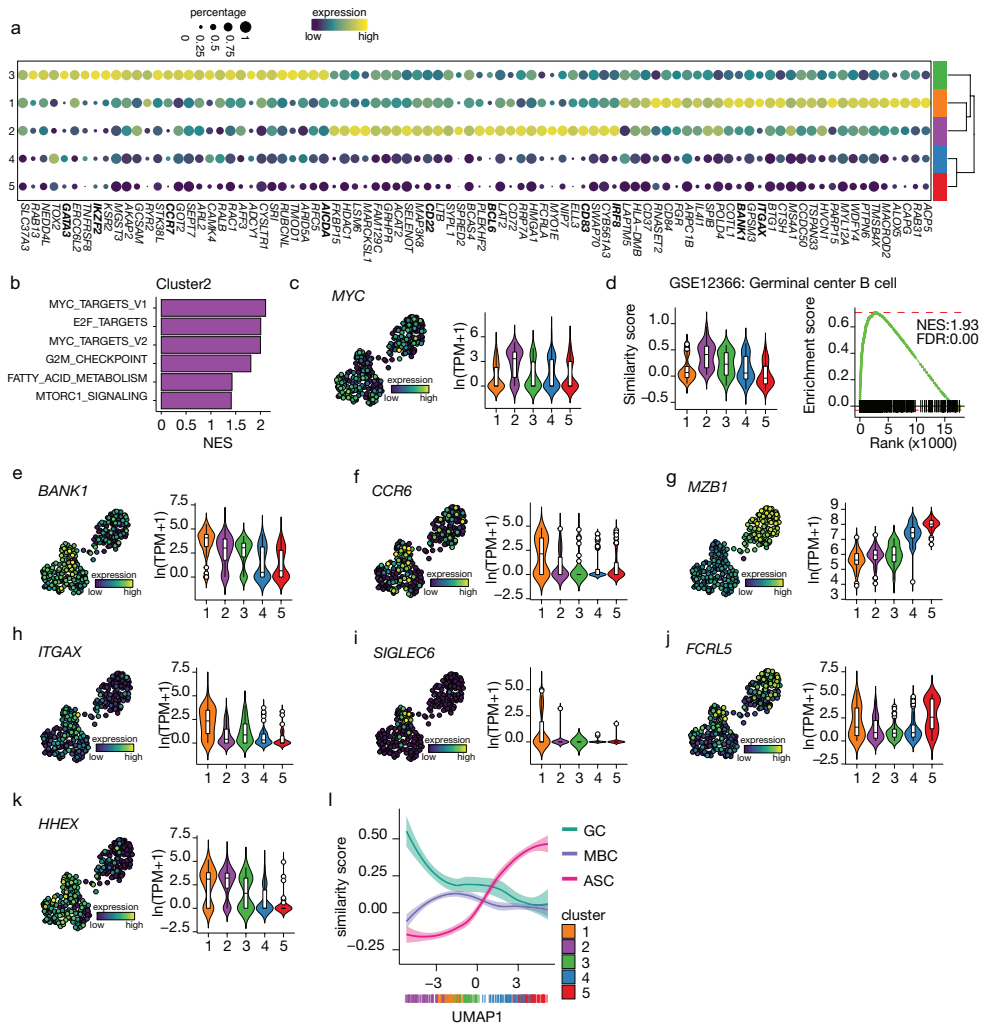


Figure 4 | Terminal differentiation into antibody-secreting cells starts from germinal center (GC) like cells. a, Top 30 differentially expressed genes identified in clusters 1-3. The size of the dot encodes the percentage of cells within a cluster, while the color encodes the average gene expression across all cells within a cluster. **b**, Significantly enriched hallmark gene sets overlapping with the differentially expressed genes identified in cluster 2. **c**, UMAP projection colored by expression of the transcription factors *MYC* (left), along with corresponding distribution of expression levels ($\ln(\text{TPM}+1)$) within each cluster (right). **d**, Corresponding distribution of the germinal center (GC) similarly score within each cluster (left) and GSEA enrichment plot (right) for GC B cell gene signature in cells from cluster 2 (NES: Normalized Enrichment Score, FDR: False Discovery Rate). **e-k**, UMAP projection colored by expression of the *BANK1* (e), *CCR6* (f), *MZB1* (g), *ITGAX* (h), *SIGLEC6* (i), *FCRL5* (j), *HHEX* (k; left), along with corresponding distribution of expression levels ($\ln(\text{TPM}+1)$) within each cluster (right). **l**, The similarity score of *ex vivo* germinal center B cell (GC), memory B cell (MBC), and antibody-secreting cell (ASC) gene sets ordered by UMAP1.

memory B cells.

To confirm the above findings of an *in vitro* B differentiation system in which GC-like B cells are directed towards both a memory and an ASCs cell phenotype, we analyzed the similarity score of all cells in our dataset ordered based on UMAP1 with gene signatures obtained from *ex vivo* sorted B cell at different differentiation stages, namely GC B cell, memory B cells and ASCs (**Figure 41**). As expected, the ASCs similarity score increases following UMAP1-based differentiation, starting at the lowest in cluster 2 and gradually increasing going through clusters 3, 4, and 5. Conversely, the similarity with GC B cell starts at the highest in cluster 2 and rapidly decreases going toward cluster 1; a slight stagnation is then observed in correspondence to cluster 3, followed by an additional decrease going through clusters 4 and 5. Finally, the similarity with memory B cells starts low with cluster 2, picks up in cluster 1, and decreases again through clusters 3 to 5. Thus, the differentiation dynamics observed in our *in vitro* system recapitulate *ex vivo* naive B cell differentiation processes, including both a memory and an ASC differentiation route.

To conclude, these results indicate that B cells with a GC-like phenotype are identified *in vitro* from human naive B cells after culture in presence of IL-4 and IL-21, and CD40L costimulation. Additionally, we find a post-GC B cell population with increased connectivity to the novel B cell to ASCs intermediate and a B cell population with a memory-like phenotype.

DISCUSSION

In this study, we set out to elucidate different stages of naive human B cell differentiation into ASCs by performing single-cell transcriptomics, B cell receptor reconstruction, and trajectory inference analysis on *in vitro* differentiated human naive B cells and integrating these data with *ex vivo* transcriptomes of isolated B cells and ASC subsets derived from different human tissues. We demonstrated that the *in vitro* generated antibody-secreting cells (ASC) are highly comparable to *ex vivo* ASCs. This led to the identification of an unknown B cell in ASCs intermediate population still active in antigen presentation and processing that can also be found *ex vivo* in lymphoid tissue with active ASCs differentiation processes (like tonsils). Finally, B cells with a germinal-center-like (GC-like) and a pre-memory phenotype were identified in our *in vitro* system thus recapitulating the different naive B differentiation processes observed *in vivo*.

To the best of our knowledge, this is the first study in which GC-like B cells are identified *in vitro* from human naive B cells. This finding could help us to decode one important and still unanswered question in B cell biology, i.e. which factors control the decisions for a GC-B cell to differentiate into a memory B cell or a plasma cell⁶³. In our system, we were able to clearly define cells with an ASCs phenotype (clusters 4 and 5) and cells with a gene signature that pointed towards a memory-like B cell phenotype (cluster 1). Surprisingly, the fact that both analyses focused on connection and dynamics between clusters, i.e., PAGA and RNA velocity, did not indicate a direct strong connection between the B cells clusters and the ASCs clusters raises the question of whether these two populations are related. In this respect, the *in vitro* generated

ASCs could be differentiating from a cell population that is lost at the time of our analysis or independently of a GC reaction. Additional research including time-course experiments is needed to further explore this possibility.

In line with this, the higher connectivity observed among the three B cell clusters rather than with the ASCs cluster, could indicate the presence of an alternative differentiation wave *in time*. In fact, the GC B cells of cluster 2 might represent the next GC reaction after the one that gave rise to the ASCs of clusters 4 and 5, and that would have generated new ASCs, possibly from cluster 3 if the culture would not be interrupted for analysis. This hypothesis raises the intriguing question of whether the memory cells of cluster 1 are again an alternative end-point or the starting point of this second GC reaction. Unfortunately, this is bioinformatically difficult to rule out as current methods to infer cellular trajectory do require a priori knowledge of the start point of differentiation⁶⁴, while unbiased analysis of cellular stage transition, such as RNA velocity, can still not be corrected for possible other drivers of cellular stage transition such as cell cycle⁶⁵.

A concept that is now supported by several studies is that different levels of antigen-affinity and different timing of generation during the GC reaction, dictate the fate of a GC B cell to become either a memory B cell or a long-lived plasma cell^{9,66}. Memory B cells that arise from GC reactions are an earlier output in the GC reaction than plasma cells and therefore accumulate somewhat less (albeit is mostly still considerable) affinity-increasing SHM⁹. Conversely, long-lived plasma cells are generated at a later stage of the GC reaction and are equipped with highly affine and highly mutated BCRs. Additionally, mouse studies have highlighted the role of Tfh-produced cytokines such as IL-21 and IL-4 in respectively inducing long-lived plasma cells or memory B cells upon *in vivo* transfer of *in vitro* induced GC-like B cells⁶⁷. In our *in vitro* system, IL-21 and IL-4 are provided together, explaining the possibility of having both plasma cell and memory populations at the end of the culture. It would be interesting to further analyze the output of a culture in which only one of the cytokines is provided, and in particular, if the presence of IL-4 only could boost the memory population as already demonstrated *in vivo* in mice⁶⁸. Furthermore, *in vitro* mouse studies demonstrated that naive B cells need to be primed in culture with IL-4 to obtain the GC-like phenotype and that naive B cells cultured directly in presence of IL-21 proliferate less and directly differentiate into ASCs. Whether the directly generated ASCs are identical to the ASCs generated via the GC-like intermediate stage still needs to be further investigated.

Interestingly, the metabolism of steroids and cholesterol were among the most enriched terms for the differentially expressed genes between the pre- and terminally differentiated ASCs. This is in line with the concept that the full commitment to antibody production and secretion of terminally differentiated ASCs requires a massive reprogramming of the metabolism not only to provide the molecular “bricks” for antibody production, i.e., amino acids and sugars, but also the cellular machinery to sustain such massive production, i.e. ER and Golgi expansion. In this respect, several studies demonstrated that the *de novo* synthesis of fatty acid is a crucial step in

plasma cell formation^{69,70}. Additionally, some new pieces of evidence support the hypothesis that antibody secretion and ER stress might be linked to the longevity of plasma cells^{71,72}. In future studies, we shall focus on the analysis of the changes in metabolic pathways that occur in our *in vitro* systems. A deeper analysis of the metabolic reprogramming happening at the interchange between the different cellular stages observed in our *in vitro* system might reveal that metabolism plays an additional layer of control on top of the known transcriptional ones for B cell differentiation.

To conclude, using an *in vitro* system that accurately recapitulates the *in vivo* human GC reaction we uncovered a novel intermediate population in the ASCs differentiation process and possibly an alternative route of differentiation into memory B cells. Further research is needed to further dissect the regulation of human B cell differentiation processes and in particular the choice between the two differentiation routes in both healthy and diseased conditions.

ACKNOWLEDGEMENTS

We thank the core facility at Sanquin: Erik Mul, Simon Tol, and Mark Hoogenboezem for providing technical assistance.

FUNDING

This research project was supported by a Landsteiner Foundation for Blood Transfusion Research grant, (LSBR 1609) and a Product and process development grant for cellular products by Sanquin (PPOC17-34/ L2263). MB is supported by the German Research Foundation (IRTG2168-272482170, SFB1454-432325352).

DATA AVAILABILITY

All raw fastq files and digital gene expression matrixes (DGE) are available at the Gene Expression Omnibus (GEO) repository under accession no. GSE214265.

REFERENCES

1. King, C., Tangye, S. G. & Mackay, C. R. T Follicular Helper (T FH) Cells in Normal and Dysregulated Immune Responses. *Annu Rev Immunol* **26**, 741–766 (2008).
2. Zaretsky, A. G. *et al.* T follicular helper cells differentiate from Th2 cells in response to helminth antigens. *J Exp Med* **206**, 991–999 (2009).
3. Bryant, V. L. *et al.* Cytokine-mediated regulation of human B cell differentiation into Ig-secreting cells: predominant role of IL-21 produced by CXCR5+ T follicular helper cells. *J Immunol* **179**, 8180–90 (2007).
4. Reinhardt, R. L., Liang, H.-E. & Locksley, R. M. Cytokine-secreting follicular T cells shape the antibody repertoire. *Nat Immunol* **10**, 385–93 (2009).
5. Irah L. King and Markus Mohrs. IL-4–producing CD4+ T cells in reactive lymph nodes during helminth infection are T follicular helper cells. *J. Exp. Med* **206**, 1001–1007 (2009).
6. Yusuf, I. *et al.* Germinal center T follicular helper cell IL-4 production is dependent on signaling lymphocytic activation molecule receptor (CD150). *J Immunol* **185**, 190–202 (2010).
7. Victora, G. D. & Nussenzweig, M. C. Germinal Centers. *Annu Rev Immunol* **40**, 5–10 (2022).
8. Glaros, V. *et al.* Limited access to antigen drives generation of early B cell memory while restraining the plasmablast response. *Immunity* **54**, 2005–2023.e10 (2021).
9. Weisel, F. J., Zuccarino-Catania, G. v., Chikina, M. & Shlomchik, M. J. A Temporal Switch in the Germinal Center Determines Differential Output of Memory B and Plasma Cells. *Immunity* **44**, 116–130 (2016).
10. Belnoue, E. *et al.* APRIL is critical for plasmablast survival in the bone marrow and poorly expressed by early-life bone marrow stromal cells. *Blood* **111**, 2755–64 (2008).
11. Cassese, G. *et al.* Plasma cell survival is mediated by synergistic effects of cytokines and adhesion-dependent signals. *J Immunol* **171**, 1684–90 (2003).
12. Radbruch, A. *et al.* Competence and competition: the challenge of becoming a long-lived plasma cell. *Nat Rev Immunol* **6**, 741–50 (2006).
13. Verstegen, N. J. M., Ubels, V., Westerhoff, H. V., van Ham, S. M. & Barberis, M. System-Level Scenarios for the Elucidation of T Cell-Mediated Germinal Center B Cell Differentiation. *Front Immunol* **12**, 1–19 (2021).
14. Victora, G. D. *et al.* Identification of human germinal center light and dark zone cells and their relationship to human B-cell lymphomas. *Blood* **120**, 2240–2248 (2012).
15. Loken, M. R., Shah, V. O., Dattilio, K. L. & Civin, C. I. Flow cytometric analysis of human bone marrow. II. Normal B lymphocyte development. *Blood* **70**, 1316–24 (1987).
16. Tangye, S. G., Liu, Y. J., Aversa, G., Phillips, J. H. & de Vries, J. E. Identification of functional human splenic memory B cells by expression of CD148 and CD27. *J Exp Med* **188**, 1691–703 (1998).
17. Terstappen, L. W., Johnsen, S., Segers-Nolten, I. M. & Loken, M. R. Identification and characterization of plasma cells in normal human bone marrow by high-resolution flow cytometry. *Blood* **76**, 1739–47 (1990).
18. Sanderson, R. D., Lalor, P. & Bernfield, M. B lymphocytes express and lose syndecan at specific stages of differentiation. *Cell Regul* **1**, 27–35 (1989).
19. Tarte, K., Zhan, F., De Vos, J., Klein, B. & Shaughnessy, J. Gene expression profiling of plasma cells and plasmablasts: toward a better understanding of the late stages of B-cell differentiation. *Blood* **102**, 592–600 (2003).
20. Halliley, J. L. *et al.* Long-Lived Plasma Cells Are Contained within the CD19(-)CD38(hi)CD138(+) Subset in Human Bone Marrow. *Immunity* **43**, 132–45 (2015).
21. Minnich, M. *et al.* Multifunctional role of the transcription factor Blimp-1 in coordinating plasma cell differentiation. *Nat Immunol* **17**, 331–43 (2016).
22. Chung, W. *et al.* Single-cell RNA-seq enables comprehensive tumour and immune cell profiling in primary breast cancer. *Nat Commun* **8**, 15081 (2017).
23. Andor, N. *et al.* Single-cell RNA-Seq of follicular lymphoma reveals malignant B-cell types and coexpression of T-cell immune checkpoints. *Blood* **133**, 1119–1129 (2019).
24. Miyai, T. *et al.* Three-step transcriptional priming that drives the commitment of multipotent progenitors toward B cells. *Genes Dev* **32**, 112–126 (2018).
25. Alberti-Servera, L. *et al.* Single-cell RNA sequencing reveals developmental heterogeneity among early lymphoid progenitors. *EMBO J* **36**, 3619–3633 (2017).
26. Canzar, S., Neu, K. E., Tang, Q., Wilson, P. C. & Khan, A. A. BASIC: BCR assembly from single cells. *Bioinformatics* **33**, btw631 (2016).

27. Upadhyay, A. A. *et al.* BALDR: a computational pipeline for paired heavy and light chain immunoglobulin reconstruction in single-cell RNA-seq data. *Genome Med* **10**, 20 (2018).
28. Rizzetto, S. *et al.* B-cell receptor reconstruction from single-cell RNA-seq with VDJpuzzle. *Bioinformatics* **34**, 2846–2847 (2018).
29. Lindeman, I. *et al.* BraCeR: B-cell-receptor reconstruction and clonality inference from single-cell RNA-seq. *Nat Methods* **15**, 563–565 (2018).
30. Milpied, P. *et al.* Human germinal center transcriptional programs are de-synchronized in B cell lymphoma. *Nat Immunol* **19**, 1013–1024 (2018).
31. Dominguez-Sola, D. *et al.* The FOXO1 Transcription Factor Instructs the Germinal Center Dark Zone Program. *Immunity* **43**, 1064–74 (2015).
32. Sander, S. *et al.* PI3 Kinase and FOXO1 Transcription Factor Activity Differentially Control B Cells in the Germinal Center Light and Dark Zones. *Immunity* **43**, 1075–86 (2015).
33. Unger, P.-P. A. *et al.* Minimalistic In Vitro Culture to Drive Human Naive B Cell Differentiation into Antibody-Secreting Cells. *Cells* **10**, 1183 (2021).
34. Urashima, M. *et al.* CD40 ligand triggers interleukin-6 mediated B cell differentiation. *Leuk Res* **20**, 507–515 (1996).
35. Souwer, Y. *et al.* B cell receptor-mediated internalization of salmonella: a novel pathway for autonomous B cell activation and antibody production. *J Immunol* **182**, 7473–81 (2009).
36. Picelli, S. *et al.* Full-length RNA-seq from single cells using Smart-seq2. *Nat Protoc* **9**, 171–81 (2014).
37. Andrews, S. FastQC: a quality control tool for high throughput sequence data. (2010).
38. Bray, N. L., Pimentel, H., Melsted, P. & Pachter, L. Near-optimal probabilistic RNA-seq quantification. *Nat Biotechnol* **34**, 525–7 (2016).
39. Sonesson, C., Love, M. I. & Robinson, M. D. Differential analyses for RNA-seq: transcript-level estimates improve gene-level inferences. *F1000Res* **4**, 1521 (2015).
40. Li, B., Ruotti, V., Stewart, R. M., Thomson, J. A. & Dewey, C. N. RNA-Seq gene expression estimation with read mapping uncertainty. *Bioinformatics* **26**, 493 (2010).
41. Hao, Y. *et al.* Integrated analysis of multimodal single-cell data. *Cell* **184**, 3573–3587.e29 (2021).
42. Butler, A., Hoffman, P., Smibert, P., Papalexi, E. & Satija, R. Integrating single-cell transcriptomic data across different conditions, technologies, and species. *Nat Biotechnol* **36**, 411–420 (2018).
43. Korsunsky, I., Nathan, A., Millard, N. & Raychaudhuri, S. Presto scales Wilcoxon and auROC analyses to millions of observations. *bioRxiv* 653253 (2019) doi:10.1101/653253.
44. Liberzon, A. *et al.* The Molecular Signatures Database (MSigDB) hallmark gene set collection. *Cell Syst* **1**, 417–425 (2015).
45. Rizzetto, S. *et al.* B-cell receptor reconstruction from single-cell RNA-seq with VDJpuzzle. *Bioinformatics* **34**, 2846–2847 (2018).
46. Attaf, N. *et al.* FB5P-seq: FACS-Based 5-Prime End Single-Cell RNA-seq for Integrative Analysis of Transcriptome and Antigen Receptor Repertoire in B and T Cells. *Front Immunol* **11**, 795575 (2020).
47. Jardine, L. *et al.* *Blood and immune development in human fetal bone marrow and Down syndrome*. *Nature* vol. 598 (2021).
48. Longo, N. S. *et al.* Analysis of somatic hypermutation in X-linked hyper-IgM syndrome shows specific deficiencies in mutational targeting. *Blood* **113**, 3706–3715 (2009).
49. Wolf, F. A. *et al.* PAGA: graph abstraction reconciles clustering with trajectory inference through a topology preserving map of single cells. *Genome Biol* **20**, 1–9 (2019).
50. Roper, S. I. *et al.* B cells extract antigens at arp2/3-generated actin foci interspersed with linear filaments. *Elife* **8**, (2019).
51. Bolger-Munro, M. *et al.* Arp2/3 complex-driven spatial patterning of the BCR enhances immune synapse formation, BCR signaling and b cell activation. *Elife* **8**, (2019).
52. Bergen, V., Lange, M., Peidli, S., Wolf, F. A. & Theis, F. J. Generalizing RNA velocity to transient cell states through dynamical modeling. *Nature Biotechnology* 2020 38:12 **38**, 1408–1414 (2020).
53. Meyer, S. J. *et al.* CD22 Controls Germinal Center B Cell Receptor Signaling, Which Influences Plasma Cell and Memory B Cell Output. *J Immunol* **207**, 1018–1032 (2021).
54. Basso, K. & Dalla-Favera, R. BCL6: master regulator of the germinal center reaction and key oncogene in B cell lymphomagenesis. *Adv Immunol* **105**, 193–210 (2010).

55. Wang, H. *et al.* Transcription factors IRF8 and PU.1 are required for follicular B cell development and BCL6-driven germinal center responses. *Proceedings of the National Academy of Sciences* 201901258 (2019) doi:10.1073/pnas.1901258116.
56. Calado, D. P. *et al.* The cell-cycle regulator c-Myc is essential for the formation and maintenance of germinal centers. *Nat Immunol* **13**, 1092–1100 (2012).
57. Dominguez-Sola, D. *et al.* c-MYC is required for germinal center selection and cyclic re-entry HHS Public Access. *Nat Immunol* **13**, 1083–1091 (2012).
58. Béguelin, W. *et al.* EZH2 enables germinal centre formation through epigenetic silencing of CDKN1A and an Rb-E2F1 feedback loop. *Nat Commun* **8**, (2017).
59. Holmes, A. B. *et al.* Single-cell analysis of germinal-center B cells informs on lymphoma cell of origin and outcome. *Journal of Experimental Medicine* **217**, (2020).
60. Wang, S. *et al.* IL-21 drives expansion and plasma cell differentiation of autoreactive CD11c^{hi}T-bet⁺ B cells in SLE. *Nature Communications* 2018 9:1 **9**, 1–14 (2018).
61. Sutton, H. J. *et al.* Atypical B cells are part of an alternative lineage of B cells that participates in responses to vaccination and infection in humans. *Cell Rep* **34**, (2021).
62. Laidlaw, B. J., Duan, L., Xu, Y., Vazquez, S. E. & Cyster, J. G. The transcription factor Hhex cooperates with the corepressor Tle3 to promote memory B cell development. *Nat Immunol* **21**, 1082–1093 (2020).
63. Akkaya, M., Kwak, K. & Pierce, S. K. B cell memory: building two walls of protection against pathogens. *Nat Rev Immunol* **20**, 229–238 (2020).
64. Saelens, W., Cannoodt, R., Todorov, H. & Saeys, Y. A comparison of single-cell trajectory inference methods. *Nature Biotechnology* 2019 37:5 **37**, 547–554 (2019).
65. Bergen, V., Soldatov, R. A., Kharchenko, P. V & Theis, F. J. RNA velocity—current challenges and future perspectives. *Mol Syst Biol* **17**, e10282 (2021).
66. Smith, K. G. C., Light, A., Nossal, G. J. & Tarlinton, D. M. The extent of affinity maturation differs between the memory and antibody-forming cell compartments in the primary immune response. *EMBO J* **16**, 2996–3006 (1997).
67. Nojima, T. *et al.* In-vitro derived germinal centre B cells differentially generate memory B or plasma cells in vivo. *Nat Commun* **2**, 465 (2011).
68. Duan, L. *et al.* Follicular dendritic cells restrict interleukin-4 availability in germinal centers and foster memory B cell generation. *Immunity* **54**, 2256–2272.e6 (2021).
69. Dufort, F. J. *et al.* Glucose-dependent de novo lipogenesis in B lymphocytes: a requirement for atp-citrate lyase in lipopolysaccharide-induced differentiation. *J Biol Chem* **289**, 7011–7024 (2014).
70. Fagone, P. *et al.* Phospholipid biosynthesis program underlying membrane expansion during B-lymphocyte differentiation. *J Biol Chem* **282**, 7591–7605 (2007).
71. Goldfinger, M., Shmuel, M., Benhamron, S. & Tirosh, B. Protein synthesis in plasma cells is regulated by crosstalk between endoplasmic reticulum stress and mTOR signaling. *Eur J Immunol* **41**, 491–502 (2011).
72. Pengo, N. *et al.* Plasma cells require autophagy for sustainable immunoglobulin production. *Nat Immunol* **14**, 298–305 (2013).

SUPPLEMENTARY INFORMATION

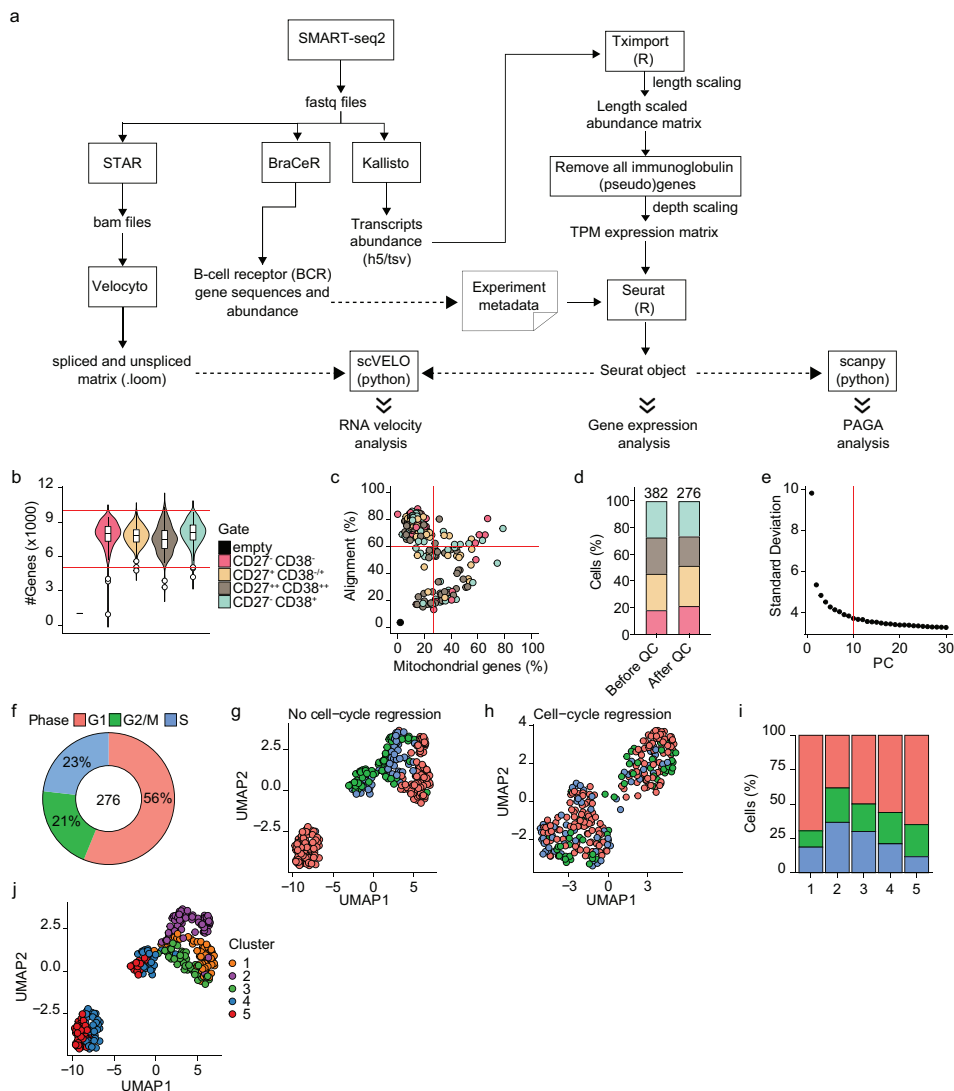


Figure 1—figure supplement 1 | scRNA-seq analysis of differentiating human B cells. **a**, Schematic overview of the analysis pipeline. **b**, Violin plot depicting the number of genes in each of the four sorted populations based on CD27 and CD38 expression. **c**, Scatter plot showing the percentage alignment and the proportion of mitochondrial genes per single cell. **d**, Stacked bars denote the frequency of the four sorted populations based on CD27 and CD38 expression before and after quality control. **e**, The number of principal components (PC; x-axis) with the variance in gene expression explained by each component. The top 10 principal components were selected for further analysis. **f**, Distribution of the different cell-cycle phases (Gap 1 (G1), Gap 2/mitosis (G2/M), and synthesis (S)) among the 276 high-quality single cells. **g–h**, UMAP projection of single-cell transcriptomes of *in vitro* differentiated human naive B cells without (**g**) and with (**h**) cell-cycle regression. Each point represents one cell, and colors indicate the cell-cycle phase. **i**, Mean cell-cycle phase frequencies within each of the B cell subsets that were identified after cell-cycle regression. **j**, UMAP projection of single-cell transcriptomes of *in vitro* differentiated human naive B cells without cell cycle regression. Each point represents one cell, and colors indicate graph-based cluster assignments identified with cell-cycle regression.

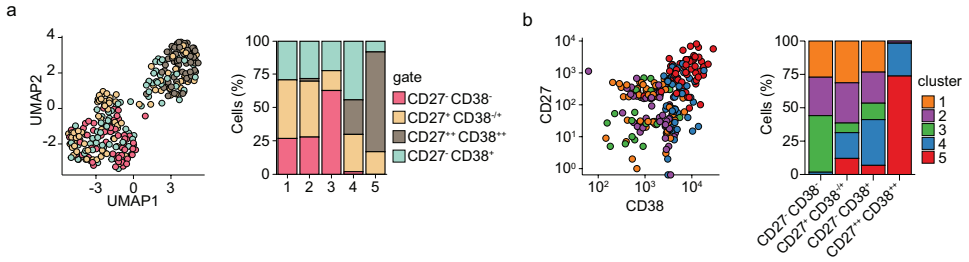


Figure1—figure supplement 2 | Subset distribution of differentiating primary human B cells. a, UMAP projection (left) as in figure 1i colored by the four sorted populations based on CD27 and CD38 expression. Barplot show the relative abundance of CD27⁻CD38⁻, CD27⁺CD38⁺⁺, CD27⁺⁺CD38⁺⁺, CD27⁻CD38⁺ cells among the five transcriptionally distinct clusters (right). **b**, Dot plot showing combined CD27 and CD38 protein expression values of cells from each cluster (left). Barplot show the relative abundance of the five transcriptionally distinct clusters within the CD27⁻CD38⁻, CD27⁺CD38⁺⁺ and CD27⁻CD38⁺ populations (right).

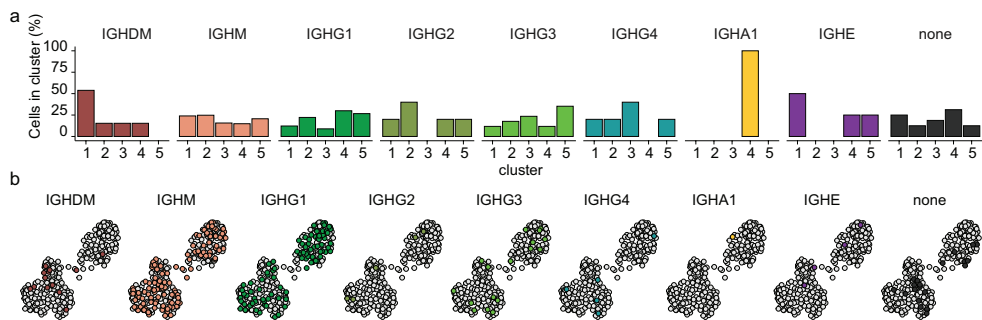


Figure2—figure supplement 1 | The distribution of heavy immunoglobulin gene in differentiating primary human B cells. a, Mean antibody subclass frequencies within each B cell subset. b, UMAP projection as in *figure 1i* colored by the reconstructed immunoglobulin heavy chain isotype.

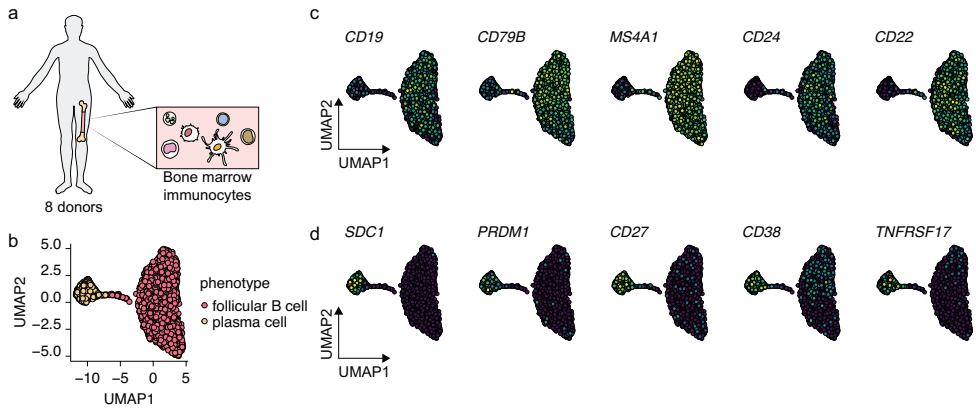


Figure2—figure supplement 2 | Selection of bone marrow-derived mature B cells and antibody-secreting cells.
a, Schematics of scRNA-seq on bone marrow-derived immunocytes derived from 8 human donors. **b**, UMAP plot of single-cell transcriptomes of bone marrow-derived B cells and antibody-secreting plasma cells. Each point is one cell, and colors indicate graph-based cluster assignments. **c–d**, UMAP plot of single-cell transcriptomes of bone marrow-derived B cells and antibody-secreting plasma cells, colored by expression of indicated B cell (**c**) and plasma cell (**d**) marker genes.

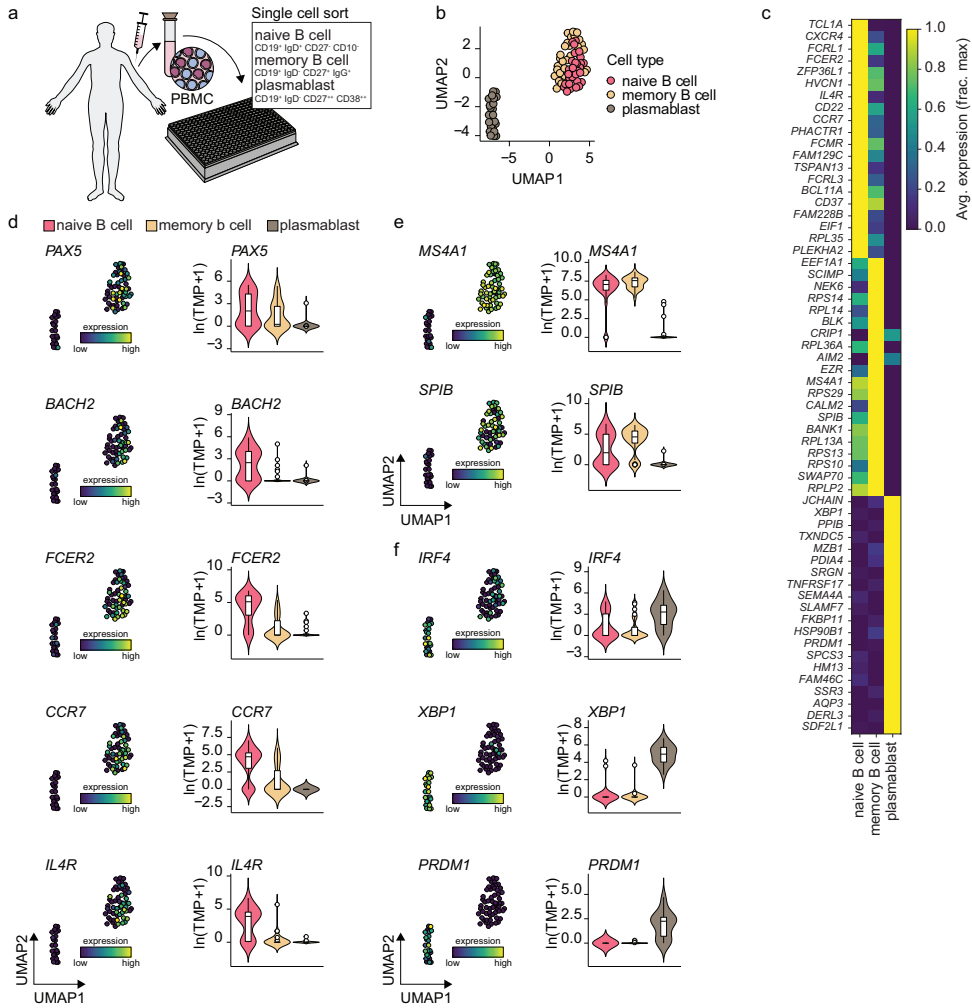


Figure2—figure supplement 3 | Gene expression characteristics of peripheral blood naive B cells, memory B cells, and plasmablast. **a**, Schematics of scRNA-seq on sort purified naive B cells, memory B cells, and plasmablast derived from healthy human peripheral blood. **b**, UMAP plot of single-cell transcriptomes of peripheral human naive B cells and plasmablast. Each point is one cell, and colors indicate graph-based cluster assignments. **c**, Heatmap of the 15 most differentially expressed genes significantly enriched in each cell cluster. **d**, Violin plots of previously characterized cluster-specific marker genes.

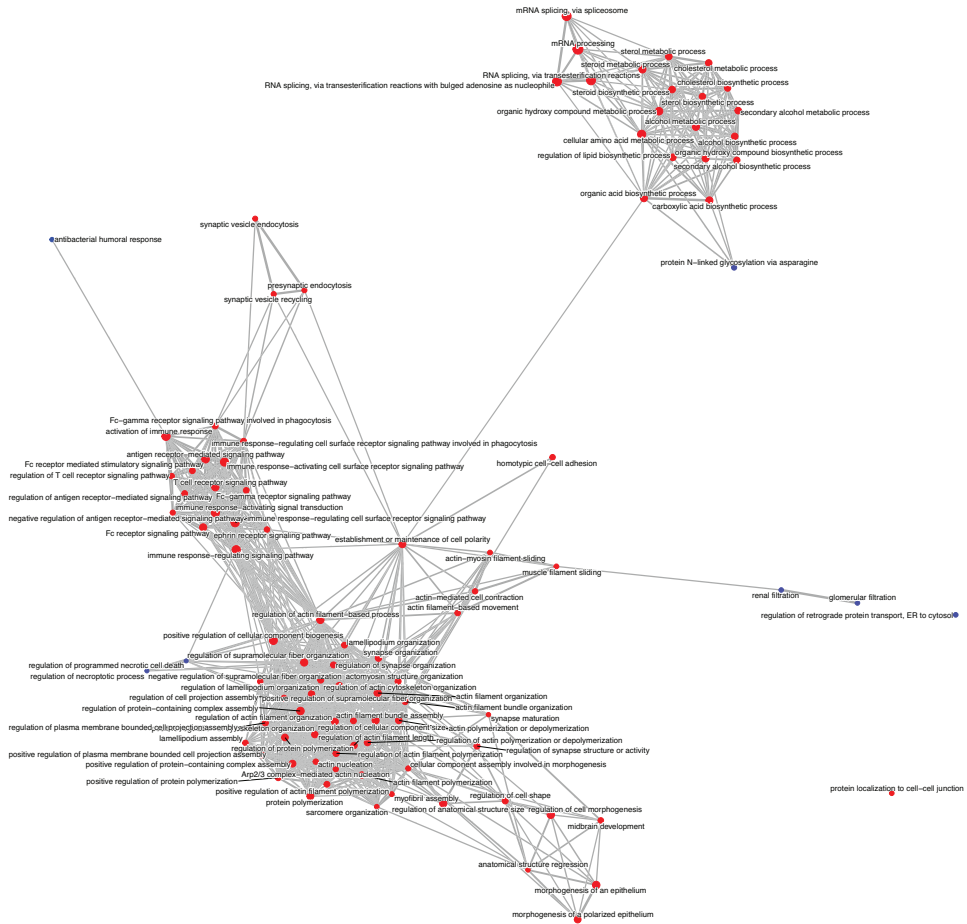


Figure3—figure supplement 1 | Enrichment Map of gene set enrichment analysis comparing clusters 4 and 5. The dot size and the dot color represent the number of genes in the pathway and the NES, respectively.

Supplementary file 1. Primer sequences

Genes		Sequence (5'-3')
<i>18S-rRNA</i>	Forward	CGGCTACCACATCCAAGGAA
	Reverse	GCTGGAATTACCGCGGCT
<i>PRDM1</i>	Forward	AACGTGTGGGTACGACCTTG
	Reverse	ATTTTCATGGTCCCCTTGGT
<i>XBP1</i>	Forward	CCGCAGCACTCAGACTACG
	Reverse	TGCCCAACAGGATATCAGACT
<i>IRF4</i>	Forward	CCACCACTGGCAAGGCCAG
	Reverse	GCAGCCGGCAGTCTGAGAACG
<i>PAX5</i>	Forward	ACGCTGACAGGGATGGTG
	Reverse	CCTCCAGGAGTCGTGTACG
<i>BACH2</i>	Forward	TTGCCTGAGGAGGTCACAG
	Reverse	ACAGGCCATCCTCACTGTTC

Chapter 7

Summarizing discussion

In response to T cell-dependent (TD) antigens, B cells differentiate into memory B cells and antibody-secreting plasmablast/plasma cells. The response is initiated in secondary lymphoid organs and requires recognition of antigens and repeated short but extensive cell-cell contacts with (early) T follicular helper (Tfh) cells providing help for B cells undergoing selection and differentiation. Early Tfh cell differentiation is induced by antigen-presenting dendritic cell interaction with naive helper T cells and is impacted by the T cell receptor (TCR) signaling strength. Crucial components of help provided by (early) Tfh cells are the expression of CD40L and cytokines IL-21 and IL-4. These minimal components are *in vivo* sufficient to drive naive B cell proliferation followed by effector B cell differentiation. Tfh cell differentiation and function are tightly interconnected with the B cell response. Like differentiation of B cells into memory B cells and antibody-secreting cells is dependent on Tfh-dependent selection, finalization of Tfh cell differentiation is regulated by B cells. B cells and Tfh cells have a highly symbiotic relationship, making the interactions between this pair specifically interesting in, for example, efficient vaccine development. *In this thesis, we sought to understand how the communication signals provided to the B and naive helper T cells integrate and steer their differentiation.*

BCR-mediated particle phagocytosis

B cells engage in a TD antigen response after recognizing specific antigens using the BCR. Antigen recognition facilitates the internalization of antigen-containing particles and surface presentation of antigen-derived peptides by major histocompatibility complex (MHC) class II proteins, which allows cognate interaction with (early) Tfh cells. Studies on BCR-mediated antigen responses have focused on soluble antigens for decades. However, most of the antigens encountered *in vivo* are large insoluble antigens, like particulate antigens such as viruses and antigens coated with antibodies and complement^{1,2}. Interestingly, it has been proposed that the predominant form of antigen encountered by germinal center (GC) B cells *in vivo* is associated with membranes and in a particulate form^{3,4}. Large antigens are acquired by direct uptake from the membranes of antigen-presenting cells through force-dependent extraction or enzymatic liberation⁵⁻⁷. Traditionally, it was believed that B cells could not internalize large antigen-containing particles (>0.5 μm) in the process of phagocytosis, which requires intense remodeling of the actin cytoskeleton. Recently phagocytic capacity was described for human B cells after BCR binding⁸⁻¹¹. **Chapter 3** of this thesis characterized the signaling pathways downstream of the BCR necessary for internalizing large non-membrane bound polystyrene beads and *Salmonella Typhimurium* previously coated with anti-IgM antibodies to target primary human B cells expressing IgM BCRs. We demonstrate that human primary B cells can recognize, take up, and destroy particulate antigens and then present those processed antigens to CD4⁺ T cells to elicit adaptive immune responses in a BCR-dependent manner. Antibody- and complement-mediated opsonization targeting the FC γ receptor IIB and the complement receptor 2 (CR2) were not required for large particle phagocytosis in B cells. Nevertheless, highly efficient particle binding was achieved through complement-opsonization. A similar observation has been made

regarding the function of non-cognate B cells in transporting complement-opsonized antigen to FDCs via binding to CR2 *in vivo*^{12,13}.

Although the vast proportion of circulating IgM-expressing human B cells are antigen-inexperienced naive B cells, some have an unswitched IgM memory phenotype, which may contain mutations¹⁴. These antigen-activated memory B cells of low affinity typically develop from the pre-GC and early GC stages^{15,16}. Isotype-switched IgG-BCR requires a significantly lower threshold of activation as compared to the activation of IgM-BCRs¹⁷. IgM-BCR memory B cells did not switch the isotype of the BCR and may still have an activation threshold like IgD-IgM naive-inexperienced B cells. Nevertheless, these IgM-BCR memory B cells may require different signaling pathways for particulate antigen phagocytosis. Given the heterogeneity among the IgM-BCR B cells, some of our findings may be specific to one of these populations.

Using a series of inhibitors that act on activation of BCR-signaling proteins, we demonstrate that IgM BCR-mediated phagocytic events rely on active SYK and PI3K signaling. In the cascade of BCR activation, PI3K plays an essential role in regulating conversion of phosphatidylinositol 4,5-bisphosphate (PIP₂) to phosphatidylinositol 3,4,5-triphosphate (PIP₃). In most cases, PIP₃ functions as docking phospholipids that recruit proteins to the plasma membrane, thereby initiating signaling cascades. The BCR-activating coreceptor CD19 recruits various signaling molecules, including PI3K, to the BCR signalosome upon antigen stimulation. CRISPR-Cas9 mediated genome editing revealed that the coreceptor CD19 was not required for IgM-BCR-induced phagocytosis or endocytosis of anti-IgM particles in a knockout human B cell line. Previously, however, it was demonstrated that CD19 reduces the threshold of BCR-signaling by amplifying signal transduction^{4,18}. Although BCR signaling and BCR-mediated internalization are interconnected, they appear mutually exclusive¹⁹. As such, CD19 may be critical for BCR activation, whereas receptor internalization requires other adaptors.

Detailed analysis that we performed to identify the link between BCR and PI3K activation established that in BCR-mediated phagocytosis, and not endocytosis, NCK is involved as the adaptor protein. NCK directly propagates the BCR signal to PI3K and facilitates the RAC1-dependent regulation of actin dynamics, which plays an essential role in cytoskeleton remodeling during particle engulfment. Central to RAC1 activation is PIP₃-dependent recruitment and activation of guanine nucleotide exchange factors (GEFs). Among the 80 members of the GEF family, at least 20 directly activate RAC1. We did not elucidate the GEF required for BCR-mediated phagocytosis; however, VAV is the most predominant GEF expressed in B cells that activates RAC1 and is best studied in immune cells^{20,21}. VAV plays a critical role in actin remodeling, BCR endocytosis, the presentation of p:MHCII, and B cell membrane spreading^{22,23}. Like VAV, DOCK2 is a GEF that functions through RAC1 to initiate F-actin remodeling²⁴. DOCK2, in contrast to VAV, has a DHR-1 domain that allows it to bind efficiently and specifically to PIP₃, making it conceivable that PI3K activity is required for DOCK2 recruitment and RAC1 activity²⁴⁻²⁸. Indeed, DOCK2 deficiency almost completely abrogates BCR-mediated RAC1 activity, whereas the activation of VAV was unchanged, placing it upstream of DOCK2²⁸. VAV

is highly required for BCR-mediated calcium influx^{29,30}. Calcium mobilization and cytoskeletal rearrangement are key hallmarks in regulating B cell function and intertwining in complex ways. Although VAV may thus be required for the calcium signals that finely control the rearrangement of the actin cytoskeleton, DOCK2 directly activates RAC1, necessary for actin stress fiber formation during BCR-mediated phagocytosis³¹.

Although engulfment of a large particle by a B cell itself requires intense remodeling of the actin cytoskeleton, actin remodeling is also necessary for growth of BCR microclusters²⁴. The sustained growth of such microclusters relays on PI3K-mediated conversion of PIP₂ to PIP₃ and downstream DOCK2-dependent activation of RAC1. For internalization of large particles with highly repetitive protein structures, formation of such BCR microclusters is vital. Indeed, a sharp pulse of RAC1 activity at the plasma membrane is observed shortly after large particle binding using the RAC1 biosensor. After the event of phagocytosis, RAC1 activity is significantly reduced. The local activation of RAC1 at the membrane may indicate a direct role in remodeling the actin cytoskeleton for BCR microcluster formation.

The importance of particle phagocytosis in induction and continuation of the humoral immune response must be further determined. It is generally believed that during an immune response, most B cells encounter antigens retained by subcapsular sinus macrophages or follicular dendritic in a complement- and/or antibody-dependent process^{12,32-34}. Large particulate antigen enters the subcapsular sinus in lymph nodes via afferent lymph vessels^{3,35}. Macrophages in the subcapsular sinus transport opsonized particles to non-cognate follicular B cells that transport antigenic complexes to follicular dendritic cells through CR2. By contrast, small soluble antigens diffuse into the follicles through a conduit network^{36,37}. According to recent findings, follicular B cells internalize large particulate antigens, which promotes GC response and production of class-switched antibodies in mice.³⁸ It is tempting to speculate that B cell phagocytic events are essential in human responses to large pathogens during infection and auto-antigen complexes (maybe even in part cell membrane-bound) during auto-immune diseases. For example, in peripheral blood B cells of patients with systemic lupus erythematosus (SLE), which have reduced expression of PTEN, the protein that converts PIP₃ back to PIP₂, enhanced BCR-microcluster formation is observed^{24,39}. SLE is an autoimmune disease characterized by the production of antibodies to components of the cell nucleus⁴⁰. In SLE patients, many apoptotic cells accumulate in various tissues, including GCs⁴¹. During cell apoptosis, plasma membrane blebbing generates apoptotic bodies ranging from 0.5 to 5 μm in diameter⁴², size ranges internalized by follicular B cells³⁸. BCR-mediated phagocytosis of these apoptotic bodies by specific B cells may correlate with SLE pathology. As BCR-mediated internalization of soluble vs. large particulate antigens has a different mechanism of action, it is essential to study those mechanisms with a unique role in large particle B cell phagocytosis. These specific targets may be used for biological intervention to steer antibody responses in vaccination and immunopathology. For example, autoantibodies attack red blood cells (RBC) and platelets in autoimmune hemolytic anemia and thrombocytopenic purpura, respectively, causing their destruction through phagocytosis or complement-mediated

lysis^{43,44}. In addition, alloimmunization responses may occur when patients receive a transfusion of donor red blood cells or platelets, which are recognized as foreign antigens^{45,46}. The antibodies generated during these responses drive similar antibody-mediated clearance mechanisms as the auto-antibodies. RBC or platelet-derived (micro)particles are internalized by B cells for these antibodies to be formed. Targeted inhibition of these internalization events may be very beneficial to dampen these responses.

TCR signaling mediates T helper cell plasticity

A responding naive CD4⁺ T cell is expanding, gains effector function, and migrates in response to inputs such as TCR-CD3 binding, signaling downstream of CD28 costimulatory molecules, and DC-derived cytokines. Each Th subset produces a specific cytokine signature in high amounts while retaining the ability to produce other cytokines to a lesser extent. In the classical Th1/Th2 polarization dogma, the strength of TCR signaling and costimulation dictates the outcome of Th1/Th2 polarization. IL-21 is the main cytokine secreted by (early) Tfh cells to regulate B cell differentiation. We previously reported that, in addition to IL-21, human Tfh cells can plastically co-express the Th1 cytokine IFN- γ and/or the Th2 cytokine IL-4⁴⁷. In **Chapter 4**, we sought to understand the potential plasticity that allows Tfh cells to express distinct cytokines that each may steer towards different paths of B cell differentiation. T cells were stimulated with monoclonal anti-CD3 and anti-CD28 antibodies. Through crosslinking the TCR-CD3 signaling machinery, anti-CD3 activates all T cells regardless of their antigen specificity. Multiple levels of CD3 stimulation were used to mimic antigen availability to facilitate different degrees of TCR clustering on the surface of Th cells and to determine the ability to induce the different Th phenotypes.

We demonstrate that high levels of CD3-TCR stimulation led to the induction of IL-21-expressing Tfh-like cells, while low levels resulted in less IL-21 induction, but autocrine or paracrine feed-forward signals of IL-21 could enhance IL-21 production in Tfh-like cells under those conditions. We also demonstrate that the plastic co-expression of IL-4 and IFN- γ by IL-21-producing Tfh cells required a delicate balance in CD3-TCR stimulation, with low levels facilitating the production of IL-4 and high levels resulting in the co-expression of IFN- γ . The addition of exogenous IL-4 or IL-21 significantly affected the co-expression of IL-4 and IFN- γ , with exogenous IL-4 profoundly increasing the percentage of IL-21-producing Tfh cells that co-expressed IL-4 either alone or with IFN- γ , particularly after low CD3-TCR stimulation. Exogenous IL-21 slightly enhances the population of IL-21⁺IFN- γ ⁺ cells. The results of this study provide new insights into the signal 1-dependent plasticity of Tfh-like cells and the role of antigen availability in Tfh-dependent B cell differentiation during the evolution of germinal center reactions.

It is interesting to note that *in vivo*, Tfh cells progressively differentiate to regulate the GC response. A high level of IL-21 is initially secreted by Tfh cells in GCs, but as the GC response progresses, IL-21 is extinguished, and IL-4 is secreted⁴⁸. This switch may be regulated by the

amount of antigen and, consequently, the number of p:MHCII on the surface of GC B cells. A high antigen dose results in more antigen-derived p:MHCII molecules being displayed by antigen-presenting cells, which increases the amount of signaling received by specific T cells at a key time³⁷. Moreover, high antigen doses may prolong the period during which antigen-derived p:MHCII molecules are displayed by antigen-presenting cells, therefore prolonging the TCR signaling process. In agreement with the temporal switch from IL-21 to IL-4 secretion by Tfh cells, we observed that high CD3-TCR signaling promotes IL-21, stabilizing itself in an auto- and/or paracrine feed-forward loop. We demonstrate that the loss of CD3-TCR stimulation supports IL-4 secretion to extinguish IL-21 production.

Understanding the induction of an IL-21-secreting Tfh phenotype that switches to co-express other cytokines is challenging; however, obtaining a more detailed understanding of this process could provide insight into how the presence of antigens influences Tfh-mediated B cell differentiation within the dynamic germinal center reaction.

B cell fate determination into ASC

Protective, but also unwanted, humoral immunity is formed when naive B cells recognize antigens and, with the support of CD4 helper T cells, differentiate into memory B cells and antibody-secreting cells (ASCs) in GC reactions. The B cell differentiation pathways for forming ASCs and memory B cells remain largely unknown, especially in humans. Even though this subject is historically intriguing for theoretical reasons, it also attracts significant attention because the differentiation of human ASCs is needed to facilitate production of therapeutic antibodies. Furthermore, elucidation of the regulators of the ASC differentiation pathways may identify targets for preventing undesired ASC formation. Human naive B cell differentiation into ASCs is notoriously challenging in conditions where enough cell numbers remain to investigate the differentiation process. It is a significant hurdle to understanding the cues that control the complex dynamics of differentiation and hampers the development of strategies to counteract undesired antibody formation. **Chapter 5** presents a novel methodological approach to understanding how naive B cells differentiate into ASC. In a co-culture system of CD19⁺CD27⁻IgG⁻ naive B cells with murine fibroblasts expressing different levels of human CD40L and co-stimulation with IL-21 and IL-4 (alone or in combination), the interplay between B cells and (early) T follicular helper (Tfh) cells were simulated. The minimal conditions drive efficient proliferation, class switching, and ASC differentiation of human naive B cells *in vitro*.

The ASC compartment comprises mature plasma cells (PCs) and less mature plasmablasts (PBs). ASC differentiation is commonly monitored by surface markers CD27, CD38, and CD138, as well as transcription factors PRDM1 and XBP1. Expression of these surface markers and transcription factors starts at the plasmablast stage and increases with differentiation towards PC⁴⁹⁻⁵¹. We demonstrate that high CD40 co-stimulation in presence of IL-21 allows strong proliferation and prepares stimulated B cells for ASC differentiation via upregulation of the transcription factor PRDM1. As B cells continue to express transcription factors that maintain B

cell identity (e.g. PAX5, IRF8, BACH2), ASC differentiation could not be completed efficiently with the induction of CD27, CD38, and CD138 surface marker expression. When CD40 co-stimulatory signals were low, IL-4 induced a CD27+CD38^{low} population, indicative of newly activated cells, both *in vivo* and especially *in vitro*⁵².

Prominent ASC fate transition, including both plasmablast and plasma cells, occurs when CD40L and IL-21 are renewed after initial B cell priming, which extinguishes the B cell transcription program. Renewal of the culture was accompanied by a second wave of phosphorylated STAT3 in the primed B cells. Although IL-21 is known to signal to activate STAT3 in human naive B cells^{53,54}, some direct or indirect CD40-mediated induction of STAT3 phosphorylation is observed⁵⁵. IL-21-induced STAT3 activation efficiently promotes upregulation of PRDM1, the master regulator of ASC differentiation⁵³. It is interesting to delineate mechanistically why renewed CD40L and IL-21 stimulatory conditions induce ASC differentiation more efficiently than single stimulations alone. It is theoretically possible for all naive B cells to differentiate efficiently into ASC since CD40L and IL-21 are abundant at the time of initial cell culture. Still, the renewal of the culture specifically provides the essential signals that complete differentiation. Before the experiments, the CD40L-expressing fibroblasts are lethally irradiated to ensure that they do not overgrow and negatively affect experimental output. The expression level of CD40L on these fibroblasts was determined using flow cytometry when these cells were harvested and suspended. The expression dynamics of CD40L during these cell cultures have never been determined. The CD40L-expressing fibroblasts are adherent cells and will acquire orientation with an apical pole directly in contact with the B cells and basal pole in contact with tissue-culture plates. Initially, CD40L may be expressed uniformly or directed to the apical pole. During the culture, polarity may change, and CD40L availability may be affected by the interacting B cells or the lethal irradiation. Renewal of the culture provide freshly irradiated CD40L-expressing cells that exhibit the polarity to stimulate again efficiently the human B cells.

Interestingly, interference in the CD40L signaling using a blocking antibody to release CD40L stimulation after two executive days of 'normal' culture demonstrates dramatically enhanced ASC formation where proliferation was inhibited⁵⁵. This would argue against the importance of CD40L renewal to facilitate differentiation. Alternatively, differentiation in the secondary cultures may be supported by replenishing growth factors, removing accumulated inhibitory molecules, or by reducing the number of activated B cells that counter ASC formation through contact inhibition of the vastly expanded stimulated B cells in the culture. This contact inhibition in the dark zone of the germinal center where the highly proliferative B cells reside may keep these cells in check *in vivo*^{56,57}. Migration to the less densely populated light zone to encounter antigen and selection signals of the Tfh cells may be simulated by reducing the amount of densely packed B cells in the culture.

Where *in vivo* recognition of antigen by the BCR and the subsequent internalization and presentation of antigen-derived peptides in complex with MHCII is vital for B-Tfh cell interaction and receipt of the CD40L signal, triggering of the IgM BCR with soluble anti-IgM antibodies

or IgM-coated beads has not contributed to enhanced ASC differentiation in the minimalistic cultures. Due to the overlap between BCR and CD40 signaling pathways, it is possible that in our *in vitro* system, the necessary BCR signaling is bypassed by a superphysiological level of CD40 co-stimulation⁵⁸⁻⁶⁰. Alternatively, the added soluble and bead-coated IgM may not have facilitated enhanced differentiation as the BCRs may have been stimulated during isolation, culture, or both. BCR recombination in the bone marrow generates an immense amount of BCR variability that, after negative selection for self-antigens, can recognize all structures present in nature. The fibroblast cells engineered to express human CD40L are of murine origin and will most likely express loads of protein structures foreign to the naive human B cells. Similarly, loads of the reagents used in selecting CD19⁺CD27⁻IgG⁻ naive B cells may contain structures that are recognized by a fraction of the B cells put in culture and results in selective outgrowth and differentiation of a selected subset. In this situation, CD40L competition would be accompanied by fibroblast-mediated BCR stimulation, which may explain why stimulating anti-CD40 antibodies or recombinant soluble trimeric CD40L does not promote ASC differentiation⁶¹. Indeed, naive B cells search and adhere to wild-type murine fibroblasts that do not express CD40L as seen during live imaging. Even though this interaction may be integrin-mediated, BCRs could be involved. B cell differentiating in our cultures were assessed for their clonality to determine whether they represented a small antigen-specific subset, like B cells against fibroblast antigens. Strong polyclonal B cell outgrowth was observed, which is a strong argument against the differentiation of a subset of B cells recognizing fibroblast cells. While many polyreactive BCRs could recognize the heterologous cell line in the naive B cell compartment, this would result in an oligoclonal response instead of an exclusively polyclonal response. In addition, the vast amounts of secreted antibodies of unswitched IgM and class-switched IgG isotypes produced by the ASCs in the culture system did not bind fibroblasts. Although BCRs may thus be stimulated during selection, culture, or both, many results argue otherwise.

Although many questions remain on how exactly the stimulated B cells are primed to differentiate into the ASC compartment, the minimalistic *in vitro* culture system described in chapter 5 did allow the delineation of regulators of the ASC differentiation pathways to identify targets for the prevention of undesired ASC formation. Combining single-cell RNA sequencing of B cell differentiation *in vitro* with *ex vivo* datasets of isolated B cells and ASCs, as well as state-of-the-art analysis pipelines, a detailed and multi-scale analysis of stimulated human naive B cells at various stages of their differentiation to ASCs was conducted in chapter 6. Our data have led to identifying a novel ASC-precursor population and *in vitro* B cell differentiation pathways that recapitulate GC B cell reactions and memory B cell formation for the first time.

It is difficult to infer dynamic relationships between cell types from single-cell sequencing data since they represent snapshots of biological processes. The RNA velocity approach attempts to overcome this challenge by using the unspliced RNA content as a proxy for spliced RNA content in the near future and building directional relationships based on this extrapolation^{62,63}. With this approach, we could determine clear directionality in the ASC compartment, with the

pre-ASCs having prominent connections to the more terminally differentiated ASCs. Contrary to this, the three populations that still show a clear signature of B cells, including activated B cells, GC B cells, and (pre-)memory B cells, all exhibit some degree of connectivity with pre-ASC cells. If we look closely at the *in vivo* situation, this high degree of connectivity is expected. After BCR-mediated antigen engagement, B cells move to the T cell zone to receive additional signals for pre-Tfh cells⁶⁴ to differentiate into extrafollicular PB^{65,66}, early-memory B cell^{16,67,68} or propagate within the GC reaction. Several rounds of antigen- and Tfh cell-mediated selection give rise to GC-derived memory B cells and antibody-secreting plasmablast/plasma cells^{16,69}. GC-memory B cells that reencounter antigens infrequently reengage in GC for further diversification and account for most secondary antibody responses⁶⁸. Clearly, the multiple B cell compartments that arise during an immune response are highly interconnected *in vivo*. This likely explains the high degree of connectivity in our *in vitro* culture system.

BCR reconstruction and clonality inference from the single-cell RNA-seq data demonstrated that the analyzed cells carry mostly unmutated BCRs, indicating that somatic hypermutation is not occurring in our minimalistic system. In contrast, cultured B cells did switch their BCR isotype through class-switch recombination (CSR) from IgD and IgM to IgG. Both these processes are facilitated by the expression of activation-induced cytidine deaminase (AID)^{70,71}. Even though the gene encoding this protein was highly expressed in a fraction of the cells, only prominent CSR was observed. Although it has been thought for quite a while that CSR occurs predominantly during the GC reaction together with somatic hypermutation, recently, it was shown that these processes are uncoupled⁷². Multiple approaches have demonstrated that CSR is initiated before differentiation into GC B cells or extrafollicular plasmablast, and that its activity is greatly diminished in GCs. Reproduction of the somatic hypermutation process *in vitro* has proven extremely challenging. Future efforts should focus on reproducing and modulating somatic hypermutation *in vitro*. This could help us understand how affinity maturation shapes human B cell differentiation key phases and outputs.

During extrafollicular and GC B cell responses, other factors, including nutrient availability, migration patterns, and physical signals such as shear stress, may influence B cell fate decisions. As a result, 3D cultures systems or organoids replicating GC microenvironments may be beneficial for human *in vitro* B cell differentiation studies. Whether ASCs generated in the *in vitro* cultures presented in this thesis resemble extrafollicular PB or arise from the B cells with a robust GC B cell phenotype needs to be determined. A key observation that requires further exploration is that the induction of the GC B cell phenotype highly relies on the presence of IL-4. IL-21 stimulation in naive B cells does allow the immediate induction of *PRDM1* expression without going through a BCL6-driven GC phenotype. Identifying this GC-like B cell population allows the selection of specific surface markers expressed exclusively by this population. After confirming a positive correlation between mRNA and protein expression, these GC-like B cells can be purified from the cultures to define differentiation efficiency to ASCs. It may still very well be that the generated ASCs comprise a heterogenous population of both early and late ASCs. Since the

differences between extrafollicular plasmablast, circulating plasmablast/plasma cells, and long-lived plasma cells in the bone marrow are largely unknown, determining their transcriptional profiles would be interesting. This information may allow delineation of the open question what makes the plasma cells that populate the bone marrow superior to others? Did they receive other signals before their differentiation, or did they happen to make the bone marrow survival niche by chance?

Proposed model

This thesis describes the tight regulation between Tfh cell and B cell differentiation and function (**Chapter 2**). A combination of the data from the various chapters and current literature may be summarized in the following model: As a hallmark of humoral immunity, the GC reaction is orchestrated by reciprocal interactions between B and Tfh cells. The Tfh cells respond dynamically to their environment, particularly by the amount of p:MHCII presented by the B cells with the antigen-specific TCR. B cells, in turn, respond to antigen using the antigen-specific BCR (**Chapter 3**). Despite the acquisition of soluble antigens by B cells, the presentation of antigen-derived peptides is several-fold more efficient with particulate antigens⁷³, which may result in superior responses *in vivo*. The amount of p:MHCII presented positively correlates with BCR affinity or antigen density (**Figure 1**)⁷⁴. The TCR:pMHCII-dependent contact results in a prolonged dwell time of the cognate T:B cells, allowing additional signals to be received that drive the humoral response (**Figure 1**). Some of these additional signals are provided by Tfh cells and include membrane-bound inducible costimulator (ICOS), CD40L, and the cytokines IL-4 and IL-21. Interestingly, because of ICOS stimulation by ICOSL on B cells, more CD40L is expressed on Tfh cells, which provides costimulation for B cells and enhances CD40-CD40L interactions. Additionally, p:MHCII density, and with this, the amount of TCR stimulation defines the cytokines produced by the Tfh cell (**Figure 1**). We demonstrate that Th phenotypes are highly plastic with the ability to co-expressing multiple cytokines with a degree of temporal regulation. Even so, low TCR stimulation increased IL-4 production, whereas high TCR stimulation largely led to increased IL-21 production (**Figure 1**) (**Chapter 4**). As such, limited antigen availability or low/intermediate-affinity BCRs, result in the secretion of IL-4 and low CD40 signaling to drive the activation of a GC B cell and memory B cell phenotype (**Figure 1**) (**Chapter 5 and Chapter 6**)^{16,75}. Alternatively, high antigen availability or high-affinity BCRs induce the secretion of IL-21 and facilitate enhanced T:B cell dwell time to receive high CD40 costimulation that drives the induction of ASC (**Figure 1**) (**Chapter 5 and Chapter 6**)^{16,75}.

The single-cell RNA sequencing data that led to the identification of a novel ASC-precursor population and demonstrated *in vitro* B cell differentiation pathways that recapitulate GC B cell reactions and memory B cell formation (**Chapter 6**) may be used for network reconstructions. Subsequently, computational models, may be generated from these networks to describe their dynamics. These models may reveal paths for the immune system to switch between healthy and (auto)immune disease states.

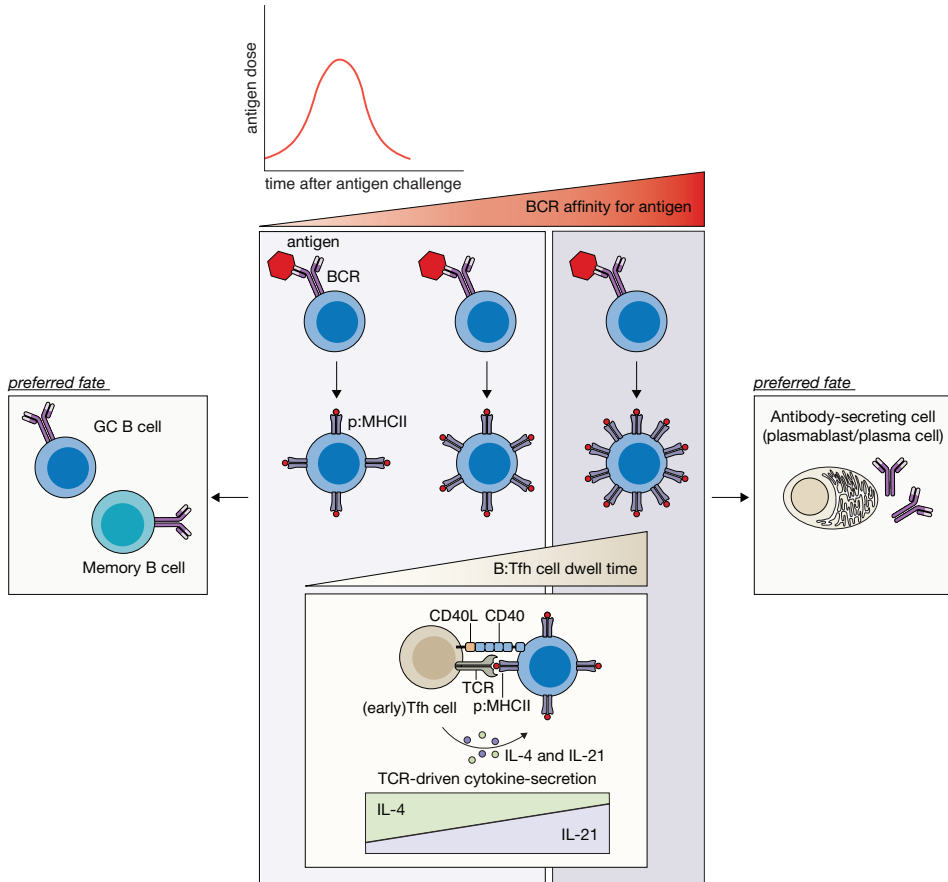


Figure 1 | Model of T cell-dependent B cell differentiation. Antigen dose and B cell receptor (BCR) affinity for the target antigen determine the amount of antigen-derived peptides loaded on major histocompatibility complex (MHC) class II (p:MHCII). The amount of p:MHCII correlates with the time B and (early) T follicular helper (Tfh) cells interact and the signals provided. IL-4 secretion is increased by low TCR stimulation, whereas IL-21 secretion is enhanced by high TCR stimulation. The dwell time and the secreted cytokines together dictate the B cell fate, with low/intermediate-affinity BCRs and corresponding T cell help predisposed to the germinal center B cell and memory B cell fate and high-affinity BCRs and strong T cell help favorably for antibody-secreting cell (plasmablast and plasma cell) differentiation.

REFERENCES

1. Batista, F. D. & Neuberger, M. S. B cells extract and present immobilized antigen: implications for affinity discrimination. *EMBO J* **19**, 513–20 (2000).
2. Hoogeboom, R. & Tolar, P. Molecular mechanisms of B cell antigen gathering and endocytosis. *Curr Top Microbiol Immunol* **393**, 45–63 (2015).
3. Carrasco, Y. R. & Batista, F. D. B Cells Acquire Particulate Antigen in a Macrophage-Rich Area at the Boundary between the Follicle and the Subcapsular Sinus of the Lymph Node. *Immunity* **27**, 160–171 (2007).
4. Depoil, D. *et al.* CD19 is essential for B cell activation by promoting B cell receptor-antigen microcluster formation in response to membrane-bound ligand. *Nat Immunol* **9**, 63–72 (2008).
5. Tolar, P., Sohn, H. W., Liu, W. & Pierce, S. K. The molecular assembly and organization of signaling active B-cell receptor oligomers. *Immunol Rev* **232**, 34–41 (2009).
6. Spillane, K. M. & Tolar, P. B cell antigen extraction is regulated by physical properties of antigen-presenting cells. *Journal of Cell Biology* **216**, 217–230 (2017).
7. Natkanski, E. *et al.* B cells use mechanical energy to discriminate antigen affinities. *Science (1979)* **340**, 1587–1590 (2013).
8. Minton, A. R. *et al.* B-cell receptor dependent phagocytosis and presentation of particulate antigen by chronic lymphocytic leukemia cells. *Explor Target Antitumor Ther* **3**, 37–49 (2022).
9. Zhu, Q. *et al.* Human B cells have an active phagocytic capability and undergo immune activation upon phagocytosis of *Mycobacterium tuberculosis*. *Immunobiology* **221**, 558–567 (2016).
10. Souwer, Y. *et al.* B cell receptor-mediated internalization of salmonella: a novel pathway for autonomous B cell activation and antibody production. *J Immunol* **182**, 7473–81 (2009).
11. de Wit, J. *et al.* Antigen-Specific B Cells Reactivate an Effective Cytotoxic T Cell Response against Phagocytosed *Salmonella* through Cross-Presentation. *PLoS One* **5**, e13016 (2010).
12. Phan, T. G., Grigorova, I., Okada, T. & Cyster, J. G. Subcapsular encounter and complement-dependent transport of immune complexes by lymph node B cells. *Nat Immunol* **8**, 992–1000 (2007).
13. Cinamon, G., Zachariah, M. a, Lam, O. M., Foss, F. W. & Cyster, J. G. Follicular shuttling of marginal zone B cells facilitates antigen transport. *Nat Immunol* **9**, 54–62 (2008).
14. Koers, J. *et al.* CD45RB Glycosylation and Ig Isotype Define Maturation of Functionally Distinct B Cell Subsets in Human Peripheral Blood. *Front Immunol* **13**, 1936 (2022).
15. Weisel, F. J., Zuccarino-Catania, G. v., Chikina, M. & Shlomchik, M. J. A Temporal Switch in the Germinal Center Determines Differential Output of Memory B and Plasma Cells. *Immunity* **44**, 116–130 (2016).
16. Victora, G. D. & Nussenzweig, M. C. Germinal Centers. *Annu Rev Immunol* **40**, 413–442 (2022).
17. Wan, Z. *et al.* The activation of IgM- or isotype-switched IgG- and IgE-BCR exhibits distinct mechanical force sensitivity and threshold. *Elife* **4**, 1–24 (2015).
18. Fujimoto, M., Poe, J. C., Jansen, P. J., Sato, S. & Tedder, T. F. CD19 amplifies B lymphocyte signal transduction by regulating Src-family protein tyrosine kinase activation. *J Immunol* **162**, 7088–94 (1999).
19. Hou, P. *et al.* B cell antigen receptor signaling and internalization are mutually exclusive events. *PLoS Biol* **4**, e200 (2006).
20. Malhotra, S., Kovats, S., Zhang, W. & Coggeshall, K. M. B cell antigen receptor endocytosis and antigen presentation to T cells require Vav and dynamin. *J Biol Chem* **284**, 24088–97 (2009).
21. Turner, M. & Billadeau, D. D. VAV proteins as signal integrators for multi-subunit immune-recognition receptors. *Nat Rev Immunol* **2**, 476–86 (2002).
22. Weber, M. *et al.* Phospholipase C-gamma2 and Vav cooperate within signaling microclusters to propagate B cell spreading in response to membrane-bound antigen. *J Exp Med* **205**, 853–68 (2008).
23. Malhotra, S., Kovats, S., Zhang, W. & Coggeshall, K. M. Vav and Rac activation in B cell antigen receptor endocytosis involves Vav recruitment to the adapter protein LAB. *J Biol Chem* **284**, 36202–12 (2009).
24. Wang, J. *et al.* Growth of B Cell Receptor Microclusters Is Regulated by PIP2 and PIP3 Equilibrium and Dock2 Recruitment and Activation. *Cell Rep* **21**, 2541–2557 (2017).
25. Nishikimi, A. *et al.* Sequential regulation of DOCK2 dynamics by two phospholipids during neutrophil chemotaxis. *Science (1979)* **324**, 384–387 (2009).
26. Floc'h, A. le *et al.* Annular PIP3 accumulation controls actin architecture and modulates cytotoxicity at the immunological synapse. *Journal of Experimental Medicine* **210**, 2721–2737 (2013).
27. Dobbs, K. *et al.* Inherited DOCK2 Deficiency in Patients with Early-Onset Invasive Infections. *N Engl J Med* **372**, 2409–2422 (2015).

28. Ushijima, M. *et al.* The rac activator DOCK2 mediates plasma cell differentiation and IgG antibody production. *Front Immunol* **9**, (2018).
29. Tedford, K. *et al.* Compensation between Vav-1 and Vav-2 in B cell development and antigen receptor signaling. *Nat Immunol* **2**, 548–555 (2001).
30. Doody, G. M. *et al.* Signal transduction through Vav-2 participates in humoral immune responses and B cell maturation. *Nat Immunol* **2**, 542–547 (2001).
31. Guo, F., Debidda, M., Yang, L., Williams, D. A. & Zheng, Y. Genetic deletion of Rac1 GTPase reveals its critical role in actin stress fiber formation and focal adhesion complex assembly. *J Biol Chem* **281**, 18652–9 (2006).
32. Cyster, J. G. B cell follicles and antigen encounters of the third kind. *Nat Immunol* **11**, 989–996 (2010).
33. Phan, T. G., Green, J. A., Xu, Y. & Cyster, J. G. Immune complex relay by subcapsular sinus macrophages and noncognate B cells drives antibody affinity maturation. *Nat Immunol* **10**, 786–796 (2009).
34. Kranich, J. & Krautler, N. J. How Follicular Dendritic Cells Shape the B-Cell Antigenome. *Front Immunol* **7**, 225 (2016).
35. Batista, F. D. & Harwood, N. E. The who, how and where of antigen presentation to B cells. *Nat Rev Immunol* **9**, 15–27 (2009).
36. Roozendaal, R. *et al.* Conduits mediate transport of low-molecular-weight antigen to lymph node follicles. *Immunity* **30**, 264–76 (2009).
37. Pape, K. A., Catron, D. M., Itano, A. A. & Jenkins, M. K. The Humoral Immune Response Is Initiated in Lymph Nodes by B Cells that Acquire Soluble Antigen Directly in the Follicles. *Immunity* **26**, 491–502 (2007).
38. Martínez-Riaño, A. *et al.* Antigen phagocytosis by B cells is required for a potent humoral response. *EMBO Rep* **19**, 1–15 (2018).
39. Wu, X. N. *et al.* Defective PTEN regulation contributes to B cell hyperresponsiveness in systemic lupus erythematosus. *Sci Transl Med* **6**, (2014).
40. Mok, C. C. & Lau, C. S. Pathogenesis of systemic lupus erythematosus. *J Clin Pathol* **56**, 481 (2003).
41. Shao, W. H. & Cohen, P. L. Disturbances of apoptotic cell clearance in systemic lupus erythematosus. *Arthritis Res Ther* **13**, 202 (2011).
42. Kakarla, R., Hur, J., Kim, Y. J., Kim, J. & Chwae, Y. J. Apoptotic cell-derived exosomes: messages from dying cells. *Experimental & Molecular Medicine* **52**, 1–6 (2020).
43. Berentsen, S. & Sundic, T. Red Blood Cell Destruction in Autoimmune Hemolytic Anemia: Role of Complement and Potential New Targets for Therapy. *Biomed Res Int* **2015**, 1–11 (2015).
44. Pos, W., Luken, B. M., Sorvillo, N., Kremer Hovinga, J. A. & Voorberg, J. Humoral immune response to ADAMTS13 in acquired thrombotic thrombocytopenic purpura. *J Thromb Haemost* **9**, 1285–91 (2011).
45. Zimring, J. C., Stowell, S. R., Johnsen, J. M. & Hendrickson, J. E. Effects of genetic, epigenetic, and environmental factors on alloimmunization to transfused antigens: Current paradigms and future considerations. *Transfus Clin Biol* **19**, 125–31 (2012).
46. Zimring, J. C. & Hudson, K. E. Cellular immune responses in red blood cell alloimmunization. *Hematology* **2016**, 452–456 (2016).
47. de Wit, J. *et al.* Human B cells promote T-cell plasticity to optimize antibody response by inducing coexpression of TH1/TFH signatures. *J Allergy Clin Immunol* **135**, 1053–60 (2015).
48. Weinstein, J. S. *et al.* TFH cells progressively differentiate to regulate the germinal center response. *Nat Immunol* **17**, 1197–205 (2016).
49. Fink, K. Origin and Function of Circulating Plasmablasts during Acute Viral Infections. *Front Immunol* **3**, (2012).
50. McCarron, M. J., Park, P. W. & Fooksman, D. R. CD138 mediates selection of mature plasma cells by regulating their survival. *Blood* **129**, 2749–2759 (2017).
51. Sanz, I. *et al.* Challenges and opportunities for consistent classification of human B cell and plasma cell populations. *Front Immunol* **10**, 2458 (2019).
52. Shlomchik, M. J. & Weisel, F. Germinal center selection and the development of memory B and plasma cells. *Immunol Rev* **247**, 52–63 (2012).
53. Deenick, E. K. *et al.* Naive and memory human B cells have distinct requirements for STAT3 activation to differentiate into antibody-secreting plasma cells. *J Exp Med* **210**, 2739–53 (2013).
54. Avery, D. T. *et al.* B cell-intrinsic signaling through IL-21 receptor and STAT3 is required for establishing long-lived antibody responses in humans. *J Exp Med* **207**, 155–71 (2010).
55. Marsman, C. *et al.* Termination of CD40L co-stimulation promotes human B cell differentiation into antibody-secreting cells. *Eur J Immunol* **1–14** (2022) doi:10.1002/eji.202249972.

56. Allen, C. D. C., Okada, T. & Cyster, J. G. Germinal-center organization and cellular dynamics. *Immunity* **27**, 190–202 (2007).
57. Cyster, J. G. Germinal Centers: Gaining Strength from the Dark Side. *Immunity* **43**, 1026–8 (2015).
58. Mizuno, T. & Rothstein, T. L. B cell receptor (BCR) cross-talk: CD40 engagement enhances BCR-induced ERK activation. *J Immunol* **174**, 3369–76 (2005).
59. Elgueta, R. *et al.* Molecular mechanism and function of CD40/CD40L engagement in the immune system. *Immunol Rev* **229**, 152–72 (2009).
60. Luo, W., Weisel, F. & Shlomchik, M. J. B Cell Receptor and CD40 Signaling Are Rewired for Synergistic Induction of the c-Myc Transcription Factor in Germinal Center B Cells. *Immunity* **48**, 313–326.e5 (2018).
61. Marasco, E. *et al.* B-cell activation with CD40L or CpG measures the function of B-cell subsets and identifies specific defects in immunodeficient patients. *Eur J Immunol* **47**, 131–143 (2017).
62. Bergen, V., Lange, M., Peidli, S., Wolf, F. A. & Theis, F. J. Generalizing RNA velocity to transient cell states through dynamical modeling. *Nature Biotechnology* **2020 38:12 38**, 1408–1414 (2020).
63. la Manno, G. *et al.* RNA velocity of single cells. *Nature* **2018 560:7719 560**, 494–498 (2018).
64. Crotty, S. Follicular helper CD4 T cells (TFH). *Annu Rev Immunol* **29**, 621–63 (2011).
65. O'Connor, B. P. *et al.* Imprinting the fate of antigen-reactive B cells through the affinity of the B cell receptor. *J Immunol* **177**, 7723–32 (2006).
66. Paus, D. *et al.* Antigen recognition strength regulates the choice between extrafollicular plasma cell and germinal center B cell differentiation. *J Exp Med* **203**, 1081–91 (2006).
67. Viant, C. *et al.* Germinal center-dependent and -independent memory B cells produced throughout the immune response. *Journal of Experimental Medicine* **218**, (2021).
68. Mesin, L. *et al.* Restricted Clonality and Limited Germinal Center Reentry Characterize Memory B Cell Reactivation by Boosting. *Cell* **180**, 92–106.e11 (2020).
69. Mesin, L., Ersching, J. & Victora, G. D. Germinal Center B Cell Dynamics. *Immunity* **45**, 471–482 (2016).
70. Okazaki, I. M., Kinoshita, K., Muramatsu, M., Yoshikawa, K. & Honjo, T. The AID enzyme induces class switch recombination in fibroblasts. *Nature* **416**, 340–345 (2002).
71. Chua, K. F., Alt, F. W. & Manis, J. P. The Function of AID in Somatic Mutation and Class Switch Recombination: Upstream or Downstream of DNA Breaks. *J Exp Med* **195**, f37 (2002).
72. Roco, J. A. *et al.* Class-Switch Recombination Occurs Infrequently in Germinal Centers. *Immunity* **51**, 337–350.e7 (2019).
73. Vidard, L. *et al.* Analysis of MHC class II presentation of particulate antigens of B lymphocytes. *J Immunol* **156**, 2809–18 (1996).
74. Phan, T. G. *et al.* High affinity germinal center B cells are actively selected into the plasma cell compartment. *J Exp Med* **203**, 2419–24 (2006).
75. Laidlaw, B. J. & Cyster, J. G. Transcriptional regulation of memory B cell differentiation. *Nat Rev Immunol* **21**, 329–343 (2020).

Appendix

Nederlandse samenvatting

List of publications

Author contributions

PhD portfolio

Curriculum Vitae

Dankwoord

NEDERLANDSE SAMENVATTING (ook voor niet-ingewijden)

Door de recente SARS-CoV-2-pandemie is het voor het publiek steeds duidelijker geworden hoe afhankelijk we zijn van een efficiënt functionerend immuunsysteem. Het immuunsysteem beschermt het lichaam tegen ziekteverwekkers, zoals bacteriën, schimmels, parasieten en virussen, maar ook tegen abnormale lichaamseigen cellen die kanker kunnen veroorzaken. Het immuunsysteem is een complex biologisch systeem dat bestaat uit twee sterk samenwerkende delen: het aangeboren (natuurlijke) immuunsysteem en het verworven (aangeleerde) immuunsysteem. Een goede samenwerking tussen deze twee delen leidt tot zeer efficiënte herkenning en verwijdering van ziekteverwekkers.

Nadat een ziekteverwekker het lichaam is binnengedrongen, dient het aangeboren immuunsysteem als eerste verdedigingslinie. Het aangeboren immuunsysteem bevat complementeiwitten en gespecialiseerde cellen zoals macrofagen, neutrofielen en dendritische cellen. Een primaire rol van deze cellen is om met behulp van specifieke antennes, ook wel receptoren genoemd, de ziekteverwekkers te herkennen om ze vervolgens op te ruimen. Macrofagen doen dat door de ziekteverwekkers heel efficiënt op te eten en in kleine stukjes af te breken. Hoewel macrofagen erg goede eters zijn, raken ze op een gegeven moment verzadigd en uitgeput. De macrofagen geven signalen af die neutrofielen uit het bloed naar de plek waar de ziekteverwekker is binnengedrongen zullen lokken. Net als macrofagen kunnen neutrofielen ziekteverwekkers opeten en verteren tot kleine stukjes. Daarnaast kunnen neutrofielen ook dodelijke stoffen uitstoten die de ziekteverwekkers, maar ook de eigen cellen aantasten en vernietigen. Tijdens deze eerste fase van de bescherming zullen de bloedvaten een beetje vloeistof gaan lekken naar het geïnfecteerde weefsel of orgaan waardoor miljoenen complementeiwitten bij de plek van infectie terechtkomen. De complementeiwitten kunnen aan de ziekteverwekkers binden en geactiveerd raken en ze vervolgens doden door ze lek te prikken met gaatjes. Soms is het aangeboren immuunsysteem zo efficiënt dat een groot deel van de ziekteverwekkers al snel is opgeruimd. Vaak zal echter het verworven immuunsysteem worden geactiveerd. Activatie van het verworven immuunsysteem gebeurt met behulp van dendritische cellen. Dendritische cellen kunnen de ziekteverwekkers opnemen en zichzelf bekleden met kleine stukjes van de ziekteverwekker. De dendritische cellen zullen nu de plek van de infectie verlaten en via lymfevaten, een soort snelweg voor de cellen en moleculen van het immuunsysteem, naar de lymfeknopen migreren. De lymfeknopen zijn het lokale hoofdkwartier van het immuunsysteem die onder andere worden bewoond door cellen van het verworven immuunsysteem. Het verworven immuunsysteem bestaat uit twee soorten cellen, B-cellen en T-cellen.

De T-cellen worden onderverdeeld in helper-T-cellen en cytotoxische-T-cellen. De cytotoxische-T-cellen maken cellen dood die zijn besmet door ziekteverwekkers. De helper-T-cellen helpen B-cellen om antilichamen te maken (later hierover meer) en moedigen de uitgeputte macrofagen aan de ziekteverwekker op te ruimen. B- en T-cellen herkennen delen van een ziekteverwekker,

ook wel antigenen genoemd, met hun antigeen receptor, respectievelijk B-cel receptor (BCR) en T-cel receptor (TCR). Ons lichaam kent miljarden B- en T-cellen die allemaal een unieke antigeen receptor over het hele celoppervlak klaar hebben staan. B- en T-cellen kunnen met deze antigeen receptor ziekteverwekkers makkelijk uit elkaar houden. Dit kan worden vergeleken met het sleutel-slot principe, waarbij elke sleutel een specifiek slot open kan maken. In het geval van een infectie met een specifieke ziekteverwekker, wil je er uiteindelijk voor zorgen dat de cel met de juiste antigeen receptor wordt gevonden en geactiveerd, zodat de cel zich kan vermenigvuldigen en vervolgens die ziekteverwekker gericht kan opruimen zonder bijkomende specifieke reacties te geven. Voor het vinden en activeren van de juiste helper-T-cel is de dendritische cel belangrijk. De dendritische cellen die bekleed zijn met stukjes ziekteverwekker en zijn afgereisd van de plek van infectie naar de lymfeknopen, zullen op zoek gaan naar de helper-T-cel met juiste TCR. De dendritische cel wrijft als het ware tegen elke helper-T-cel die tegengekomen wordt. De niet specifieke helper-T-cellen zullen zich hier niets van aantrekken, maar wanneer een specifieke cel wordt gedetecteerd zal er een connectie worden gemaakt; twee immuun cellen geven elkaar als het ware de immunologische hand. Naast de initiële handdruk zullen extra signalen worden gegeven waarmee de dendritische cel de helper-T-cel activeert. Deze activatie zorgt ervoor dat de helper-T-cel gaat delen. Eén cel worden er twee, twee worden er vier enzovoort tot er duizenden cellen zijn die allemaal hetzelfde stukje van de ziekteverwekker herkennen. Daarnaast geeft de activatie de helper-T-cel bepaalde eigenschappen die essentieel zijn voor het verwijderen van de ziekteverwekkers. Een deel van de helper-T-cellen zal naar de plek van infectie gaan om daar uitgeputte macrofagen te wekken, terwijl andere in de lymfeknoop blijven om de B-cellen te helpen.

B-cellen zullen in sommige gevallen ook reageren op delen van ziekteverwekkers zonder de hulp van helper-T-cellen. In dit proefschrift staat echter de T-cel-afhankelijke B-cel reactie centraal. Daar waar helper-T-cellen met stukjes ziekteverwekker beklede dendritische cellen nodig hebben voor de herkenning van de ziekteverwekker, kunnen B-cellen ziekteverwekkerstukjes direct herkennen als onderdeel van de ziekteverwekker zelf. Hoewel ziekteverwekkers je lijf binnenkomen via bijvoorbeeld een wond, kunnen ze daarna geheel of vaker in de vorm van stukken daarvan door het lichaam verspreiden en via de lymfevaten terechtkomen in de lymfeknopen. Wanneer een specifieke B-cel wordt geactiveerd door een T-cel-afhankelijk antigeen, wordt het eerste activeringssignaal afgegeven wanneer het antigeen bindt aan de BCR. Na herkenning wordt het antigeen door de B-cel opgenomen. Lang werd gedacht dat B-cellen alleen kleine stukjes van de ziekteverwekker en niet de volledige ziekteverwekker zelf op konden nemen. In de afgelopen jaren hebben meerdere onderzoeken, waaronder onderzoek van onze groep, laten zien dat B-cellen deze eigenschap wel degelijk bevatten. Na herkenning en opname, bekleedt de B-cel, net als de dendritische cel, zich met kleine stukjes ziekteverwekker. Nu pas kunnen de door de dendritische cel geactiveerde en gedeelde helper-T-cellen een connectie aangaan met de B-cel en de extra hulp afgeven die de B-cel nodig heeft om te kunnen deelnemen aan een T-cel-afhankelijke B-cel reactie. Net als de geactiveerde helper-T-cel zal de geactiveerde B-cel

gaan delen om zichzelf te vermeerderen, dit gebeurt veelal in de kiemcentrumreactie. Tijdens deze reactie verandert het genetisch materiaal, ofwel het recept, dat de antigeen receptor op de delende B-cellen maakt een beetje. Dit proces is willekeurig een vaak zal het recept niet verbeteren. Soms zorgt de verandering er echt voor dat de ziekteverwekker nog beter kan worden herkend, zodat de sleutel nog beter op het slot past. De B-cellen die een sterkere antigeen receptor hebben gekregen, zullen de ziekteverwekker beter herkennen en zichzelf met meer kleine stukjes van de ziekteverwekker bekleden. Opnieuw zullen de helper-T-cellen een connectie aangaan met B-cellen, maar nu specifiek met de B-cellen met een sterkere antigeen receptor en een betere bedekking met stukjes ziekteverwekker. De sterkste afstammelingen zullen uiteindelijk transformeren in antilichamen-makende cellen en geheugen-B-cellen. De antilichamen-makende cellen maken, zoals de naam al doet vermoeden, grote hoeveelheden antilichamen, tot wel 1000 per seconde. Een antilichaam is de uitgescheiden vorm van de antigeen receptor die initieel gebonden was aan de voorvader B-cel. De antilichamen komen terecht in het bloed en zullen door het hele lichaam verspreiden en aan de ziekteverwekker binden als ze deze tegenkomen. Antistoffen zorgen ervoor dat de ziekteverwekker beter uit ons lichaam wordt verdreven. Zo kunnen ze bijvoorbeeld aan virussen vastplakken, waardoor de virussen niet meer de cellen van ons eigen lichaam kunnen binnendringen. Deze lichaamseigen cellen hebben virussen nodig om zichzelf te vermenigvuldigen. Daarnaast kunnen antilichamen binden aan bijvoorbeeld bacteriën zodat de macrofagen ze nog beter kunnen opeten, en maken ze het lekprikken van ziekteverwekkers door de complementeiwitten efficiënter. De antilichamen-makende cellen kunnen zich nestelen in het beenmerg en daar jarenlang antistoffen uitscheiden, zodat een latere infectie met eenzelfde ziekteverwekker sneller geklaard wordt. De geheugen-B-cellen kunnen de ziekteverwekkers onthouden nadat het er eenmalig mee in aanraking is geweest en kunnen in sommige gevallen meteen transformeren naar een antilichamen-makende cel die nu enorme hoeveelheden antilichamen maken in een paar dagen in plaats van er een hele week over te doen.

Helper-T-cel activatie en functie zijn dus nauw verbonden met de B-cel reactie. In dit proefschrift hebben we geprobeerd te begrijpen hoe de communicatiesignalen die aan de B- en helper-T-cellen worden geleverd, ervoor zorgen dat er uiteindelijk antilichamen-makende cellen en geheugen-B-cellen worden gevormd. De resultaten hiervan worden in dit proefschrift beschreven in verschillende hoofdstukken.

In de **hoofdstukken 1 en 2** van dit proefschrift beschrijven we uitvoerig alle betrokken partijen en facetten van een efficiënte B-cel reactie. We beschrijven hoe de ziekteverwekkers worden herkend door de BCR, hoe het precies kan dat de helper-T-cel en de B-cel elkaar tegenkomen, welke signalen er door de helper-T-cel aan de B-cel worden gegeven en hoe deze signalen in de B-cel een domino-effect van signaalroutes activeert waarmee de B-cel 'besluit' of hij uiteindelijk een antilichamen-makende cel of geheugen-B-cel wordt. Zwakke en sterke signalen zorgen voor verschillende activatie van de extreem geconnecteerde signaalroutes en het begrijpen hiervan is erg complex. We geven een perspectief van hoe het domino-effect van signaalroutes mogelijk beter kan worden begrepen met behulp van rekenkundige modellen.

In **hoofdstuk 3** hebben we uitvoerig onderzocht hoe een B-cel een groot partikel, zoals een hele bacterie, opneemt. Zoals hierboven beschreven werd lang gedacht dat B-cellen dit vermogen niet hebben. We laten zien dat de B-cel dit wel degelijk kan en dat dit proces afhankelijk is van herkenning door de BCR. We beschrijven welke signaalroutes na BCR-stimulatie in de B-cel worden geactiveerd en welke essentieel zijn voor het naar binnen trekken van volledige bacteriën. We laten zien dat een specifieke receptor, CD19, die onderdeel is van het BCR-signaleringscomplex en vaak betrokken is bij de opname van kleine oplosbare antigenen, niet betrokken is bij de opname van grote bacteriën. In tegenstelling ontdekken we dat het BCR-signaaleiwit NCK zorgdraagt voor de activatie van het eiwit PI3K dat vervolgens RAC1 activeert. Uiteindelijk is deze signalering nodig voor het remodeleren van de buitenkant van de B-cel zodat de bacterie naar binnen kan worden getrokken.

In **hoofdstuk 4** hebben we de focus van onderzoek naar de helper-T-cellen verlegd. We bekijken hoe de sterkte van de immunologische handdruk, die in het lichaam wordt gegeven door met stukjes ziekteverwekker beklede dendritische cellen of B-cellen aan de helper-T-cellen door herkenning met de TCR, de functie van de helper-T-cellen beïnvloedt. De TCR-stimulatie zorgt ervoor dat helper-T-cel bepaalde signaaleiwitten, die wij cytokine noemen, gaan uitscheiden die vervolgens een effect kunnen hebben op de B-cel reactie. We laten zien dat een zwak signaal voornamelijk productie van de cytokine IL-4 induceert, terwijl een sterk signaal de helper-T-cellen juist aanzet tot IL-21 productie. Daarnaast observeren we dat de helper-T-cellen verschillende cytokines tegelijkertijd kunnen uitscheiden. Dit is interessant, want elke cytokine heeft een ander effect op de B-cel en het integreren van al de mogelijkheden zorgt er waarschijnlijk voor dat het immuunsysteem zo flexibel is.

In de **hoofdstukken 5 en 6** hebben we de vorming van antilichamen-makende cellen en geheugen-B-cellen onderzocht. In **hoofdstuk 5** beschrijven we een door ons opgezet kweeksysteem waarmee we geïsoleerde menselijke B-cellen efficiënt kunnen laten transformeren tot antilichamen-makende cellen. We laten zien dat sterke stimulatie met het helper-T-cel eiwit CD40L samen met de hierboven genoemde cytokine IL-21 ervoor zorgen dat er specifieke signaalroutes worden geïnduceerd die zorgdragen voor deze transformatie. In **hoofdstuk 6** gebruiken we deze methode om specifieker te kijken naar deze transformatie. We gebruiken een nieuwe techniek waarbij we een overzicht van de genexpressie in individuele cellen krijgen. Ons DNA is een blauwdruk voor de eiwitten die een cel produceert en die de functie van een cel bepalen. Elke cel bevat hetzelfde DNA, maar verschillende cellen variëren de mate waarin dit DNA wordt gebruikt om de eiwitten te maken. Door de individuele genexpressie te bestuderen kunnen we achterhalen welke eiwitten er in verschillende stadia van de B-cel reactie tot expressie worden gebracht. We zien duidelijk dat antilichamen-makende cel een erg afwijkend expressie patroon hebben als we deze vergelijken met het B-cel voorstadium. We vergelijken het expressiepatroon van de door ons in het lab 'gemaakte' antilichamen-makende cellen met de antilichamen-makende cellen die we in het lichaam tegenkomen en zien dat de patronen erg overeenkomen. Dit systeem kan ertoe leiden dat we belangrijke factoren vinden die de transformatie naar antilichamen-

makende cel mogelijk maakt. Deze informatie kunnen we vervolgens gebruiken om de reactie tegen ziekteverwekkers te verbeteren, maar ook om antilichamen-makende celvormig tijdens een reactie gericht tegen ons eigen lichaam, wat we auto-immuniteit noemen, te remmen.

Hoofdstuk 7 vat de bevindingen van dit proefschrift samen en onderzoekt de implicaties voor toekomstig onderzoek naar T-cel-afhankelijke B-cel reacties.

LIST OF PUBLICATIONS

Wieske L, Stalman EW, Dam PJK van, Kummer LY, Steenhuis M, Kempen ZLE van, Killestein J, Volkens AG, Tas SW, Boekel L, Wolbink G, Kooi A van der, Raaphorst J, Löwenberg M, Takkenberg B, D'Haens GRAM, Spuls PI, Bekkenk MW, Musters AH, Post NF, Bosma AL, Hilhorst ML, Vegting Y, Bemelman FJ, Voskuyl A, Broens B, Sanchez AP, Els CACM van, Wit J de, Rutgers A, Leeuw K de, Horváth B, Verschuuren JJGM, Ruiters AM, Ouwerkerk L van, Woude D van der, Allaart CF, Teng YKO, Paassen P van, Busch MH, Jallah PBP, Brusse E, Doorn PA van, Baars AE, Hijnen D, Schreurs CRG, Pol WL van der, Goedee HS, Keijzer S, Keijser J, Cristianawati O, Brinke A ten, **Verstegen NJM**, Zwinderman KAH, Ham SM van, Kuijpers TW, Rispens T, Eftimov F. 2023. Persistence of seroconversion at 6 months following primary immunisation in patients with immune-mediated inflammatory diseases. *Ann Rheum Dis* ard-2022-223464. doi:10.1136/ARD-2022-223464

van Dam KPJ, Wieske L, Stalman EW, Kummer LYL, Roosen J, van Kempen ZLE, Killestein J, Volkens AG, Boekel L, Wolbink GJ, van der Kooi AJ, Raaphorst J, Löwenberg M, Takkenberg RB, D'Haens GRAM, Spuls PI, Bekkenk MW, Musters AH, Post NF, Bosma AL, Hilhorst ML, Vegting Y, Bemelman FJ, Voskuyl AE, Broens B, Sanchez AP, van Els CACM, de Wit J, Rutgers A, de Leeuw K, Horváth B, Verschuuren JJGM, Ruiters AM, van Ouwerkerk L, van der Woude D, Allaart RCF, Teng YKO, van Paassen P, Busch MH, Jallah PBP, Brusse E, van Doorn PA, Baars AE, Hijnen DJ, Schreurs CRG, van der Pol WL, Goedee HS, Steenhuis M, Keijzer S, Keijser JBD, Cristianawati O, Rispens T, Brinke A ten, **Verstegen NJM**, Marieke van Ham S, Tas SW, Kuijpers TW, Eftimov F. 2023. Disease activity in patients with immune-mediated inflammatory diseases after SARS-CoV-2 vaccinations. *J Autoimmun* **135**:102984. doi:10.1016/J.JAUT.2022.102984

Verstegen NJM, Pollastro S, Unger PA, Marsman C, Elias G, Jorritsma T, Streutker M, Baßler K, Händler K, Rispens T, Schultze JL, ten Brinke A, Beyer M van HS. 2022. Single-cell analysis reveals dynamics of human B cell differentiation and identifies novel B and antibody-secreting cell intermediates. *bioRxiv*. doi:10.1101/2022.10.03.510595

Stalman EW, Wieske L, van Dam KPJ, Kummer LY, van Kempen ZLE, Killestein J, Volkens AG, Tas SW, Boekel L, Wolbink GJ, van der Kooi AJ, Raaphorst J, Löwenberg M, Takkenberg RB, D'Haens GRAM, Spuls PI, Bekkenk MW, Musters AH, Post NF, Bosma AL, Hilhorst ML, Vegting Y, Bemelman FJ, Voskuyl AE, Broens B, Parra Sanchez A, van Els CACM, Wit J de, Rutgers A, de Leeuw K, Horváth B, Verschuuren JJGM, Ruiters AM, van Ouwerkerk L, van der Woude D, Allaart CF, Teng OYK, van Paassen P, Busch MH, Jallah PBP, Brusse E, van Doorn PA, Baars AE, Hijnen DJ, Schreurs CRG, van der Pol WL, Goedee HS, Steenhuis M, Keijzer S, Keijser JBD, Boogaard A, Cristianawati O, ten Brinke A, **Verstegen NJM**, Zwinderman

KAH, Rispens T, van Ham SM, Kuijpers TW, Eftimov F. 2022. Breakthrough infections with the SARS-CoV-2 omicron (B.1.1.529) variant in patients with immune-mediated inflammatory diseases. *Ann Rheum Dis* **81**:1757–1766. doi:10.1136/ARD-2022-222904

Marsman C, **Verstegen NJM**, Streutker M, Jorritsma T, Boon L, ten Brinke A, van Ham SM. 2022. Termination of CD40L co-stimulation promotes human B cell differentiation into antibody-secreting cells. *Eur J Immunol* **52**:1662–1675. doi:10.1002/EJI.202249972

van den Dijssel J, Hagen RR, de Jongh R, Steenhuis M, Rispens T, Geerdes DM, Mok JY, Kragten AH, Duurland MC, **Verstegen NJM**, van Ham SM, van Esch WJ, van Gisbergen KP, Hombrink P, ten Brinke A, van de Sandt CE. 2022. Parallel detection of SARS-CoV-2 epitopes reveals dynamic immunodominance profiles of CD8+ T memory cells in convalescent COVID-19 donors. *Clin Transl Immunology* **11**:e1423. doi:10.1002/cti2.1423

Verstegen NJM, Hagen RR, van den Dijssel J, Kuijper LH, Kreher C, Ashhurst T, Kummer LYL, Steenhuis M, Duurland M, de Jongh R. 2022. Immune dynamics in SARS-CoV-2 experienced immunosuppressed rheumatoid arthritis or multiple sclerosis patients vaccinated with mRNA-1273. *Elife* **11**:e77969.

Palomares Cabeza V, Kummer LYL, Wieske L, Hagen RR, Duurland M, Konijn VAL, van Dam KPJ, Stalman EW, van de Sandt CE, Boekel L, **Verstegen NJM**, Steenhuis M, Rispens T, Tas SW, Wolbink G, Killestein J, Kuijpers TW, van Ham SM, Eftimov F, Brinke A ten, van Kempen ZLE, Target-to-B! (T2B!) SARS-CoV-2 study group. 2022. Longitudinal T-Cell Responses After a Third SARS-CoV-2 Vaccination in Patients With Multiple Sclerosis on Ocrelizumab or Fingolimod. *Neurology(R) neuroimmunology & neuroinflammation* **9**. doi:10.1212/NXI.0000000000001178

Boekel L, Stalman EW, Wieske L, Hooijberg F, van Dam KPJ, Besten YR, Kummer LYL, Steenhuis M, van Kempen ZLE, Killestein J, Volkens AG, Tas SW, van der Kooi AJ, Raaphorst J, Löwenberg M, Takkenberg RB, D'Haens GRAM, Spuls PI, Bekkenk MW, Musters AH, Post NF, Bosma AL, Hilhorst ML, Vegting Y, Bemelman FJ, Voskuyl AE, Broens B, Parra Sanchez A, van Els CACM, de Wit J, Rutgers A, de Leeuw K, Horváth B, Verschuuren JJGM, Ruiters AM, van Ouwkerk L, van der Woude D, Allaart CF, Teng YKO, van Paassen P, Busch MH, Jallah PBP, Brusse E, van Doorn PA, Baars AE, Hijnen DJ, Schreurs CRG, van der Pol WL, Goedee HS, Vogelzang EH, Leeuw M, Atiqi S, van Vollenhoven R, Gerritsen M, van der Horst-Bruinsma IE, Lems WF, Nurmohamed MT, Boers M, Keijzer S, Keijser J, van de Sandt C, Boogaard A, Cristianawati O, ten Brinke A, **Verstegen NJM**, Zwinderman KAH, van Ham SM, Rispens T, Kuijpers TW, Wolbink G, Eftimov F, T2B! immunity against SARS-CoV-2 study group. 2022. Breakthrough SARS-CoV-2 infections with the delta (B.1.617.2) variant in vaccinated patients with immune-mediated inflammatory diseases using immunosuppressants:

a substudy of two prospective cohort studies. *Lancet Rheumatol* **4**:e417–e429. doi:10.1016/S2665-9913(22)00102-3

Wieske L, van Dam KPJ, Steenhuis M, Stalman EW, Kummer LYL, van Kempen ZLE, Killestein J, Volkens AG, Tas SW, Boekel L, Wolbink GJ, van der Kooi AJ, Raaphorst J, Löwenberg M, Takkenberg RB, D'Haens GRAM, Spuls PI, Bekkenk MW, Musters AH, Post NF, Bosma AL, Hilhorst ML, Vegting Y, Bemelman FJ, Voskuyl AE, Broens B, Sanchez AP, van Els CACM, de Wit J, Rutgers A, de Leeuw K, Horváth B, Verschuuren JJGM, Ruiter AM, van Ouwkerk L, van der Woude D, Allaart RCF, Teng YKO, van Paassen P, Busch MH, Jallah PBP, Brusse E, van Doorn PA, Baars AE, Hijnen DJ, Schreurs CRG, van der Pol WL, Goedee HS, Keijzer S, Keijser JBD, Boogaard A, Cristianawati O, ten Brinke A, **Verstegen NJM**, Zwinderman KAH, van Ham SM, Kuijpers TW, Rispens T, Eftimov F, de Jongh R, van de Sandt CE, Kuijper L, Duurland M, Hagen RR, van den Dijssel J, Kreher C, Bos A, Palomares Cabeza V, Konijn VAL, Elias G, Vallejo JG, van Gils MJ, Ashhurst TM, Nejentsev S, Mirfazeli ES. 2022. Humoral responses after second and third SARS-CoV-2 vaccination in patients with immune-mediated inflammatory disorders on immunosuppressants: a cohort study. *Lancet Rheumatol* **4**:e338–e350. doi:10.1016/S2665-9913(22)00034-0

Wieske L, Kummer LYL, van Dam KPJ, Stalman EW, van der Kooi AJ, Raaphorst J, Löwenberg M, Takkenberg RB, Volkens AG, D'Haens GRAM, Tas SW, Spuls PI, Bekkenk MW, Musters AH, Post NF, Bosma AL, Hilhorst ML, Vegting Y, Bemelman FJ, Killestein J, van Kempen ZLE, Voskuyl AE, Broens B, Sanchez AP, Wolbink G, Boekel L, Rutgers A, de Leeuw K, Horváth B, Verschuuren JJGM, Ruiter AM, van Ouwkerk L, van der Woude D, Allaart CF, Teng YKO, van Paassen P, Busch MH, Jallah BP, Brusse E, van Doorn PA, Baars AE, Hijnen D, Schreurs CRG, van der Pol WL, Goedee HS, Steenhuis M, Rispens T, ten Brinke A, **Verstegen NJM**, Zwinderman KAH, van Ham SM, Kuijpers TW, Eftimov F. 2022. Risk factors associated with short-term adverse events after SARS-CoV-2 vaccination in patients with immune-mediated inflammatory diseases. *BMC Med* **20**:100. doi:10.1186/s12916-022-02310-7

van Kempen ZLE, Wieske L, Stalman EW, Kummer LYL, van Dam PJ, Volkens AG, Boekel L, Toorop AA, Strijbis EMM, Tas SW, Wolbink GJ, Löwenberg M, van Sandt C, ten Brinke A, **Verstegen NJM**, Steenhuis M, Kuijpers TW, van Ham SM, Rispens T, Eftimov F, Killestein J. 2022. Longitudinal humoral response after SARS-CoV-2 vaccination in ocrelizumab treated MS patients: To wait and repopulate? *Mult Scler Relat Disord* **57**:103416. doi:10.1016/j.msard.2021.103416

Unger P-PA, **Verstegen NJM**, Marsman C, Jorritsma T, Rispens T, ten Brinke A, van Ham SM. 2021. Minimalistic *In Vitro* Culture to Drive Human Naive B Cell Differentiation into Antibody-Secreting Cells. *Cells* **10**:1183. doi:10.3390/cells10051183

Verstegen NJM, Ubels V, Westerhoff H v., van Ham SM, Barberis M. 2021. System-Level Scenarios for the Elucidation of T Cell-Mediated Germinal Center B Cell Differentiation. *Front Immunol* **12**:734282. doi:10.3389/fimmu.2021.734282

Verstegen NJM, Unger P-PA, Walker JZ, Nicolet BP, Jorritsma T, van Rijssel J, Spaapen RM, de Wit J, van Buul JD, ten Brinke A, van Ham SM. 2019. Human B Cells Engage the NCK/PI3K/RAC1 Axis to Internalize Large Particles via the IgM-BCR. *Front Immunol* **10**:1–14. doi:10.3389/fimmu.2019.00415

Kersten K, Coffelt SB, Hoogstraat M, **Verstegen NJM**, Vrijland K, Ciampricotti M, Doornebal CW, Hau C-S, Wellenstein MD, Salvagno C, Doshi P, Lips EH, Wessels LFA, de Visser KE. 2017. Mammary tumor-derived CCL2 enhances pro-metastatic systemic inflammation through upregulation of IL1 β in tumor-associated macrophages. *Oncoimmunology* **6**:e1334744. doi:10.1080/2162402X.2017.1334744

Coffelt SB, Kersten K, Doornebal CW, Weiden J, Vrijland K, Hau C-S, **Verstegen NJM**, Ciampricotti M, Hawinkels LJAC, Jonkers J, de Visser KE. 2015. IL-17-producing $\gamma\delta$ T cells and neutrophils conspire to promote breast cancer metastasis. *Nature* **522**:345–348. doi:10.1038/nature14282

van Aalderen MC, Remmerswaal EBM, **Verstegen NJM**, Hombrink P, ten Brinke A, Pircher H, Kootstra NA, ten Berge IJM, van Lier RAW. 2015. Infection History Determines the Differentiation State of Human CD8 + T Cells. *J Virol* **89**:5110–5123. doi:10.1128/JVI.03478-14

AUTHOR CONTRIBUTIONS

Chapter 2

System-level scenarios for the elucidation of T cell-mediated germinal center B cell differentiation.

Niels J. M. Versteegen^{1,2}, Victor Ubels^{3,4}, Hans V. Westerhoff^{2,5}, S. Marieke van Ham^{1,2,†} and Matteo Barberis^{2,3,4,†}

¹Department of Immunopathology, Sanquin Research and Landsteiner Laboratory, Amsterdam University Medical Centers, University of Amsterdam, Amsterdam, The Netherlands

²Synthetic Systems Biology and Nuclear Organization, Swammerdam Institute for Life Sciences, University of Amsterdam, Amsterdam, The Netherlands

³Systems Biology, School of Biosciences and Medicine, Faculty of Health and Medical Sciences, University of Surrey, Guildford, United Kingdom

⁴Centre for Mathematical and Computational Biology, CMCB, University of Surrey, Guildford, United Kingdom

⁵Department of Molecular Cell Physiology, VU University Amsterdam, Amsterdam, The Netherlands

[†]These authors contributed equally to the study as last co-authors

MB and SvH conceived the study. MB and NJMV designed the study. NV, VU and MB wrote the manuscript, with contribution from SvH and HW. MB and SvH provided scientific leadership and supervised the study.

Chapter 3

Human B cells engage the NCK/PI3K/RAC1 axis to internalize large particles via the IgM-BCR.

Niels J.M. Verstegen^{1,3,†}, Peter-Paul A. Unger^{1,†}, Julia Z. Walker¹, Benoit P. Nicolet¹, Tineke Jorritsma¹, Jos van Rijssel², Robbert M. Spaapen¹, Jelle de Wit¹, Jaap D. van Buul², Anja ten Brinke¹, and S. Marieke van Ham^{1,4}

¹Department of Immunopathology, Sanquin Research and Landsteiner Laboratory, Amsterdam University Medical Centers, University of Amsterdam, Amsterdam, The Netherlands

²Molecular Cell Biology, Sanquin Research, Amsterdam, The Netherlands, and Landsteiner Laboratory, Amsterdam UMC, University of Amsterdam, Amsterdam, The Netherlands.

³Synthetic Systems Biology and Nuclear Organization, Swammerdam Institute for Life Sciences, University of Amsterdam, Amsterdam, The Netherlands.

⁴Swammerdam Institute for Life Sciences, University of Amsterdam, Amsterdam, The Netherlands.

[†]Both authors contributed equally

NV, PU, AtB, and SvH conceived the ideas and designed the experiments. NV, PU, JW, BN, TJ, JvR, performed the experiments. NV, PU, JW, BN, TJ, JvR, RS, JdW, JvB, AtB and SvH analyzed the data. NV, PU, AtB and SvH wrote the manuscript. All authors have read and approved the manuscript.

Chapter 4

TCR signal strength regulates plastic co-expression of IL-4 and IFN- γ by Tfh-like cells.

Niels J. M. Verstege^{1,2}, Tineke Jorritsma¹, Matteo Barberis^{2,3,4}, Anja ten Brinke¹ and S. Marieke van Ham^{1,5,†}

¹Department of Immunopathology, Sanquin Research and Landsteiner Laboratory, Amsterdam University Medical Centers, University of Amsterdam, Amsterdam, Netherlands

²Synthetic Systems Biology and Nuclear Organization, Swammerdam Institute for Life Sciences, University of Amsterdam, Amsterdam, The Netherlands

³Systems Biology, School of Biosciences and Medicine, Faculty of Health and Medical Sciences, University of Surrey, Guildford, United Kingdom

⁴Centre for Mathematical and Computational Biology, CMCB, University of Surrey, Guildford, United Kingdom

⁵Swammerdam Institute for Life Sciences, University of Amsterdam, Amsterdam, The Netherlands

NV, and SvH conceived the ideas and designed experiments. NV and TJ performed the experiments and analyzed the data. NV, MB, AtB, and SvH reviewed the data and wrote the manuscript. All authors have read and approved of the manuscript.

Chapter 5

Minimalistic *in vitro* culture to drive human naive B cell differentiation into antibody-secreting cells.

Peter-Paul A. Unger^{1,†}, Niels J. M. Verstegen^{1,2,†}, Casper Marsman¹, Tineke Jorritsma¹, Theo Rispens¹, Anja ten Brinke¹ and S. Marieke van Ham^{1,3}

¹Department of Immunopathology, Sanquin Research and Landsteiner Laboratory, Amsterdam University Medical Centers, University of Amsterdam, Amsterdam, The Netherlands

²Synthetic Systems Biology and Nuclear Organization, Swammerdam Institute for Life Sciences, University of Amsterdam, Amsterdam, The Netherlands.

³Swammerdam Institute for Life Sciences, University of Amsterdam, Amsterdam, The Netherlands.

[†]These authors contributed equally to this work.

PU, NV, AtB, and SvH conceived the ideas and designed the experiments. PU, NV, CM, TJ, performed the experiments. PU, NV, CM, TJ, TR, AtB and SvH analyzed the data. NV, PU, AtB and SvH wrote the manuscript. All authors have read and agreed to the published version of the manuscript.

Chapter 6

Single-cell analysis reveals dynamics of human B cell differentiation and identifies novel B and antibody-secreting cell intermediates.

Niels J.M. Versteegen^{1,2,†}, Sabrina Pollastro^{1,†}, Peter-Paul A. Unger¹, Casper Marsman¹, George Elias¹, Tineke Jorritsma¹, Marij Streutker¹, Kevin Baßler³, Kristian Händler^{3,4}, Theo Rispens¹, Joachim L. Schultze^{3,4}, Anja ten Brinke¹, Marc Beyer^{3,4,5}, S. Marieke van Ham^{1,6}

¹Department of Immunopathology, Sanquin Research and Landsteiner Laboratory, Amsterdam University Medical Centers, University of Amsterdam, Amsterdam, The Netherlands

²Synthetic Systems Biology and Nuclear Organization, Swammerdam Institute for Life Sciences, University of Amsterdam, The Netherlands

³Genomics and Immunoregulation, LIMES Institute, University of Bonn, Bonn, Germany

⁴Platform for Single Cell Genomics and Epigenomics, German Center for Neurodegenerative Diseases (DZNE) and University of Bonn, Bonn, Germany

⁵Immunogenomics & Neurodegeneration, German Center for Neurodegenerative Diseases (DZNE), Bonn, Germany

⁶Swammerdam Institute for Life Sciences, University of Amsterdam, The Netherlands

[†]These authors contributed equally to this work.

SvH conceived the study. SvH led the study. SvH, MB, and AtB supervised the study. NV, SP and PU designed the experiments. PU, CM, MS, and TJ, performed the experiments. NV, SP, and GE analyzed the data. NV, SP, KB, KH, TR, JLS, AtB, and SvH provided intellectual input to the study. NV, SP, PU, AtB, and SvH wrote the manuscript. All of the authors reviewed and approved the manuscript.

PHD PORTFOLIO

Name PhD student: Niels J.M.C. Verstegen
 PhD period: 1 October 2015 – 31 October 2020
 Promotor: prof. dr. S.M. van Ham

Copromotores: dr. J.A ten Brinke
 dr. M. Barberis

Courses	Year	ECTS
Postgraduate Course Advanced Immunology	2016	2.9
Summer School on Advanced Immunology	2016	2
Indesign Workshop	2018	0.2
Analysis tools to understand metabolic networks	2018	1
Personal development programme: The last step & what next?	2019	0.4

Seminars & Workshops	Year	ECTS
Weekly Sanquin IP Department meetings	2015-2020	5
Biweekly Journal Club	2015-2020	2.5
Monthly Department Science Evening	2015-2020	2
Weekly Sanquin Research Staff meeting	2015-2020	5
Landsteiner lectures & guest speaker seminars	2015-2020	5
Sanquin Science Day	2016, 2018, 2019	0.75

Masterclasses	Year	ECTS
dr. André Veillette	2017	0.2
Professor dr. Meinrad Busslinger	2017	0.2

(Inter)national conferences	Year	ECTS
Dutch Society for Immunology – Noordwijkerhout, NL <i>poster presentation</i>	2015	1.5
Dutch & British Society for Immunology – Liverpool, UK <i>poster presentation</i>	2016	1.5
Amsterdam Infection & Immunology Institute retreat – Heemskerk, NL <i>oral presentation</i>	2017	2.5
Amsterdam Institute for Molecules, Medicines and Systems – Amsterdam, NL <i>poster presentation</i>	2017	1

(Inter)national conferences	Year	ECTS
Dutch Society for Immunology – Noordwijkerhout, NL <i>oral presentation</i>	2017	1.5
Bioinformatics and Systems Biology (BioSB) – Lunteren, NL <i>poster presentation</i>	2017	1.5
Amsterdam Infection & Immunology Institute retreat – Heemskerk, NL <i>oral presentation</i>	2018	2.5
Keystone Symposia - B Cells and T Follicular Helper Cells Controlling Long-Lived Immunity – Whistler, CA <i>poster presentation</i>	2017	3
European Congress of Immunology – Amsterdam, NL <i>poster presentation</i>	2018	3
Keystone Symposia - B Cell-T Cell Interactions – Keystone, US <i>poster presentation</i>	2019	3
Dutch Society for Immunology – Noordwijkerhout, NL <i>oral presentation</i>	2019	1.5
European B Cell Network – Remote <i>oral presentation</i>	2021	1.5
 Supervising & teaching	 Year	 ECTS
Master student Julia Walker <i>Internship, 9 months</i>	2016	3.6
Lab assistent immunologie research en kliniek	2017-2019	1
 Parameters of esteem	 Year	
Poster Prize for best poster presentation, Sanquin Science Day	2018	
Travel grant Amsterdam Infection & Immunology Institute	2019	
Travel grant Amsterdams Universiteitsfonds	2019	

CURRICULUM VITAE

Niels Josephus Martinus Cornelis Verstegen was born on August 18th, 1991 in Goirle. In 2010, he graduated from Mill-Hill College in Goirle, majoring in the Nature and Health track, where he developed a fascination for the molecules that govern life. In 2010, he began his studies in Biomedical Science at the University of Amsterdam, obtaining his bachelor's degree in 2013. During his undergraduate studies, he conducted research in the department of experimental immunology at Amsterdam UMC. In 2013, he enrolled in the research Master's program in Biomedical Sciences, Infection and Immunity track, at the University of Amsterdam. His first internship was conducted at the Netherlands Cancer Institute, where he investigated the mechanism by which the mammary tumor-derived cytokine, CCL2, promotes the pro-metastatic functions of gamma delta T cells in transgenic breast cancer mouse models, in the laboratory of Prof. dr. Karin de Visser. He completed his final internship at Sanquin Research, where he studied the mechanism by which primary human B cells perform phagocytosis on antigen particles in the laboratory of Prof. dr. Marieke van Ham. He graduated from the Master's program (*cum laude*) and obtained his Master of Science degree in 2015. That same year, he began his Ph.D. as a collaboration between the Department of Immunopathology of Sanquin Research and the Department of Synthetic Systems Biology and Nuclear Organization of the University of Amsterdam, under the supervision of Prof. dr. Marieke van Ham, with a main focus on the regulation of human B cell differentiation by the nature of the immunizing antigen and regulatory factors from follicular helper T cells. The results of this work are presented in this thesis. From 2021 onwards, he continued his academic career by examining the SARS-CoV-2 vaccination response in patients with immune-mediated inflammatory disorders treated with specific immunosuppressants, as a postdoctoral researcher in the Target-to-B consortium. His work aims to provide a deeper understanding of the impact of these disorders and treatments on the immune system's response to the SARS-CoV-2 vaccination to improve vaccination strategies and outcomes for these patients.



DANKWOORD

“The lone wolf dies but the pack survives” (George R.R. Martin). Dit proefschrift zou er niet zijn zonder alle mensen die er direct bij betrokken waren, en zeker niet zonder de mensen die me van buitenaf hebben gesteund. Het was een uitdagend traject met hoogte- en dieptepunten, maar ook met ontzettend veel gezelligheid, mooie herinneringen en nieuwe vrienden. Er zijn een aantal mensen die ik in het bijzonder wil bedanken.

Marieke, toen ik mijn eerste college van jou bijwoonde, wist ik meteen dat je een bijzonder fijn persoon bent. Het is dan ook geen verrassing dat ik mijn laatste stage voor mijn biomedische master bij jou heb afgerond en daarna misschien iets te lang ben blijven plakken. Dit kwam niet alleen door de passende PhD- en postdoc-projecten, maar ook door het familiegevoel dat mede dankzij jou heerst op de afdeling immunopathologie. Een stukje Brabantse gezelligheid in Amsterdam-West. Soms halen we niet het beste in elkaar naar boven als het gaat om het afronden van projecten, maar het resultaat mag er altijd zijn. En uiteindelijk gaat het daar toch om. Bedankt voor alle kansen, steun en wijze raad in de afgelopen jaren.

Anja, het is echt bewonderenswaardig om te zien hoe jij en Marieke elkaar aanvullen. Soms is het gewoon nodig om even op de rem te trappen om het overzicht weer terug te krijgen. Ik wil je bedanken voor de hoeveelheid tijd en energie die je in de projecten hebt gestoken en ervoor hebt gezorgd dat ze naar een hoger niveau werden getild. Je snelle en doeltreffende feedback was van onschatbare waarde, zeker in de afrondende fase.

Matteo, thank you for showing me that there are more interesting research topics beyond immunology. Together, we explored the use of systems biology approaches in the field of immunology, which has already yielded noteworthy results and will definitely lead to further celebrations. I appreciate your guidance, both in person and remotely.

Casper, “the (B cell) boys are back in town”, bedankt voor alle mooie dingen die we samen mee hebben gemaakt gedurende dit promotietraject. Of we nu serieus discussieerden over data, SLAM! MixMarathon-proeven deden in het lab, samen borrelden of op congresreisjes gingen, jij stond altijd voor me klaar. We hebben veel gelachen en veel aan elkaar gehad. Ik bewonder jouw no-stress mentaliteit en hoop dat ik daar tijdens mijn verdediging ook een beetje van kan lenen.

Sabrina, ik zou willen dat ik dit stukje in het Italiaans kon schrijven, maar eigenlijk ben je al een grotere kaaskop dan je misschien zou willen. Dus daarom gewoon zo. Hoewel we al goed op weg waren met het analyseren van de single-cell RNA-sequencing data, hebben we het samen naar een hoger niveau gebracht. Je was mijn bioinformatica-partner in crime en ik heb veel nieuwe dingen van je mogen leren. Bedankt ook voor de gezellige boottochtjes en de beachvolleybalfeestjes. Grazie di tutto!

Peter-Paul, ooit begonnen als mijn begeleider tijdens mijn masterstage en uitgegroeid tot een waardige collega binnen onze B-cel groep. Ik wil graag mijn waardering uitspreken voor de inzet die je hebt geleverd als 'grootvader' van de B-cel differentiatieprojecten. Het is fantastisch om te zien dat al deze projecten hebben geleid tot prachtige publicaties.

Tineke, bedankt dat je de boel georganiseerd en draaiende houdt. Ik vind het geweldig hoe je keer op keer fantastische datasets weet te genereren met je vele B- en T-celproeven. Ik ben ervan overtuigd dat we van deze inspanningen nog een paar geweldige publicaties kunnen genereren. Keep up the good work!

Julia, nog geen drie maanden begonnen met mijn promotietraject en toen al een masterstudent begeleiden. Dat was nog best uitdagend. Super bedankt voor al je hulp bij het fagocytose project en natuurlijk ook voor de gezelligheid buiten het lab.

Benoit, all of your efforts with the chemical inhibitors used in the phagocytosis project have made my life easier. Thanks for learning all the ins and outs of using the ImageStream and your willingness to assist whenever needed.

Jos en Jaap, zonder jullie hulp had het fagocytose project een open einde gehad. Mooi om te zien dat jullie kennis van de moleculaire celbiologie het project een andere dimensie heeft gegeven.

Robbert, ik waardeer je bijdrage aan mijn ervaring met Alpe d'HuZes, het feit dat je me met beide benen op de grond hebt gezet omtrent Nature publicaties, en jou hulp bij het genereren van de knock-out cellen en natuurlijk de gezelligheid buiten het lab.

Jelle, bedankt voor je hulp en feedback rondom het fagocytose project en voor het deelnemen aan mijn promotiecommissie.

Theo, bedankt voor je kritische blik en voor je waardevolle input bij alle projecten.

Dankzij jullie bijdrage, **Victor** en **Hans**, ben ik de immunologie met een andere blik gaan bekijken.

George, thanks for the helpful single-cell RNA-sequencing discussion and for always being up-to-date with the recent literature and tools.

Marij, bedankt voor je hulp bij het zoeken naar nieuwe regulatoren van humane B cel differentiatie en de gezelligheid daarbuiten.

Kevin, Kristian, Joachim, and Marc, thanks for your help and guidance in exploring single-cell RNA-sequencing data.

Aan alle (voormalige) PhD-studenten. Naast jullie wetenschappelijke bijdragen hebben we ook, zoals Guus Meeuwis dat zo mooi verwoordt, vele tranen gelachen onnozelen gedaan, maar ook heel vaak tevreden, het licht uit gedaan. Iedereen bedankt voor deze onvergetelijke tijd, met ontzettend veel mooie herinneringen. Labuitjes, labweekendjes, borrels, reisjes, playbackshows, etentjes, you name it, allemaal nog mooier dankzij jullie (L): **Jana, Dorit, Lea, Richard, Anna Kroeze, Anna van Beek, Anno, Twan, Laura Delvasto Núñez, Sanne, Nieke, Juulke, Judith, Karin, Willem, Gerben, Inge, Nienke, Esther, Tamara, Astrid, Saskia, Jorn, Yasmin, Myrdinn, Milou, Lisan, Laura Kummer, Laura Fernandez, Jet, Anouk, Christine, Charlotte, Joanne, Stefan, Bert, Jim en Marlieke** (jij hoort hier ook gewoon bij).

Aan alle IP-ers die ervoor zorgen dat iedereen hartelijk wordt ontvangen, waarbij je lekker jezelf kunt zijn, die altijd in zijn voor een praatje en je helpen en van feedback voorzien waar nodig: **Maurice, Rocco, Daniela, Jerry, Virginia, Amélie, Maaïke, Ina, Christina, Jolinde, Henk, Annelies, Mariël, Veronique, Pleuni, Miranda, Angela, Ingrid, Irma, Dorina, Dorien, Olvi, Julian, Sofie, John, Suzanne, Ilse, Ninotska, Kristof, Iris, Elizabeth, Gillian, Gerard, Diana, Sacha, Jolanda, Floris, Nadine, Steven, Dominique, Sinead, Rob, Milena, Gertjan, Arend, Iris, Mieke, Ellen, Marja, Lisanne, Simone, Gijs, Sophie, Brenda en Bruno**.

Fatima en Kaoutar, bedankt dat jullie ervoor zorgen dat alles altijd soepel verloopt. Jullie bijdrage aan de afdeling is onmisbaar. **Fatima**, bedankt voor het regelen van de laatste loodjes. Zonder jou promoveert er uiteindelijk niemand.

Voor iedereen die de Sanquin tijd nog een stukje kleuriger hebben gemaakt. Dank voor de borrels, BBQ-sessies, feestjes, tuin chillings en kickboks avonturen: **Arthur, Rivelino (guardian angel), Max, Erik, Robin, Thijs, Carlijn, Felix, Anna Oja, Florencia, Roos, Zoltan en Franscesca**.

Aan de boys van de beste instituut Faciliteit: **Erik, Simon, Mark, Floris en Tom**. Ik wil jullie bedanken voor het dagelijks up-and-running houden van de apparatuur. Bedankt voor het meedenken en voor het repareren, ontstoppen of back-uppen wanneer dat nodig is. Bedankt voor de gezelligheid op Y3 en daarbuiten.

Dorian, Irene en Yorick, bedankt voor de gezellige avondjes uit, de wetenschappelijke discussies, en voor de onvoorwaardelijke vriendschap die je kunt overhouden van studeren.

Aan de vrienden uit het zuiden. De ene keer zien we elkaar meer dan de ander, maar als we bij elkaar zijn weten we dat het goed zit. Bedankt voor jullie streken, voor alle avonturen en voor de

steun door dik en dun: **Milan, Jaap, Teun, Koen, Jip** en **Guido**. En natuurlijk ook jullie plus-one: **Michelle, Jasmijn, Balou, Karlijn** en **Esther**

Aan de Utrechters die me hebben geadopteerd. Bedankt voor de ontspanning, relativering, de vele racefiets kilometers, een luisterend oor of gewoon even gek doen: **Mark, Mart, Twan, Robbin, Yvet, Aida, Mark, Lori, Ingeborg, Luuk, Eric, Ilse, Yara, Sjors, Nadine** en **Volkert**.

Veerle, in tijde van quasimodo werd al vrij snel duidelijk wat ik aan je had. Bedankt voor je zorgzaamheid, je support, je liefde en het avontuur. Voor de lach en de traan.

De familie, een goede achterban is het halve werk. Bedankt voor de Brabantse nuchter- en gezelligheid: **opa's** en **oma's, Desirée, Joost, Daan, Denise, Koen, Marion, Marty, Simone, Erik, Jinthe, Quinty, Dennis, Chantal, Senn, Jim, Erik, Conny, Dennis, Nicole, Manon** en **Bob**.

Malou en **Dirk**, bedankt voor de bourgondische avondjes, voor jullie gastvrijheid, voor de gezelligheid en steun.

En dan **ons pap** en **ons mam**, bedankt voor jullie onvoorwaardelijke liefde, vertrouwen en steun. Jullie staan altijd voor me klaar en helpen waar nodig. Wie ik ben, zou ik niet zijn zonder jullie. Ik ben jullie ontzettend dankbaar!

If I can live through this
What comes next
Will be
Marvellous

—Fred again.. - Marea—

A

